AFFDL-TR-74-123

LOW AND HIGH FREQUENCY AIRCRAFT GUNFIRE VIBRATION: PREDICTION AND LABORATORY SIMULATION

ENVIRONMENTAL CONTROL BRANCH
VEHICLE EQUIPMENT DIVISION

DECEMBER 1975

TECHNICAL REPORT AFFDL-TR-74-123
FINAL REPORT FOR PERIOD 1 OCTOBER 1972 – 11 DECEMBER 1974

AIR FORCE FLIGHT DYNAMICS LABORATORY
AIR FORCE WRIGHT AERONAUTICAL LABORATORIES
Air Force Systems Command
Wright-Patterson Air Force base, Ohio 45433

NOTICE

When Government drawings, specifications, or other data are used for any purpose other than in connection with a definitely related Government procurement operation, the United States Government thereby incurs no responsibility nor any obligation whatsoever; and the fact that the government may have formulated, furnished, or in any way supplied the said drawings, specifications, or other data, is not to be regarded by implication or otherwise as in any manner licensing the holder or any other person or corporation, or conveying any rights or permission to manufacture, use, or sell any patented invention that may in any way be related thereto.

This report has been reviewed by the Information Office (OI) and is releasable to the National Technical Information Service (NTIS). At NTIS, it will be available to the general public, including foreign nations.

ROBERT W. SEVY
Project Engineer

ELBERT E. RUDDELL
Project Engineer

FOR THE COMMANDER

WILLIAM C. SAVAGE
Chief, Environmental Control Branch
Vehicle Equipment Division

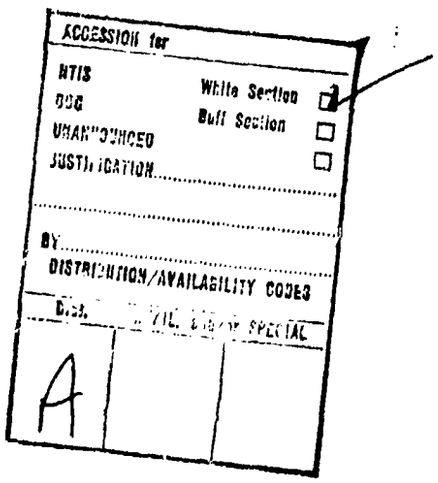

Copies of this report should not be returned unless return is required by security considerations, contractual obligations, or notice on a specific document.

AFSC FORCE / APRIL 1976 - 150

UNCLASSIFIED
SECURITY CLASSIFICATION OF THIS PAGE (When Data Entered)

REPORT DOCUMENTATION PAGE

READ INSTRUCTIONS BEFORE COMPLETING FORM

1. REPORT NUMBER: AFFDL-TR-74-123	2. GOVT ACCESSION NO.
3. RECIPIENT'S CATALOG NUMBER	
4. TITLE (and Subtitle): LOW AND HIGH FREQUENCY AIRCRAFT GUNFIRE VIBRATION: PREDICTION AND LABORATORY SIMULATION	5. TYPE OF REPORT & PERIOD COVERED: Final Report. 1 Oct 72 - 11 Dec 1974
6. PERFORMING ORG. REPORT NUMBER	
7. AUTHOR(s): Robert W. Sevy, Elbert E. Ruddell	8. CONTRACT OR GRANT NUMBER(s)
9. PERFORMING ORGANIZATION NAME AND ADDRESS: Environmental Control Branch (FEE), Air Force Flight Dynamics Laboratory, Wright-Patterson Air Force Base, Ohio 45433	10. PROGRAM ELEMENT, PROJECT, TASK AREA & WORK UNIT NUMBERS: AF- Task No. 329A 0301
11. CONTROLLING OFFICE NAME AND ADDRESS: Environmental Control Branch (FEE), Air Force Flight Dynamics Laboratory, Wright-Patterson Air Force Base, Ohio 45433	12. REPORT DATE: Dec 1975
	13. NUMBER OF PAGES: 219
14. MONITORING AGENCY NAME & ADDRESS (if different from Controlling Office)	15. SECURITY CLASS. (of this report): Unclassified
	15a. DECLASSIFICATION/DOWNGRADING SCHEDULE

16. DISTRIBUTION STATEMENT (of this Report)

Approved for public release; distribution unlimited

17. DISTRIBUTION STATEMENT (of the abstract entered in Block 20, if different from Report)

18. SUPPLEMENTARY NOTES

19. KEY WORDS (Continue on reverse side if necessary and identify by block number)
Vibration
Gunfire Induced Vibration
Prediction Model
Test Method

20. ABSTRACT (Continue on reverse side if necessary and identify by block number)

This study describes in-house efforts ~~comprising two~~ primary objectives: (1) ~~One, the~~ generation of a gunfire-induced vibration prediction model that defines the equipment vibration spectrum in terms of four low frequency sinusoidals superimposed on a high frequency random vibration field; and (2) ~~Two, the~~ synthesis of an economic laboratory test method by which the spectral characteristics of the prediction model are simulated. In the process, a flexible prediction function is introduced to the technology as a promising

DD FORM 1 JAN 73 1473 EDITION OF 1 NOV 65 IS OBSOLETE

UNCLASSIFIED
SECURITY CLASSIFICATION OF THIS PAGE (When Data Entered)

012070

vehicle through which more accurate and realistic vibration fields might be predicted and portrayed in the future.

A gunblast power model is invoked, from previous work, that relates the vibration magnitude and spectral character of the aircraft structural response to the gun power parameters and the distance separating the equipment from the gun muzzles.

The test method development necessitated the modification of existing commercial vibration equipment resulting in general improvement of the vibration system, as a whole.

The prediction technique and test method, developed in this program, is being integrated into MIL-STD-810C and will appear as Method 519.2.

FOREWORD

This report was prepared in the Vehicle Equipment Division (FEE), Air Force Flight Dynamics Laboratory, Wright-Patterson Air Force Base, Ohio. The report contains the results of an in-house research program to develop a vibration prediction technique and a laboratory test method for aircraft equipments exposed to gunfire environments.

This work was conducted from 1 October 1972 to 11 December 1974 under Task 329A0301 with Robert W. Sevy as project engineer.

The authors gratefully acknowledge the contribution of Mark Haller, 4950th/Digital Processing Branch, Computer Center. Special mention must be made of the in-house laboratory contributions of Harold Johnson in the fabrication of special equipment and assisstance in the tests.

TABLE OF CONTENTS

TABLE OF CONTENTS (CONTINUED)

LIST OF ILLUSTRATIONS

LIST OF ILLUSTRATIONS (CONTINUED)

LIST OF ILLUSTRATIONS (CONTINUED)

LIST OF ILLUSTRATIONS (CONTINUED)

LIST OF TABLES

SYMBOLS

$G_{s\ max}$	maximum value of the function enveloping the sinusoids (mean squared g, sine)
$G_{r\ max}$	maximum value of the function enviloping the high frequency random spectrum (g^2/Hz)
$G_{s\ 1,2,3,4}$	mean squared sinusoidal amplitudes at f_1, f_2, f_3, and f_4 (g^2)
r_s	sinusoidal value of $G_{s\ max}$ of the reference gun (M-61)
r_r	sinusoidal value of $G_{r\ max}$ of the reference gun (M-61)
E_o	blast energy of reference gun (ft-lbs/gun)
r_o	basic firing rate of reference gun (100 Hz)
n	number of reference guns = 1
E,r,n	corresponding parameters of unknown gun
E^c	charge energy of explosive (ft-lbs/rd)
m	projectile mass which is equal to the projectile weight W_p/g
g	gravitational constant (32.17 ft/sec^2)
v	muzzle velocity (ft/sec)
f	specific impetus of the charge (ft-lbs/lb)
W_c	weight/rd of the charge
α	specific heat ratio = 1.3
D	vector distance from gun muzzle to equipment location (in.)
R_s	distance from aircraft skin to nearest point of equipment
θ	angle (rads)
β_f	low frequency slope factor of arc tan function
$\beta_{f'}$	high frequency slope factor of arctan function

SYMBOLS (CONTINUED)

ω, f	frequency (rads/sec) (Hz/sec)
ω_o, f_o	low frequency locator frequency (rads/sec) (Hz/sec)
ω_o', f_o'	high frequency locator frequency (rads/sec) (Hz/sec)
a	generalized acceleration (ft/sec^2)
a^2_{max}	maximum value of a (ft/sec^2)
G_D	value of G_s or G_r in the amplitude-distance plane
$G_{D\ max}$	maximum value of G_D
D_o	locator distance (in)
β_D	slope factor of arctan function in the amplitude distance plane
p(x)	amplitude probability density
σ	standard deviation
M	mean value
η	loss factor = $1/Q$
Q	response amplication = $1/\eta$

SECTION I

GUNFIRE VIBRATION PREDICTION

1. INTRODUCTION

This work results from follow-on areas delineated in a previous study (Reference 1) -- a study which involved the development of a prediction rationale for aircraft vibration induced by the gun blast pressure fields of aircraft armaments. The bulk of this past effort required the synthesis of a prediction technique based on energy coupling between the gunfire blast pulses and the resultant structural response. The response spectrum was defined for the high frequency region and was expressed in terms of acceleration power spectral density. In contrast, the low frequency region (below 300 Hz) remained largely undefined. It is this subject, its explication and final integration into the high frequency random portion of the prediction rationale, that constitutes the first objective of this work. The second objective involves the development of a viable and economic laboratory test method to accommodate the low and high frequency elements. In the process of developing the first theme a flexible prediction function is summoned forth and adapted to the special conditions and requirements of this technology and so becomes the medium through which the idea conduces to the achievement. Among the results of this work is Revision C to MIL-STD-810, "Method 519.2 Gunfire Vibration, Aircraft" which is included as Appendix A.

2. GUNFIRE VIBRATION SPECTRUM

From Reference 1 a composite vibration spectrum is shown (Figure 1) consisting of a low frequency assemblage of sinusoids blended with a high frequency random spectrum.

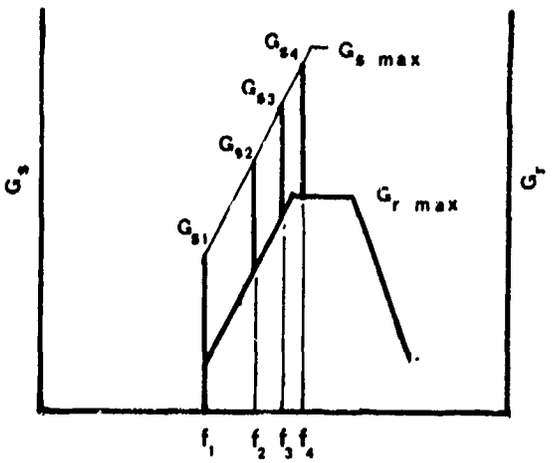

Figure 1. Composite Vibration Spectrum

The sinusoidal spectrum comprises structural response elements whose amplitudes and frequencies constitute the fundamental gunfire rate (G_{s1}) together with the second third and fourth orders (G_{s2}, G_{s3}, G_{s4}): The full nomenclature of the spectrum elements are listed as follows:

$G_{s\ max}$ = maximum value of the function enveloping the sinusoids (mean squared g)

$G_{r\ max}$ = maximum value of the function enveloping the high frequency random spectrum (g^2/Hz)

G_{s1}, G_{s2}, G_{s3}, G_{s4} = the mean squared sinusoidal amplitudes at f_1, f_2, f_3 and f_4 (g^2)

From the same reference, the power equations are listed which identify the element magnitudes of Figure 1 with the induced vibration response resulting from the power coupling from the gunfire blast.

$$G_{s\ max} = \Gamma_s\ E/E_o\ r/r_o\ n/n_o \qquad (1)$$

$$G_{r\ max} = \Gamma_r\ E/E_o\ r/r_o\ n/n_o \qquad (2)$$

Γ_s = the sinusoidal value of $G_{s\ max}$ of the reference gun (g^2)-mean squared g.

Γ_r = the random vibration value of $G_{r\ max}$ of the reference gun (g^2/H_z)

E_o = blast energy of the reference gun (ft-lbs/gun)

r_o = basic firing rate of the reference gun = 100 Hz

n_o = number of reference guns = 1

E, r, n = the corresponding parameters for the unknown gun

Finally, to couple the set of energy associations, the gunblast energy parameters are defined and related by two equations (Reference 2).

$$E = E^C - mv^2/2 \tag{3}$$

E = blast energy (ft-lbs/gun)

E^C = charge energy (ft-lbs/rd)

m = projectile mass which is equal to the projectile weight (W_p) divided by g(32.17 ft/sec^2)

v = muzzle velocity (ft/sec)

$$E^C = f(W^C)/\alpha - 1 \tag{4}$$

f = the specific impetus of the charge (ft-lbs/lb)

W^C = weight/round of the charge (lbs/rd)

α = specific heat ratio = 1.3

These expressions, Equations 1 and 2, will be recalled later in Section III where they mesh with the gunfire induced vibration data of Section II to complete the quantitative requirement of the prediction process.

3. SUMMARY

We complete this section with a brief review of the impending work areas. Section II describes, processes, and presents low frequency sine and high frequency random vibration data of the F-4 and A-7D aircraft -- the data being presented as a three dimensional display involving the parameters of magnitude, frequency, and distance. Section III invokes special prediction surface equations with which to umbrella the data display. The prediction surface parameters are then related to the power equation of Section I. Section IV evolves a laboratory test technique by which the sinusoids and random vibration spectrum are synthesized, combined, applied, and controlled.

SECTION II

DATA DESCRIPTION AND PROCESSING

1. SOURCES

Two sources for gunfire data were used: A-7D data and data from the F-4E. The F-4E data was selected from the data bank used in past works (Reference 1) and as such may be regarded as older and somewhat less reliable; the accelerometer locations being less precisely stated. In contrast, the A-7D gunfire data is recent (1970), the accelerometer locations are rather precisely defined and sufficiently detailed information concerning the structural characteristic (i.e., primary or secondary) was at hand such that, on balance, the A-7D data was elected to have the greatest weighting. Nonetheless the F-4E data served to reinforce that of the A-7D. Figures 2 and 3 show the accelerometer locations for the A-7D and F-4E. As in earlier works only those accelerometers were used that were located relatively close to the skin surface and attached on primary structure (skin, frames, stringers, bulkheads, etc). The average depth of the accelerometers was approximately three inches. Accelerometers located on instrument panels, gunsights, shelves, equipment arrays, and seats were excluded - these accelerometers, by our own imposed definition, are classified as being associated with secondary structure and must be treated separately.

a. Gunfire Flight Conditions

Both gunfire cases were reduced from airborne tape records. Gunfire recording was generally at 5000 feet altitude and Mach 0.85. However, the A-7D data included other flight conditions and maneuvers. But this element was of no great concern since gunfire levels are high compared to contributions from other sources and so gunfire levels tend to mask the contributions from most flight conditions.

b. 1/3 Octave Data

The reduced data originally appeared in 1/3 octave form. Though some narrow band A-7D data was available, past experience has shown (for

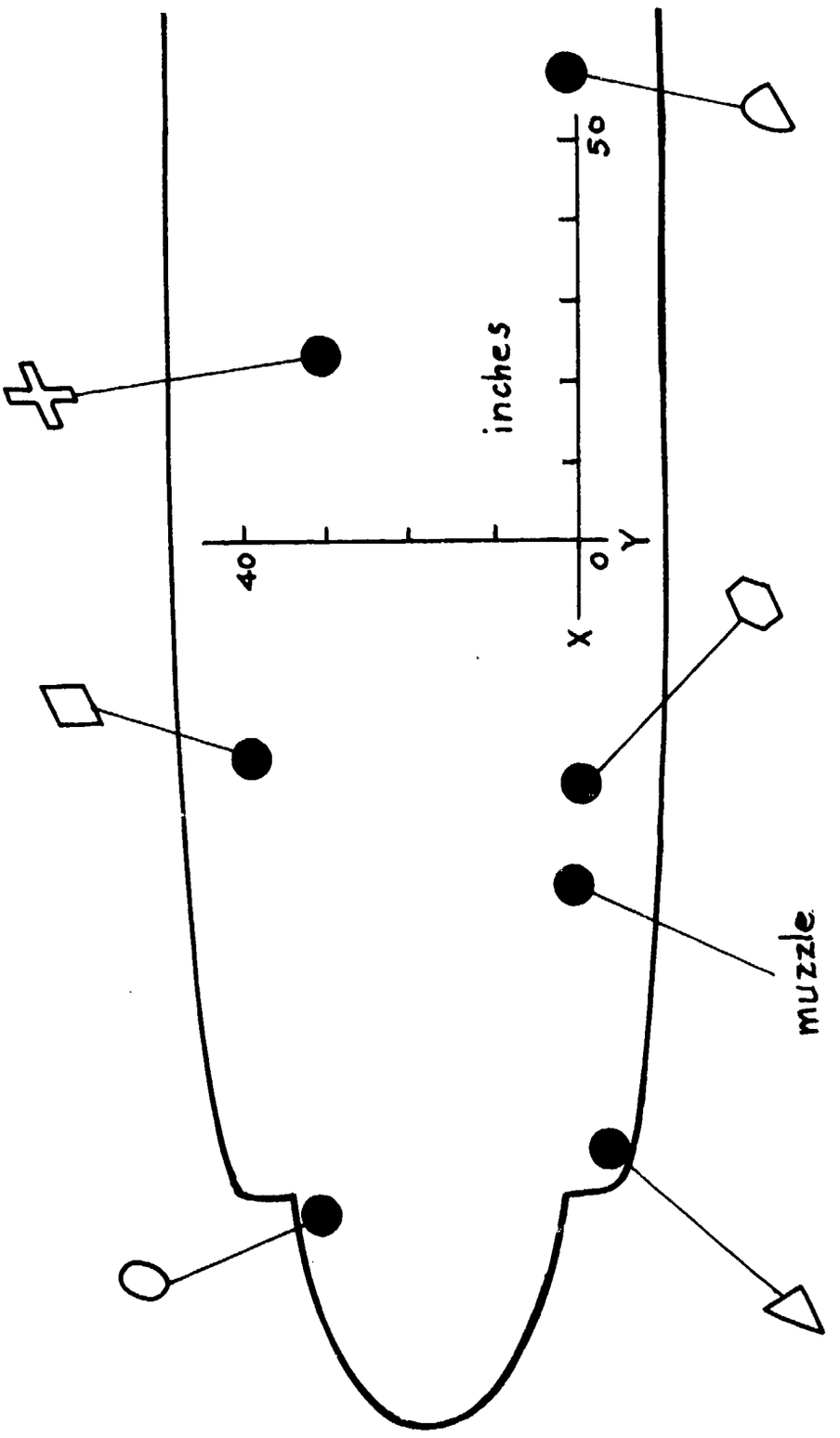

Figure 2(a). Accelerometer Locations (Primary Structure) of the A-7D

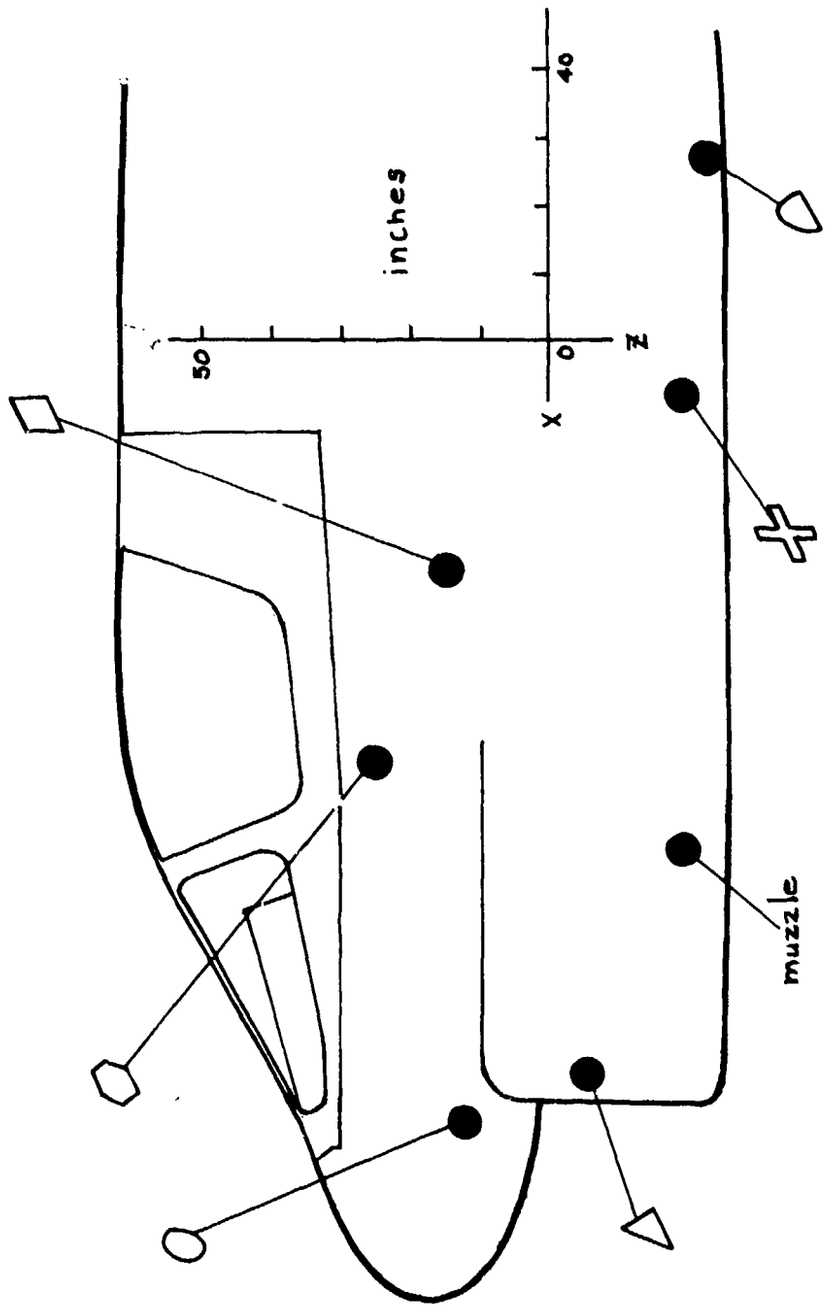

Figure 2(b). Accelerometer Locations (Primary Structure) of the A-7D

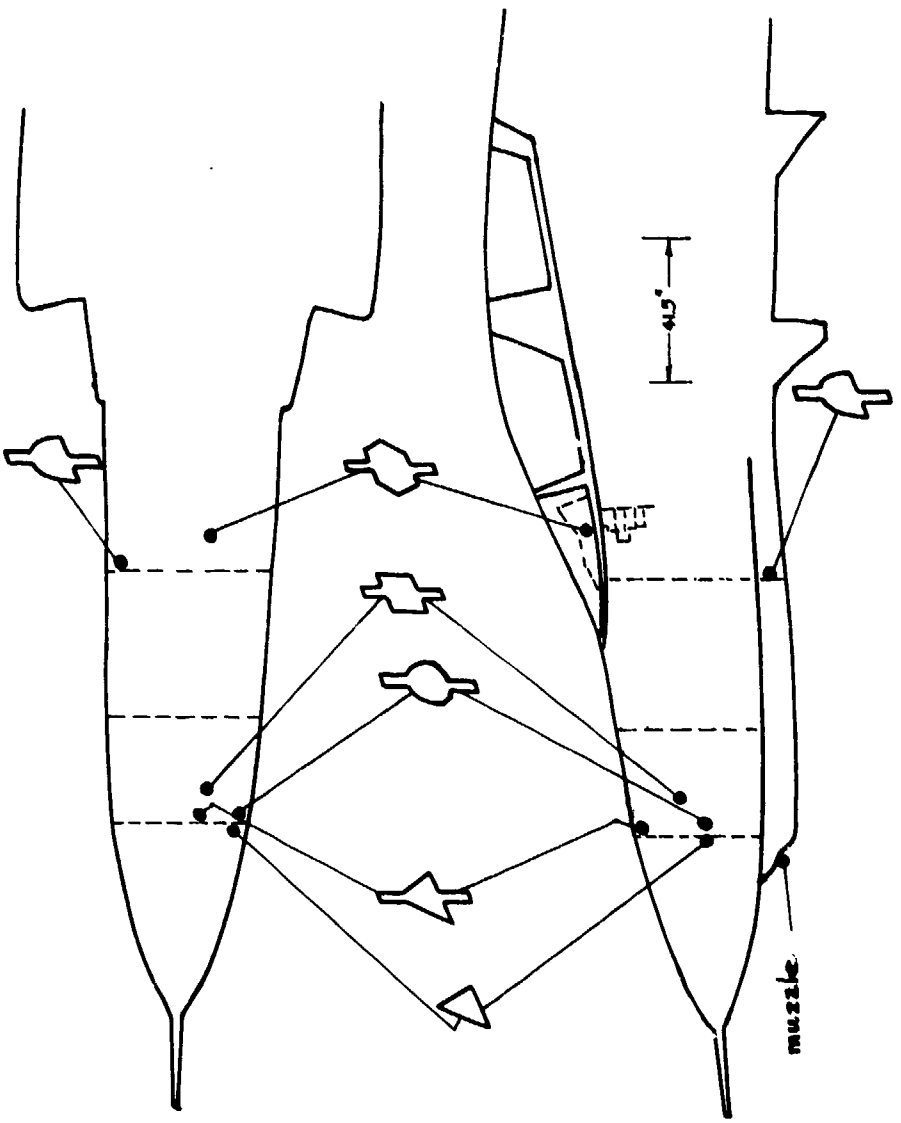

Figure 3. Accelerometer Locations (Primary Structure) of the F-4E

the higher gunfire rates) that 1/3 octave reduction does a reasonably good job of representing the spectral analysis at the basic gunfire rate and at the second, third and fourth harmonics. Admittedly, the bandwidth is somewhat high at 400 Hz (92 Hz) but, on the average, one-third octave readings, at this frequency, seldom exceed narrow band values by more than several dB.

In summary, from considerations of data quality, locational details, and applicability, (in that order) the 1/3 octave analysis employed was deemed suitable for the purposes of this study.

c. Gun Parameters and Configuration

Both guns are of the M-61, rotating barrel, 20 mm class. Both were firing at a 100 Hz rate, both muzzles are sufficiently close to or integral with the aircraft structure such that the gun standoff distance may be considered zero (Reference 1); that is, the expectation that the structural vibration would be reduced in amplitude due to a spatial separation between the gun muzzle and the aircraft structure is minimized.

Finally, the gun ballistic parameters that figure importantly in the gunfire model are presented in Table 1 for convenient reference. The table is repeated in the second row to show the parameters in metric units (Newton-meter-sec).

2. DATA DISPLAY

In previous work (Reference 1) it was shown that data analysis of gunfire vibration is facilitated by arranging the vibration field in three dimensional form consisting of the variables amplitude and frequency, both represented as a function of the distance from the gun muzzle.

a. Determination of the D Parameter

The D parameter represents the vector distance from the gun muzzle point to the selected accelerometer location and was calculated from the three orthogonal distances referenced from the butt line, fuselage, and the water line corrdinates. Figure 4 represnts a typical spatial arrangment from which D is determined.

TABLE 1

GUNFIRE BALLISTIC PARAMETERS

(English Units)							
Gun	Gun Caliber	Firing Rate r		Muzzle Vel. v	Muzzle Energy $W_p v^2/2g$	Blast Energy E	E/E_o
	(mm) (in.)	Hz/min	Hz/sec	(ft/sec)	(ft-lbs)	(ft-lbs)	
M61	20 .79	6,000 (nom)	100 (max)	3,380 (nom)	39,600	55,000	1.0
(Metric Units)							
	(mm) (in.)	Hz/min.	Hz/sec	m/sec	Newton Meters	Newton Meters	E/E_o
M61	20 .79	6,000 (nom)	100 (max)	1,030	53,700	74,600	1.0

b. Low Frequency Sinusoidals (G_s).

The data was divided into two major regimes, the low frequency sinusoidal region and the high frequency random domain. The first category consists of the low frequency spectral outputs representing the basic gunfire rate $r = f_1 = 100$ Hz together with the second, third and fourth orders, that is, $f_2 = 200$ Hz, $f_3 = 300$ Hz and $f_4 = 400$ Hz. Note that the 1/3 octave bandwidth of the third order analysis is sufficiently broad (73 Hz) to accommodate the 300 Hz component even though the nearest analyzer center frequency is 315 Hz. The rms values of these spectra were squared and plotted in a three dimensional, isometric display of the mean squared magnitudes (G_s), the frequency (f) and the distance parameter (D). The plots are shown respectively for the A-7D and the F-4E, as Figures 5 and 6. Note that the symbols are keyed to transducer locations as shown previously in Figures 2 and 3.

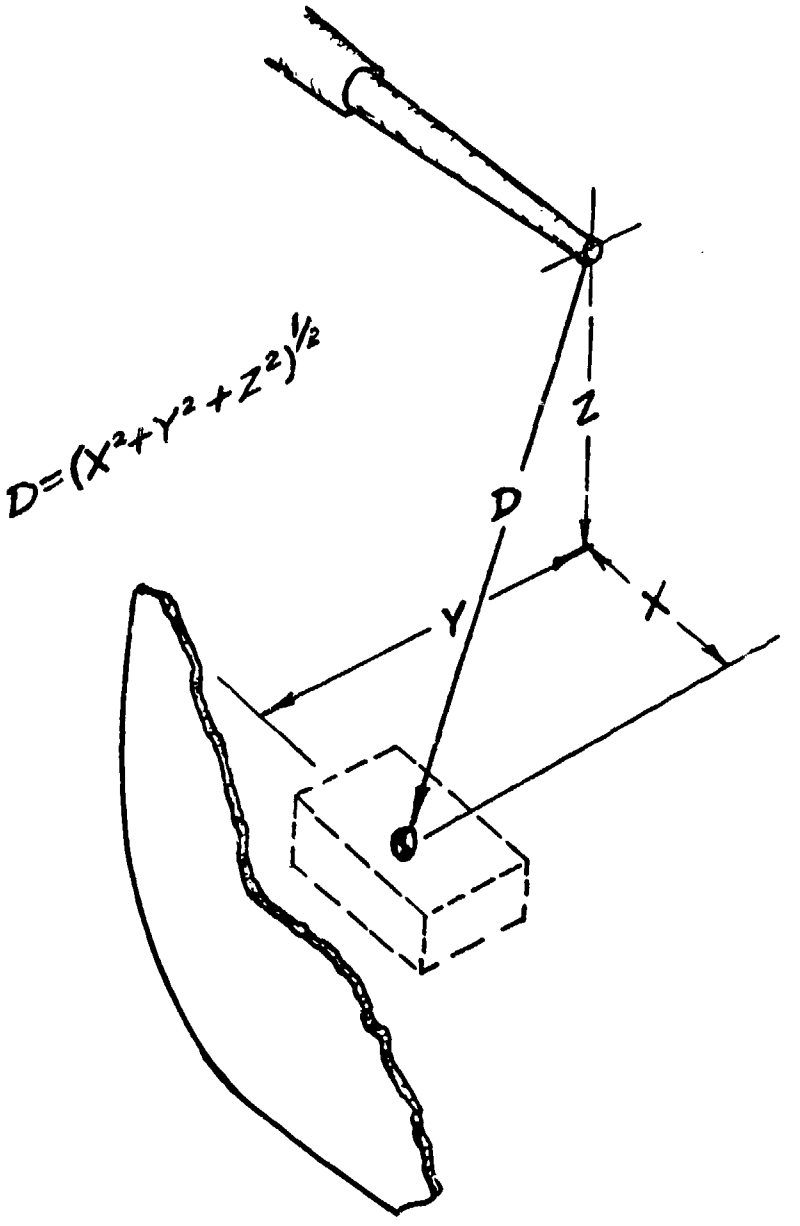

Figure 4. Determination of the Distance Parameter; D

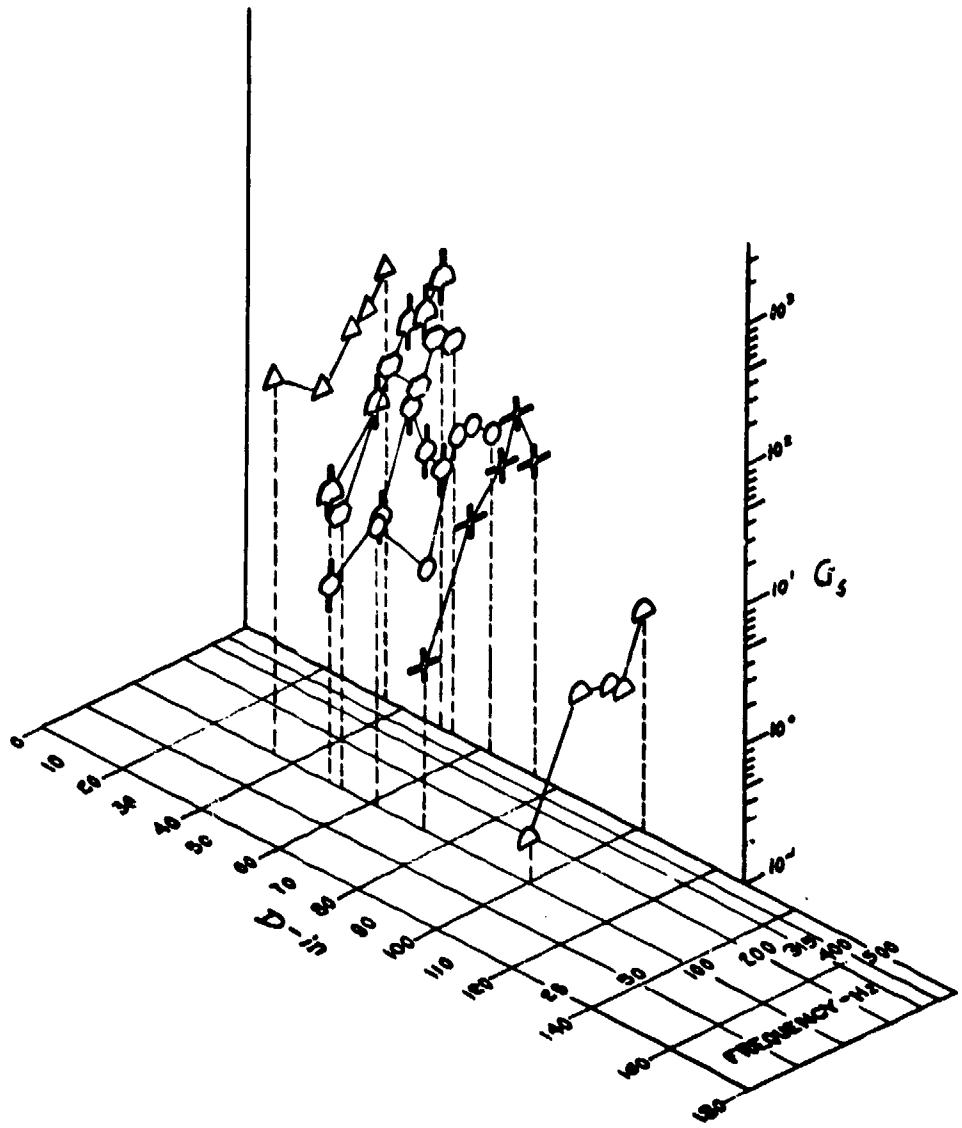

Figure 5. Three Dimensional Plot of A-7D Gunfire Vibration (Sinusoidal)

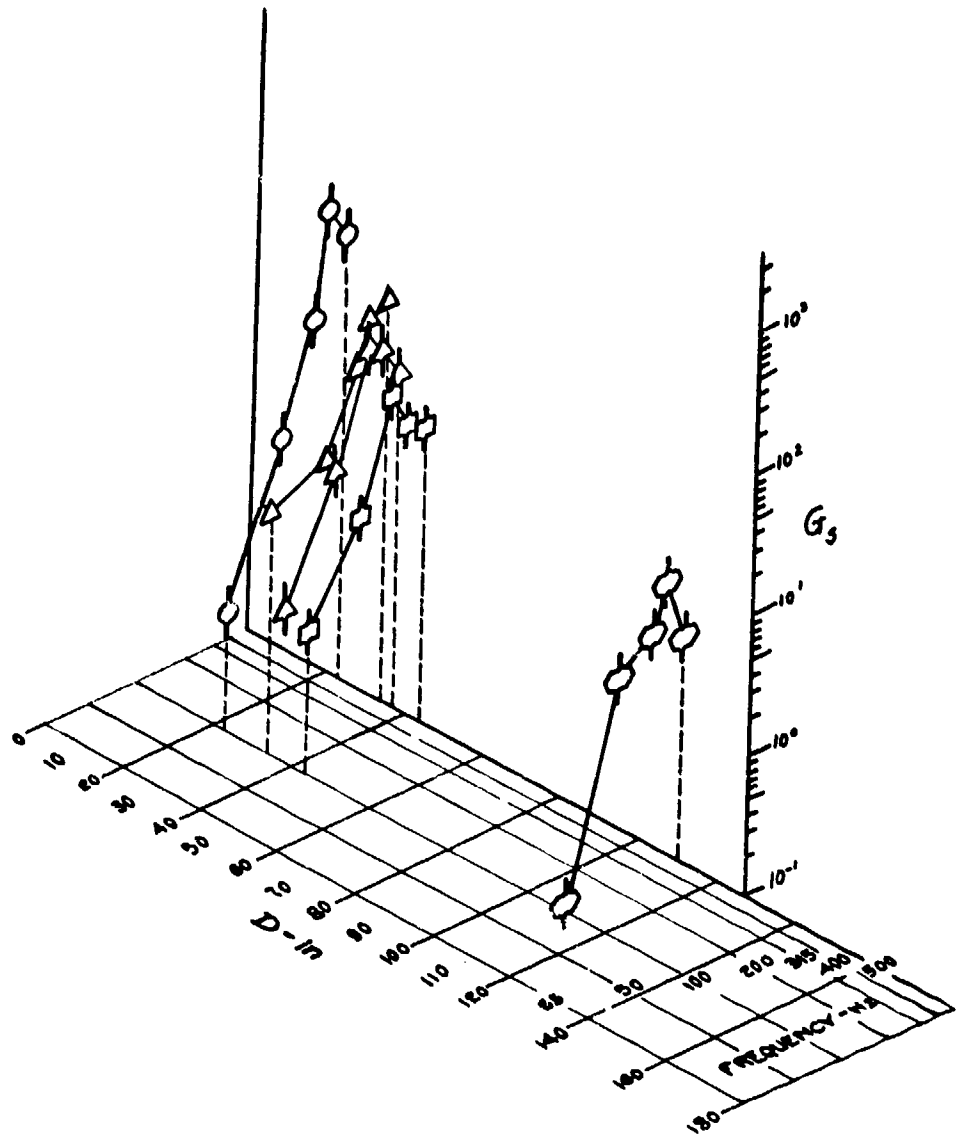

Figure 6. Three Dimensional Plot of F-4E Gunfire Vibration (Sinusoidal)

c. High Frequency Random (G_r)

Similarly, the mean squared outputs of the 1/3 octave analysis beginning at 630 Hz and extending to 2 KHz were divided by their respective 1/3 octave bandwidths to derive the corresponding acceleration power spectral densities (G_r). The isometric display for the A-7D and F-4E are seen in Figures 7 and 8.

d. SUMMARY

To recapitulate, we have constructed, in consonance with our earlier objectives and power models, a three dimensional array of reduced gunfire vibration data involving three elements: the mean squared magnitude, the frequency, and the vector distance D.

Our next step is to synthesize a surface embodying the variables G_s, G_r, f and D in such a way as to constitute a surface of sufficient conformal virtuosity to permit a suitable fit for the data display and this step serves to introduce, in the following section, what we believe to be a function of the requisite versatility.

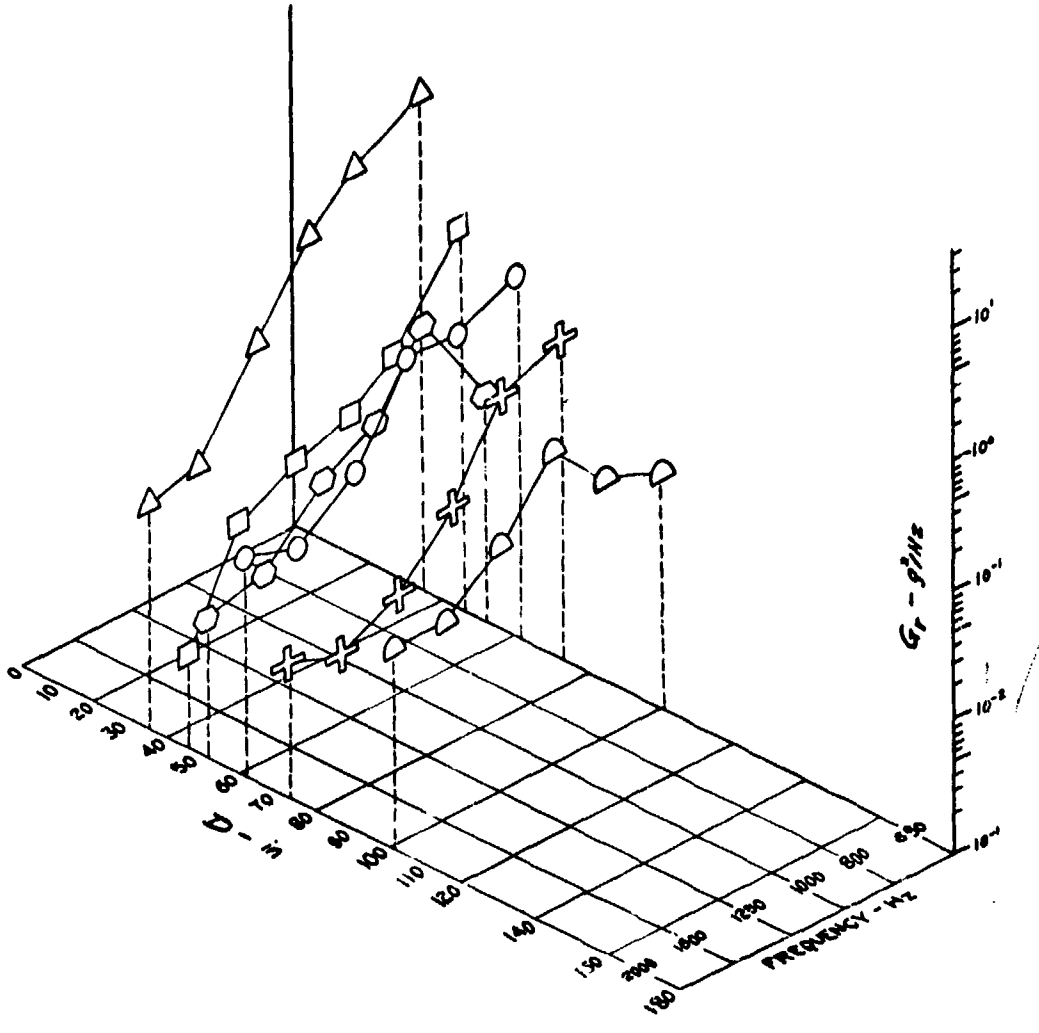

Figure 7. Three Dimensional Plot of A-7D Gunfire Vibration (Random)

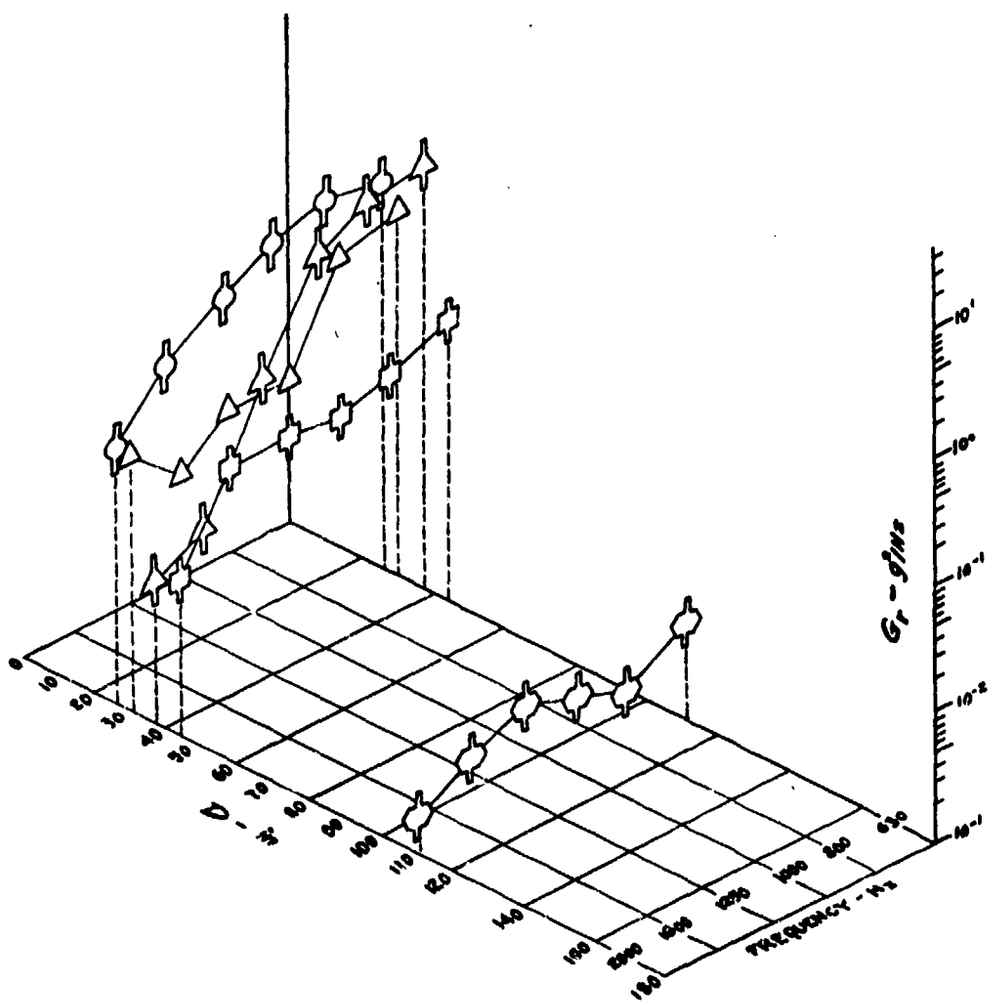

Figure 8. Three Dimensional Plot of F-4E Gunfire Vibration (Random)

SECTION III

VIBRATION PREDICTION SYNTHESIS

1. VIBRATION CHARACTERISTICS

If the vibration prediction process for aircraft is to be substantially improved more flexible means must be devised to describe the variegated transfer functions and response characteristics that are encountered when ranging through the vehicle structures. A few examples are discussed and shown for illustration.

a. Typical Cases

A typical transfer function for the aircraft skin is shown in Figure 9(a). Here, a transfer function is defined as a function (a/p) which when multiplied by the boundary layer pressure spectrum (p) yields the acceleration response spectrum (a).

If we move across the skin joints and several inches into the aircraft interior, say on a frame or bulkhead, we see a response curve whose high frequencies are being rolled off as in Figure 9(b). If we move further in on the primary structure (10 inches or so) the response continues to roll off in the high frequency region; usually with an attendant decrease in the a_{max} region. Now, if we add mass near the region (an equipment item) both the curve leading edge and the high frequency roll-off portion of the curve will down shift further as shown in Figure 9(c); also a_{max} is further diminished, depending on the load. Figure 9(d) represents a typical transfer function for the wing section and tail section. Figure 9(e) shows the engine orders and gear frequencies of the accessory section superimposed on a random background - a typical spectral picture of vibration response as it is seen at locations near the engine. Finally, a reasonably good approximation to helicopter vibration response of the primary structure can be simulated with four rotor blade frequencies blended with an upper frequency random spectrum as shown in Figure 9(f).

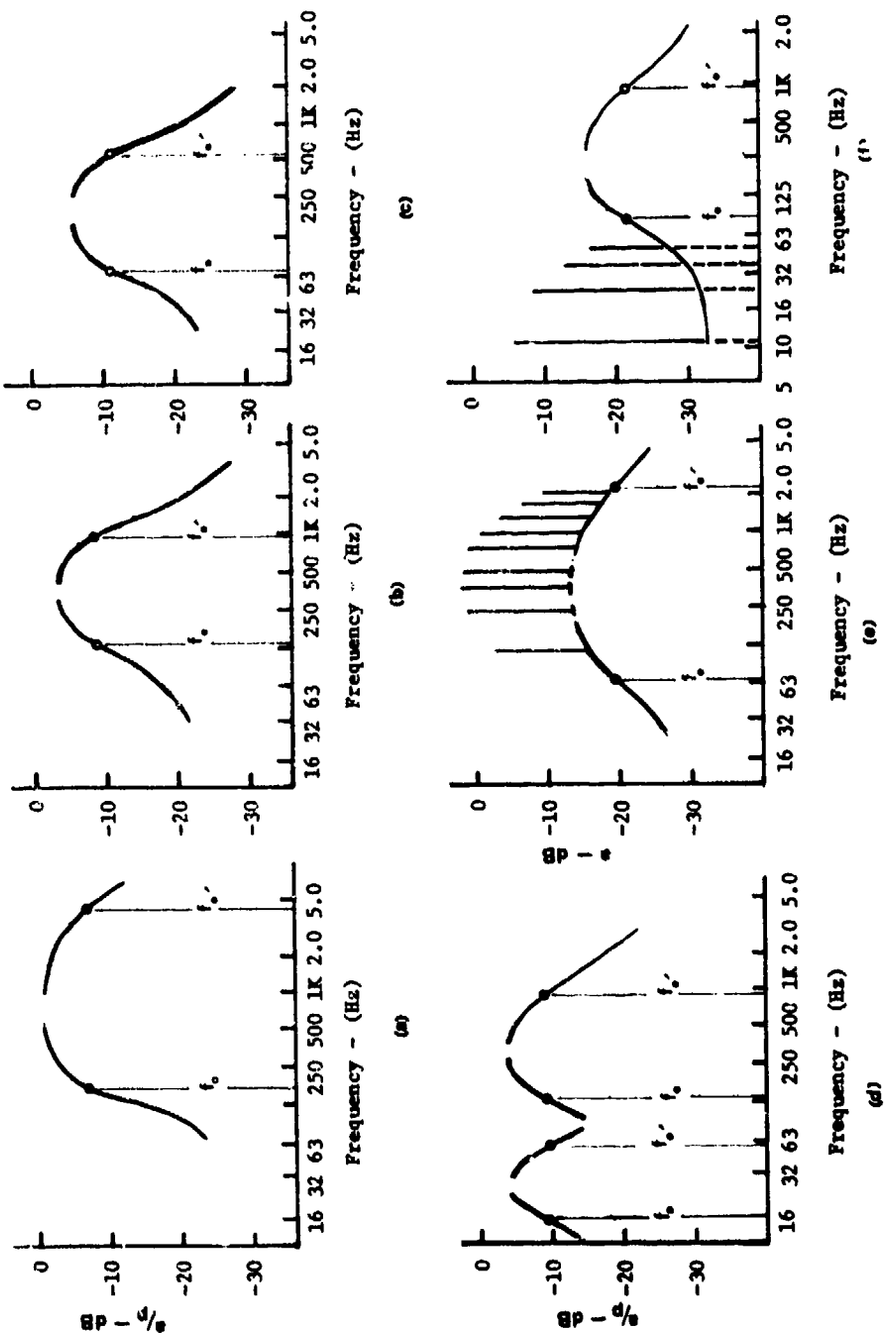

Figure 9. Typical Transfer Functions and Response Spectra of Aircraft

From these examples, we see that what we need is a function that can be split into a high and low frequency region; each region independently translatable up and down the frequency range and each with independently adjustable slopes. Given a function with these convenient properties we can pretty well cover most transfer and response functions for aircraft primary structure.

2. SELECTION OF A FUNCTION

A promising function (encountered during the work detailed in Appendix B) having these properties is of the arctan class. More properly, it is an elaboration of this form, which appears as follows for the low and high frequency regions, respectively.

$$\theta = \arctan A \tag{1}$$

$$\theta = \pi - \arctan A \tag{2}$$

where:

θ = angle (rads)

$$A = \frac{2\beta(\omega/\omega_o)}{1 - (\omega/\omega_o)^2}, \quad 0 \leq \beta \leq 1.0$$

ω = angular frequency (rads/hz)

β = slope factor

Many readers will recognize the arctan expression as a form that establishes the phase angle between the force and displacement of a simple, viscously damped, single degree of freedom oscillator--the force acting on the mass.

In this form, frequency translation occurs by control of ω_o. Slope control is readily obtained by adjusting β (Figure 10(a).

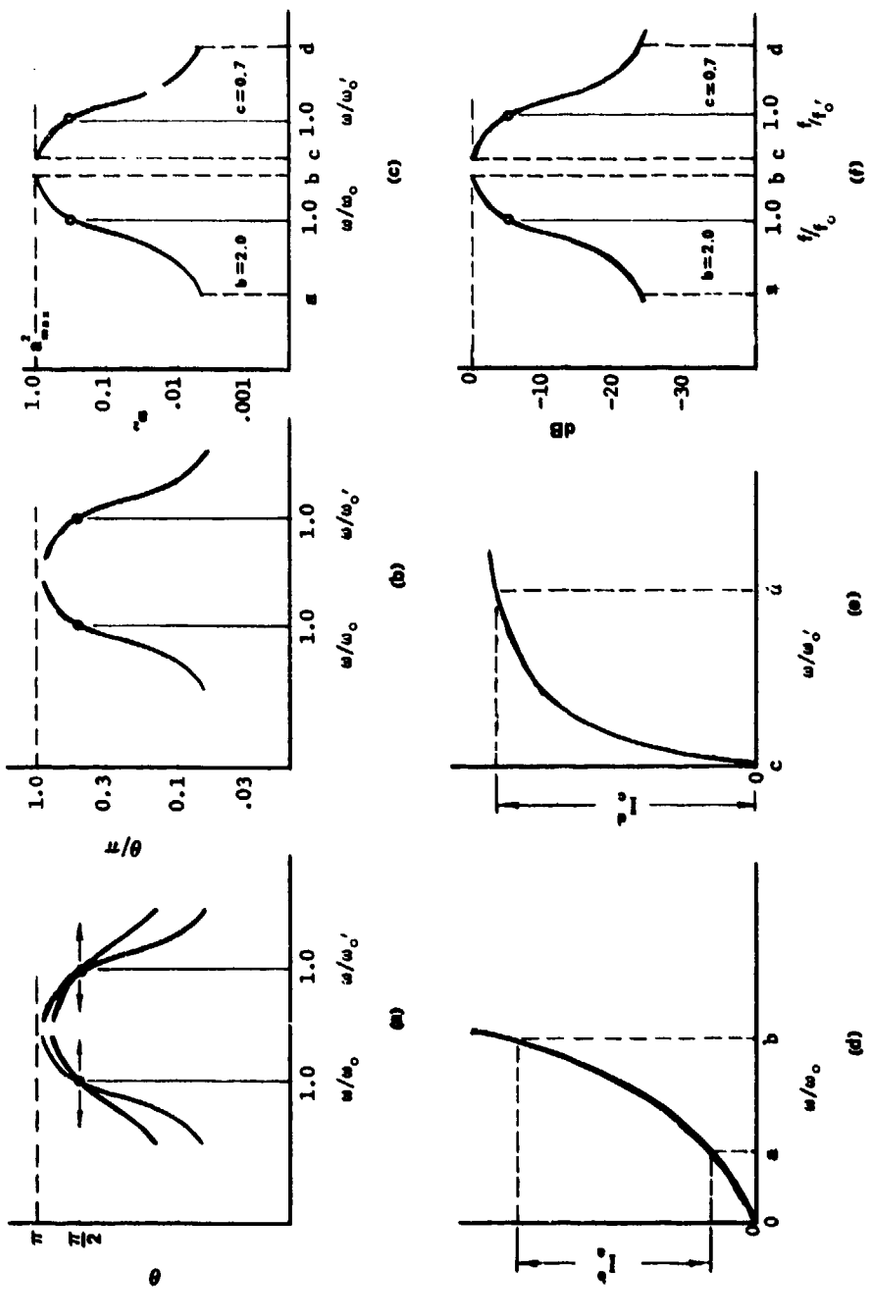

Figure 10. Synthesis of the Flux-Function

Normalization of the curve is desirable for general use:

$$\frac{\theta}{\pi} = \frac{\arctan A}{\pi} \tag{3}$$

$$\frac{\theta}{\pi} = \frac{\pi - \arctan A}{\pi} \tag{4}$$

The curves to Equations 3 and 4 are shown in Figure 10(b).

a. Further Adjustments

However, there remains an objection to the curve in this form owing to the asymptotic properties of the function. That is, $\theta \rightarrow \pi$ as $\omega/\omega_o \rightarrow \infty$. To terminate the curve at the top we need to readjust the vertical axis somewhat to obtain a convergent expression at some finite, real value of ω/ω_o. We can do this utilizing normalization techniques, as follows:

$$\frac{\theta}{\theta_{2.0}} = \frac{\arctan A}{\theta_{2.0}} \tag{5}$$

where

$$\theta_{2.0} = \arctan \frac{2\beta\, \omega/\omega_o}{1-(\omega/\omega_o)^2} \quad @\ \omega/\omega_o = 2.0$$

Here, ω/ω_o is chosen to provide a good shape approximation to the vibration characteristics, usually a ratio between two and three will provide a suitable fit for our needs. In this case, we have selected $\omega/\omega_o = 2.0$.

Now, let $\frac{\theta}{\theta_{2.0}} = Ka$ and substitute in Equation 5:

$$a = \frac{1}{K} \frac{\arctan A}{\theta_{2.0}} \tag{6}$$

where: $\frac{\arctan A}{\theta_{2.0}} = C$

a = vibration in acceleration units

We see that when $\omega = 2\ \omega_o$, then C = 1.0, and $a = a_{max}$. From inspection of Equation 6, $1/K = a_{max}$. If we substitute this into Equation 6 we have a generalized form for the independent variable, a.

$$a = a_{max} \frac{\arctan A}{\theta_{2.0}} \tag{7}$$

$$0 \leq \omega/\omega_o \leq 2.0$$

Next, we treat the high frequency rolloff curve in similar fashion noting that our frequency ratio directions are reversed, that is, as $\omega/\omega_o' \rightarrow 0$, $\theta \rightarrow \pi$ rads. From our familiarity with vibration high frequency rolloff characteristics we select $\omega/\omega_o' = 0.7$ as a reasonably good lower limit producing an acceptable fit. Note that the prime mark is used to identify the variables in the high frequency (rolloff) section.

Using the same approach as before we have:

$$a = a_{max} \left[\frac{\pi - \arctan A}{\theta_{.7}} \right] \tag{8}$$

$$0.7 \leq \omega/\omega_o'$$

A good deal of the time we will be concerned with mean squared values of the acceleration and the acceleration power spectral densities. Thus, Equations 7 and 8 may be squared as follows:

$$a^2 = a_{max}^2 \left[\frac{\arctan A}{\theta_{2.0}} \right]^2 \tag{9}$$

$$a^2 = a_{max}^2 \left[\frac{\pi - \arctan A}{\theta_{.7}} \right]^2 \tag{10}$$

The squared curves are shown in Figure 10(c). When using power spectral densities we will also be concerned with overall mean squared acceleration, thus the integrals of Equations 9 and 10 appear as follows:

$$I_a^b = a_{max}^2 \int_a^b \left[\frac{\arctan A}{\theta_{2.0}}\right]^2 d(\omega/\omega_o) \qquad (11)$$

$$I_c^d = a_{max}^2 \int_c^d \left[\frac{\pi - \arctan A}{\theta_{0.7}}\right]^2 d(\omega/\omega_o) \qquad (12)$$

Figures 10(d) and (e) show the integrals of the low and high frequency curves, respectively. Finally, since most of the time we will use the log of the independent variable a^2 (referenced to a_{max}^2) we present Equations 9 and 10 as follows.

$$dB = 10 \log_{10} \left[\frac{\arctan A}{\theta_{2.0}}\right]^2 \qquad (13)$$

$$dB = 10 \log_{10} \left[\frac{\pi - \arctan A}{\theta_{2.0}}\right]^2 \qquad (14)$$

where:

$$a^2 = a_{max}^2 \text{ @ zero dB}$$

Also, since we will be using hertz for the frequency variable, we substitute f in lieu of ω. The final set of curves are shown in Figure 10(f).

3. SYNTHESIS OF THE VIBRATION PREDICTION SURFACE

Our task is now to use the foregoing expressions, and variations of them, to produce a three dimensional surface sufficiently plastic to conform well with our plotted data as seen in Figures 5 through 8. If we recall the concluding notes of Section I ... the differentiation of

a proposed gunfire envelope into three elements; sinusoidal, low frequency random, and high frequency random, then we begin the synthesis with the sinusoidal surface. It is seen as a generalized surface, Figure 11(a), and appears in more detailed break down as Figure 11(b).

The surface is represented by the following function:

$$\frac{G_s}{G_{smax}} = \left[\frac{\theta}{\theta_{2.0}}\right]^2 \quad G_D/G_{Dmax} \tag{15}$$

where:

G_s = mean squared g (sine) of the surface

G_{smax} = value of G_s @ $f/f_o = 2.0$

$\theta = \frac{\arctan A}{\pi}$, $0 \leq f/f_o \leq 2.0$

$\theta_{2.0} = \frac{\arctan A}{\pi}$, $f/f_o = 2.0$

G_D = value of G_s in the amplitude-distance plane

G_{Dmax} = value of G_D @ $D/D_o = 0$

Before proceeding further with the surface it is necessary to introduce some variations on an arctan theme. We have seen that the arctan form as previously used provides good shaping for the usual vibration fields of aircraft primary structure but for gunfire induced structural response the curve is too far down in the low frequency end. This is not surprising since the Fourier spectrum of the blast pressure pulse converges to a maximum value at the basic gunfire rate (which corresponds to the low frequency end of the arctan function) and, in consequence, the structural response in this region is noticeably higher.

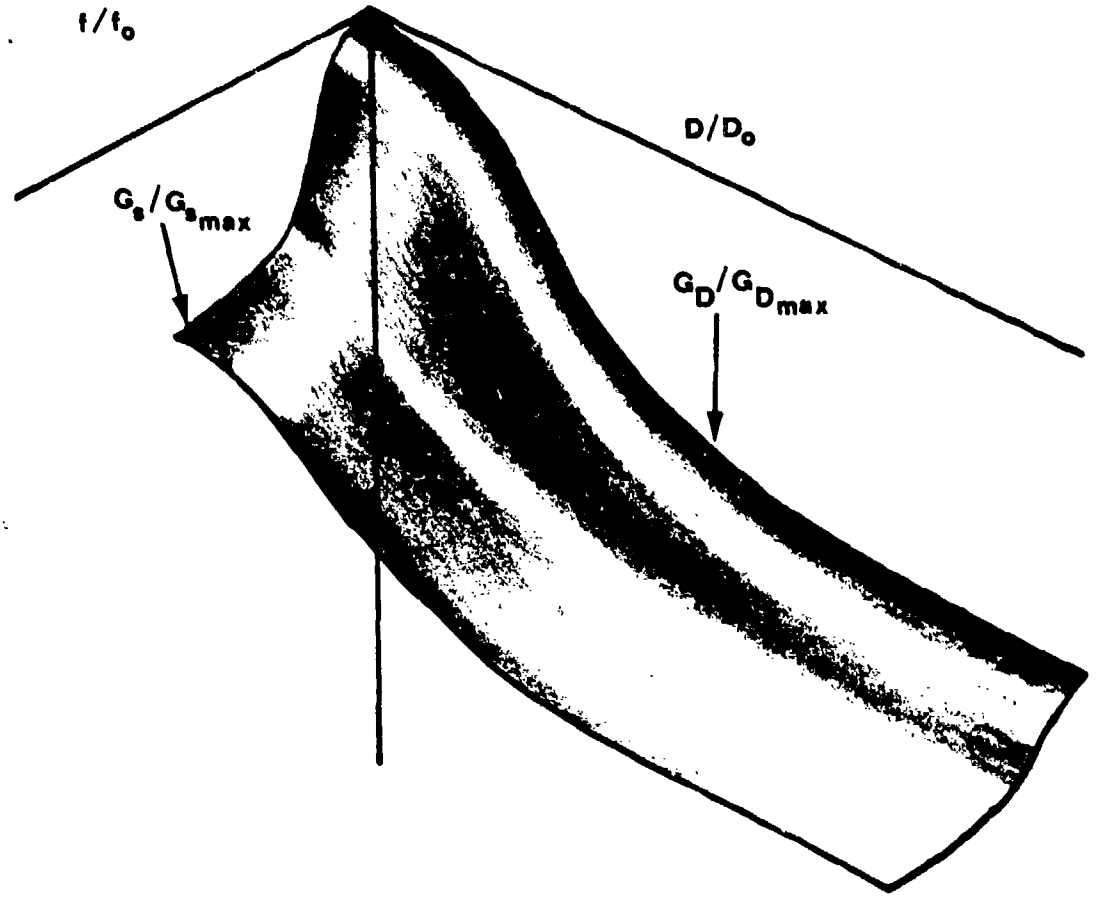

Figure 11(a). Generalized Gunfire Vibration Surface (Sinusoidal)

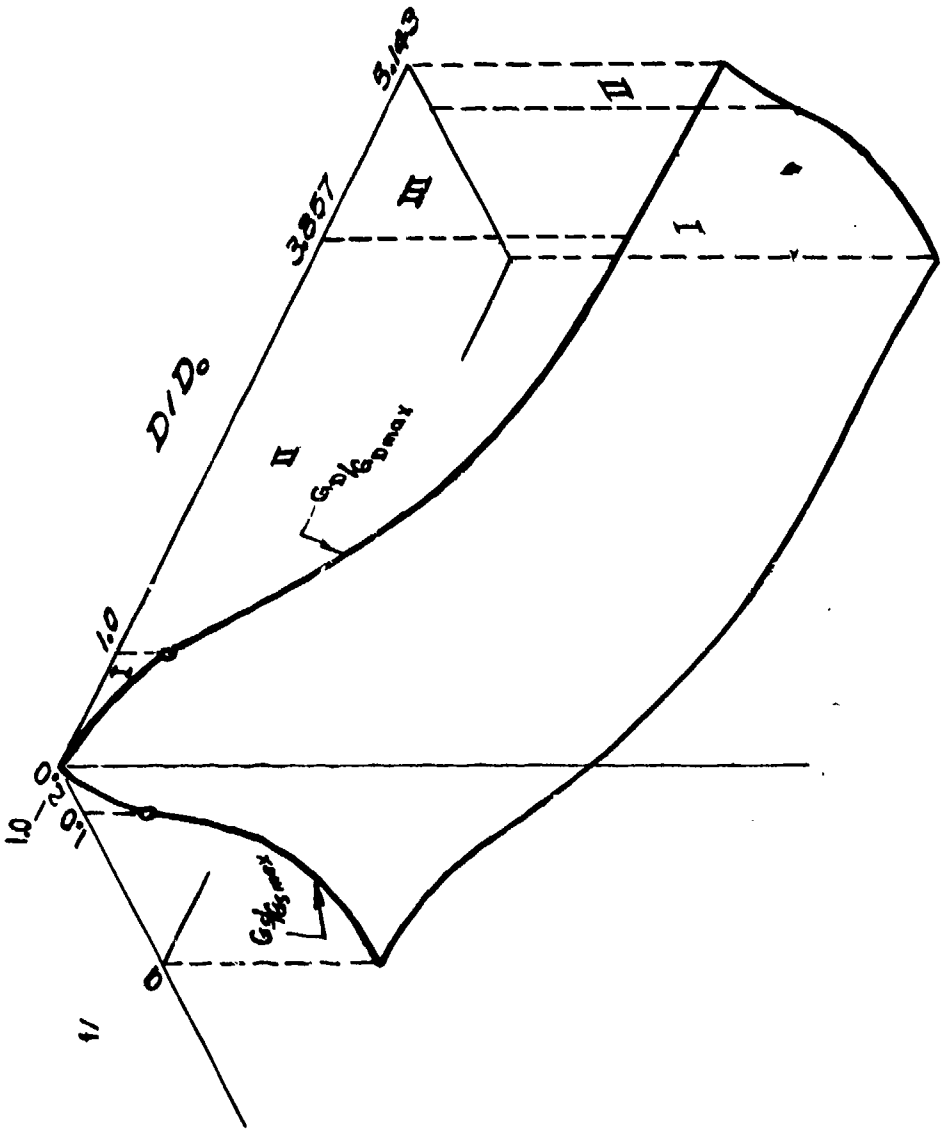

Figure 11(b). Generalized Gunfire Vibration Surface (Sinusoidal)

We can overcome this difficulty by dividing the arctan into two parts thus:

PART I

$$\text{let } \arctan A = \arctan \frac{2\beta_f}{1-(f/f_o)^2}$$

$$\text{for } f/f_o \leq 1.0$$

PART II

$$\text{let } \arctan A = \arctan \frac{2\beta_f \, f/f_o}{1-(f/f_o)^2}$$

$$\text{for } 1.0 \leq f/f_o \leq 2.0$$

We see that Part I differs from Part II only by the absence of the (f/f_o) term in the numerator. This results in about 6 dB of low frequency emphasis-just about what we require. A further bonus evolves from the variations: both first derivatives (with respect to f/f_o) converge to each other and are equal at $f/f_o = 1$, thus presenting us with a smooth, continuous function throughout the transition.

a. The Distance Function, G_D

We look into the magnitude-distance (D) plane (Figure 11b) and imagine a function that has a maximum value of one at D = 0; decreasing as a function of D. Here again, the arctan form proves effective but to get good conformity with the data surface we shall once again have to introduce some variations, in fact, four of them.

First, we set up the general equation:

$$\frac{G_D}{G_{max}} = \left[\frac{\theta_D}{\pi}\right]^2 \qquad (16)$$

Then, we define $\left[\frac{\theta_D}{\pi}\right]^2$ in three parts:

PART I

$$\theta_D = 1 - \frac{1}{\pi} \arctan \frac{2\beta_D \, D/D_o}{1-(D/D_o)^2} \qquad (17)$$

$$\text{for } 0 \leq D/D_o < 1.0$$

where:

D = vector distance from a point on the aircraft primary structure to the gun muzzle (inches)

D_o = locator distance (inches)

β_D = slope factor

PART II

$$\theta_D = 1 - \frac{1}{\pi} \arctan \frac{2\,\beta_D}{1-(D/D_o)^n} \qquad (18)$$

$$\text{for } 1.0 \leq D/D_o \leq 3.857$$

where:

$n = 1.534-0.167\ D/D_o$

PART III

$$\theta_D = \frac{0.3175-0.017\ D/D_o}{\pi} \qquad (19)$$

$$\text{for } 3.857 \leq D/D_o \leq 5.143$$

Part III is a simple linear function with a negative slope that enters into the scheme because Part II rises very slightly at values of $n > 2$.

In retrospect, we probably would have fared better, at least more simply, by programming $\beta_D = f(D/D_o)$, perhaps beginning back at Part II, to compensate for the slight rise.

One final variation which emphasizes the flexibility of this function arises from the well known observation that the rate of vibration amplitude decay (vs distance from the source) is also frequency dependent. Stated another way: the high frequencies decay (vs D) more than the low frequencies.

If we let $\beta_f = g(D)$ and program the function to take the form of Figure 12 we have a resultant variation of the arctan that has the effect of rotating the surface, G_s, clockwise about G_{Dmax} as D/D_o increases. This results in a warped surface whose low frequency area is being lifted at a greater rate than the high frequency portion of the surface; thereby giving us the desired frequency selective property. We shall make further use of this innovation when we consider the high frequency random surface.

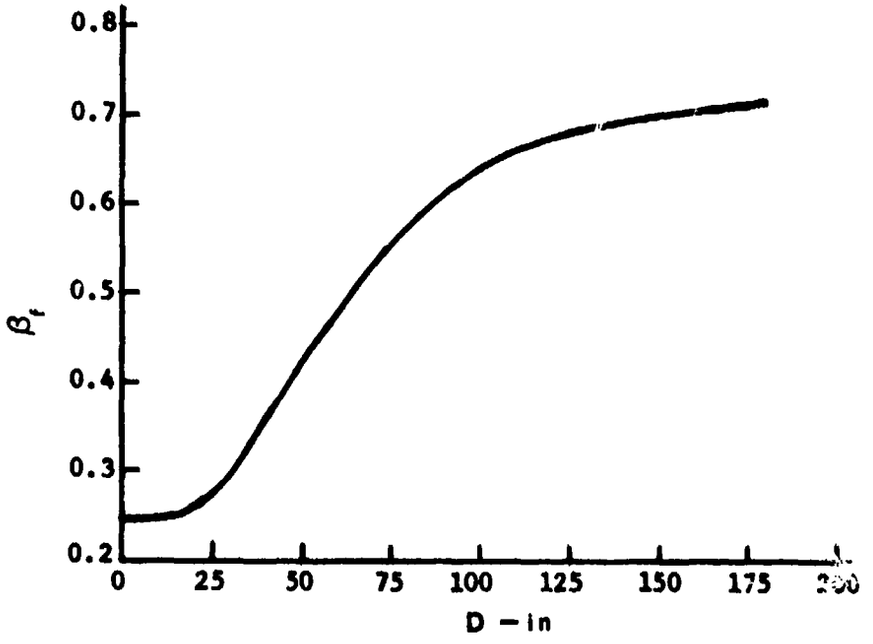

Figure 12. The Slope Parameter, β_f, as a function of Distance, D

To summarize, we have constructed a surface, in the main, using the arctan form and its variations to provide us with a flexible cover by which we now propose to conform a mantle for the data surfaces of Figures 5 and 6.

4. FITTING THE SURFACE TO THE DATA

a. Low Frequency Sinusoidal Surface

The equations, cumbersome in normal engineering practice, become tractable when inserted into a digital computer. The variables and parameters are adjusted and a calcomp plotter produces curves (scaled to Figures 5 and 6) such that we can place each new surface over the data (Figures 13 and 14). Visually, we obtain a best fit that envelops about 90% of the data points. This process yields averaged surface parameters derived from A-7D and F-4E data, that are summarized as follows:

G_{smax} = 2000 g^2 = 0 dB = Γ_s of Equation 1

β_f = see Figure 12

f_o = 250 Hz

β_D = 0.3

D_o = 35 inches

Having done this, it is only necessary to graduate the three axes of the surface with the proper scalars and it, when conjoined with gunfire Equation 1, provides a general prediction surface for the low frequency sines. The surface is seen as Figure 15 and reappears in Appendix A as part of the new gunfire specification, Method 519.2, MIL-STD-810(C).

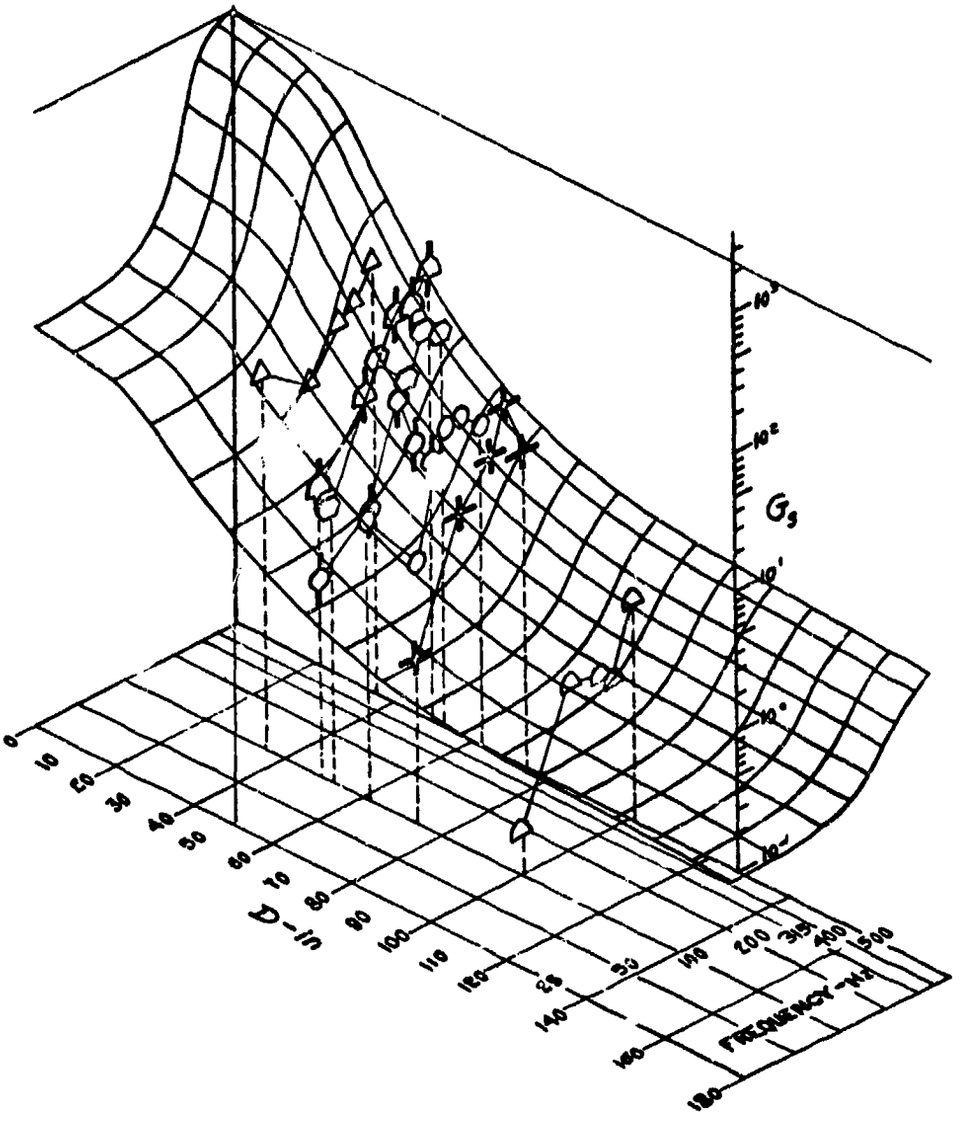

Figure 13. Prediction Surface Fitted to the A-7D Data (Sinusoidal)

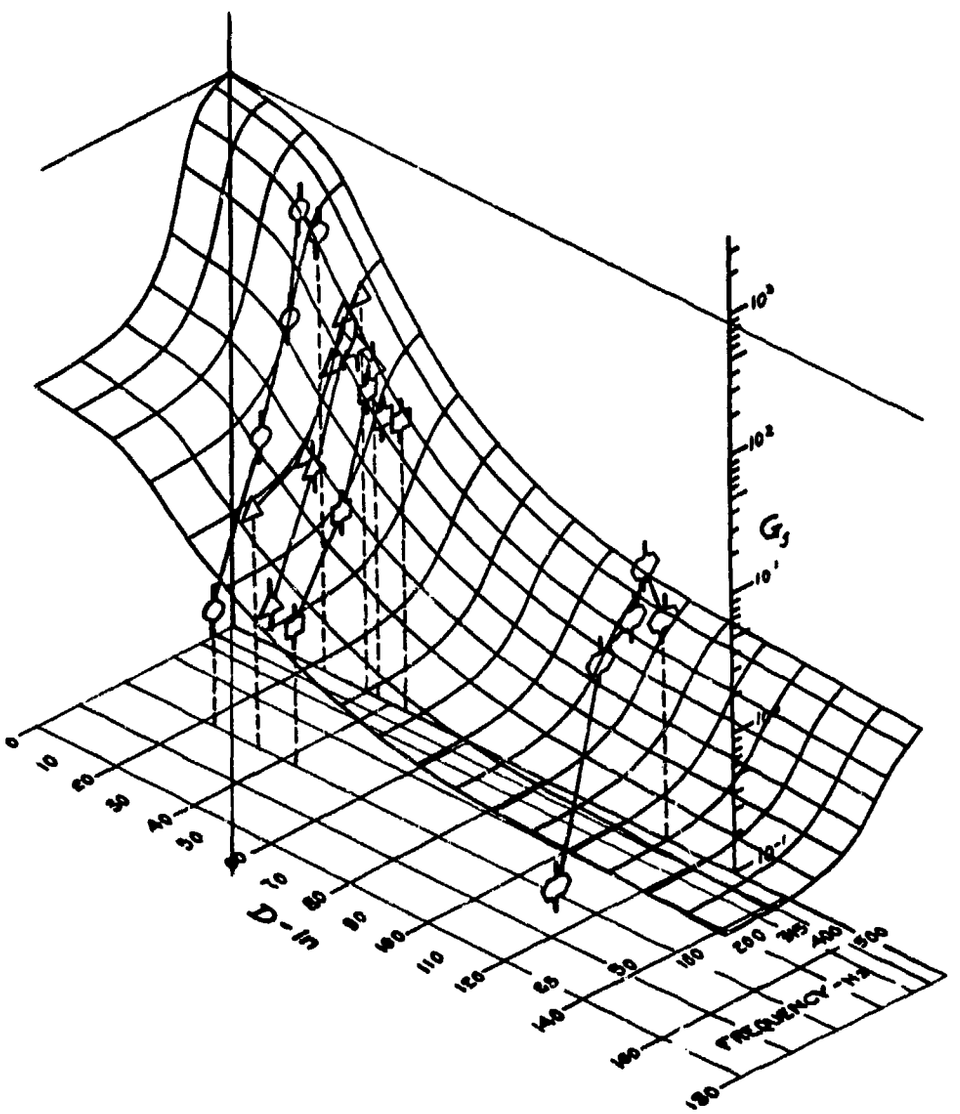

Figure 14. Prediction Surface Fitted to the F-4E Data (Sinusoidal)

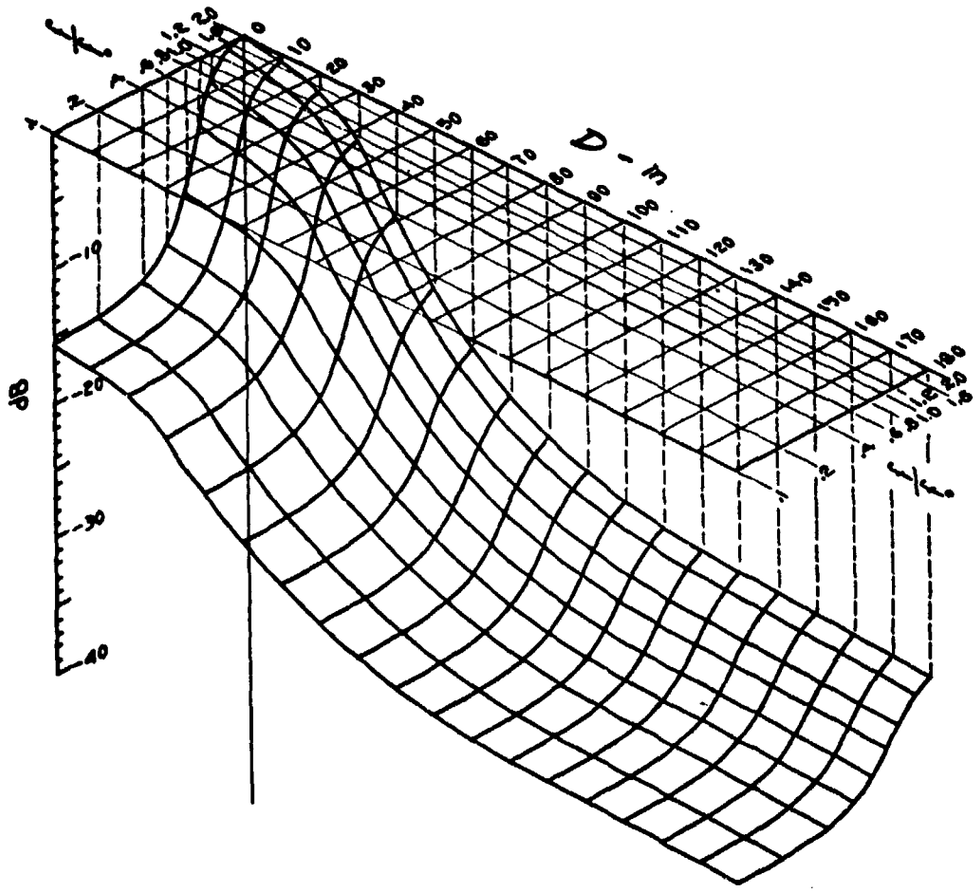

Figure 15. Final Gunfire Prediction Surface (Sinusoidal)

b. High Frequency Random Surface

We treat the high frequency random surface in similar fashion. Figures 16a and 16b show a surface described by the following general function:

$$G_r/G_{rmax} = \left[\frac{\theta}{\theta_{.7}}\right]^2 G_D/G_{Dmax} \tag{20}$$

where:

G_r = accel. power spectral density (g^2/H_z)

G_{rmax} = value of G_r at $f/f_{o'}$ = 0.7

$\theta = \pi - \arctan A, \; 0.7 \leq f/f_{o'}$ (21)

$\theta_{.7} = \pi - \arctan A, \; @ \; f/f_{o'} = 0.7$

$$A = \frac{2\beta_{f'} \, f/f_{o'}}{1-(f/f_{o'})^2}$$

$\beta_{f'} = g(D)$

$D_o = h(f)$

β_D = constant

G_D = same as sine surface

As was done with β_f earlier, $\beta_{f'}$ is cast in similar functional form and is shown as Figure 17. A further variation is inserted by making D_o a function of frequency as shown in Figure 18.

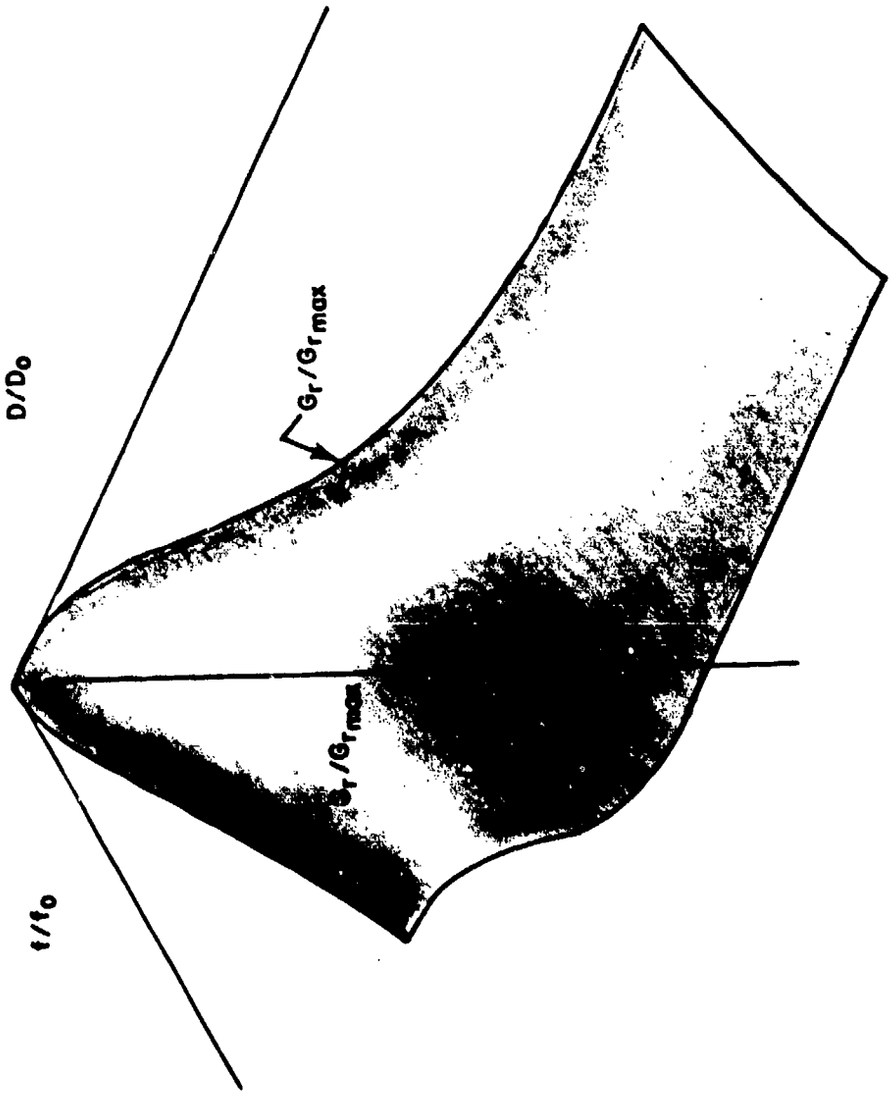

Figure 16(a). Generalized Gunfire (High Frequency Random)

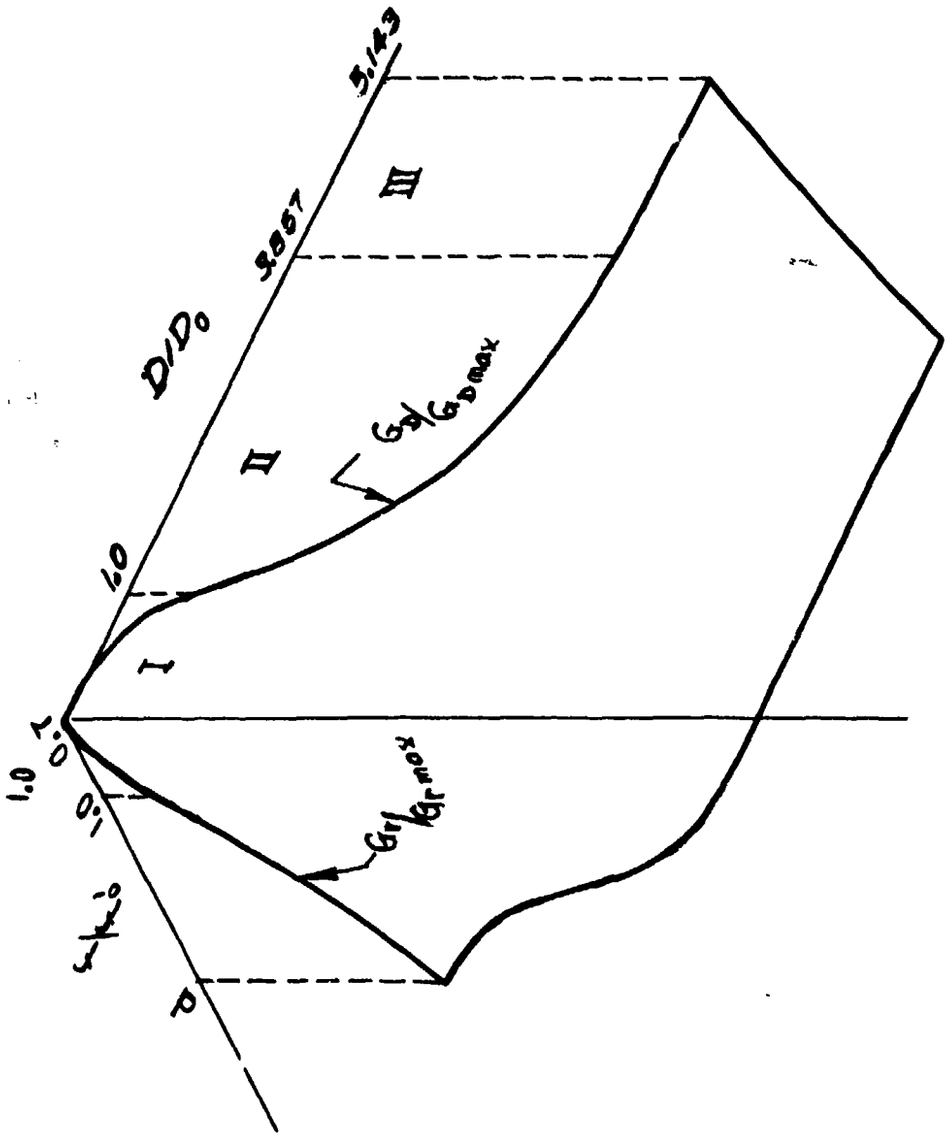

Figure 16(b). Generalized Gunfire (High Frequency Random)

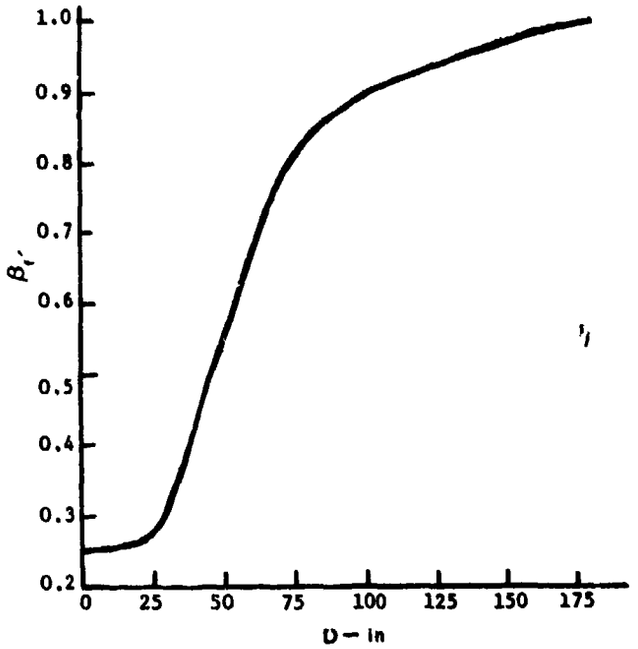

Figure 17. The Slope Parameter, β_f', as a Function of Distance, D

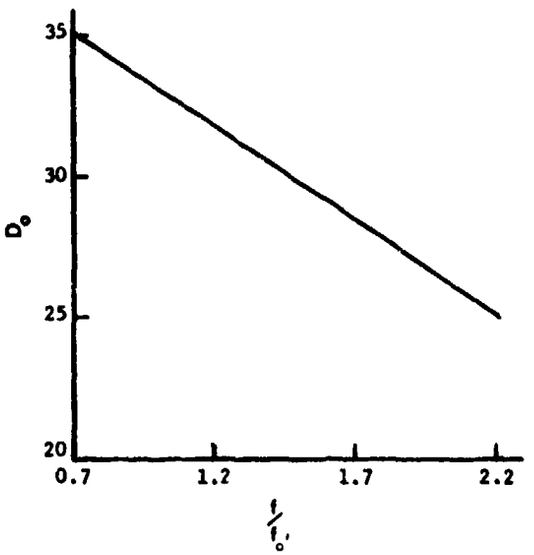

Figure 18. The Distance Locator, D_o, as a Function of Distance D

After a number of fitting trials the final constants and variables were selected. The envelopes are shown in Figures 19 and 20 and the appropriate values are listed as follows:

G_{rmax} = 35 g^2/Hz = 0 dB = Γ_r of Equation 2

β_f = see Figure 17

$f_{o'}$ = 900 Hz

β_D = 0.20

D_o = see Figure 18

The high frequency random surface is scaled. G_{rmax} is related to the gunfire prediction equation (see Equation 2, Section II). The surface is shown as Figure 21 and it, too, is included in Appendix A.

c. Low Frequency Random Surface

The low frequency random surface is of secondary importance; it simply provides a random background signal for the sine surface. G_{rmax} for the surface is keyed to that of the high frequency random surface and is, therefore, 35 g^2/Hz. All other properties are the same as those of the sine surface excepting for f_o which is set at 300 Hz and the function β_f; which is down shifted 60%. Both changes are introduced to produce a sharp, low frequency random rolloff..

Finally, the surface is shown with scalar values (Figure 22) and the surface is also entered in Appendix A.

5. SUMMARY

Several comments are appropriate before we enter Section IV to describe the development of a combination sine and random test technique.

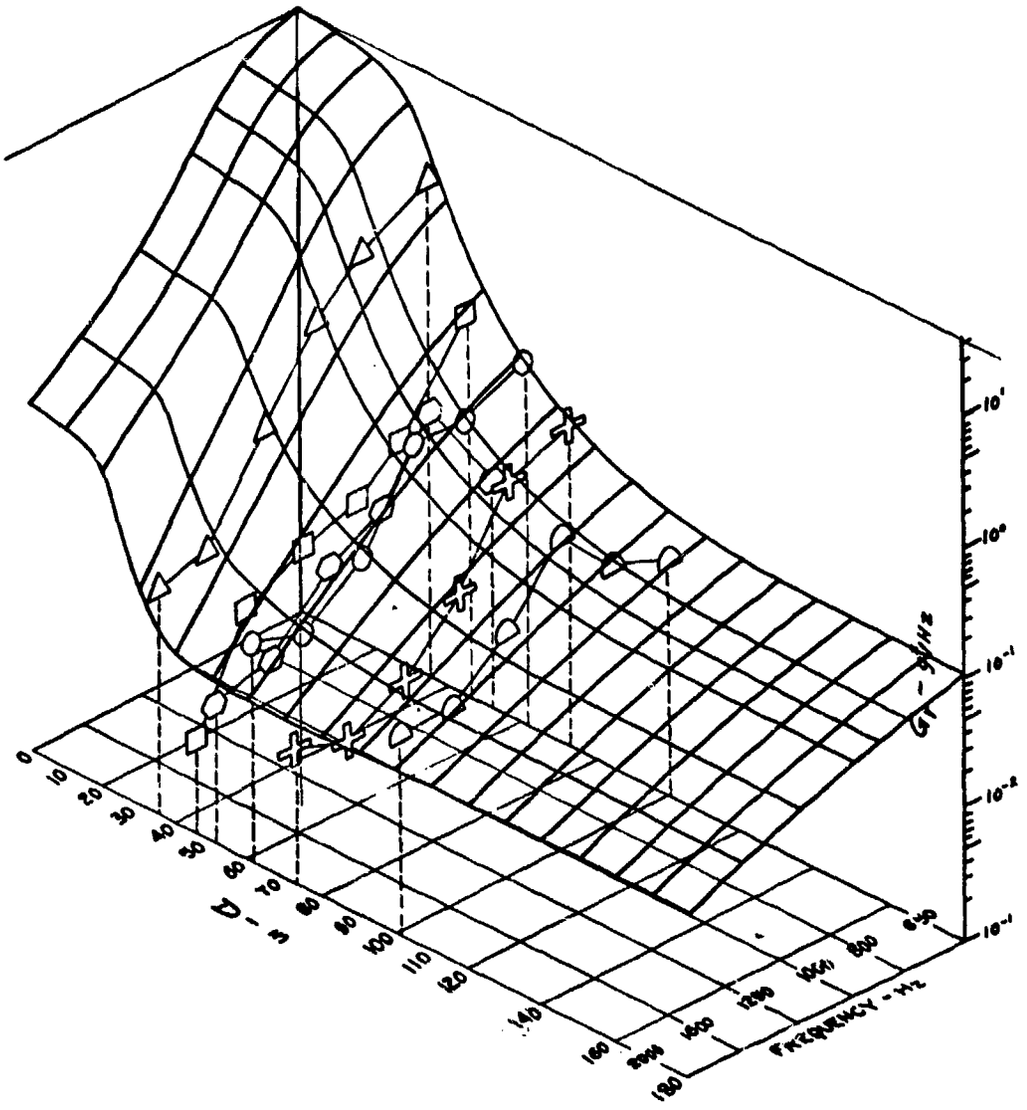

Figure 19. Prediction Surface Fitted to A-7D Data (Random)

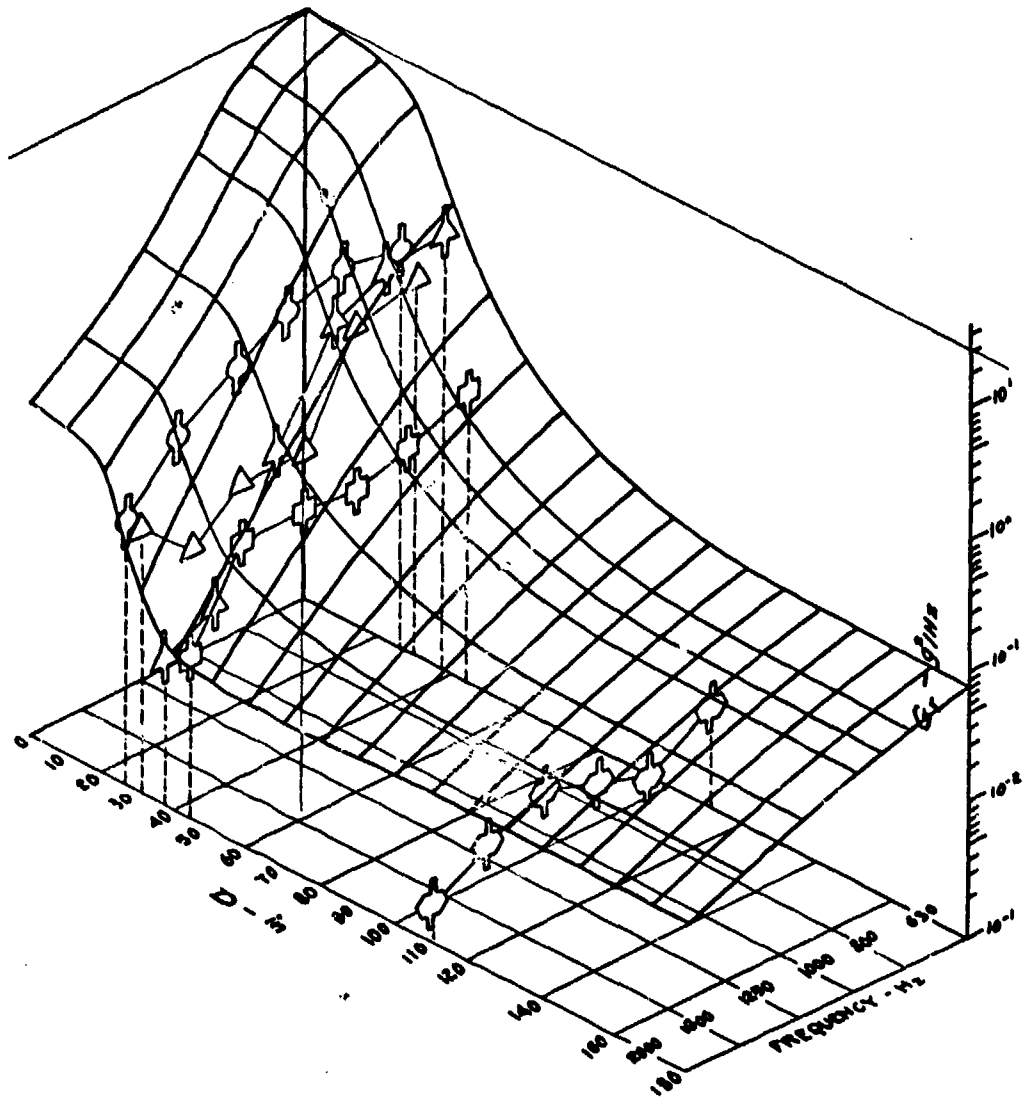

Figure 20. Prediction Surface Fitted to F-4E Data (Random)

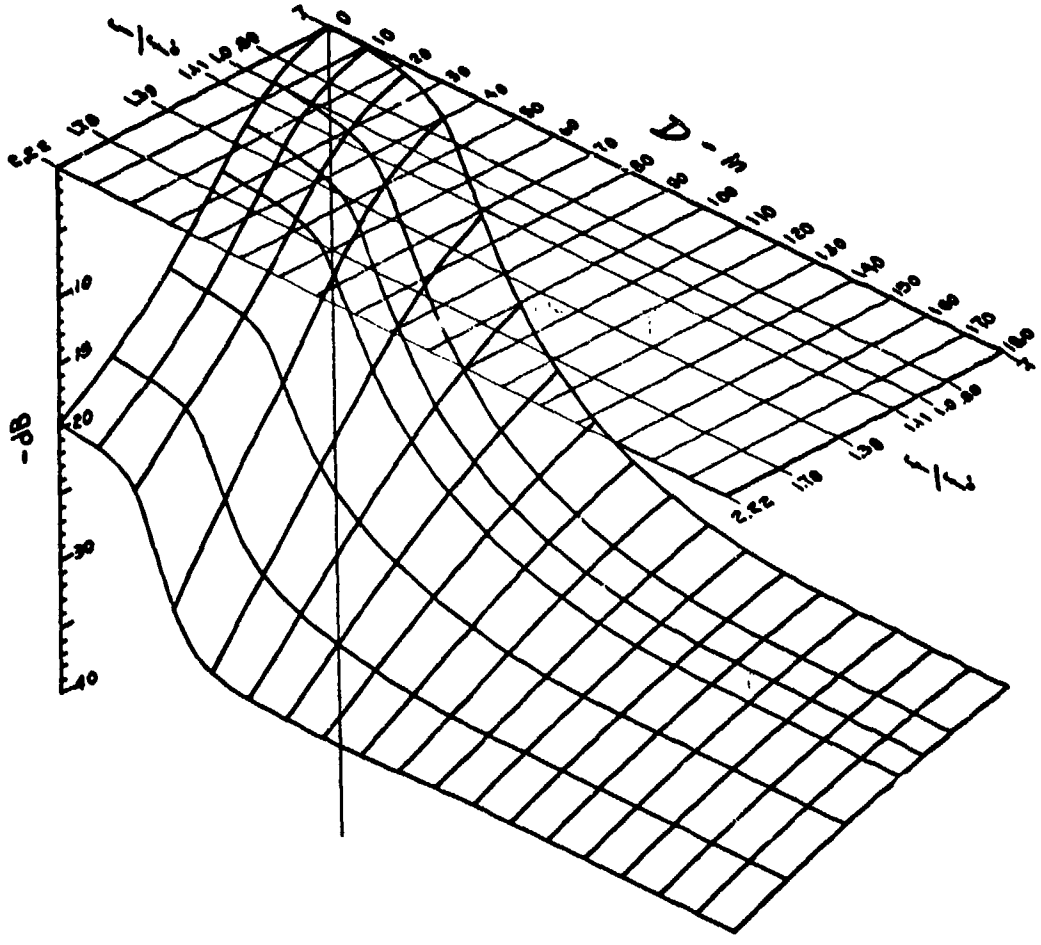

Figure 21. Final Gunfire Prediction Surface (High Frequency Random)

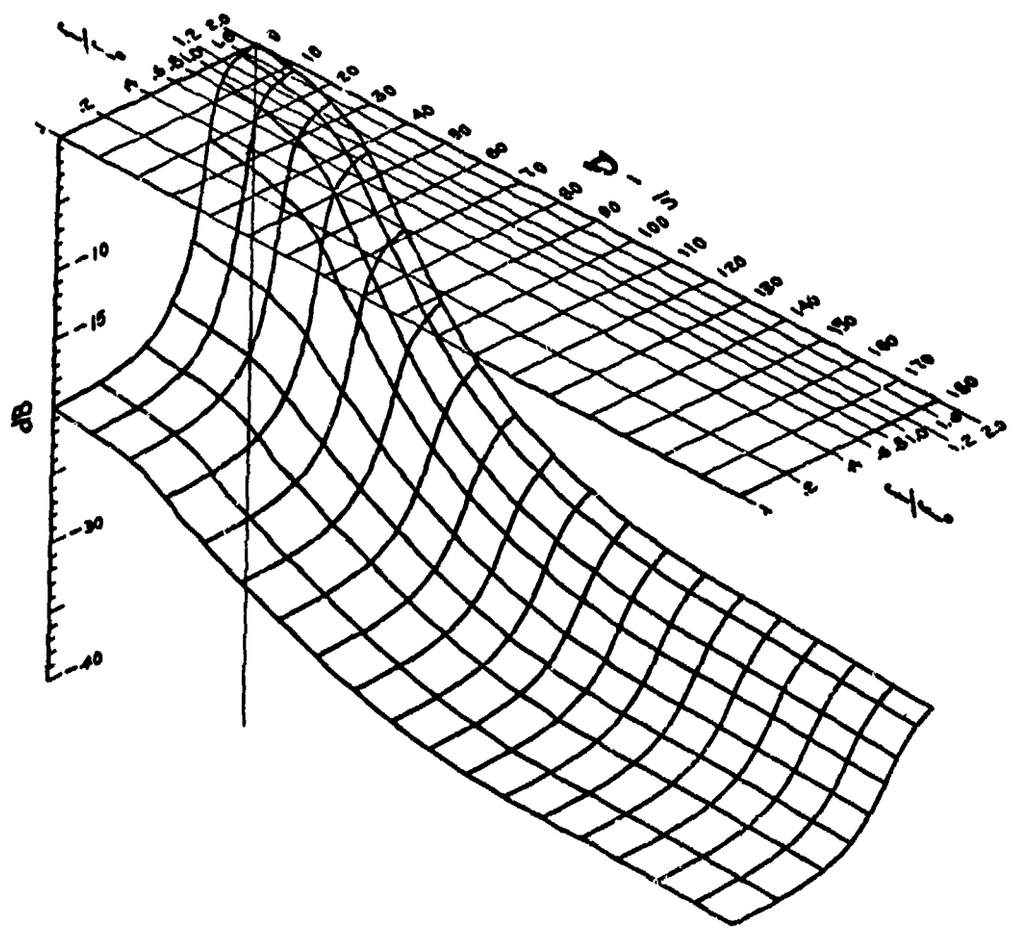

Figure 22. Final Gunfire Prediction Surface (Low Frequency Random)

It would be advantageous to assemble a computer program such that when key envelope parameters and initial locator estimates are inserted into the computer (along with the vibration data) a best fit surface is generated. This approach would require a utilization of three dimensional statistics and regresssion techniques. Very likely, a number of trial insertions would be required and the number of routines, not to mention subroutines, might turn out to be formidable; nonetheless the possible gains are sufficiently promising to warrant investigation. In conclusion, the versatility of this function has been demonstrated; its great flexibility allows surface modulations as well as surface deformations combined with translations and attenuations--all interacting in such a way as to provide an envelope that can almost be said to have been sculptured. It is for this reason that we term it the flex function.

As noted, the next section is concerned with the development of relatively economic control means by which four swept, sinusoids may be superimposed on a random background. Figure 23 shows a typical test spectrum that we have chosen to simulate. What we wish to do is to approximate the spectrum on our 80 channel shaker system and then determine how close and within what limits we can maintain control of that spectrum.

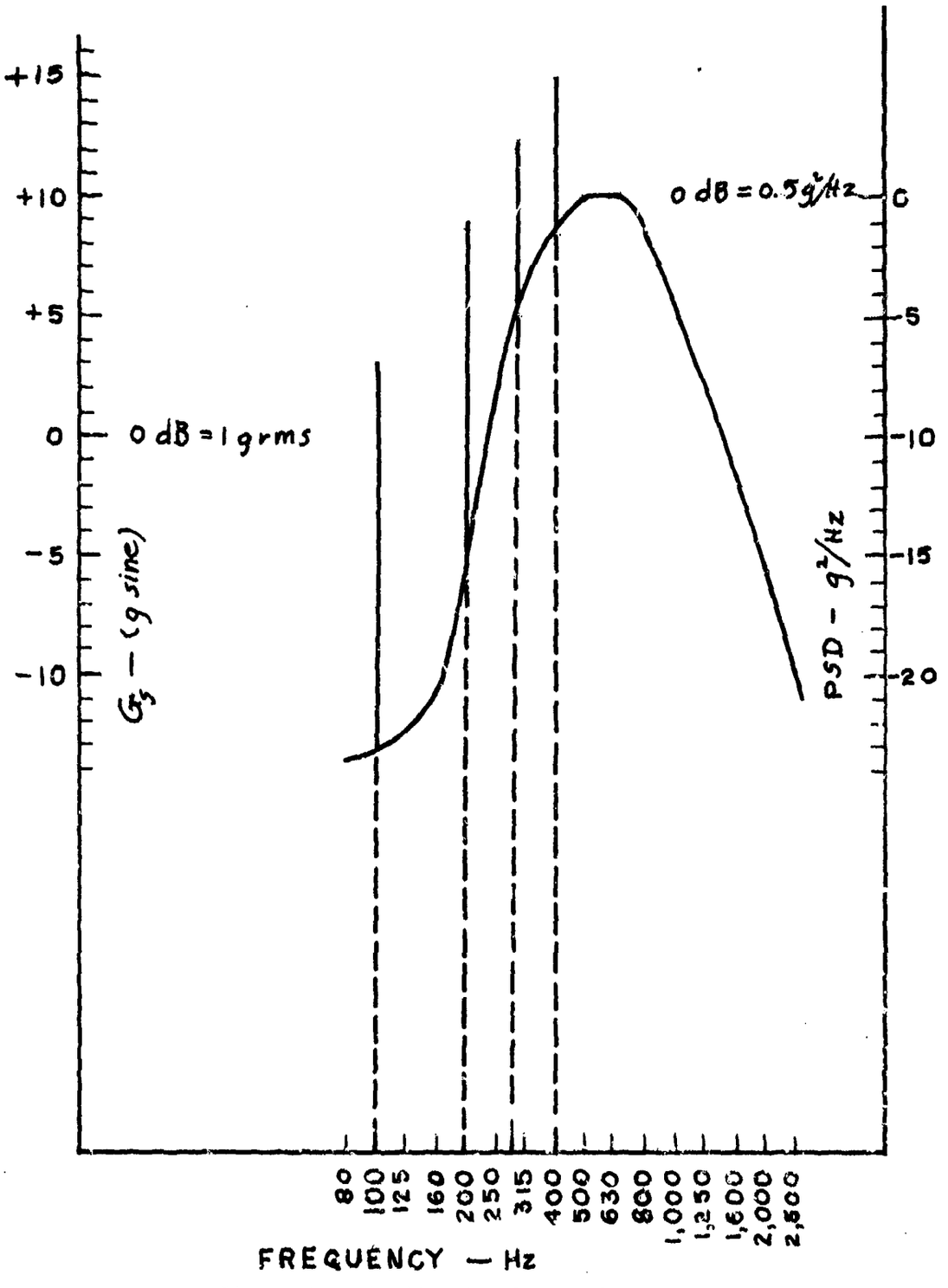

Figure 23. Gunfire Simulation Spectrum

SECTION IV

TEST METHOD DEVELOPMENT

1. SYSTEM DESCRIPTION

How does one superimpose swept sinusoids, including programmed amplitude versus frequency properties, on a broadband random background? That is, how does one do so without incurring considerable equipment expense and circuit complexity? We suspect that we can do this if four individual servo systems are paired-off with a corresponding set of tracking filters as shown in Figure 24 but the cost, equipment-wise, is sobering.

a. Instrumentation

We undertook to study this problem and after several unsuccessful approaches evolved a technique which is at least suitable for the necessity that occasions it. We found that by plugging two operators into the loop, a loop which includes controlling, switching, and monitoring circuitry, we could control, monitor, and record all four sinusoids with; four voltage controlled generators, two tracking filters, two log converters, X-Y recorders, and several inexpensive black boxes consisting of potentiometers, a motor, switches, and other itinerant components assembled from the junk parts bin. For our application, the system was integrated into an MB T589 Random System. The configuration is essentially compatible with other analog random systems. Even though several circuit modifications of the T589 were required, all changes were reasonably straight forward, involving only moderate complexity and minor expense. In fact, the modifications themselves provide advantages or improvements for applications other than those specifically sought for in this experiment. Appendix C contains the details of these circuit changes together with a discussion of their purpose, use, and advantages.

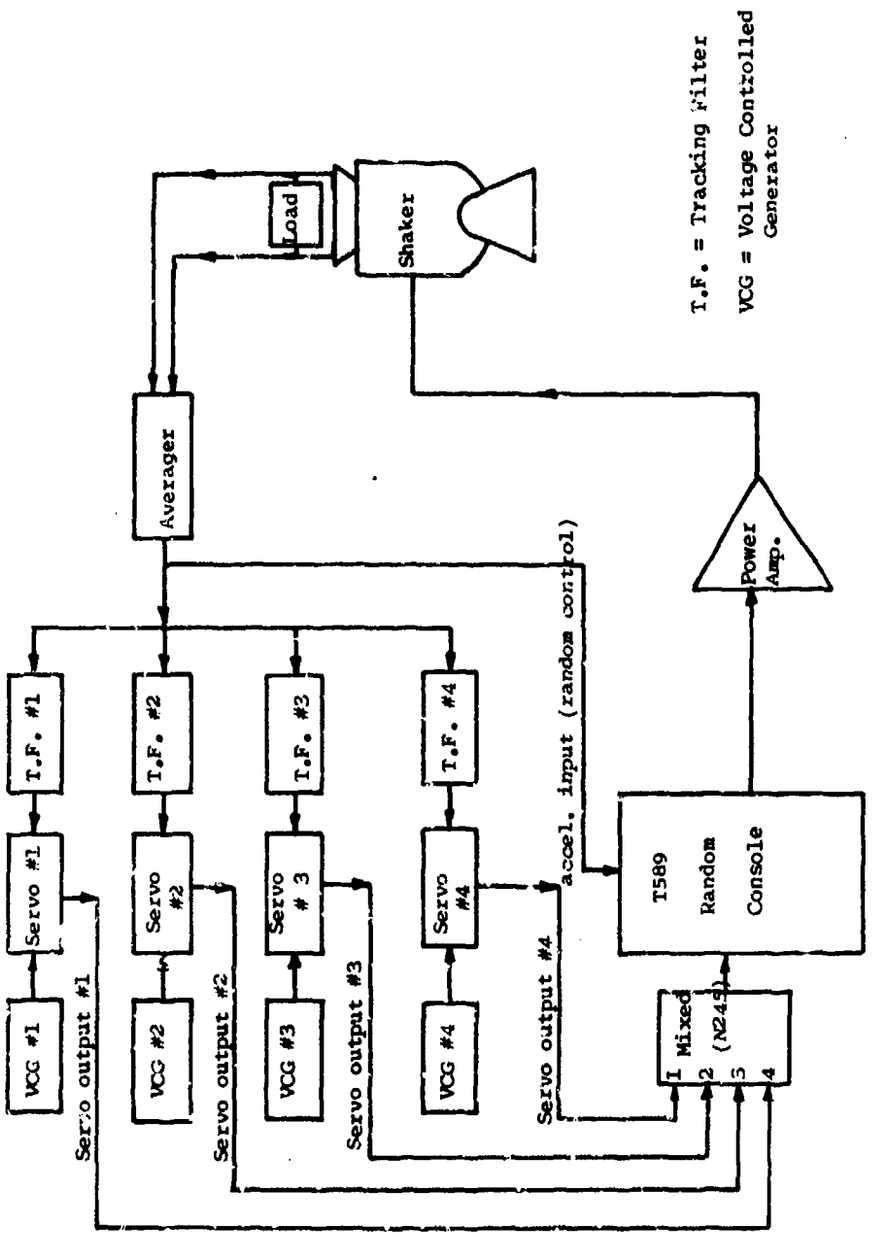

Figure 24. Simulation Spectrum Using Four Servos

b. System Function

The heart of the sinusoidal system resides in the primary unit called the Control Console. Figure 25 shows a somewhat simplified schematic in order to better illustrate the circuit operation. Swept sinusoidal inputs to the console are provided by two voltage controlled generators, hereafter referred to as VCG's one and two. The first VCG is set at a basic gunfire rate, say f_1 = 100 H_z (6000 rpm) and VCG_2 is set at the first harmonic, f_2, or 200 Hz. The VCG signal outputs enter the console, pass through control potentiometers P-1 and P-2, leave the console and enter the random console mixer (MB, N245) at inputs one and two. This mixer unit, excepting the demodulator circuitry employed, may be considered typical and serves to combine signals at f_1 and f_2 with the random noise part of the spectrum. The summed signal, after having passed through the master gain circuitry, then enters the power amplifier and drives the shaker.

The monitor accelerometer signal passes through a tracking filter (T.F.) whose band pass center frequency is either f_1 or f_2 (achieved through switching means to be described shortly). The filtered output signal is rectified and appears as a DC filtered signal output (FSO_{DC}) which, after passing through a log converter, terminates at the Y axis of an X-Y recorder.

At a given switch position (position one or two), one of the VCG outputs is transferred through a section of the ganged two pole switch and enters the tuning signal input of the T.F. Simultaneously, the second section of a two pole switch transfers one leg of the cycling voltage (DC $\propto$ to f_1) to the X axis of the recorder. Briefly, the system works in this manner: with the transfer switch in, say, position one the VCG_1 output is transferred to the tuning input of the T.F. and this shifts the T.F. band pass center frequency to f_1. Sequentially, the log FSO_{DC} drives the Y axis of the recorder to an ordinate position equal to the rms g level of f. At the same time, the DC $\propto f_1$ voltage, the voltage that originally establishes the VCG frequency f_1, is transferred through the second section of the selector switch to drive the X or horizontal axis to an abscissa value equal to f_1.

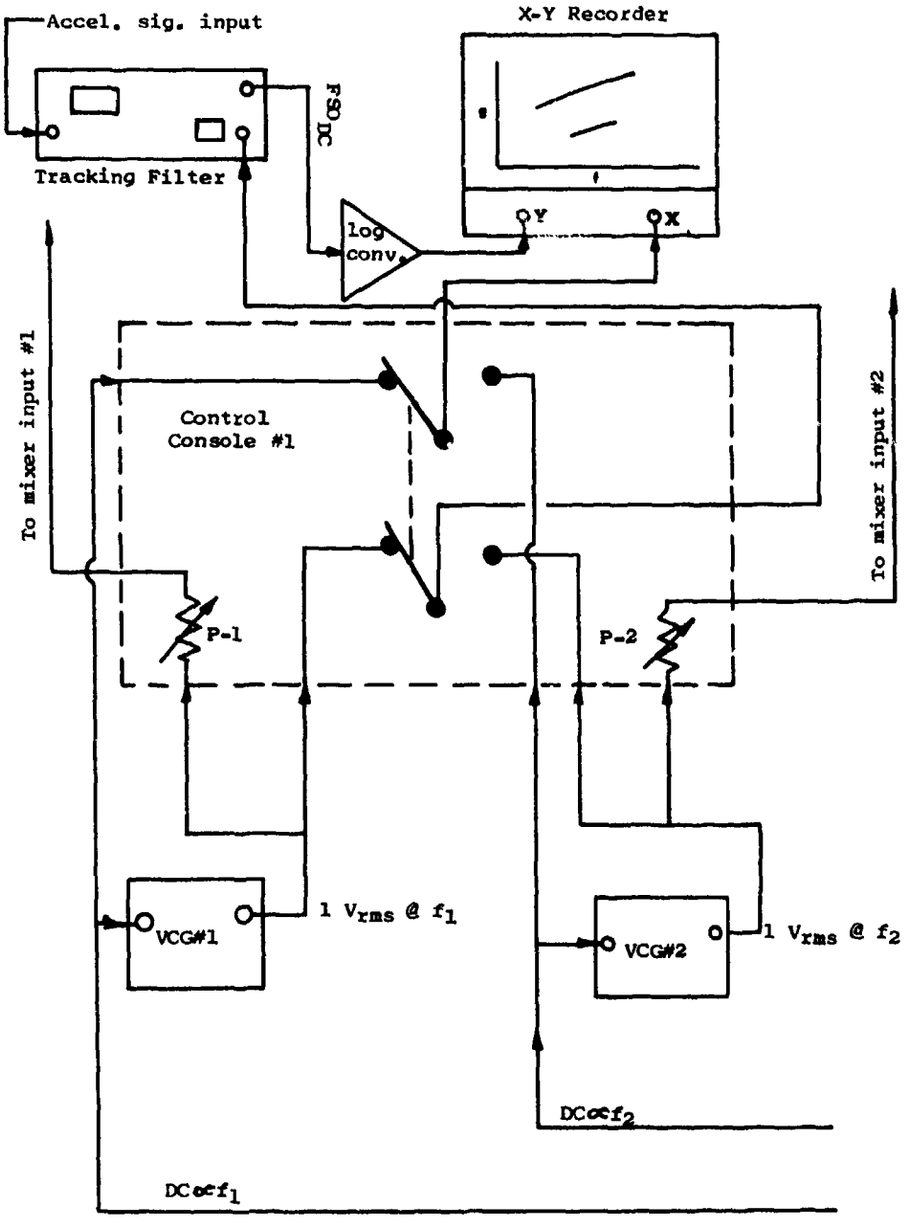

Figure 25. Control Console (Simplified Schematic)

Meanwhile, back at the console, the operator adjusts pot number one such that Y_1 remains within the tolerances of a test curve that has been pregraphed on the X-Y recorder paper. The operator presses a push button switch on the console to lower the recorder pen for a spot record.

In this manner, one operator alternately switching between positions one and two, monitors, adjusts, controls, and records the shaker output levels of f_1 and f_2. Now, if we duplicate the setup just described, call it console number two, we then have a configuration which allows two operators to accommodate four sinusoids (f_1, f_2, f_3, f_4). Sinusoids that are intended to represent the gunfire fundamental plus three harmonics. A third operator is utilized to monitor and occasionally adjust the random spectrum portion of the combined vibration. In practice, especially for the smaller and simpler test loads (approximately 25 pounds or less), the third operator is seldom required.

A flow diagram for the complete setup is shown in Figure 26 and the photos of Figure 27 show the two consoles, recorders, VCG's, and associated equipments. A detailed schematic of the complete sinusoidal system, together with a comprehensive discussion concerning circuit operation, setup procedures, and adjustments are contained in Appendices C and D.

c. Operational Notes

At this juncture, it is appropriate to pause and emphasize several factors that play a key role in the successful operation of this laboratory configuration.

First, the system works well provided that the cycling rate is low; low, that is, with respect to the system time constants and with respect to the rate of resonant response that obtains when the test item is swept, sinusoidally, over the cycling range. Here, the cycling range is defined in terms of the percent deviation of the gunfire rate about its mean or center value. The results of data obtained through Eglin AFB sources suggested that a deviation of $\pm$20% (for a 3 sigma confidence level) was suitable as an estimate for a 20mm cannon firing at a basic mean rate of 100 Hz.

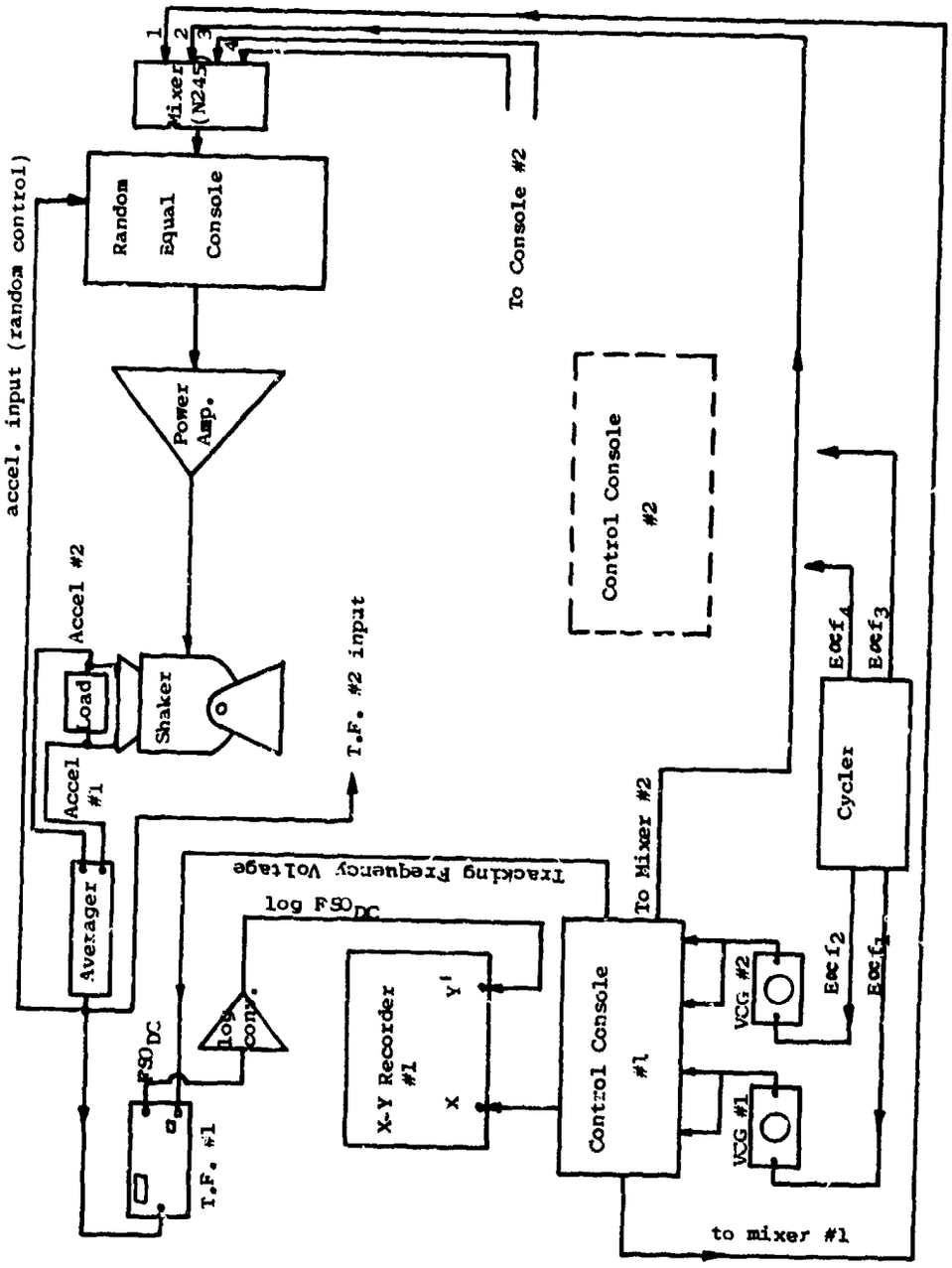

Figure 26. Block Diagram of Complete System

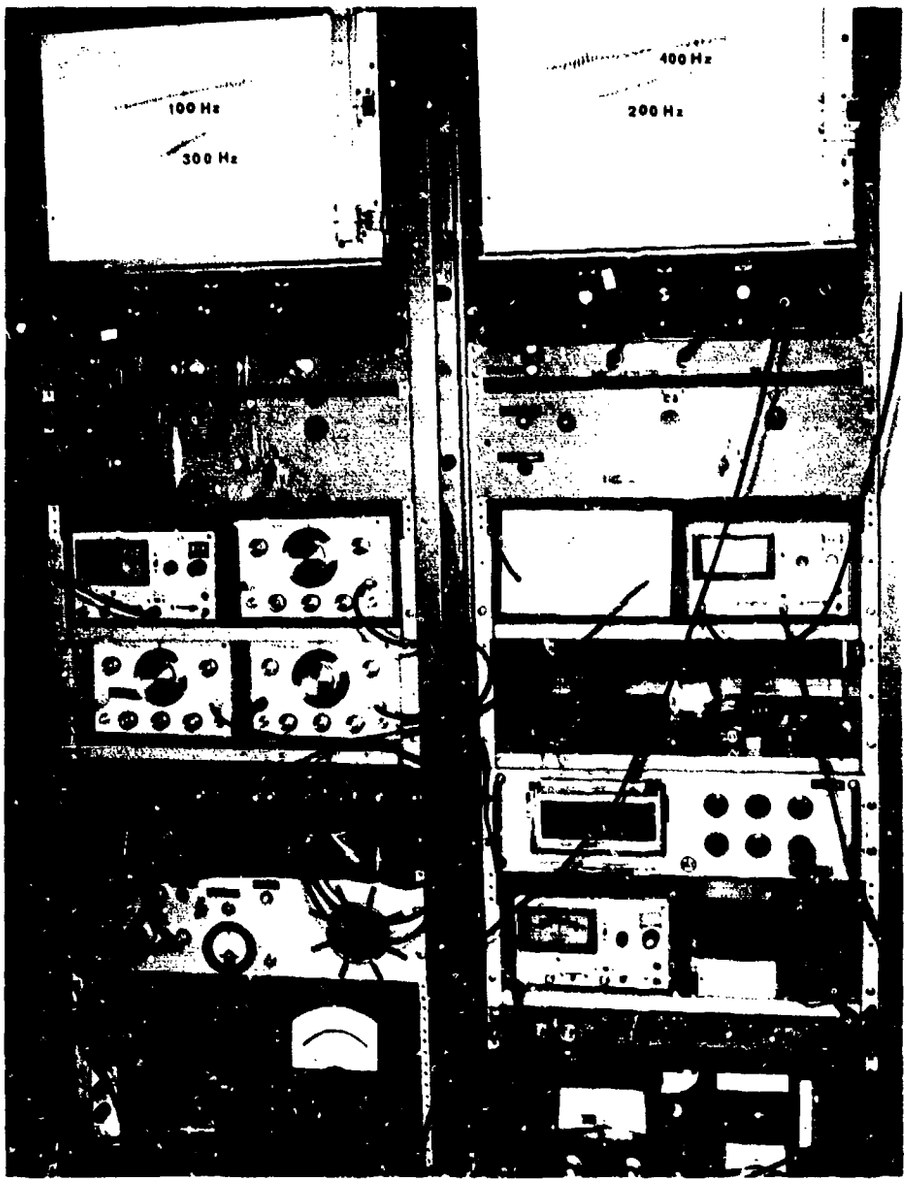

Figure 27. Consoles, Recorder, and Associated Equipments

Consistent with the frequency interrelationships of harmonic series, the deviations of f_2, f_3, and f_4 are also set proportional to their frequencies; so the array of deviations and ranges appear as follows:

Deviation, f(Hz)				Range (Hz)
$\pm f_1$	= $\pm$ 0.2(100)	= $\pm$	20 Hz	80 - 120 Hz
$\pm f_2$	= $\pm$ 0.2(200)	= $\pm$	40 Hz	160 - 240 Hz
$\pm f_3$	= $\pm$ 0.2(300)	= $\pm$	60 Hz	240 - 360 Hz
$\pm f_4$	= $\pm$ 0.2(400)	= $\pm$	80 Hz	320 - 480 Hz

During the course of this study, we determined that manual amplitude control became noticeably difficult if the sweep time was reduced to 6 or 7 minutes; but control was improved when the time duration for one complete sweep (from low to high frequency) was increased. For a good compromise the rate was finally set at 15 minutes, a time which also corresponds to the total test time of Method 519, MIL-STD-810C. For this time duration, the high and low sweep rates were 10.67 Hz/min and 2.67 Hz/min, for 400 and 100 Hz, respectively. With a low cycling rate then, we have sufficient time to switch frequencies, make amplitude adjustments, switch back, and so on. Second, and of comparable relevance, we experimentally determined that a time constant of 1/2 to 1 second for a filter bandwidth of 5 Hz was sufficient to permit rapid switching from one frequency to another. With a little familiarization through practice runs, amplitude deviations about the mean could be held within $\pm$ 1.5 to 2.0 db for the worst cases (300 and 400 Hz). The bandwidth, 5 Hz, represents a good compromise between system response and sine amplitude error owing to the random noise contributions.

Finally, it is important that the monitoring load be equally divided between the two operators. Since the Q of equipments tends to increase with frequency one would expect the sharper responses to occur in the higher frequencies, which in our situation was in the 300 to 400 Hz region.

By sweeping the range at low levels (see Appendix D, para 4.1) one can determine which peak-notches are the sharpest (have the greatest dynamic spread) and therefore require the greatest vigilance. One can then switch appropriate cables about and thus reprogram the system such that the division of vigilance is more nearly equal. The 400 and 300 Hz sinusoids, in our case, exhibited the greatest dynamic range so the channels were redistributed. One operator was allocated 100 and 300 Hz; the other 200 and 400 Hz.

2. TEST PROCEDURE

This section is concerned chiefly with the laboratory application and a review of the results of this method as it relates to an actual equipment package. In doing so, the work establishes a test technique which references detailed procedures through which the method may be facilitated and by means of which some procedural pitfalls may be avoided. Operationally, there is a good deal more to this technique than is suggested by the following simplified view, a view that has been deliberately condensed for the general reader. For those readers concerned with the important and necessary details such as setting the dynamic range of control pots P-1 and P-2 predetermining the peaknotch range of the test level, establishing ground loop criteria, maximizing servo compression control, and so on, they are invited to review Appendix D.

For our test load we chose a communications block box (weight: 50 lbs). The box represents an assembly of printed circuit boards, lumpy masses, relays, cables, leads, connectors, etc. In short, of a composition that one might expect of a typical equipment package. This package is bolted to a cast shaker base plate through two "U" channels set on edge. The channels, of aircraft aluminum, are 6 inches web height, 0.230 inch web thickness, and feature 2 inch flanges. One accelerometer was mounted on each side of the box at the interface of the channel flange and box edge. (Figure 28 and 29). The channel mounting structure was chosen to be sufficiently compliant to guarantee equalization difficulties, yet not so deviant as to lie outside the expectation of aircraft mounting

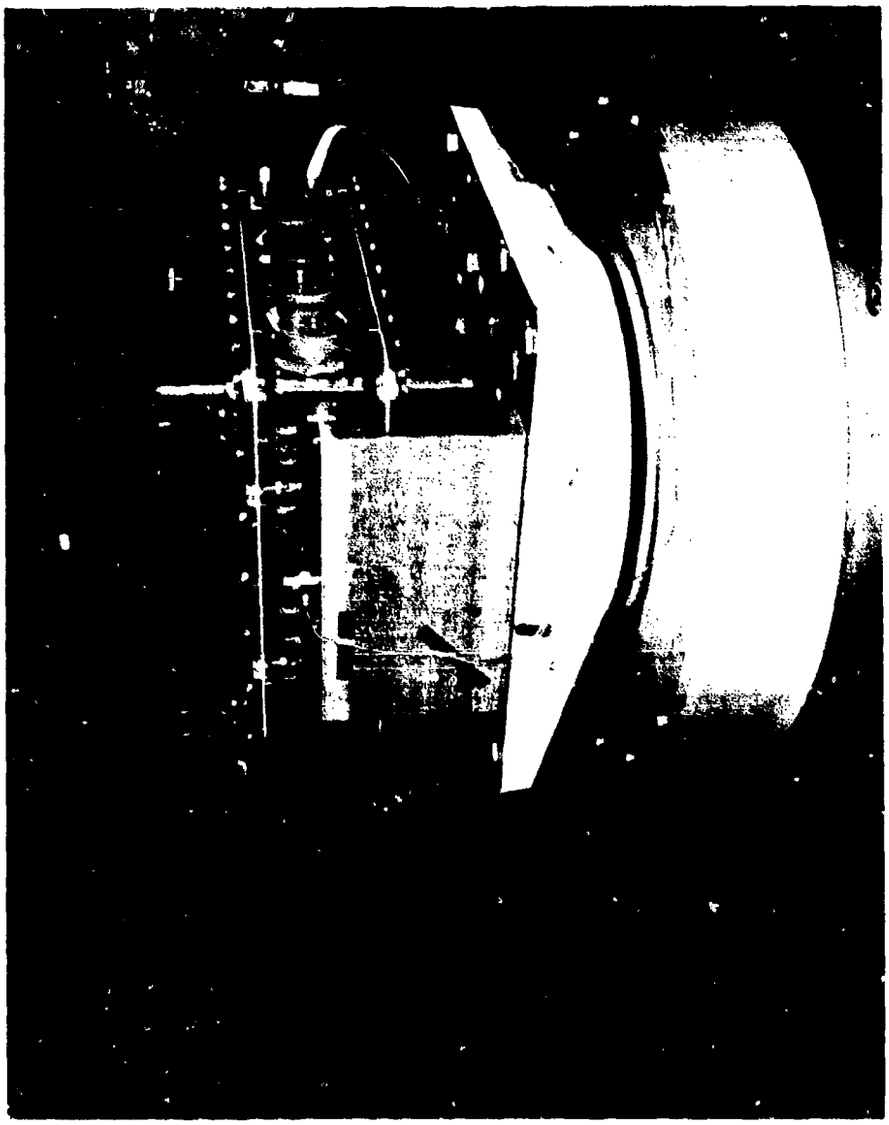

Figure 28. Test Load and Accelerometer Setup

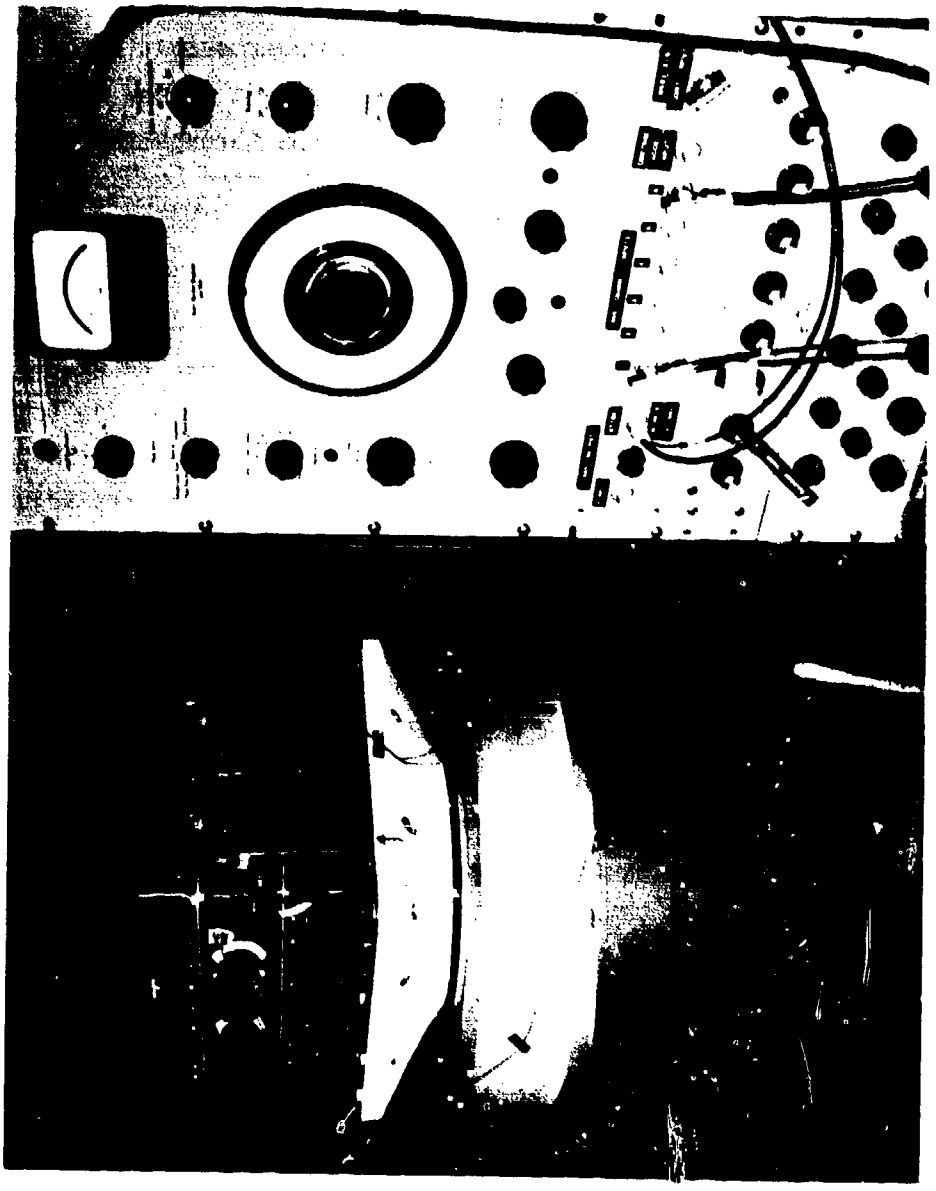

Figure 29. Test Load and Accelerometer Setup

structure impedances. Finally, some sensor details: Two accelerometers were calibrated at a relatively high sensitivity (31.6 mv/g); sufficiently low to prevent preamplifier saturation but high enough to yield a good signal to noise figure as the signals are processed through an averager (MB N681) which, being essentially a sampling switch, is something of a noise contributor. A normalizing pot at the averager output returns the accelerometer sensitivity back to the standard 10 mv/g value, whereupon the signal enters the tracking filters and proceeds through the system as described earlier.

As noted earlier (Section III, par. 5) the combined random and sinusoidal spectrum that we wish to approximate is shown in Figure 23. The cycler has been positioned at the low end of the sweep range, all recorder pens raised, and we are ready to run, that is, assuming that the important preliminaries in Appendix D have been completed; the ground loops minimized, booster amplifier set, peaknotch filter adjusted, sine and random spectrum properly shaped, and a number of other necessary steps the details of which are noted in Appendix D.

We begin vibration at a level -30dB from the test levels, sequentially switching up in 10 dB increments until the full test level is reached at zero dB. Upon completion of the checks detailed in Appendix D the two sine operators (after one of them turns on the cycler) are henceforth preoccupied with the switch, adjust, and record procedures described earlier.

Before launching further into this final cycling phase it is worth digressing to note that sinusoidal control is not only enhanced by sets of acceleration vs frequency curves drawn on the X-Y recorder sheets but further improvement can be realized by placing these sheets (normally translucent) over the corresponding sets of frequency response curves recorded earlier. The two operators thus have in the background a running history, hence a continuous reminder of the amount of control compensation needed to smooth out the frequency responses of each sinusoidal system. This works well especially at the lower vibration levels

where system responses are apt to remain linear. Here, the frequency response curve provides a background reference that is a good reflection of the inverse function needed to produce the desired test profile. At the extreme upper level, say 0.5 g^2/Hz and above, nonlinearity is present. The system response becomes soft, sluggish, and, oddly, easier to control. In counterpoint to this, the random spectrum control (in the high frequency end) becomes, as we shall presently see, ever more tenuous.

A final point before we review the results. We did not switch as quickly through the levels as is implied; rather a recording pause was interjected at each level. Accelerometer records were run off on the T-589 scanning recorder, on a 1/3 octave system, and on an Ampex FR 1200 tape recorder. Moreover, after the 0.5 g^2/Hz run was completed we raised the level up to 1.0 g^2/Hz and ran a set of records at this level also.

3. RESULTS

The first results are reviewed as presented by the T-589 system, which is to say, the power spectral density (PSD) vs frequency output of the MB N275 analyzer and X-Y plotter configuration. Briefly, the 80 channel analyzer output is plotted as the log PSD as each filter channel is sequentially stepped through the spectrum from channel 1 (center frequency, 20 Hz) to channel 80 (center frequency, 3 KHZ). The channel bandwidth for each of the first 40 channels is 25 Hz and for each of the last 40 channels it is 50 Hz.

At the -30 dB level (re. 0.5 g^2/Hz) the 4 sinusoids are shown (Figure 30) with some obvious 60 Hz present. Still, the 60 Hz, its multiples for that matter, are quite low and will drop lower, relatively, as we raise the vibration level.

The sharp high frequency roll-off in the noise spectrum, beginning at about 1300 Hz, requires elaboration. As discussed in Appendix D we note that at this phase of the test procedure we have already been at higher levels to locate and place peak-notch filters to boost the low frequency portion of the spectrum to shape the equalizer slider pots. All this was

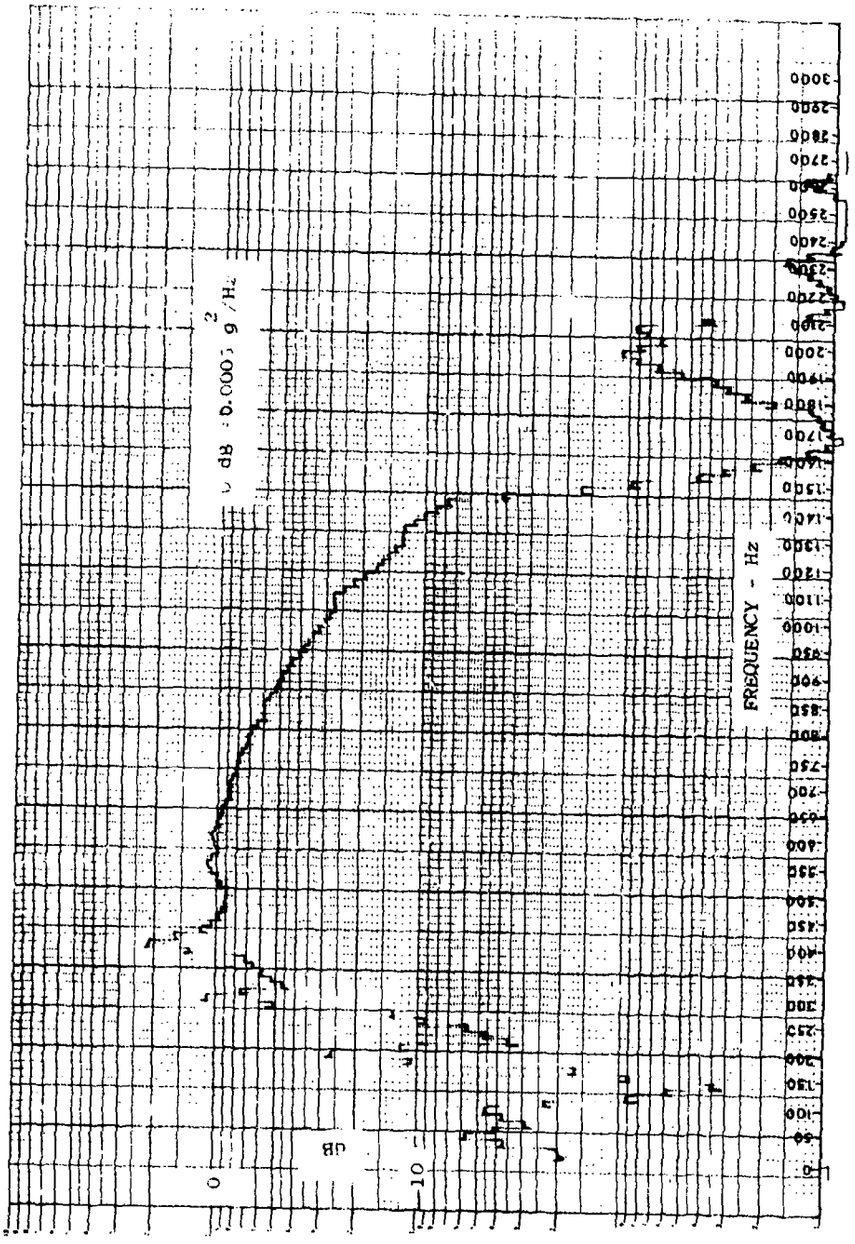

Figure 30. Gunfire Spectrum at the -30 dB Level

done to obtain the best possible spectral fit, not at the lower levels but at the higher levels. Why the higher levels only? Because this is where the spectral control problems are. The lower levels, on the whole, can be controlled reasonably well as a glance at an earlier spectrum (Figure 31) will show.

When we switch to -20dB the high signal to noise content of the low frequency region is quite marked (Figure 32). The four sinusoids are distinct and are located at their respective low range values ready for the sweep up phase when we switch up to the 0 dB level. Notice that already the high frequency content is beginning to come up, a harbinger of difficulties to come. All in all, though, control is still firm.

At the -10dB level (Figure 33) we see early signs of spectral breakthrough. The peaks at 1950 and 2200 Hz now exceed the test curve but the spectral exceedences are still within 3.5dB and one can say, at this point, that spectral control remains positive.

Figure 34 shows the spectrum when we switch to 0 dB (0.5 g^2/Hz). Here spectral control begins to show signs of mounting difficulty -- breakout is beginning at 1.95 KHz where the PSD looms 13 dB above the test curve.

Elsewhere, the spectrum rises along a frequency segment beginning at 1.45 KHZ and extending to 3.0 KHz. Still, over a test bandwidth of 2 KHz (a common value spelled out in test specifications) the PSD does not greatly exceed the +6 dB tolerance level if we except the prominence at 1.95 KHz. However, it is clear by this time that the ±6DB tolerance of the test curve (from 1 to 2 KHz) will be exceeded and that revisions in the tolerance level, that reflect test level and test load, will have to be entertained. This conclusion is buttressed when we raise the level +3 dB to 1.0 g^2/Hz as shown in Figure 35. The peak at 1.95 KHz increases 3 dB to approximately 16 dB, and the low end of the spectral breakout band has moved down to about 1.2 KHz. We are reaching some sort of limit to high frequency spectral control. Note that throughout all of this, the low frequency end of the spectrum appears well behaved even during the 15 min. sweep cycle, a phase that now seems appropriate to introduce.

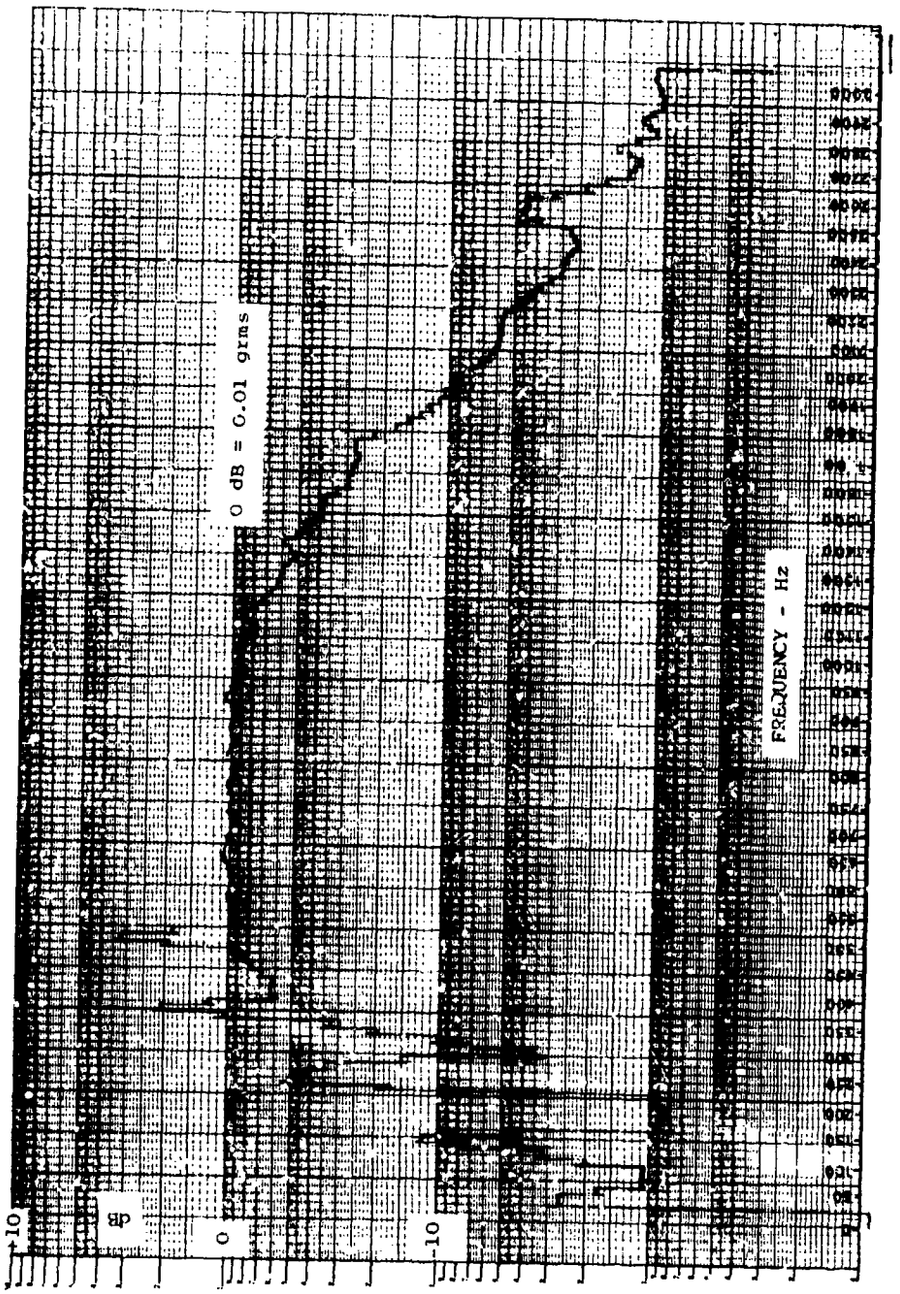

Figure 31. Spectrum Showing Good Control

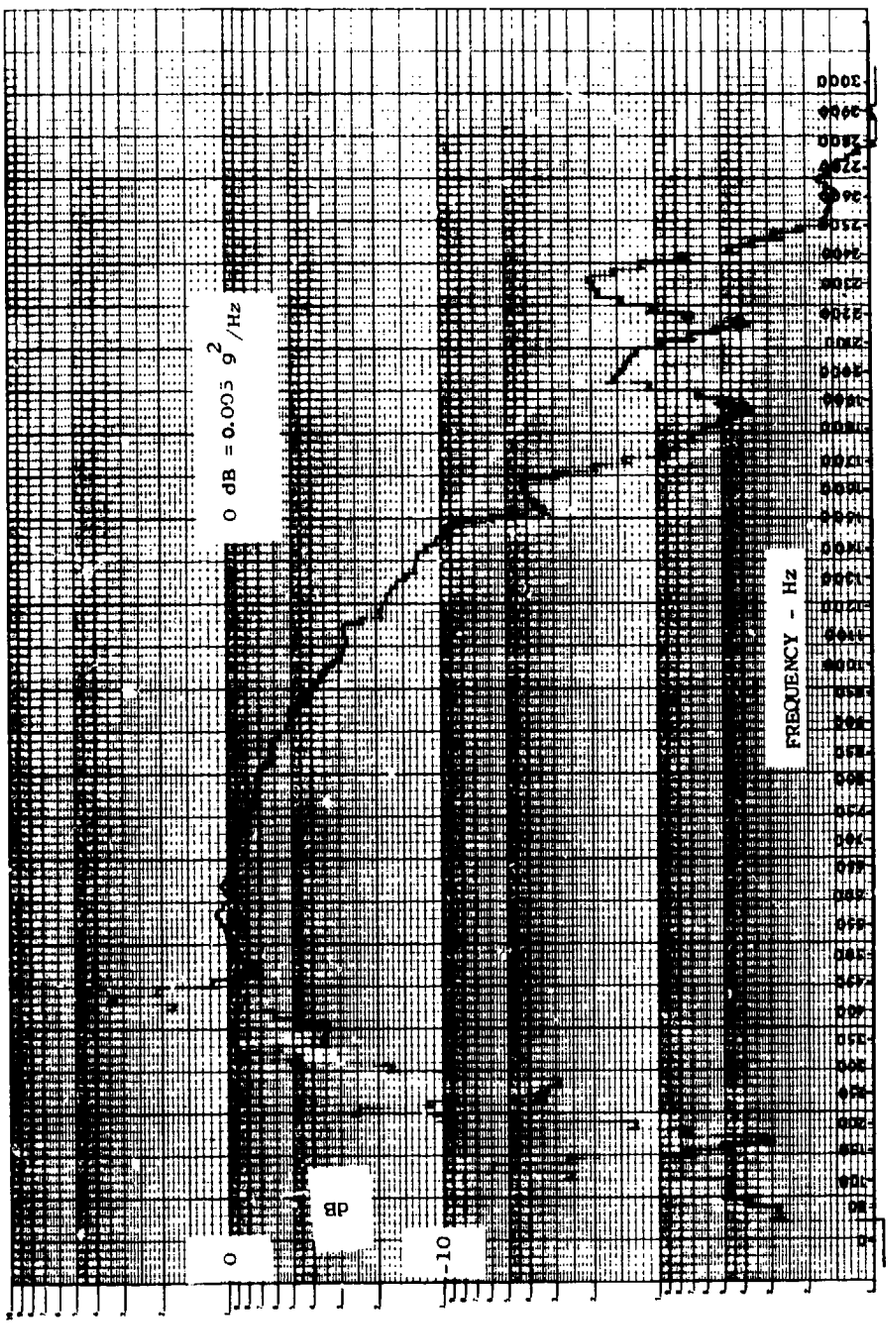

Figure 32. Gunfire Spectrum at the -20 dB Level

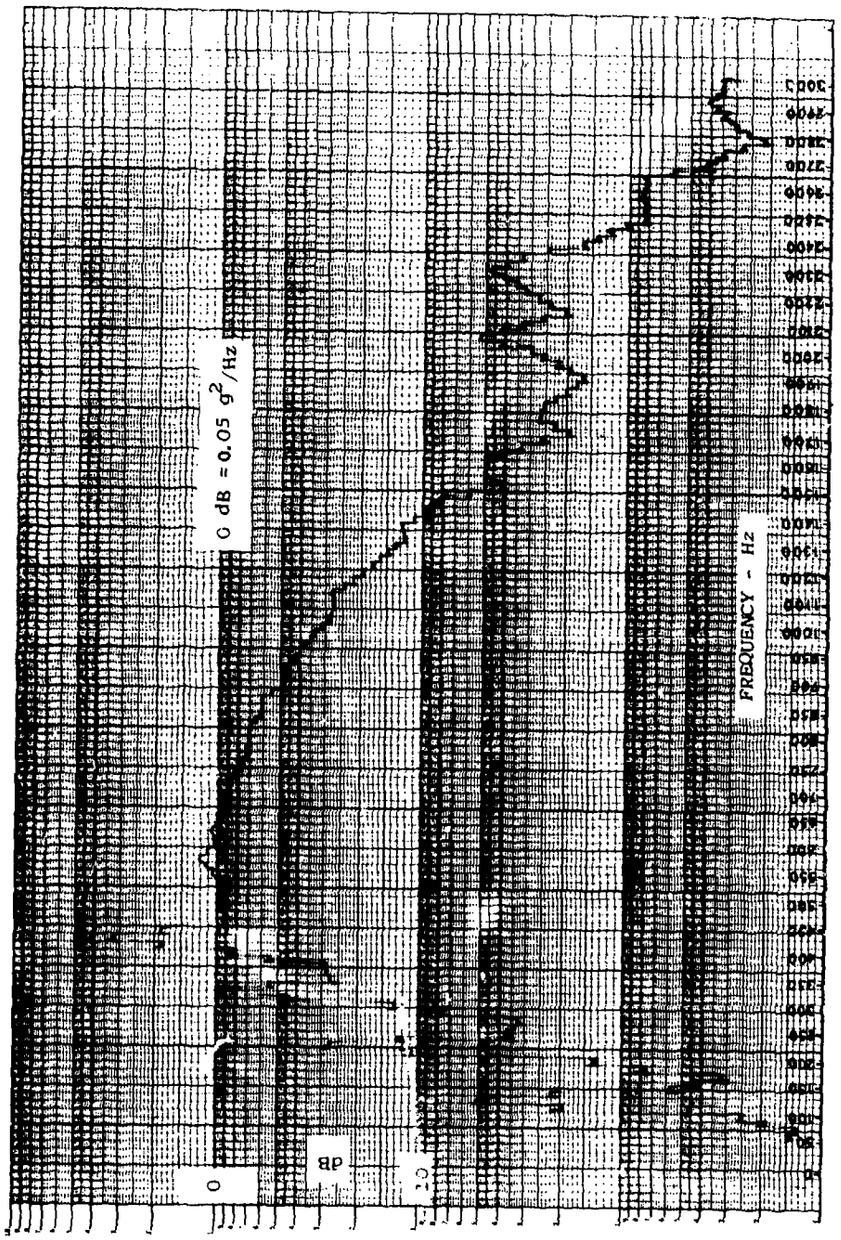

Figure 33. Gunfire Spectrum at the -10 db Level

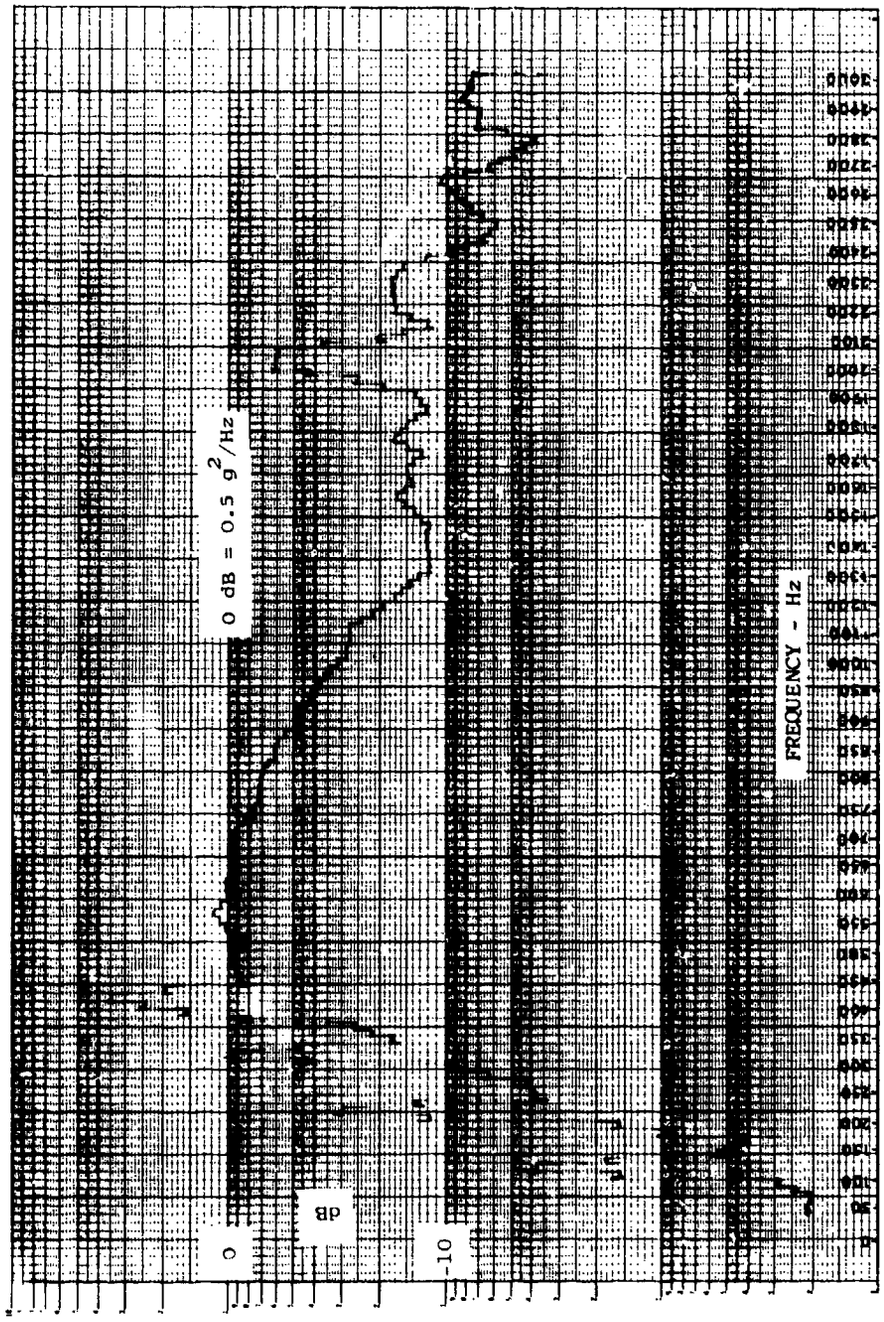

Figure 34. Gunfire Spectrum at the 0 dB Level

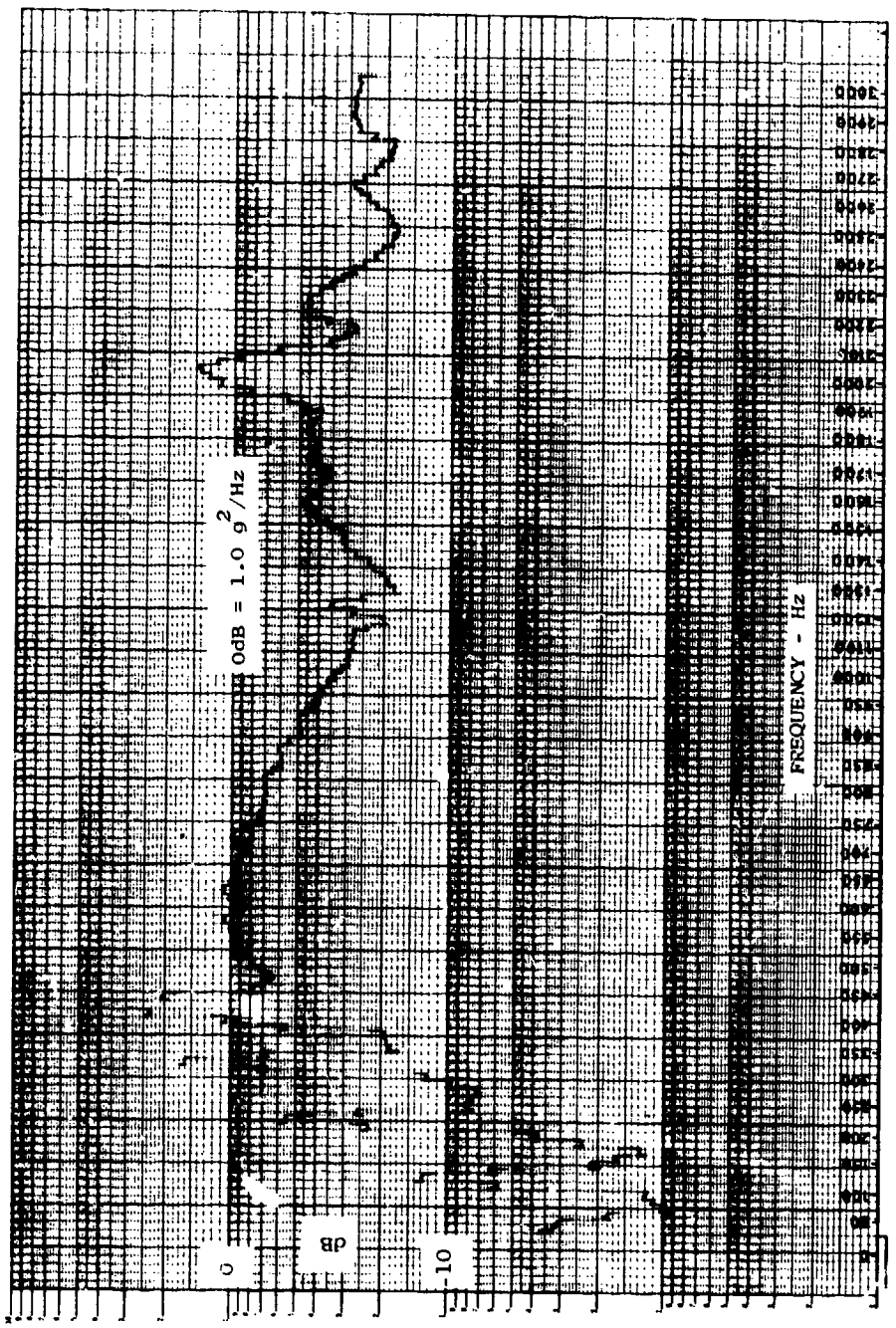

Figure 35. Gunfire Spectrum at the +3 dB Level

It will be remembered that at the 0.5 g^2/Hz level the cycler was switched on and the two operators addressed themselves to the proper performance of their respective sets of sinusoids. Their preoccupation is the reason why the spectral depressions between f_2 and f_3; and f_3 and f_4 were not touched in and brought closer to the curve (Figure 34). In fact, the experiment was run with only two operators and we can see now there is profit in having a third man to attend to this and other matters. At any rate, the cycling phase has been entered and we look at a section of the tape record of that run through the eyes of a 5 Hz filter with a one-half second time constant, the same used in the control system. Figure 36 shows a 1 1/2 minute sample of the four sinusoids. One can see that control is, on the whole, good; $\pm$2 dB easily covering the deviations of the 400 Hz trace. The spread progressively converges as one goes down frequency. Finally, at 100 Hz, control within $\pm$1dB is readily obtainable. The flat part of 200 Hz trace, in the center of Figure 36, is due to a momentarily jammed X-Y recorder.

4. SPECTRAL ANOMALIES

There are some interesting spectral responses induced in the higher frequency range during certain periods of the cycle phase and these responses invite comment. Spectral prominences appear during exposure to the higher level of excitation (0.5 g^2/Hz and above) and decrease markedly at the lower level. Also, they appear only at certain times so the N-275 readout may, during its single scan, overlook them. However, we have taped the entire cycling phase at 0.5 g^2/Hz and, also, we have at least 2 minute recordings at all other levels. This reservoir of data allows us to catch the spectral bulges at our leisure, subject them to narrow band analysis and plot their probability density distributions.

The narrow band analysis (5 Hz) taken at the +3 dB (1.0 g^2/Hz) level is shown in Figure 37. The X axis of the recorder system has drifted during analysis; thus actual frequencies (measured by a counter) are entered over each peak for more precise identification. Conspicuous, are the narrow band spectra at 599, 708, 1200, and 2038 Hz. A quick look at the time histories of the 5 Hz filtered signal output identifies

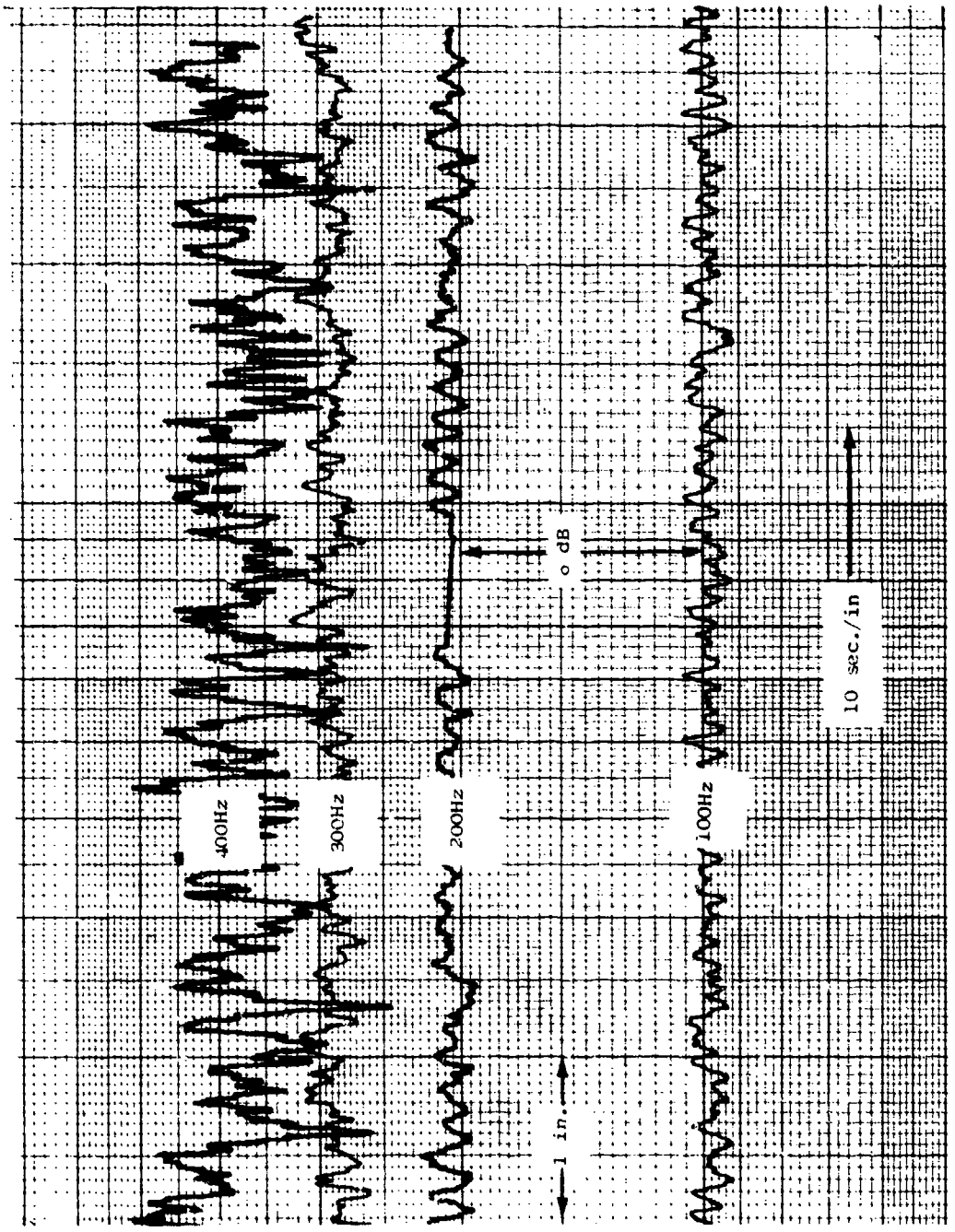

Figure 36. Control Tolerances of Sinusoids

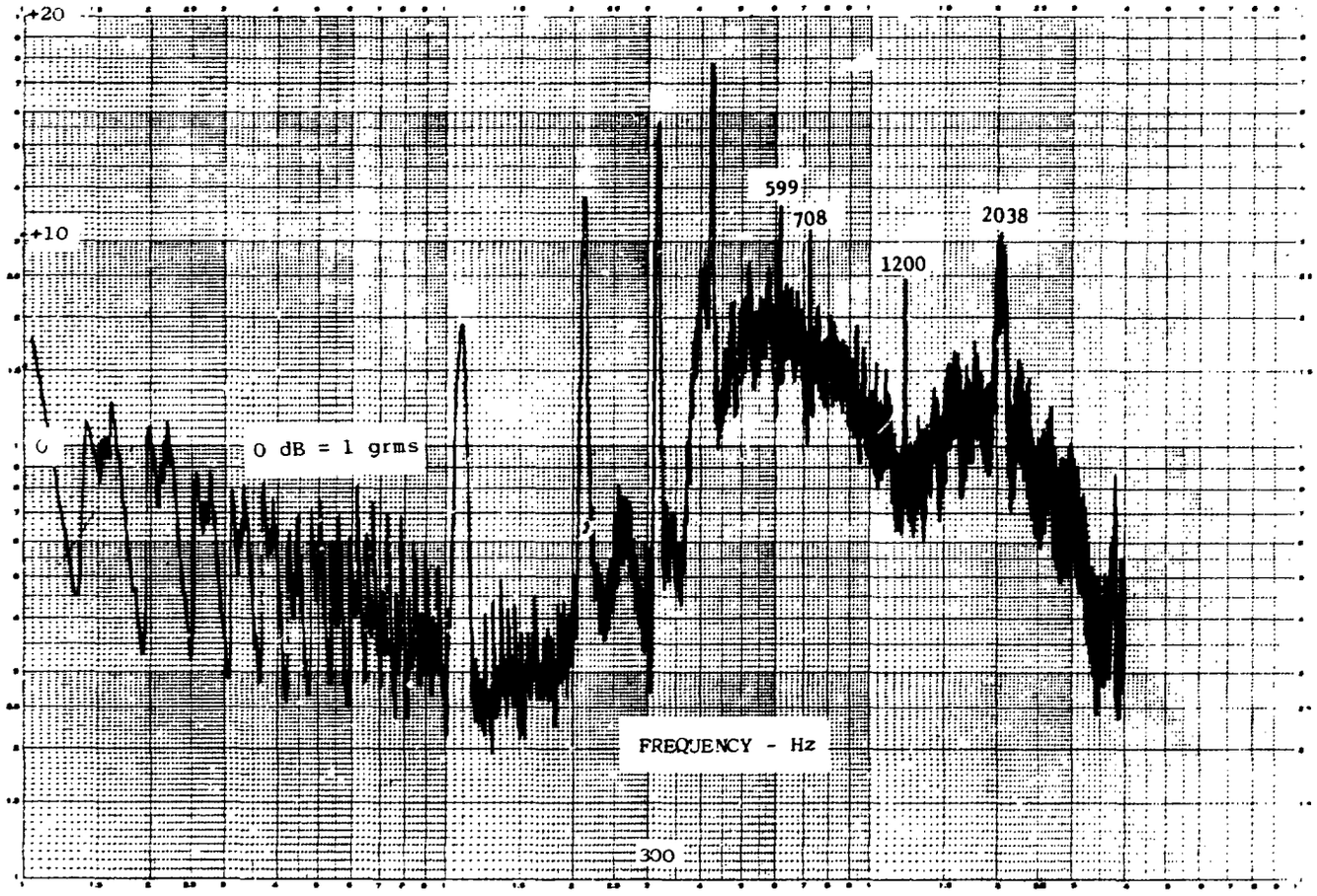

Figure 37. 5 Hz Analysis of Gunfire Spectrum at the +3 dB Level

the first three as being predominately sinusoidal. Also, this observation can be verified by reference to their amplitude probability densities (APD). A typical sample is shown in Figure 38.

The peak at approximately 2 KHz is our old equalization nemesis encountered earlier. In contrast to the other spectra this is narrow band and predominately noise as the APD of Figure 39 illustrates. The 2 KHz response is, in great part, due to the 1, 1 mode of the "U" channel as shown in Figure 40.

As might be anticipated for thick metallic members of this sort the Q is very high and the price paid for it is an unruly high frequency response in the test spectrum. Moreover this response is, very likely, aggravated by inputs generated from nonlinear behavior and from chattering down frequency where such antics are most likely to occur. This brings us to the narrow band analysis taken at 0 dB (0.5 g^2/Hz) as seen in Figure 41. In the upper frequency range note that most of the previous discretes have largely dropped out. In this particular record the low frequency part of the spectrum (below 400 Hz) includes rather large spectral intrusions that should be considered spurious -- these unwanteds are due to ground loops and tape splice kicks. They are identified on Figure 41 as (l) and (s), respectively, and should be ignored. These difficulties were pretty well cleaned up, as can be seen in the remaining figures. Again, look at Figure 42 which is -10 dB re. 0.5 g^2/Hz. The spectral differences between this level and the 1.0 g^2/Hz level are striking. Clearly the sinusoidals induced up frequency are related to the low frequency end and this suggests nonlinear behavior. Along the lines of this observation our visicorder records indicate that considerable chatter is going on inside the package. At the lower levels (Figure 43 is a trace at -20 dB down level) the traces show a normal pattern. The upper trace is a record of one of the control accelerometers through an 8 KHz galvo, the center trace is a 100 Hz timing record and the lower trace is the same as the upper trace but as seen through a 1 KHz galvo. Even at -10 dB down (Figure 44) the traces are still rather normal, however as we go 0.5 g^2/Hz (Figure 45) one observes an increasingly hashy

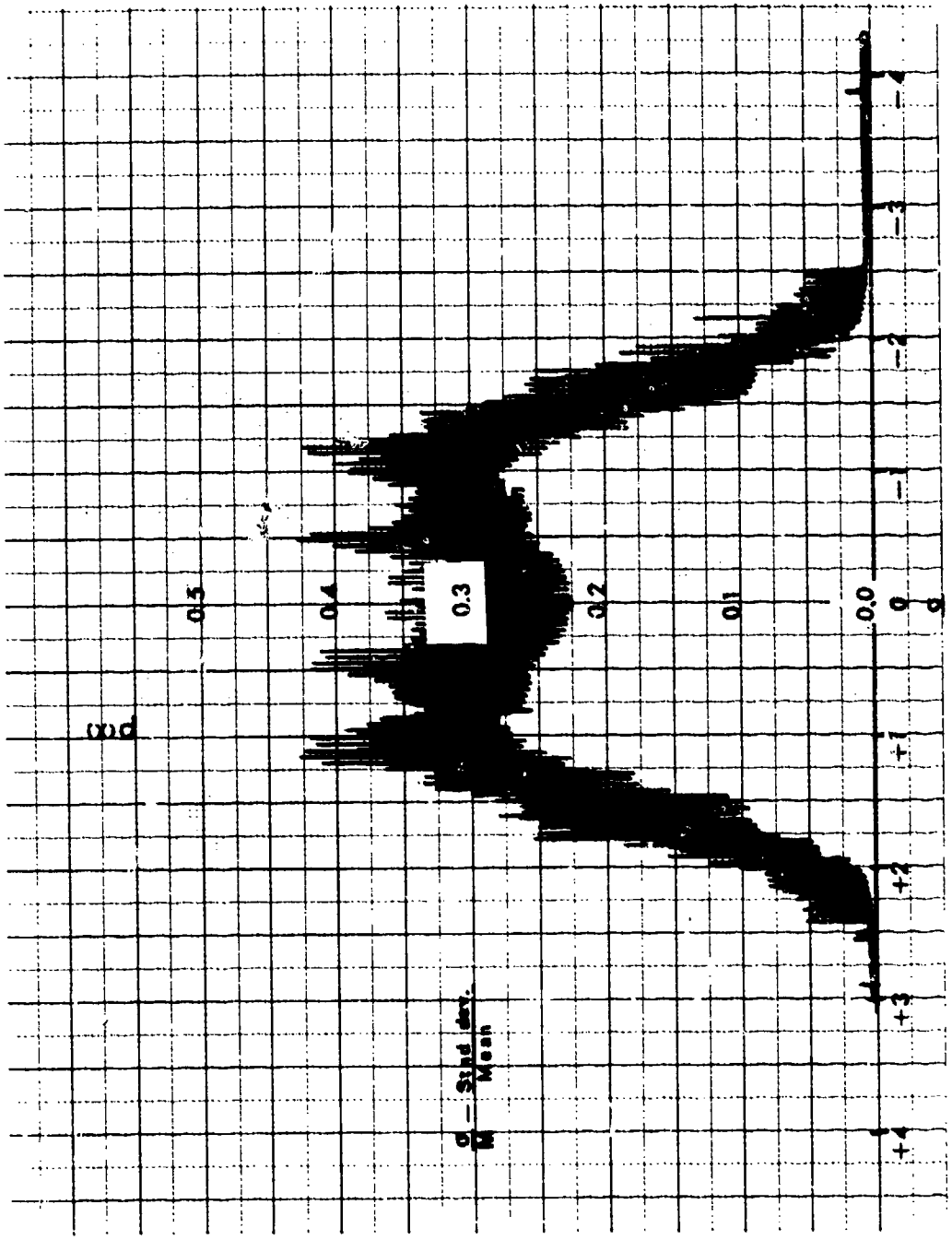

Figure 38. 5 Hz Probability Density Analysis

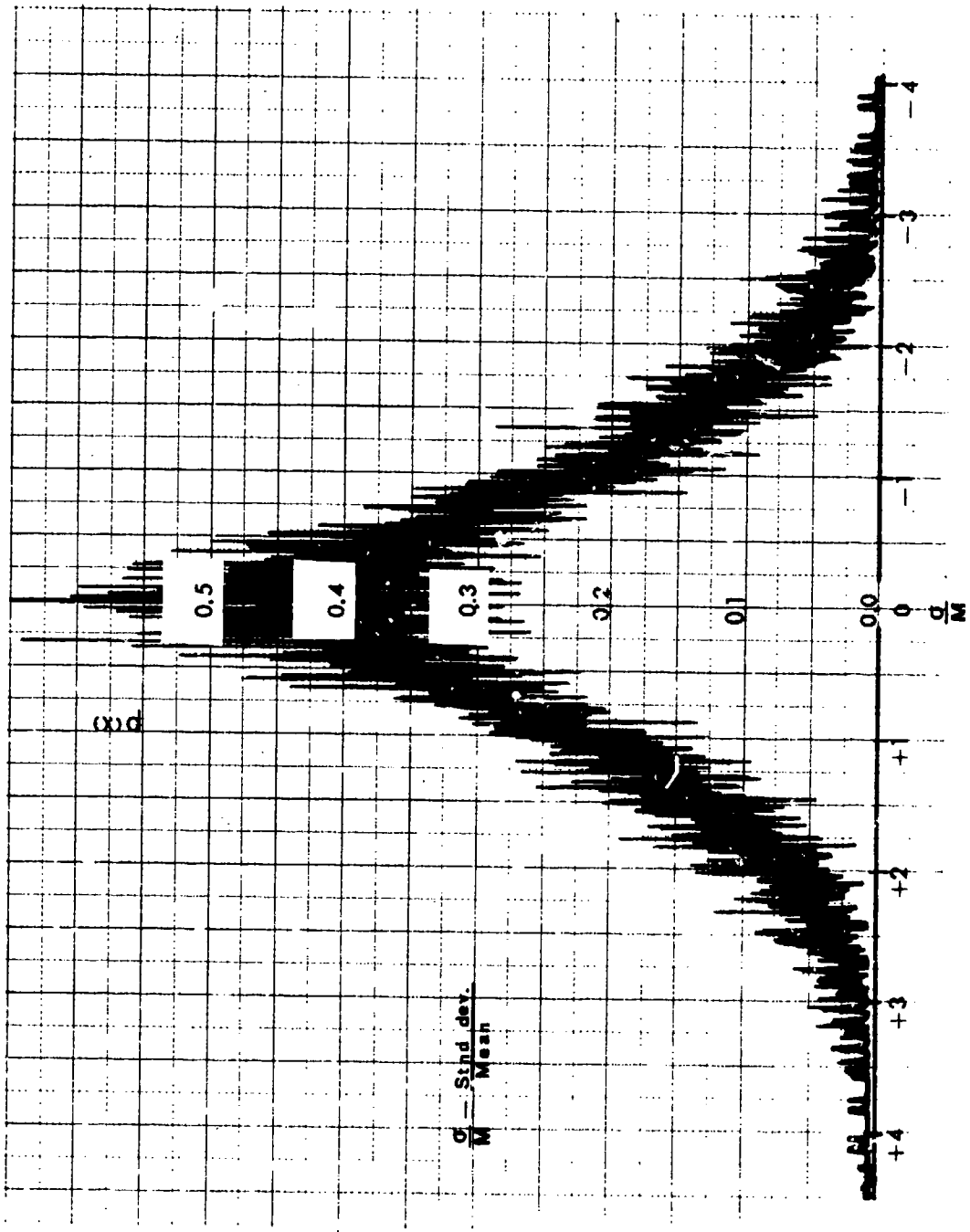

Figure 39. 5 Hz Probability Density Analysis (2kHz)

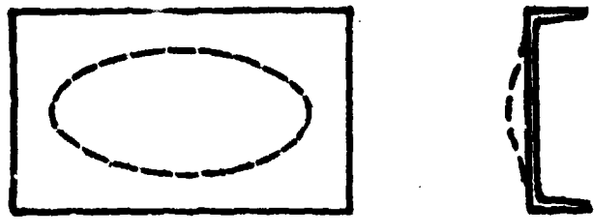

Figure 40. High Frequency Mode of Equipment Support

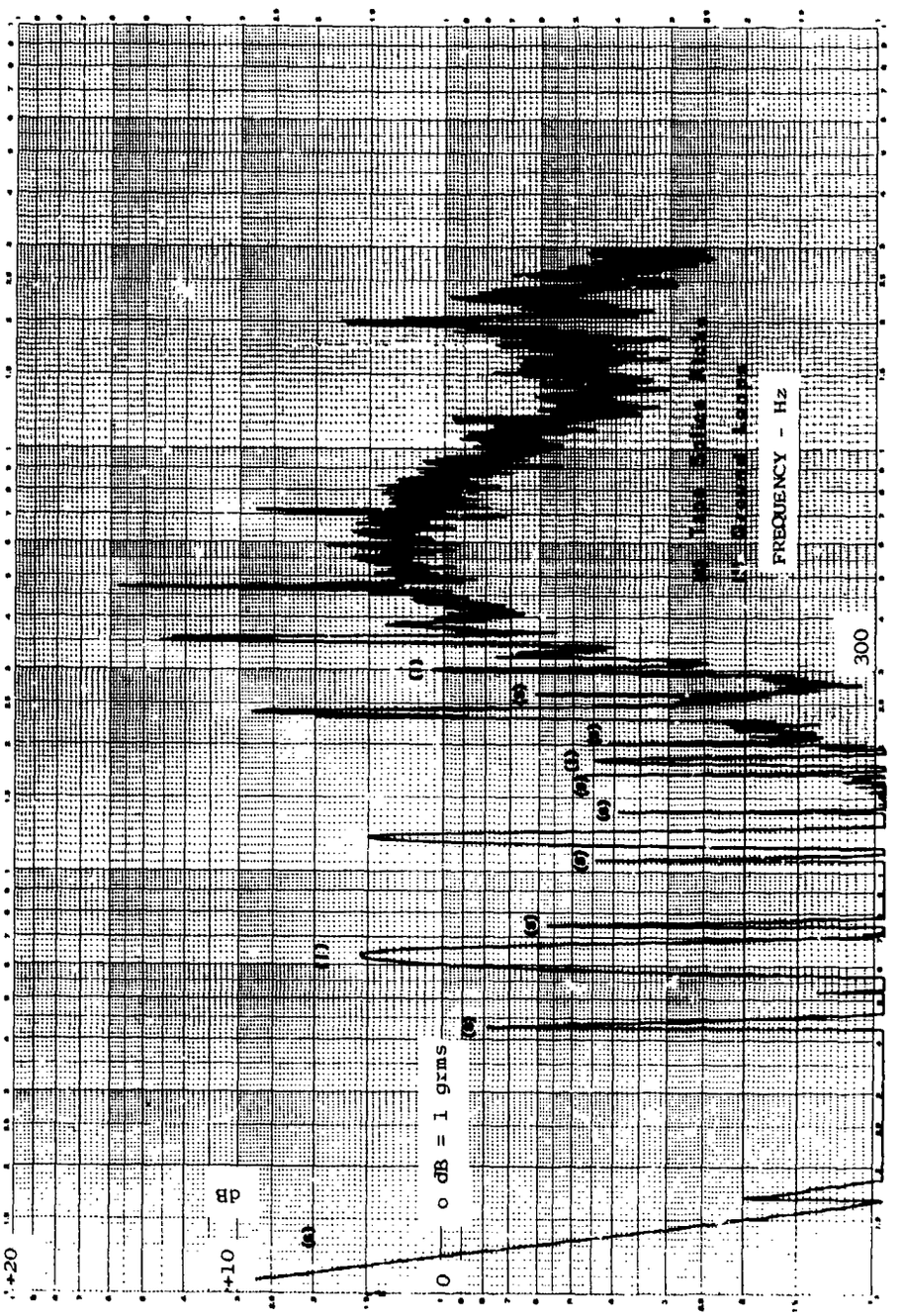

Figure 41. 5 Hz Analysis of Gunfire Spectrum at the 0 dB Level

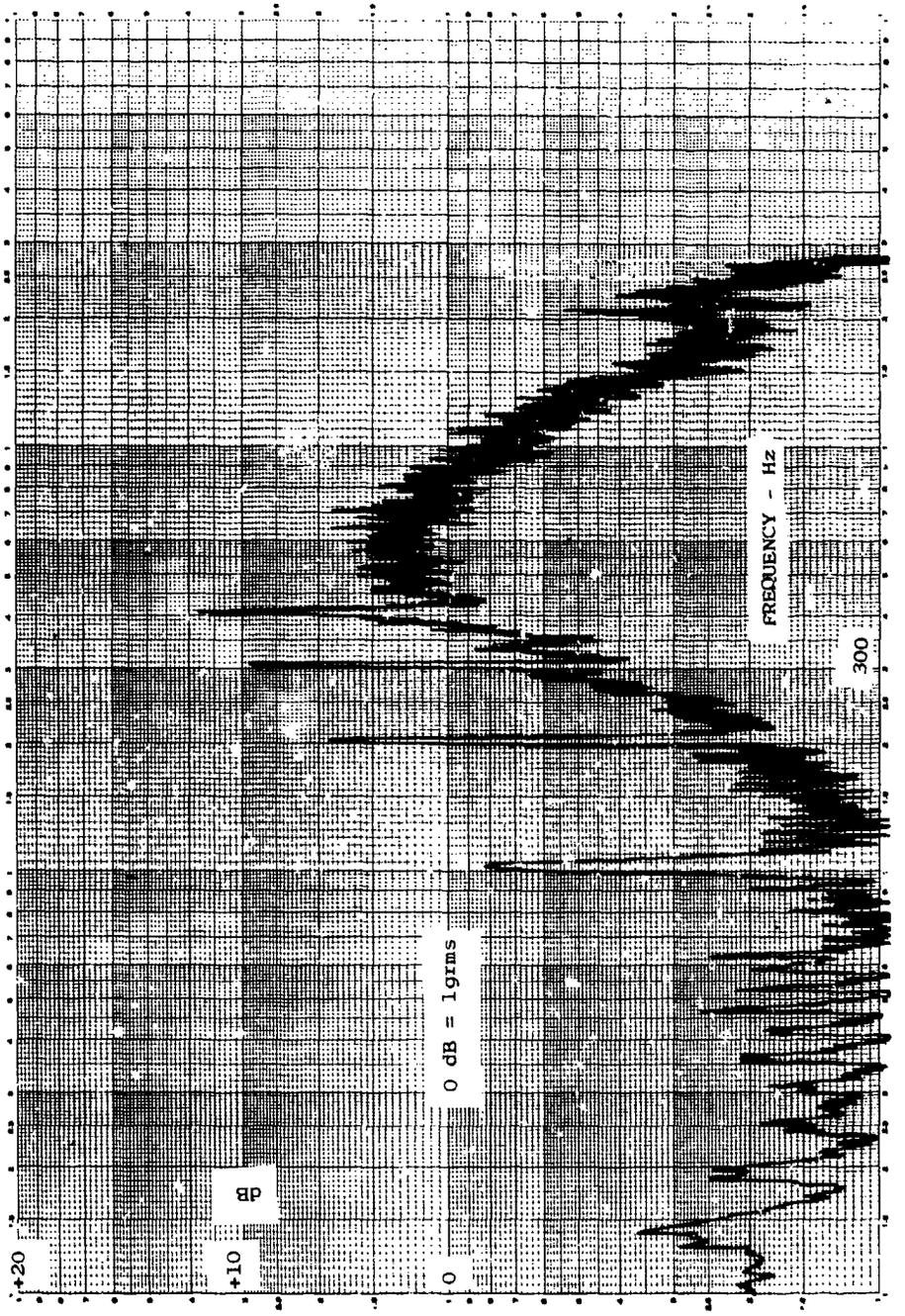

Figure 42. 5 Hz Analysis of Gunfire Spectrum at the -10 dB Level

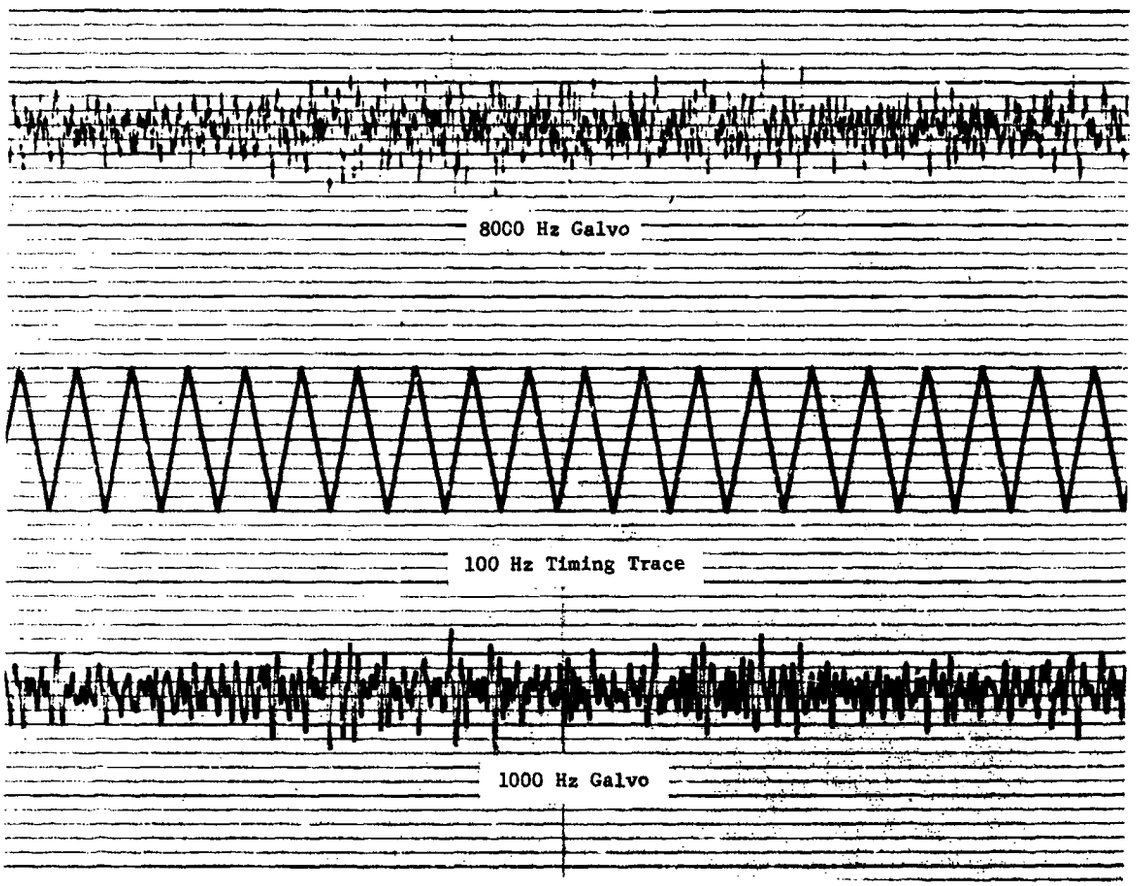

Figure 43. Galvanometer Traces of a Control Accelerometer at the -20 dB Level

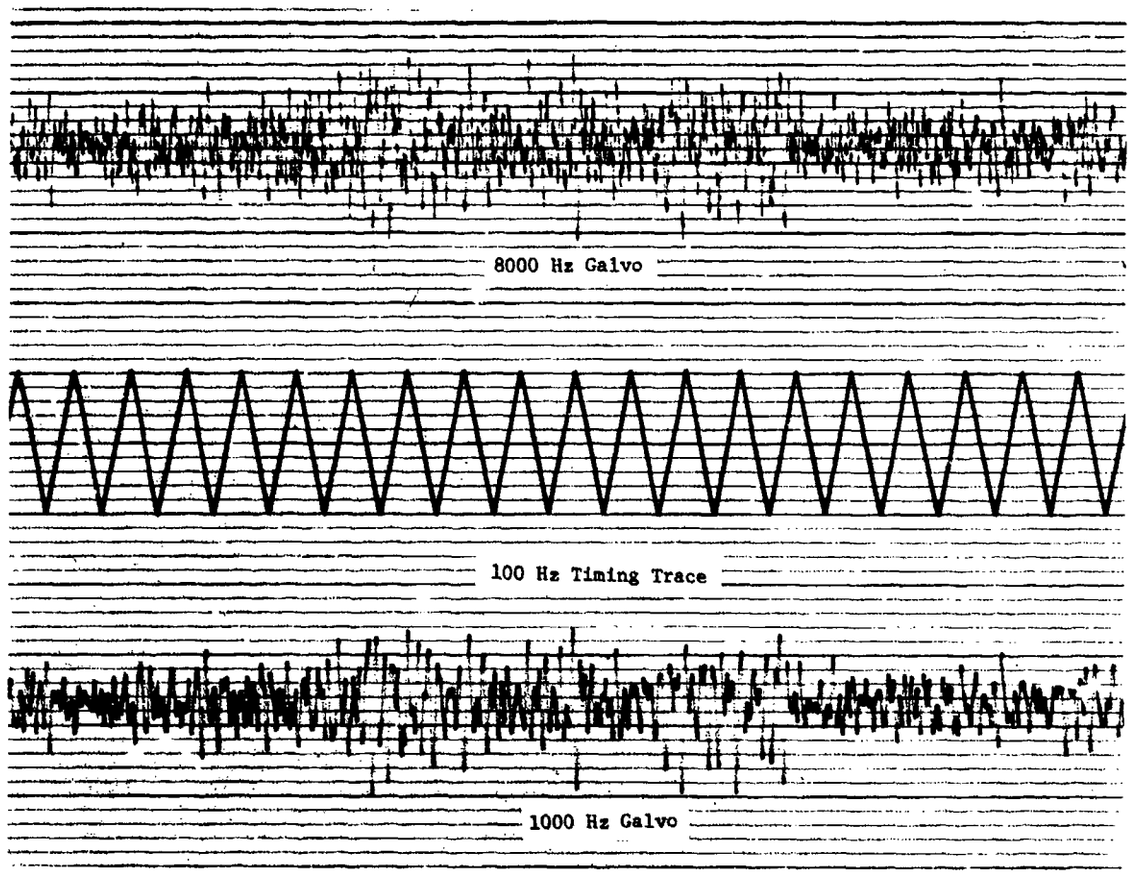

Figure 44. Galvanometer Traces of a Control Accelerometer at the -10 dB Level

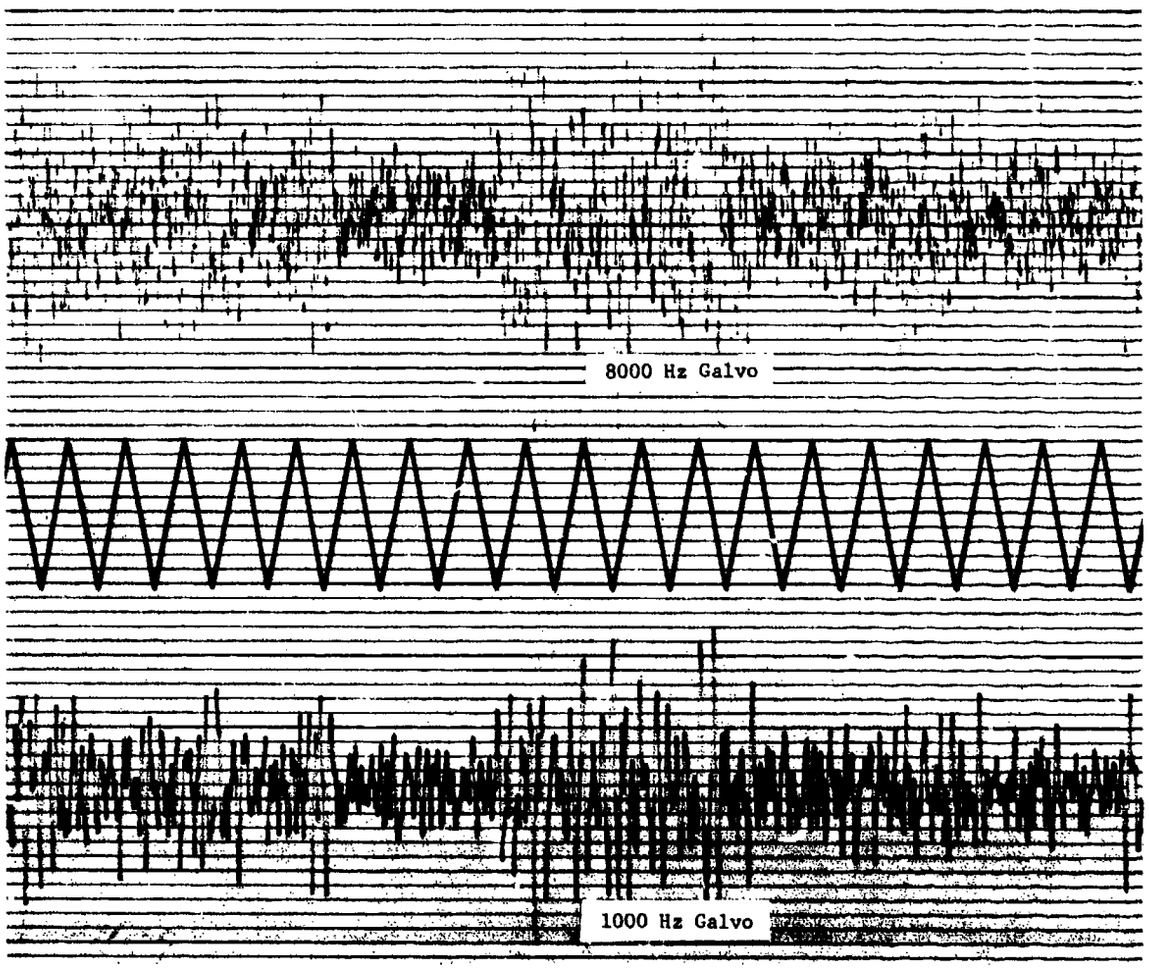

Figure 45. Galvanometer Traces of a Control Accelerometer at the 0 dB Level

spectrum; especially is this noticeable in the upper trace. The high frequency content has jumped significantly. Patterns of this sort usually indicate an internal chatter situation. At high input levels nonlinear offshoots from the four sinusoids couple into the test package at appropriate higher frequencies (usually multiples of 100, 200, 300, and 400 Hz) and result in spectral prominences. Since the servo system is not aware that the excitation source comes from down frequency it is unable to reduce channel gain at the source; hence the up channel servos are readily overloaded. The same may be said of itinerant high frequencies induced because of component chattering. Such behavior appears to be a serious problem at high inputs only; but nonetheless, specifications should attempt to take this anomaly into account, at least for the larger equipment packages.

a. Amplitude Probability Density of the Four Sinusoids

In past works (Reference 1 and 3) it has been shown how the APD of the gunfire harmonics undergo transformation. A sine-like APD appears at the basic firing frequency; gradually shifting to gaussian-like form as we proceed up frequency. Figures 46 through 49 represent typical APD specimens reduced from 5 Hz filtered gunfire tape data acquired during this study. The distributions for 100, 200, 300, and 400 Hz, not surprisingly, exhibit a similar trend. It should be noted that the uniformly spaced spikes of the APD plots are due to kicks induced by the tape splice and should be ignored.

5. TEST SPECTRUM TOLERANCES

As was noted earlier, control in the low frequency region ($f < 500$) proved to be reasonably tight even with a 50 pound load excited at high vibration input levels. This is in sharp contrast with specification control in the high frequency region where the deviation about the specification mean increases gradually at first, then markedly accelerates to large values as one leaves 1 KHz and approaches the 2 KHz region.

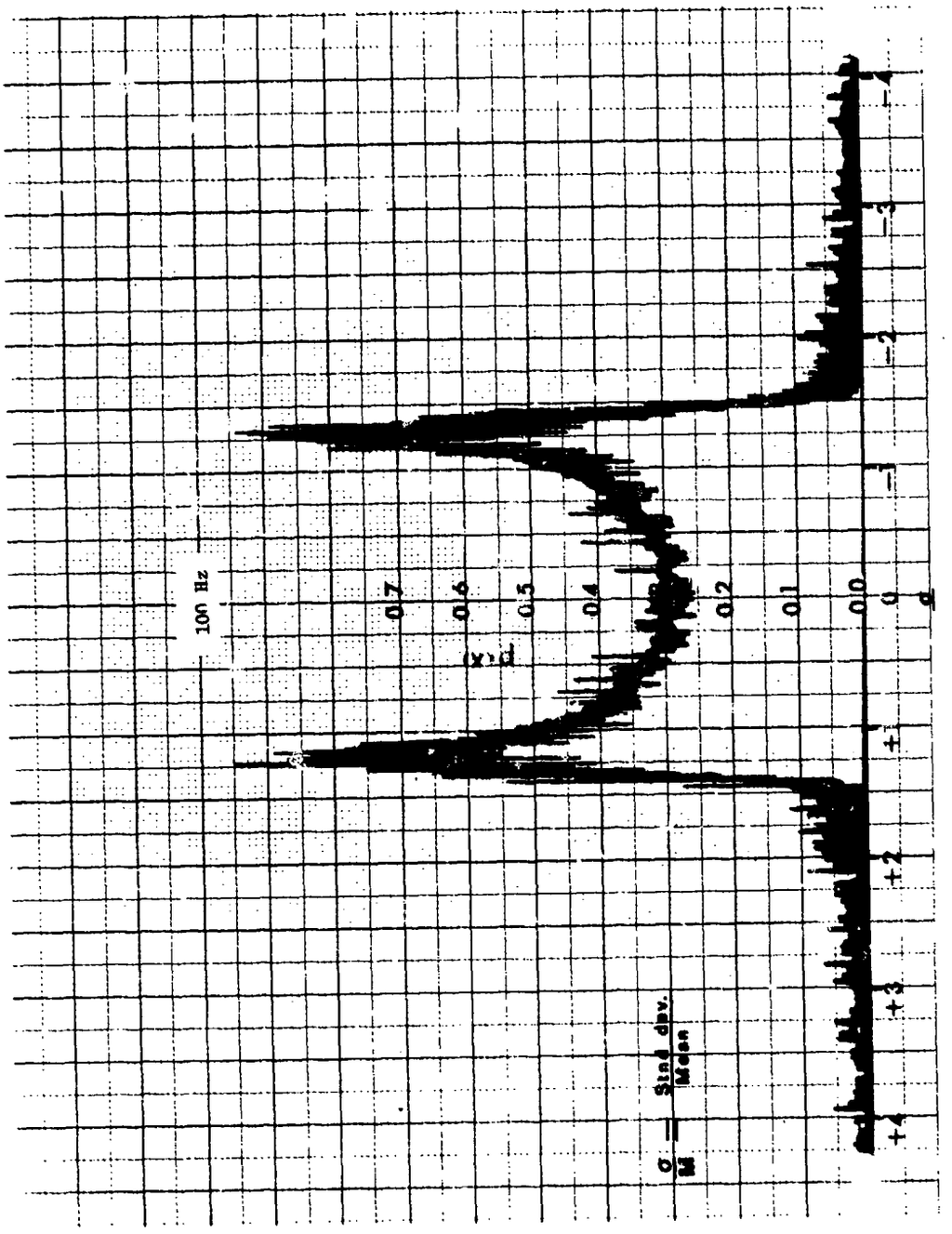

Figure 46. 5 Hz Probability Density of Gunfire Spectrum at 100 Hz

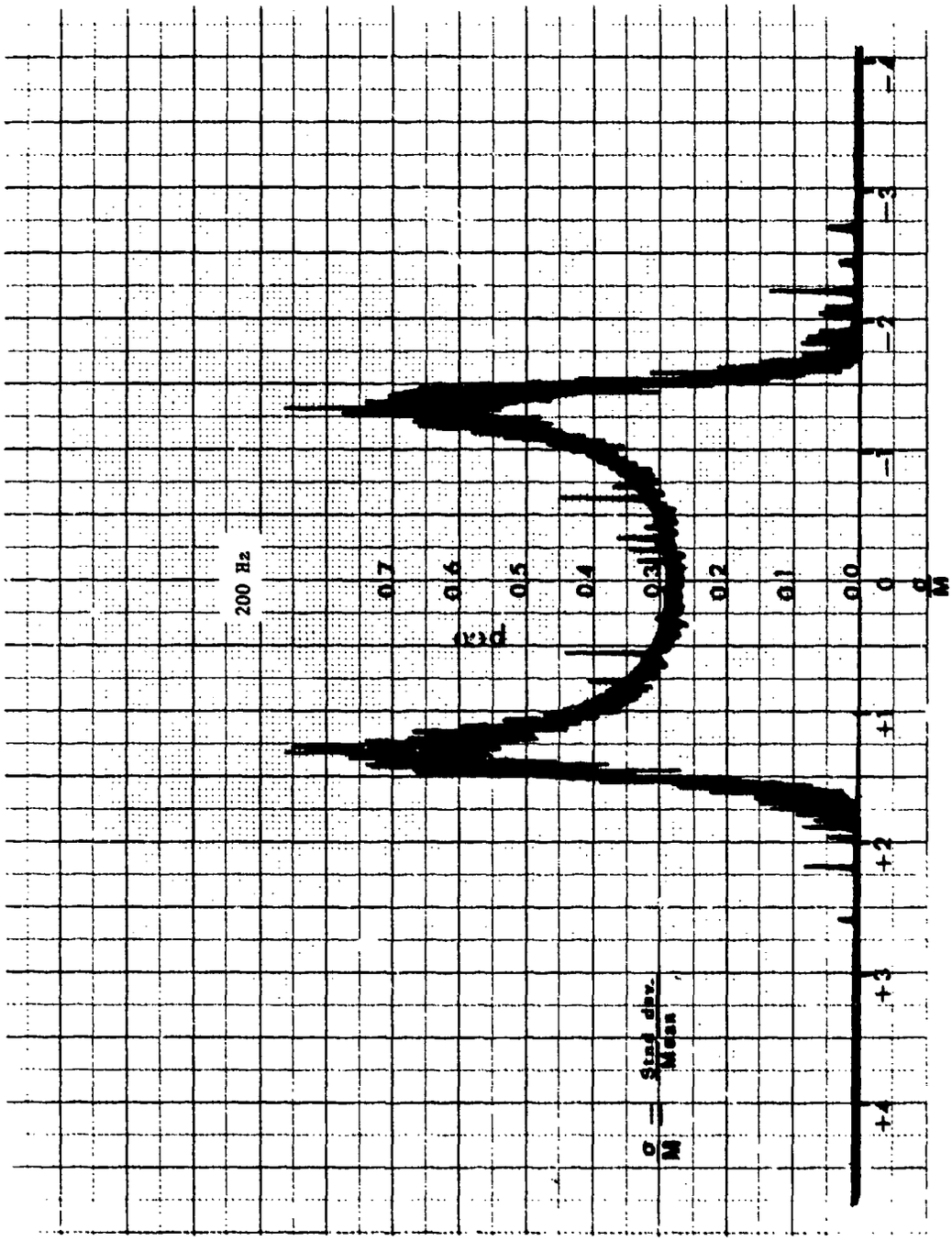

Figure 47. 5 Hz Probability Density of Gunfire Spectrum at 200 Hz

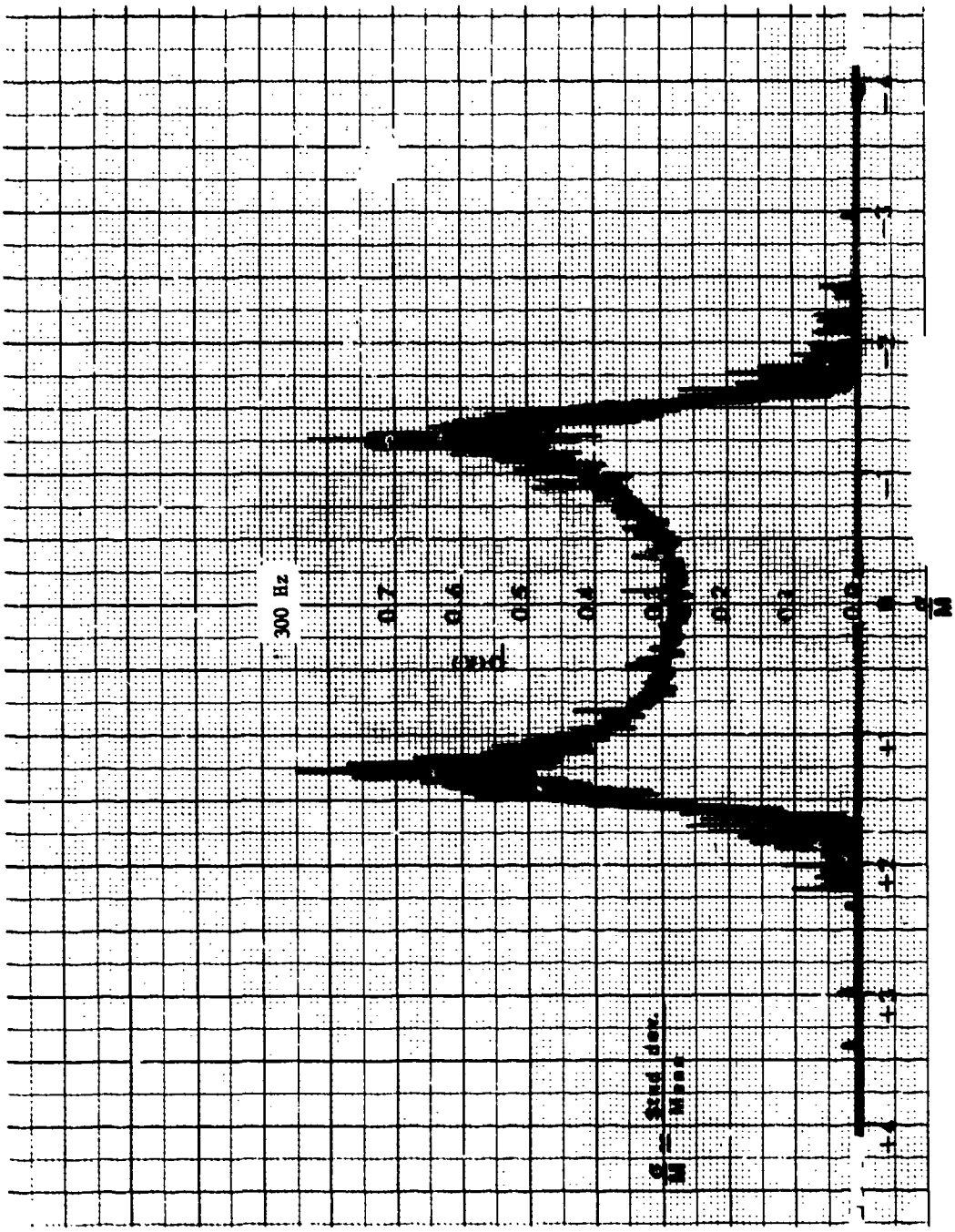

Figure 48. 5 Hz Probability Density of Test Spectrum at 300 Hz

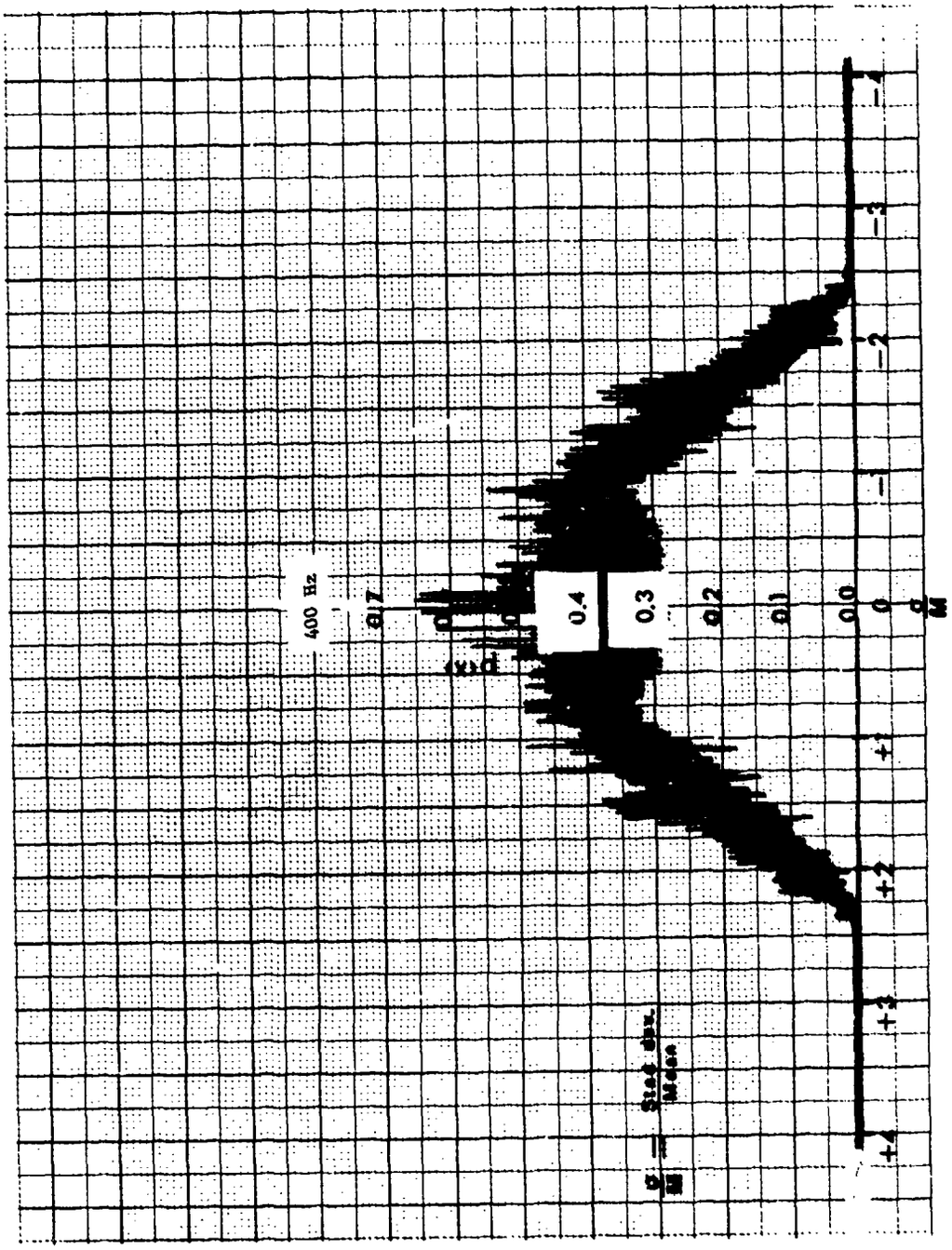

Figure 49. 5 Hz Probability Density of Test Spectrum at 400 Hz

Since the low frequency region is the most tractable of all we devised a set of diverging boundary lines based, in great part, on the results of this study augmented by some judgments from past experience. The very lowest gunfire frequency, in this case 100 Hz, amplitude is the most docile with an obvious need to increase ones tolerance with frequency. By the time we have reached the fourth harmonic (400 Hz) the spreading tolerances are being weighted by the random noise contributions.

The high frequency tolerances are set by the test jig and load characteristics (usually related to load magnitude), the levels of the random vibration spectrum, the frequency, and the equalizer-shaker capabilities. But in the main, we shall consider that tolerances are dominated, chiefly, by test load size. For small loads (weights less than 10 pounds, for example) one can control the spectrum of a typical shaker system within 3 to 4 dB. Such a tolerance curve is shown in Figure 50 and represents the basic tolerance curve (A) for both sine and random spectral control. This curve is restricted, in the random case, to test loads less than 10 pounds. For the sine tolerances no restrictions are set on either load or test level.

For loads equal to or greater than 10 pounds Figure 51 shows a curve surface (B) which allows random spectral tolerances to be added (as a function of frequency) to the basic tolerance of Figure 50.

Finally, for random vibration inputs greater than $0.1 g^2/Hz$, Figure 52 is provided to supply an incremental tolerance (curve C) which is a function of the random test level, to be added to the curves of Figures 50 and 51. Table 2 recapitulates the curve applications.

TABLE 2

TOLERANCE CURVES

	Sine	Random
$W < 10$ lbs, $G_{rmax} \leq 0.1\ g^2/Hz$	A	A
$W \geq 10$ lbs, $G_{rmax} \leq 0.1\ g^2/Hz$	A	A+B
$W < 10$ lbs, $G_{rmax} > 0.1\ g^2/Hz$	A	A+C
$W \geq 10$ lbs, $G_{rmax} > 0.1\ g^2/Hz$	A	A+B+C

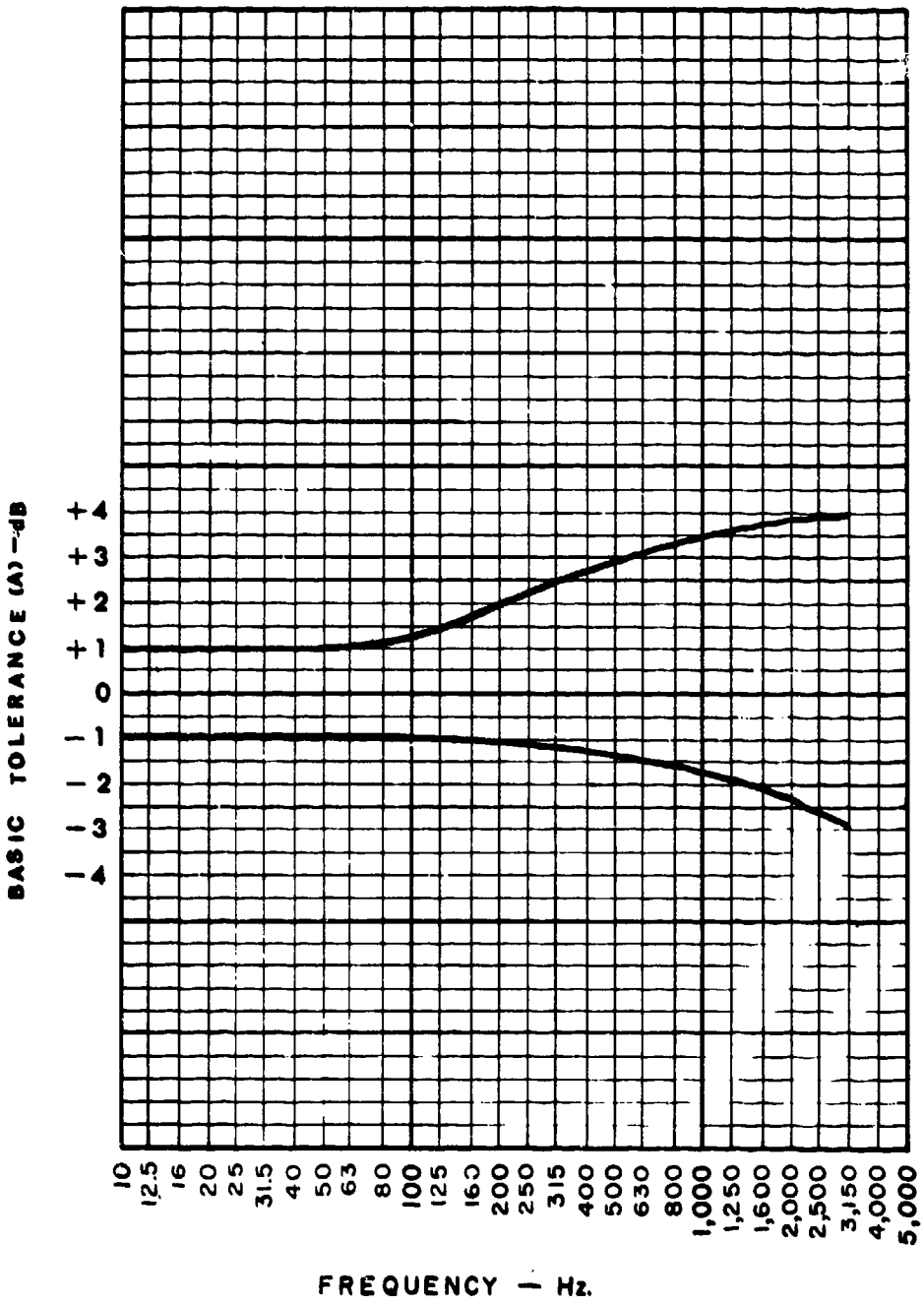

Figure 50. Basic Test Tolerance Curve for Equipments (W < 10 lbs)

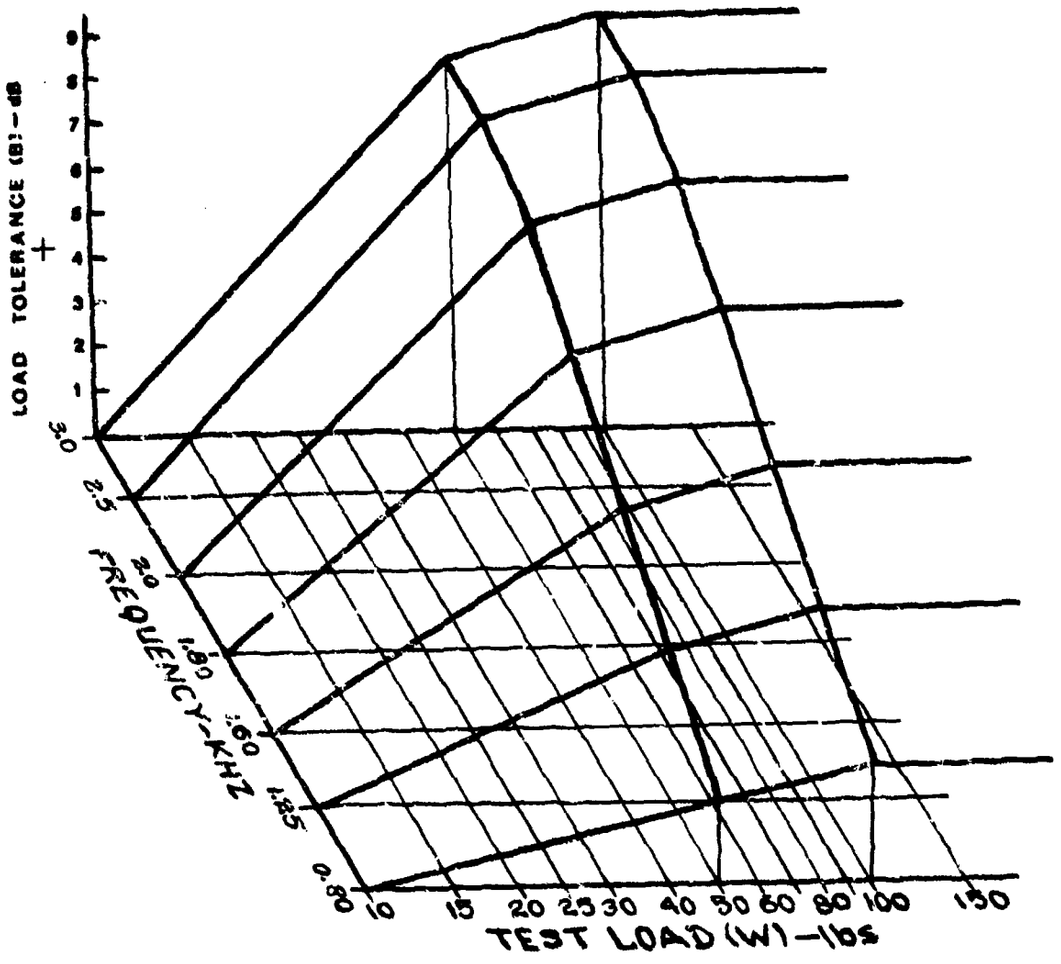

Figure 51. Test Tolerance Curve for Equipment (W ≥ 10 lbs)

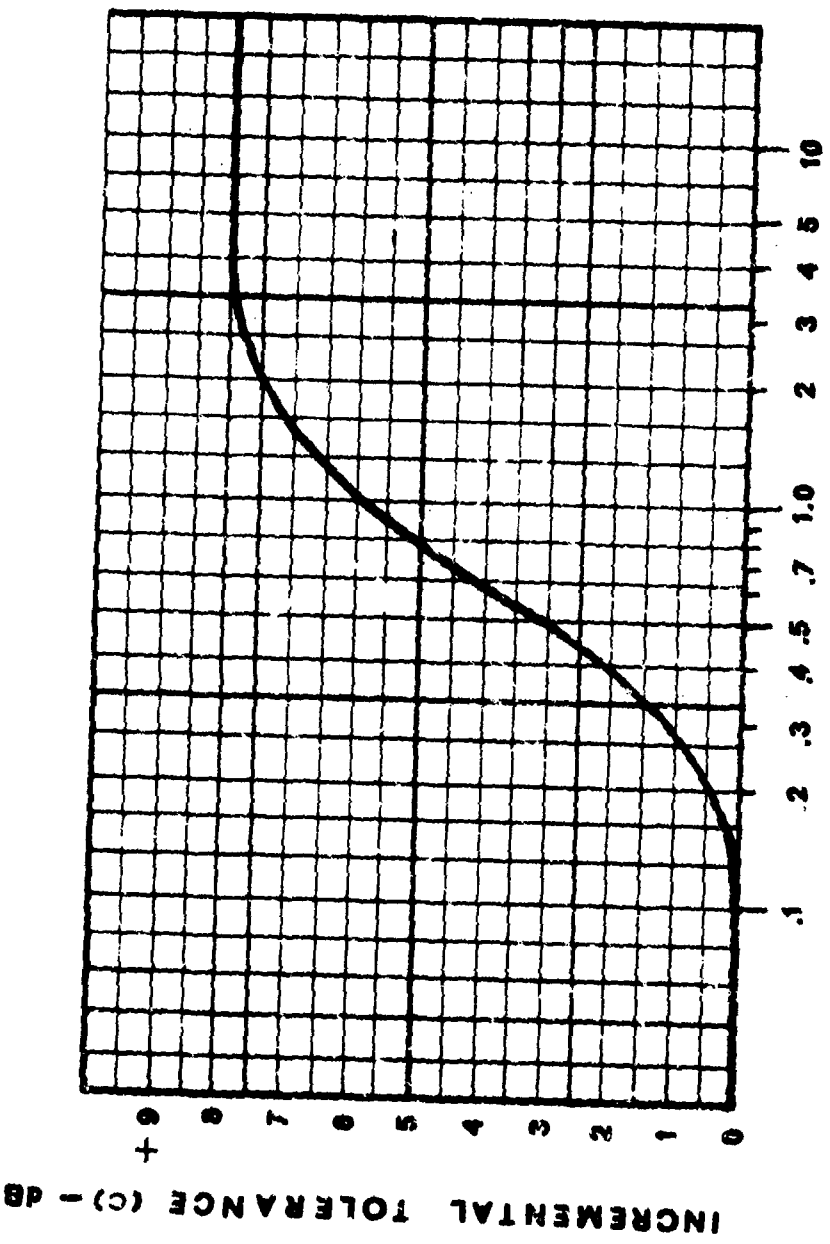

Figure 52. Test Incremental Tolerance for Levels ($G_{r\,max} > 0.1\ g^2/Hz$)

6. TEST ECONOMICS

Earlier, we had mentioned that there were other ways to approach gunfire simulation, noting the multiple servo method and its rather formidable costs. Here, we compare the two methods in order to provide a more concrete comparison of the costs between the two approaches.

The differences between the two, in the main, consist of the extra tracking filters and the four servo units. Thus for the four servo approach we have:

Four Tracking Filters		$14,000
Four Servos		10,000
	Total	$24,000

For the method developed in this program we have:

Two Tracking Filters		$7,000
Two Switching Consoles		400
	Total	$7,400

In practice the cost ratio advantage is even higher since most vibration test laboratories usually have one or two tracking filters on hand.

7. CONCLUSIONS

We have seen that the gunfire spectrum as originally synthesized can be successfully simulated utilizing existing vibration test facilities and in the following summary we review the more specific conclusions derived from this laboratory study.

(1). Four amplitude controlled, swept sinusoids can be mixed with a separate programmed random noise spectrum using relatively simple monitoring, recording, and switching techniques.

(2). Satisfactory tracking, monitoring, and control can be achieved using two tracking filters of 5 Hz bandwidth with RC averaging in accordance with the following criteria: 0.5 sec $\leq$ RC $\leq$ 1 sec.

(3). For optimum control the sweep time of the sinusoids (from low to high frequency) should be equal to or greater than 15 minutes.

(4). The necessary internal circuit modifications (see Appendix C) to current shaker systems are straight forward and inexpensive.

(5). The cost savings of this method compared to the multiple servo approach is approximately $17,000 per test facility.

APPENDIX A

METHOD 519.2 - GUNFIRE VIBRATION, AIRCRAFT

METHOD 519.2

GUNFIRE VIBRATION, AIRCRAFT

1. PURPOSE. The gunfire vibration test is conducted to simulate the relatively brief but very intense vibration fields resulting from blast pressure fields generated by repetitive firing guns mounted in, on or near the aircraft structure. This method applies to gun pod configurations and may also be used for helicopter gunships.

2. APPARATUS. Vibration shaker system with peripheral equipment and instrumentation.

3. CRITERIA FOR APPLICATION. The most severe vibration field results, primarily, from blast pressure pulses that transfer to the aircraft primary structure inducing a vibration field of maximum intensity near the gun muzzle region. This field, in an inverse relationship, decreases sharply as a function of the distance from the gun muzzle. Because of this marked variation; guns, physical locations, and ballistic parameters should be carefully and accurately identified prior to application of this test method.

In no case should this test method be substituted for conventional vibration tests but if the maximum test spectrum level of the gunfire configuration is equal to or less than the other specified vibration test levels the gunfire method need not be conducted.

3.1 Sensitive equipment. Equipments found most susceptible to gunfire are those equipments that are usually located within a 3-foot radius of the gun muzzle and are mounted on the structural surface exposed to the gun blast. Prime examples are UHF antennas of the blade, V, and the flush-mounted configurations, including their bracketry, coaxial connectors, and cables. Next in order of failure susceptibility is equipment mounted on drop-down doors and access panels, equipment mounted in cavities adjacent to and near the aircraft surface structure, and finally, equipment located in the interior of the vehicle. Typical vulnerable equipments in these latter categories are auxiliary hydraulic and power units (including mounting bracketry), switches, relays, IR, photographic, communication and navigation equipment and radar systems; including items either shock or hard mounted.

3.2 Equipments associated with mounting structures. Equipments are classified in accordance with the structure to which they are attached and are identified as either equipments mounted on primary structure or as equipments mounted on secondary structure.

3.2.1 Primary structure. Primary structure is that structure of the aircraft which comprises the main load carrying members or elements of the aircraft. Examples of primary structure are skin, frames, rings, bulkheads, stringers and includes those consoles structurally integrated with the aircraft outer walls.

3.2.2 Secondary structure. Secondary structure is that structure to which equipment is attached onto or contained in and whose mounting points terminate at the outer frame, skin, stringers, bulkheads, floors, spars or cast framing of the primary structure. Examples of secondary structure are instrument panels, trays, racks, shelves, trusses, beams, and consoles.

3.3 Determination of test spectrum. This method requires that the test spectrum for primary structure be determined first and then, if applicable--that is, for those equipments associated with secondary structure; the primary spectrum be modified to represent the final test spectrum.

The test spectrum consists of low frequency sinusoidals (basic gunfire rate and the second, third and fourth harmonics) superimposed on a continuous random vibration spectrum (see figure 519.2-1). The vibration prediction surfaces from which the spectrum for the primary structure is derived are shown in figures 519.2-2 through 519.2-4. Figure 519.2-2 represents the prediction surface for the sinusoids. Figure 519.2-3 is the surface used to obtain the high frequency random part of the spectrum. Figure 519.2-4 is the surface used to define the low frequency portion of the random spectrum. All surfaces are three dimensional isometric projections in which the surface shape varies as a function of the normalized frequency parameters f/f_0, f/f_0, and the vector distance, D. The frequency parameters are presented in this form since they are treated as variables. The distance parameter, D, represents the vector distance measured from the gun muzzle to the mean distance between equipment support points.

Note that the amplitude (vertical) scale is represented as a dB scalar ($10 \log_{10}$); thus, all values of the surfaces are referenced to 0 dB. To utilize these surfaces it is necessary to: first establish the magnitudes of the sine and the random vibration at the 0 dB level and then proceed to the D = x slice of the surface and pick off the required spectral values, relative to 0 dB.

3.3.1 Determination of the 0 dB level. The 0 dB level for the sine and random vibration is defined by the following equations.

$$G_{os} = \Gamma_s \, E/E_o \, r/r_o \, n/n_o \qquad (1)$$

$$G_{or} = \Gamma_r \, E/E_o \, r/r_o \, n/n_o \qquad (2)$$

G_{os} = 0 dB vibration level, mean squared g, sine (g^2)

G_{or} = 0 dB vibration level, accel. power spectral density (g^2/Hz)

E = blast energy of gun (ft-lbs/gun)

r = gun firing rate (Hz)

n = number of guns

E_o = blast energy of reference gun (M-61) = 55,000 ft-lbs/gun

r_o = gunfire rate of reference gun = 100 Hz

n_o = 1

Γ_s = maximum sine vibration level of reference gun = 2,000 mean squared g (g^2)

Γ_r = maximum random vibration level of reference gun = 35 g^2/Hz

A shortened form of (1) and (2) results when the reference parameters are inserted.

$$G_{os} = 3.64 \times 10^{-4} \, E \, r \, n \qquad (1a)$$

$$G_{or} = 6.36 \times 10^{-6} \, E \, r \, n \qquad (2a)$$

3.3.1.1 Determination of the gun blast energy (E). The gun blast energy is determined by the following equation.

$$E = fW^c/.3 - mv^2/2 \qquad (3)$$

f = specific impetus of explosive ($ft/lbs/_{lb}$)

W^c = weight/round of ammunition (lb/rd)

m = W_p/g = mass of projectile ($lbs\text{-}sec^2/ft$)

W_p = weight of projectile (lbs)

v = muzzle velocity of projectile (ft/sec)

g = 32.17 ft/sec^2

Table 519.2-IA is a general table which relates typical gunfire configurations to aircraft types. To facilitate identification of the ballistic parameters that are necessary to determine the gunfire vibration levels of 3.3, table 519.2-IB is provided. The table includes values of E, r, n and the muzzle velocity v; the table also includes the reference gun parameters of the M61. Table 519.2-IC is a repeat of this table using metric equivalents. Finally, a brief array of English-to-metric conversion constants are provided as specified in table 519.2-ID.

3.3.2 Adjustments of G_{os}, G_{or} (primary structure). The two 0 dB parameters shall be adjusted to account for the following additional conditions: gun standoff distance (H), gun muzzle configuration (M), equipment depth parameter (R) and equipment mass loading (W). The adjusted values G^a_{os} and G^a_{or} are the final 0 dB values from which the magnitude of any point (G_s, G_r) is established on the prediction surfaces of figures 519.2-2 through 4. These values and the individual adjustments are expressed in decibel form as follows:

$$10 \log_{10} \frac{G^a_{os}}{\Gamma_s} = 10 \log_{10} \frac{G_{os}}{\Gamma_s} + \Delta_h + \Delta_M + \Delta_R + \Delta_W \qquad (4)$$

$$10 \log_{10} \frac{G^a_{or}}{\Gamma_r} = 10 \log_{10} \frac{G_{or}}{\Gamma_r} + \Delta_h + \Delta_M + \Delta_R + \Delta_W \qquad (5)$$

$10 \log_{10} \frac{G^a_{os}}{\Gamma_s}$ = final, adjusted 0 dB value of the sine surface; referenced to Γ_s

$10 \log_{10} \frac{G^a_{or}}{\Gamma_r}$ = final, adjusted 0 dB value, of the random surface; referenced to Γ_r

Δ_h = reduction due to gun standoff distance (dB)

Δ_M = reduction due to gun muzzle configuration (dB)

Δ_R = reduction due to depth parameter (dB)

Δ_W = reduction due to mass loading (dB)

3.3.2.1 Test level reduction, Δ_h, of G_{os} and G_{or} due to gun standoff parameter (h/c). A reduction of G_{os}, G_{or} in accordance with the criteria of figure 519.2-5, shall be allowed for the case of gun configurations with muzzles mounted a perpendicular distance from the aircraft structure.

3.3.2.2 Test level reduction, Δ_M, of G_{os} and G_{or} due to free air configuration. A reduction of G_{os}, G_{or} shall be allowed for those cases in which the gun protrudes clear of and in front of the aircraft structure as shown in figure 519.2-6. The reduction shall be 6 dB; otherwise $\Delta_M = 0$ dB.

3.3.2.3 Test level reduction, Δ_R, of G_{os} and G_{or} as a function of R_s. The curve of figure 519.2-7 provides means by which G_{os} or G_{or} shall be reduced as a function of R_s.

3.3.2.3.1 Determination of the depth parameter (R_s). The depth parameter represents the shortest distance of the equipment mounting points to the aircraft surface as shown in figure 519.2-8. The measurement shall be taken from the equipment or mounting points that are nearest to the aircraft surface. If R_s is unknown or cannot be estimated, R_s shall be set at 3 inches or less.

3.3.2.4 Test level reduction, Δ_W, of G_{os} and G_{or} due to equipment mass loading. Figure 519.2-9 provides graphical means by which G_{os}, G_{or} may be reduced as a function of equipment weight. For those equipments attached directly to primary structure through vibration isolators; $\Delta_W = 0$. For equipments associated with secondary structure, $\Delta_W = 0$.

3.3.3 Determination of the distance parameter (D). The distance parameter represents the vector distance, measured (or estimated) from the gun muzzle to the mean distance between equipment support points. Where equipment support points are indeterminate, the equipment center of gravity shall represent the terminal point of D. The vector D is generated from the orthogonal distances referenced to the fuselage station, the water, and the butt line data. The D vector and the computational form is shown in figure 519.2-8.

3.3.3.1 Multiple guns, closely grouped. For configurations involving multiple guns, the origin of D is determined from the centroidal point of the gun muzzles. Figure 519.2-10 shows the origin location for a typical four-gun staggered array.

3.3.4 Application of gunfire prediction surfaces. Determine the value of D (see 3.3.3), establish the values of G^a_{os} and G^a_{or} (see 3.3.2); and using the locator grid at the top of figures 519.2-2 and 3, respectively, find the intersection points of f/f_o ($f/f_{o'}$) and D. From these points drop down vertically until the prediction surface is intersected. Measure the vertical distance with a ruler or dividers. Transfer this distance to the dB scale keeping the grid intercept in the zero dB plane. This distance, in dB, represents the magnitude of G_s or G_r referenced down from G^a_{os} or G^a_{or} (determined in 3.3.2).

The equational form for this procedure appears as the following:

$$10 \log_{10} \frac{G_s}{G^a_{os}} = dB_s \qquad (6)$$

$$10 \log_{10} \frac{G_r}{G^a_{or}} = dB_r \qquad (7)$$

G_s = a value of g^2 sine on the sinusoidal prediction surface at a given value of D and f/f_o (see figure 519.2-2)

G_r = a value of g^2/Hz on the high frequency random prediction surface at a given value of D and $f/f_{o'}$

dB_s = the value of G_s, in dB, referenced to G^a_{os}

dB_r = the value of G_r, in dB, referenced to G^a_{or}

3.3.4.1 Determination of the low frequency random spectrum. Reference to figure 519.2-4 shows that the maximum value of the low frequency random case ($G_{r\ max}$) occurs at $f/f_o = 2.0$ and has the same value for the high frequency spectrum at $f/f_{o'} = 0.7$. Since $G_{r\ max}$ has been determined for the high frequency random (3.3.4), transfer this value to figure 519.2-4 and plot (see 6. for an example).

3.3.4.2 Determination of f_o and $f_{o'}$. The value of the locator frequencies, f_o and $f_{o'}$, are as follows:

Sinusoidal Surface (Figure 519.2-2

f_o = 250 Hz

f_o = 200 Hz for items mounted on the aircraft skin

High Frequency Random Surface (Figure 519.2-3)

$f_{o'}$ = see Figure 519.2-11

Low Frequency Random Surface (Figure 519.2-4)

f_o = 300 Hz

3.3.4.3 Selection of fundamental gunfire frequency and the required harmonics. These properties shall be determined as follows:

Set the gunfire rate, r, = f_1 and let $f_2 = 2f_1$, $f_3 = 3f_1$ and $f_4 = 4f_1$

Note that the low frequency limit of the sine envelope of G_s (also the low frequency random envelop, G_r) shall be equal to $f_1 - .2f_1$. The upper frequency limit of the sine envelope, only, shall extend to $f_4 + .2f_4$.

3.3.5 Multiple guns, dispersed. For configurations characterized by guns placed at separate stations as shown in figure 519.2-12, determine each D vector to the equipment locations; and from this obtain their corresponding G_s and G_r values and, finally, add each set of values to obtain the predicted level.

3.3.6 Conversion of high frequency random spectrum, G_r. The high frequency random spectrum may be readily converted to discrete spectral values by multiplying G_r by its corresponding 1/3 octave bandwidth. The bandwidth (Δf) is determined by multiplying any given frequency (f) by .23.

3.3.7 Determination of overall RMS(OARMS). The overall RMS of the sine waves and the random noise spectrum is determined as follows:

$$OARMS = [G_{s1} + G_{s2} + G_{s3} + G_{s4} + OAMS_R]^{1/2} \qquad (8)$$

where: G_{s1}, G_{s2}, G_{s3}, G_{s4} = magnitude of sines (g^2)

$OAMS_R$ = overall mean squared g of the random noise spectrum (g^2)

3.3.7.1 Determination of overall mean squared random noise spectrum ($OAMS_R$). The $OAMS_R$ of the spectrum is determined as follows:

$$OAMS_R = A_1 + A_a^b + A_c^d \quad \text{(See figure 519.2-13)} \tag{9}$$

$$A_1 = G_{r\ max}\,[f_c - f_b] \tag{10}$$

where: $f_c = 0.7 f_{o'}$

$f_b = 600$ Hz

$$A_a^b = f_o\, G_{r\ max}\,[I_b - I_a] \tag{11}$$

where: $f/f_o = a$ and $f/f_o = b$ (See figure 519.2-13)

$[I_b - I_a]$ is the difference in ordinate values of I at $f/f_o = a$ and $f/f_o = b$ (See figure 519.2-14)

$$A_c^d = f_{o'}\, G_{r\ max}\,[I_d - I_c] \tag{12}$$

where: $f/f_{o'} = c$ and $f/f_{o'} = d$ (See figure 519.2-13)

$I_d - I_c$ is the difference in ordinate values of I at $f/f_{o'} = c$ and $f/f_{o'} = d$

(See figure 519.2-15)

3.3.7.1.1 Determination of $[I_b - I_a]$ and $[I_d - I_c]$. Refer to figure 519.2-16 and from a known value of D, select from the curve an appropriate value of β_f. From this curve pick off the appropriate values of the ordinate, I, at $f/f_o = a$ and $f/f_o = b$. Note that the properties a and b are determined from figure 519.2-13. Substitute these values in equation (11). $[I_d - I_c]$ is determined in the same manner except figure 519.2-17 is used to obtain $\beta_{f'}$; the slope factor for the high frequency random surface. Figure 519.2-15 is then used to obtain I_d and I_c. Substitute in eq. (12).

3.4 Determination of test levels (secondary structure). This paragraph shall apply to those equipment arrays located on or in secondary structure and whose aggregate of equipments and structure are of a size, weight and complexity to preclude the testing of the entire configuration as a single entity. In such cases the equipment may be removed from the secondary structure for individual vibration tests. Note that the equipment shall be excited in the isolated or hard mounted mode-in compliance with the actual mounting configuration in or on the secondary structure. All other equipments not identified with secondary structure shall be associated with primary structure and treated in accordance with 3.3.

Special transfer functions have been provided in order that the primary test spectrum G_s and G_r may be operated on to reflect a response spectrum which becomes the secondary, or input, test spectrum for the appropriate equipment. The operation and the resultant response spectrum Y_s and Y_r for the sine and the random case, respectively, is shown as follows:

$$G_s \, |H(f)|^2 = Y_s \qquad (13)$$

$$G_r \, |H(f)|^2 = Y_r \qquad (14)$$

Since G_s and G_r have been expressed in decibel form (see equations 6 and 7) and $|H(f)|^2$ is also expressed in this form (see figures 519.2-18 and 519.2-19) then Y_s and Y_r may be found by algebraically adding the spectral values of the primary structure to the appropriate transfer function as follows:

$$dB_{Y_s} = dB_s + dB_H \qquad (15)$$

$$dB_{Y_r} = dB_r + dB_H \qquad (16)$$

dB_{Y_s} = sine test spectrum for equipments associated with secondary structure

dB_{Y_r} = random test spectrum for equipments associated with secondary structure

dB_s = sine test spectrum for equipments associated with primary structure (re. $G_{s\ max}$)

dB_r = random test spectrum for equipments associated with primary structure (re. $G_{r\ max}$)

dB_H = transfer function $|H(f)|^2$ in decibel form

3.4.1 Equipment categories, secondary structure. Equipments mounted on or in secondary structures are designated in accordance with the following structural categories. Table 519.2-II provides generalized visual examples and also references corresponding transfer functions.

Category I - Equipment and groups of equipments mounted on or in racks and trays.

a. Isolated. Equipment whose secondary structure is terminated to the primary structure through vibration isolators. Examples: gen[illegible]ors, comnavigation units, data computers, forward looking radar.

b. Hard mounted. Equipments whose secondary structure is terminated to the primary structure through rigid attachments. Examples: power supplies, control boxes, switches, intervelometers, breakers, logic modules, inverters, inertial guidance and measurement units.

Category II - Equipment mounted in or on instrument panels.

a. Isolated. Equipment whose instrument panel is isolated.

b. Hard mounted. Equipment whose instrument panel is hard mounted.

Category III - Equipment mounted in or on beams, channels and trusses. These equipments are usually large, heavy and bulky.

a. Isolated. Equipments whose secondary structure is terminated to the primary structure through vibration isolators. Examples: cameras, radar packages.

b. Hard mounted. Equipments whose secondary structure is terminated to the primary structure through rigid attachments. Examples: cameras, inertial measurement units.

3.4.2 Application of $|H(f)|^2$. From table 519.2-II select the transfer function associated with the mounting category. These categories are represented by two sets of curves (figures 519.2-18 and 519.2-19) and allow envelope adjustments owing to the weight of the equipments.

The first set of curves (figure 519.2-18) involves a selection of κ as a function of equipment weight (there are exceptions to this rule noted in table 519.2-II). This value, κ, is then inserted into the f/f_{n_1} parameter as indicated at the bottom part of the transfer function curves. Normally, W is equivalent to the total equipment weight on the shelf panel, beam or truss. If stacked arrays of equipments are involved (consoles, etc.) then W is the total weight of the assembly and f_{n_1} is the average value of the shelf array.

Finally, in dB form algebraically add $|H(f)|^2$ to G_s and G_T at a sufficient number of their corresponding frequencies to insure a smooth spectral plot. In no case shall there be less than fifteen plot points over the test spectrum.

4. TEST IMPLEMENTATION. Test procedures used shall be as specified in the equipment specification or test plan.

4.1 Test item operation. Unless otherwise specified, the test item shall be operated during application of vibration so that functional effects caused by these tests may be evaluated. When a test item performance test is required during vibration and the time required for the performance is greater than the duration of the vibration test, the performance test shall be abbreviated accordingly. At the conclusion of the test, the test item shall be operated and the results obtained in accordance with General Requirements, 3.2. The test item then shall be inspected in accordance with General Requirements 3.2.

4.2 Mounting techniques. In accordance with General Requirements, 3.2, the test item shall be attached to the vibration exciter table by its normal mounting means or by means of a rigid fixture capable of transmitting the vibration conditions specified herein. Precautions shall be taken at the mechanical interfaces to minimize the introduction of undesirable responses in the test setup. Whenever possible, the test load shall be distributed uniformly on the vibration exciter table in order to minimize effects of unbalanced loads. Vibration amplitudes and frequencies shall be measured with instrumentation that will not significantly affect the test item input control or response. The input control accelerometer(s) shall be rigidly attached to the vibration table or to the intermediate structure, if used, at or as near as possible to the attachment point(s) of the test item.

5. TEST PROCEDURES

5.1 Procedure I, sine superimposed on random vibration. The test item shall be subjected to vibration along each mutually perpendicular axis. The excitation shall consist of four sinusoids superimposed over a random vibration background. The sinusoids shall be at frequencies representing the basic gunfire rate, and the second, third and fourth orders (f_1, f_2, f_3, f_4). Synchronously, the frequencies shall be swept over a bandwidth equal to $\pm.2f_1$, $\pm.2f_2$, $\pm.2f_3$, $\pm.2f_4$ beginning at the low frequency end and ending at the high frequency limit. The sweep time for the combination sine sweep and random vibration shall be 15 minutes per axis. The instantaneous peaks of the random vibration may be limited to 2.5 times the rms spectral acceleration level. The test envelope tolerances shall be as indicated in table 519.2-III and figures 519.2-20, 519.2-21 and 519.2-22.

5.2 Procedure II, single direction test. If the equipment item is mounted with the base peripherally attached onto and in the plane of the aircraft skin, then the test direction may be restricted to the direction normal to the aircraft skin (see figure 519.2-23). The total test time in this case shall be 30 minutes.

5.3 Procedure III, alternate test. For large equipment located near the gun muzzle, the overall test levels may exceed the force capabilities of all but the largest shaker systems. For such cases the sinusoidals may be separated from the random vibration and each test run independently -- each test shall run for 15 minutes per axis.

5.4 Procedure IV, alternate test (Pulse method). If no equipment is available to provide a test in accordance with Procedure I then a swept repetitive pulse technique may be used as an alternate method; provided that the pulse method is in compliance with the following requirements.

5.4.1 Spectral content. The generated spectrum shall consist of discrete acceleration magnitudes whose frequencies (f) correspond to the expression $f = nf_1$: where f_1 is the basic gunfire rate and n = 1, 2, 3 ...k. The last integer (k) is that value of n for which nf_1 is nearest to the maximum test frequency, 2 KHz.

5.4.2 Spectral magnitude and shape. The pulse test spectrum shall be defined by an envelope that outlines the discrete magnitudes of the low frequency sinusoids (formerly derived for Procedure I) and extends to connect with the envelop of the converted high frequency random spectrum as derived in 3.3.6. Note that the low frequency random spectrum of Procedure I is not used.

5.4.3 Pulse sweep parameters. The cycling time shall be the same as in 5.1 and the pulse rate (f_1) shall be continuously swept over the frequency bandwidth range as defined for f_1 in 5.1.

6. SUMMARY. The following details shall be specified in the equipment specification or test plan.

a. Gun identification and ballistic parameters (see tables 519.2-IA, 519.2-IB, 519.2-IC).

b. Gun configuration and location (see 3.3.2 and 3.3.3).

c. Equipment location on/in aircraft (fuselage station, water and butt line coordinates).

d. Equipment category (see 3.2.1, 3.2.2 and 3.4.1).

e. Distance from aircraft surface to nearest point of equipment (see 3.3.2.3.1).

f. Equipment weight (see 3.3.2.4, 3.4.2).

g. Test procedures (see 5).

REFERENCES

1. R. W. Sevy, E. E. Ruddell, "Low and High Frequency Aircraft Gunfire Vibration; Prediction and Laboratory Simulation," AFFDL-TR-74-123, August 1974.

2. R. W. Sevy, J. Clark, "Aircraft Gunfire Vibration; The Development and the Synthesis of Equipment Vibration Techniques," AFFDL-TR-70-131, November 1970.

7. EXAMPLES. The following examples are provided to facilitate the synthesis of the test spectrum for a number of typical cases ranging from equipments located on primary structure to those equipments associated with secondary structure.

7.1 An aerial refueling unit weighing 75 pounds is located in the nose section of the A-10 aircraft. The GAU/8, a 30 mm cannon is to be used and the firing rate (r) is to be 70 rounds/sec. The unit inserts into the aircraft flush with the skin and is bolted directly to the primary structure. The D vector is 48 inches and $R_s = 0$.

7.1.1 Determination of G_{os} and G_{or}. From 3.3.1 select equation (1) or (1a).

$$G_{os} = \Gamma_s \, E/_{E_o} \, r/_{r_o} \, n/_{n_o}$$

$$\Gamma_s = 2000 \ g^2$$

$$E/_{E_o} = 4.13 \text{ (see table 519.2-IB)}$$

$$r/_{r_o} = 70/_{100} = .7$$

$$n/_{n_o} = 1/_1 = 1$$

$$G_{os} = 2000 \ g^2 (4.13)(.7)(1)(1) = 5782 \ g^2$$

select equation (2) or (2a)

$$G_{or} = I_r \, E/_{E_o} \, r/_{r_o} \, n/_{n_o}$$

$$\Gamma_r = 35 \ g^2/Hz$$

$$G_{or} = 35 \ g^2/Hz \ (4.13)(.7)(1)(1) = 101.19 \ g^2/Hz$$

7.1.1.1 Test level reduction, Δ_h, of G_{os} and G_{or} due to gun standoff parameter (h/c). Owing to the gun configuration of this aircraft (see figure 519.2-5 and 519.2-6), $\Delta_h = 0$ dB.

7.1.1.2 Test level reduction, Δ_M, of G_{os} and G_{or} due to free air configuration. This is a free air configuration (see 3.3.2.2 and figure 519.2-6); Δ_M = -6 dB.

7.1.1.3 Test level reduction, Δ_R, of G_{os} and G_{or} as a function of R_s. See figure 519.2-7. Since $R_s = 0$; $\Delta_R = 0$ dB

7.1.1.4 Test level reduction, Δ_W, of G_{os} and G_{or} due to equipment mass loading. Refer to figure 519.2-9. Since the equipment weight (W) is 75 pounds G_{os} and G_{or} may be reduced 2.6 dB (10 $\log_{10}$); thus Δ_W = -2.6 dB.

7.1.2 Adjustments of G_{os}, G_{or} (primary structure). Refer to equations (5) and (6) of 3.3.2 and insert the dB reductions.

$$10 \log_{10} \frac{G_{os}^a}{\Gamma_s} = 10 \log_{10} \frac{G_{os}}{\Gamma_s} + (0) + (-6) + (0) (-2.6)$$

where: $G_{os} = 5782\ g^2$

$\Gamma_s = 2000\ g^2$

$10 \log_{10} (2.891) - 8.6$ db = 4.6 dB - 8.6 db = - 4 dB re. 2000 g^2

$G_{os}^a = (2000)(.398) = 796\ g^2 = 28.21$ grms = 0 dB (figure 519.2-2)

Also, the dB adjustments are the same for G_{or}, so using equation (6) of 3.3.2

$$10 \log_{10} \frac{G_{or}^a}{\Gamma_r} = 10 \log_{10} \frac{G_{or}}{\Gamma_r} - 8.6 \text{ dB}$$

where: $G_{or} = 101.19\ g^2/Hz$

$\Gamma_r = 35\ g^2/Hz$

$10 \log_{10} 2.891 - 8.6$ db = 4.6 dB - 8.6 dB = - 4 dB re. 35 g^2/Hz

$G_{or}^a = (35)(.398) = 13.93\ g^2/Hz$ = 0 db (figure 519.2-3)

7.1.3 Determination of the locator frequencies f_o and $f_{o'}$. From 3.3.4.2 select: f_o = 200 Hz for the sinusoidal surface, f_o = 300 Hz for the low frequency random surface and from figure 519.2-11 select (from the curve at W = 75 lbs): $f_{o'}$ = 900 Hz.

7.1.4 Determination of the sinusoidal surface, G_s. Refer to figure 519.2-2. It is useful to draw lines on the figure hence it is advantageous to make a copy. On the copy draw a line in the zero dB plane parallel to the constant D lines at D = 48 inches. Note that this line intersects the f/f_o parameter. From the intersections draw vertical lines down to the heavy, constant f/f_o lines of the prediction surface. These distances down are now transferred to the left hand dB scale (3.3.4). Recalling that f_o = 200 Hz for the sinusoidal surface arrange a table of values of G_s vs f/f_o as follows:

f/f_o	f	G_s (dB re. G^a_{os})	G^a_{os} = 796 g^2/28.2 grms
2.0	400	- 11.6 = 55.07 g^2	= 7.42 grms
1.6	320	- 12.3 = 46.86 g^2	= 6.85 grms
1.2	240	- 13.8 = 33.19 g^2	= 5.76 grms
1.0	200	- 15.5 = 22.43 g^2	= 4.74 grms
0.8	160	- 18.6 = 10.98 g^2	= 3.31 grms
0.6	120	- 20.5 = 7.09 g^2	= 2.66 grms
0.4	80	- 22.0 = 5.02 g^2	= 2.24 grms
0.2	40	- 23.0 = 3.98 g^2	= 1.99 grms

For plotting purposes it is convenient to express the values of G_s relative to G_s at f/f_o = 2.0; which is $G_{s\ max}$. This is done by subtracting $G_{s\ max}$ (-11.6 dB) from all of the values.

f/f_o	f	$G_s - G_{s\ max}$ (dB_s)
2.0	400	0 dB re. 55.07 g^2 = 7.42 grms
1.6	320	- 0.7
1.2	240	- 2.2
1.0	200	- 3.9
0.8	160	- 7.0
0.6	120	- 8.9
0.4	80	- 10.4
0.2	40	- 11.4

Before proceeding to the next step it is instructive to pause and observe that were we concerned with defining a test spectrum for secondary structure (3.4) it is now only necessary to attach the required dB_H column to the right of the present dB_s column and add the values to obtain the response, dBy_s.

7.1.4.1 Setting up the sine spectrum. Plot the envelope of G_s as a function of frequency (see 3.3.4.1) and designate the fundamental and harmonics as follows:

1. Set $f = f_1 = 70$ Hz, $f_2 = 2(70) = 140$ Hz, $f_3 = 3(70) = 210$ Hz and $f_4 = 4(70) = 280$ Hz

2. Pick off the four corresponding values of dB_s from the plot (re. 55.07 g^2 or 7.42 grms)

   - @ 70 Hz G_{s1} = - 10.7 dB = 4.69 g^2 = 2.16 grms
   - @ 140 Hz G_{s2} = - 8.1 dB = 8.53 g^2 = 2.92 grms
   - @ 210 Hz G_{s3} = - 3.9 dB = 22.43 g^2 = 4.74 grms
   - @ 280 Hz G_{s4} = - 1.3 dB = 40.82 g^2 = 6.39 grms

3. Establish the cycling range for each sinusoid.

$f_1 = \pm .2(f_1) = \pm .2(70) = 56$ to 84 Hz

$f_2 = \pm .2(f_2) = \pm .2(140) = 112$ to 168 Hz

$f_3 = \pm .2(f_3) = \pm .2(210) = 168$ to 252 Hz

$f_4 = \pm .2(f_4) = \pm .2(280) = 224$ to 336 Hz

Note that the low end of the cycling range ($f_1 - .2f_1$) is 56 Hz and is also the low end of the low frequency random spectrum (see 3.3.4.3 and figure 519.2-11).

7.1.5 Determination of the high frequency random surface, G_r. Refer to figure 519.2-3 and at the intersections of f/f_o' and D = 48 inches record the following values of G_r. Note that f_o' = 900 Hz (see 3.3.4.2).

f/f_o'	f	G_r (dB re. G_{or}^a) $G_{or}^a = .393\ g^2/Hz$
.7	630	- 13.7 = .594 g^2/Hz
.89	800	- 16.2 = .334 g^2/Hz
1.0	900	- 18.2 = .205 g^2/Hz
1.11	1000	- 20.1 = .135 g^2/Hz
1.39	1250	- 24.0 = .060 g^2/Hz
1.78	1600	- 29.2 = .056 g^2/Hz
2.22	2000	- 33.5 = .006 g^2/Hz

Make $G_{r\ max}$ the reference value by subtracting it from all the values of G_r.

f/f_o	f	G_r-$G_{r\ max}$ (dB_r)
.7	630	0 dB re. .594 g^2/Hz
.89	800	- 2.5
1.0	900	- 4.5
1.11	1000	- 6.4
1.39	1250	-10.3
1.78	1600	-15.5
2.22	2000	-19.8

Plot G_r vs f or f/f_o, as desired.

7.1.6 Determination of the low frequency random spectrum, G_r. Refer to figure 519.2-4. The maximum value ($G_{r\ max}$) occurs at f/f_o = 2.0 and D = 48 inches. Set $G_{r\ max}$ equals $G_{r\ max}$ of the high frequency random, that is, $G_{r\ max}$ = .594 g^2/Hz. Measure, as in the previous steps, the values of G_r, noting that $G_{r\ max}$ measures - 11.3 db down from 0 dB of the figure. Define the values of G_r relative to $G_{r\ max}$ by subtracting from all values of G_r. Note, finally, that f_o = 300 Hz (see 3.3.4.2).

f/f_o	f	G_r-$G_{r\ max}$ (dB_r)
2.0	600	0 db re. .594 g^2/Hz
1.6	480	- 0.7
1.2	360	- 2.5
1.0	300	- 4.7
0.8	240	- 8.3
0.6	180	- 11.1
0.4	120	- 12.8
0.2	60	- 13.8

The final test spectrum is shown in figure 519.2-1.

7.1.7 Determination of overall RMS(OARMS). Refer to 3.3.6 and figure 519.2-13. Using equation (8)

$$OARMS = [G_{s1} + G_{s2} + G_{s3} + G_{s4} + OAMS_R]^{1/2}$$

7.1.7.1 Determination of mean squared sines ($G_{s1} + G_{s2} + G_{s3} + G_{s4}$).

Sum the squares of the four sines

$$G_{s1} + G_{s2} + G_{s3} + G_{s4} = 4.69 + 8.53 + 22.43 + 40.83$$
$$= 76.5\ g^2$$

7.1.7.2 Determination of overall mean squared random noise spectrum ($OAMS_R$)

Using equation (9)

$$OAMS_R = A_1 + A_a^b + A_c^d$$

$$A_1 = G_{r\ max}\ [f_c - f_b]$$

where: $f_c = 0.7\ f_o' = 630$ Hz

$f_b = 600$ Hz (see figure 519.2.13)

$A_1 = .594(30) = 17.82\ g^2$

$A_a^b = f_o\ G_{r\ max}[I_b - I_a]$ (see figure 519.2-13)

where: $f_o = 300$ Hz

$G_{r\ max} = .594\ g^2/Hz$

$A_a^b = 178.2[I_b - I_a]$

and, $A_c^d = f_o'\ G_{r\ max}[I_d - I_c]$

where: $f_o' = 900$ KHz

$G_{r\ max} = .594\ g^2/Hz$

$A_c^d = 534.6[I_d - I_c]$

7.1.7.3 Determination of $[I_b - I_a]$ and $[I_d - I_c]$

From figure 519.2-16 select at D = 48 inches; a β_f = .300

From figure 519.2-15 select at β_f = .300 and f/f_o = a = f_1/f_o = .233; a value of I_a = .041

At f/f_o = b = 2.0 select a value of I_b = 1.053

$[I_b - I_a]$ = 1.012

substituting in eq. (11)

$A_a^b = 178.2\ [1.012] = 180.3\ g^2$

From figure 519.2-17 select at D = 48 inches; a $\beta_{f'}$ = .511

From figure 519.2-24 select at $\beta_{f'}$ = .511 and f/f_o = c = .7; a value of I_c = 0

At f/f_o = d = .222 select a value of I_d = .435

Substituting in eq. (12)

$A_c^d = 534.6\ [.435] = 232.6\ g^2$

Add random noise

$A_1 + A_a^b + A_c^d = 17.82\ g^2 + 180.3\ g^2 + 232.6\ g^2$

$= 430.7\ g^2$

Add sines: $430.7\ g^2 + 76.5\ g^2 = 507.2\ g^2$

Take the square root:

$OARMS = (507.2)^{1/2} = 22.5$ grms

7.2 An A-7D utilizes a 20 mm (M61) cannon with a firing rate of 100 Hz. The instrument panel is shock mounted (45 Hz), weighs 75 pounds and the vector distance, D, is determined to be 49.6 inches from the nearest mount of the panel. R_s is equal to 2 inches and the gun standoff distance is zero. Determine the gunfire vibration spectrum of an altimeter indicator rigidly mounted to the instrument panel.

7.2.1 Determination of G_{os} and G_{or}. From equations (1) and (2)

$$G_{os} = 2000\ (1/_1)\ (1/_1)\ (1/_1) = 2000\ g^2$$

$$G_{or} = 35\ (1/_1)\ (1/_1)\ (1/_1) = 35\ g^2/Hz$$

7.2.2 Determination of G^a_{os} and G^a_{or}.

$\Delta_h = 0$ dB (see 3.3.2.1)

$\Delta_M = 0$ dB (see 3.3.2.2)

$\Delta_{R_s} = -0.2$ dB (see 3.3.2.3)

$\Delta_W = 0$ dB (see 3.3.2.4)

Using equations (4) and (5)

$$10 \log_{10} \frac{G^a_{os}}{\Gamma_{os}} = 10 \log_{10} \frac{G_{os}}{\Gamma_{os}} - 0.2 \text{ dB}$$

$$= -0.2 \text{ dB re. } 2000\ g^2$$

$$G^a_{os} = (.9550)(2000) = 1910\ g^2 = 0 \text{ dB}$$

$$G^a_{or} = (.9559)(35) = 33.43\ g^2/Hz = 0 \text{ dB}$$

7.2.3 Determination of dB_s, dB_H and dB_{Y_s}. Utilizing the procedures detailed in 7.1 we assemble the following table. From 3.3.4.2, f_o is set at 250 Hz.

Sinusoidal Spectrum

$G^a_{os} = 1910\ g^2$

$f_o = 250$ Hz

f/f_o	f	G_s (re. G^a_{os})	dB_s (re. $G^s_{s\ max}$)	+ dB_H	= dB_{Y_s}	g^2/grms
2.0	500	-14.7	0.0	-13.0	-13.0	3.24/1.80
1.6	400	-15.2	-0.5	-11.8	-12.3	3.80/1.95
1.2	300	-16.8	-2.1	-10.0	-12.1	4.00/2.00
1.0	250	-18.6	-3.9	- 8.6	-12.5	3.65/1.91
0.8	200	-21.1	-6.4	- 6.8	-13.2	3.10/1.76
0.6 *	150	-23.0	-8.3	- 3.7	-12.0	4.00/2.00
0.4	100	-24.0	-9.3	+ 1.8	- 7.5	11.6/3.40
0.32	80	-24.4	-9.7	+ 4.0	- 5.7	17.39/4.17

The transfer function dB_H appears as a column that, in frequency correspondence, is added to dB_S. The details of this derivation now follow.

From 3.4 note equations (15) and (16). Go to table 519.2-II, Category II(a). The block, concerning a known f_{n_1}, requires that κ (figure 519.2-18) be set at 2.0; independent of equipment weight. From figure 519.2-18 insert $\kappa = 2$ as indicated in the f/f_{n_1} parameter. Also insert $f_{n_1} = 45$ Hz. This step establishes the low frequency scale. Note that each octave of frequency is divided into three bands. This scale is, therefore, 1/3 octave. To obtain the frequency in the upper adjacent 1/3 octave it is only necessary to multiply the preceding frequency by 1.26.

Establish frequencies corresponding to the sinusoidal surface (G_s), previously developed. Measure dB_H values (preferrably with dividers) and enter in the column designated dB_H. In accordance with equation (15) add dB_H to dB_S to obtain dB_{Y_s}; the desired spectrum. Remember that dB_{Y_s} is referenced to $G_{S\ max}$ which is - 14.7 dB relative to G^a_{os}. Thus, $G_{S\ max} = (.03388)(1910\ G^2) = 64.7\ g^2 = 8.04$ grms.

Plot the sinusoidal spectrum.

7.2.4 Determination of dB_r, dB_H and dBy_r (High frequency random). Following the steps detailed in 6.1 for the high frequency random curve and making use of figure 519.2-11 to obtain $f_{o'}$ = 920 Hz the following table is constructed.

High Frequency Random

G^a_{or} = 33.43 g^2/Hz

$f_{o'}$ = 920 Hz

$f/f_{o'}$	f	G_r (re. G^a_{or})	dB_r (re. $G_{r\ max}$)	+ dB_H	= dBy_r	g^2/Hz
0.7	644	-14.3	0.0	-12.2	-12.2	.075
0.89	818	-17.0	-2.7	-12.0	-14.7	.042
1.0	920	-18.5	-4.2	-12.3	-16.5	.028
1.11	1021	-20.6	-6.3	-12.1	-18.4	.019
1.39	1279	-24.5	-10.2	-12.4	-22.6	.007
1.78	1638	-29.1	-14.8	-12.7	-27.5	.002
2.22	2042	-33.6	-19.3	-13.2	-32.5	.001

Again, note that $G_{r\ max}$ is -14.3 dB down from G^a_{or} or $G_{r\ max}$ = (.03715) (33.43) = 1.241 g^2/Hz. In turn, dBy_r is referenced to $G_{r\ max}$ and represents the high frequency test spectrum for the altimeter. The final right hand column is the vibration spectrum in units of g^2/Hz. The high frequency spectrum may now be plotted.

7.2.5 Determination of dB_r, dB_H and dBy_r (Low frequency random). Repeating the past procedures of 7.1 and noting from 3.3.4.2 that f_o = 300 Hz the following table is constructed.

Low Frequency Random

$G_{r\ max} = 1.241\ g^2/Hz$
$f_o = 300$ Hz

f/f_o	f	G_r (re. 0 dB)	dB_r (re. $G_{r\ max}$)	+ dB_H	= dBY_r	g^2/Hz
2.0	600	-12.0	0.0	-12.2	-12.2	.075
1.6	480	-12.6	- 0.6	-12.4	-13.0	.063
1.2	360	-13.8	- 1.6	-12.7	-14.3	.047
1.0	300	-16.6	- 4.6	-12.9	-17.5	.023
0.8	240	-19.8	- 7.8	-13.3	-21.1	.009
0.6	180	-22.8	-10.8	-14.1	-24.9	.005
0.4	120	-24.2	-12.2	-15.0	-27.2	.002
0.27	80	-24.9	-12.9	-16.0	-28.9	.002

Note that G_r is measured relative to the 0 dB of figure 519.2-4; not relative to $G_{r_{max}}$, as was done in 7.2.3 and 7.2.4. Following this, G_r at f/f_o = 2.0, is subtracted from the G_r column to obtain dB_r which now has a 0 dB level at f/f_o = 2.0. This level (0 dB) is then set to correspond to $G_{r\ max} = 1.241\ g^2/Hz$ and dBY_r then is referenced to $G_{r\ max}$. The last column on the right indicated the spectral values in g^2/Hz.

The low frequency random spectrum may be plotted. The complete test spectrum is shown in figure 519.2-24.

7.2.6 The OAMS. The overall $(RMS)^2$ is determined for the primary structure spectrum only. This value is always greater than the spectrum for the secondary structure and, therefore, provides a conservative estimate of the overall force requirements of the shaker.

7.2.7 Determination of the blast energy, E. To illustrate the application of the blast energy equation (3) an example is presented for the reference gun (M-61).

MIL-STD-810C

$$E_o = f(W^c)/.3 - m_o v_o^2/2$$

where: $f = 330 \times 10^3$ ft-lbs/lb

$W_o^c = 600$ grains $= .086$ lb

$W_p = .223$ lb/rd

$V_o = 3380$ ft/sec

$g = 32.17$ ft/sec^2

$$E_o = \frac{330 \times 10^3 (.086)}{.3} - \frac{.223(3380)^2}{32.17(2)}$$

$E_o = 94{,}600 - 39{,}600 = 55{,}000$ ft/lb/gun

TABLE 519.2-IA. Typical gun configurations associated with aircraft classes

Gun Configuration	Aircraft	Installation (Typical)	Gun Caliber (mm)	Gun Caliber (in)
M61	F-104 F-105 F-111 F-4 F-100 B-58 B-52 A-7	Various Fixed (Forward Bomb Bay) SUU-16, on racks, tail turrets	20	.79
M39	F-5 F-100 F-101 B-57 B-52	2 or 4 in nose or back of nose or tail turret	20	.79
MK11	A-4 F-4 A-7 A-6	MK4 C.L. POD inboard wing, etc.	20	.79
MK12	A-4	1 at each wing root	20	.79
M3	A-1E	2 each wing	20	.79
M24	B-52 F-86	Tail turret 4 or 6 nose	20	.79
M3	B-52 B-26 B-57 F-86 HH-53 A-1	Tail turret up to 6 in nose	12.7	.50

TABLE 519.2-IA. (Continued)

Gun Configuration	Aircraft	Installation (Typical)	Gun Caliber (mm)	Gun Caliber (in)
GAU-2B/A	OH-6A AC-47 AC-130 A-37 UH-1 CH-3 AH-1	side-looking, nose, and up to 8 PODS	7.62	.30
GAU-4/A	F-4	POD, inboard, wing	20	.79
GAU-8/A	A-10	nose	30	1.18

TABLE 519.2-1B. Ballistic tables for typical gun configurations (English units)

Gun	Gun Caliber (mm)	Gun Caliber (in)	Propellant Weight W_c (gr)	Propellant Weight W_c (lbs)	Propellant S. Impetus I_s (ft-lbs/lb)	Chg. Energy E_c (ft-lbs)	Firing Rate F rds/min	Firing Rate F rds/sec	Projectile weight W_p (gr)	Projectile weight W_p (lbs)	Muzzle Vel. v_o (ft/sec)	Muzzle Energy $W_p v^2/2g$ (ft-lbs)	Blast Energy E (ft-lbs)	E/E_o
M61 (note 1)	20	.79	600 (nom) 590 to 610	.086	330×10^3	94.6×10^3	6,000 (nom) 1,000 (min)	100 (max) 17 (min)	1,560 (avg)	.223 (avg)	3,380 (nom) 3,250 to 3,450	39,600	55,000	1.0
M39	20	.79	See M61	See M61		See M61	1,500	25	1,560 (avg)	.223 (avg)	3,380 (nom) 3,250 to 3,450	39,600	55,000	1.0
MK11	20	.79	645 (nom) 680 to 650	.095		105×10^3	4,000 (max) 750 (min)	67 (max) 12.5 (min)	1,700	.243	3,300	41,200	63,800	1.16
MK12	20	.79	See MK11			See MK11	1,000	16.68	1,700	.243	3,300	41,200	63,800	1.16
M3	20	.79	600 (nom)	.086		See M61	800	13.33	2,000	.286	2,700	33,400	51,200	1.11
M24	20	.79	590 (nom)	.084		92,730	800	13.33	2,000	.286	2,700	33,400	59,330	1.08
M3	12.7	.50	237	.034		37,400	1,200 (nom)	20	709	.114	3,400	18,196	19,304	.351

Note 1: Reference gun, where v_o = 3380 ft/sec, r_c = 100 in, and n_g = 1

TABLE 519.2-10. (Continued)

Gun	Gun Caliber (mm) (in)	Propellant Weight W_c (gr)	Propellant Weight W_c (lbs)	Propellant S. Impetus f (ft-lbs/lb)	Propellant Chg. Energy E_c (ft-lbs)	Rifling Rate (rds/min)	Rifling Rate (rds/sec)	Projectile weight W_p (gr)	Projectile weight W_p (lbs)	Muzzle Vel. v (ft/sec)	Muzzle Energy $\frac{W_p v^2}{2g}$ (ft-lbs)	Blast Energy E (ft-lbs)	E/E_0
GAU-2B/A	7.62 .30	47	.0857	330 x 10^3	7.38 x 10^3	6,000 (sus) 1,500 (min)	100	150	.021	2,750	2,460	4,810	.087
GAU-4/A	20 .79	600	.386	See MIL		6,000 (max) 1,000 (min)	100 (max) 17 (min)	1,560 (avg)	.223 (avg)	3,300 (max) 3,250 to 3,450	39,800	58,000	1.0
GAU-8/A	30 1.18	2,300	.341		375,100	4,200 (max) 2,100 (min)	70 (max) 35 (min)	5,000	.825	3,400	140,200	227,000	4.12

TABLE 519.2-IC. Ballistic tables for typical gun configurations (Metric units)

Gun	Gun Caliber (mm)	Gun Caliber (in)	Propellant Weight W_c (gr)	Propellant Weight W_c (kg)	Propellant S. Impetus f (m-kg/kg)	Propellant Chg. Energy E_c (n-m)	Firing Rate r rds/min	Firing Rate r rds/sec	Projectile weight w_p (gr)	Projectile weight w_p (kg)	Muzzle Vel. v (m/sec)	Muzzle Energy $w_p v^2/2g$ (n-m)	Blast Energy E (n-m)	E/E_o
M61 (Note 1)	20	.79	600	.030	45,630	128,300	6,000 (nom) 1,000 (min)	100 (max) 17 (min)	1,560 (avg)	.101 (avg)	1,030	53,700	74,600	1.0
M39	20	.79	600	.030		128,300	1,500	25	1,560 (avg)	.101 (avg)	1,030	53,700	74,600	1.0
MK11	20	.79	665	.043		142,400	4,000 (max) 750 (min)	67 (max) 12.5 (min)	1,700	.110	1,006	55,867	86,500	1.16
MK12	20	.79	665	.043		142,400	1,000	16.63	1,700	.110	1,006	55,867	86,500	1.16
M3	20	.79	600	.038		128,300	800	13.33	2,000	.130	823	45,300	83,500	1.11
M24	20	.79	590	.038		125,700	800	13.33	2,000	.130	823	45,300		1.08
M3	12.7	.50	237	.015		50,700	1,200 (nom)	20	709	.046	1,036	24,700	26,000	.351

Note 1: Reference gun, where; v_o = 1030 m/sec, r_o = 100 Hz and n_o = 1

TABLE 519.2-1C. (Continued)

Gun	Gun Caliber (mm)	Gun Caliber (in)	Propellant Weight W^c (gr)	Propellant Weight W^c (kg)	Propellant S. Impetus f (m-kg/kg)	Propellant Chg. Energy E^c (m-m)	Firing Rate r rds/min	Firing Rate r rds/sec	Projectile weight W_p (gr)	Projectile weight W_p (kg)	Muzzle Vel. v (m/sec)	Muzzle Energy $W_p v^2/2g$ (m-m)	Blast Energy E (m-m)	E/E_o
GAU-2B/A	7.62	.30	47	.003	45,630	10,000	6,000 (nom) 1,500 (min)	100 25 (min)	150	.010	838	3,414	5,685	.007
GAU-4/A	20	.79	600	.039		128,300	6,000 (nom) 1,000 (min)	100 (max) 17 (min)	1,560 (avg)	.101	1,030	53,700	74,600	1.0
GAU-8/A	30	1.18	2,340	.156		508,500	4,200 (max) 2,100 (min)	70 (max) 35 (min)	5,800	.376	1,036	201,000	387,500	4.12

TABLE 519.2-IO. Conversion table - English to Metric units

lbs x (0.4536)	= kg
grams x (10^{-3})	= kg
grains x (6.480×10^{-5})	= kg
inches x (25.4)	= mm
feet x (0.3048)	= meters
feet/sec x (0.3048)	= meters/sec
feet-lbs x (.1383)	= m - kgf
kgf x (9.807)	= newtons
newton x meter	= joule

TABLE 519.2-II Secondary structure transfer functions associated with equipment categories

Equipment Category	Examples	Remarks	$\|H(f)\|^2$	
			If f_{n_1} is known	If f_{n_1} is unknown	f_{n_2}
I(a)		f_{n_1} is the lowest vertical translation frequency of the isolated system	See Fig 519.2-18	See Fig 519.2-18 select: f_{n_1} = 45 Hz	See Fig 519.2-18
I(b)			See Fig 519.2-19	See Fig 519.2-19 select: f_{n_1} = 60 Hz	See Fig 519.2-19
II(a)		For instr. panels only D is measured from the gun muzzle to the nearest panel mount or attach point.	See Fig 519.2-18 select: α = 2.0	See Fig 519.2-18 select: α = 2.0 f_{n_1} = 60 Hz	See Fig 519.2-18

TABLE 519.2-II (continued)

Equipment Category	Examples	Remarks	$b_k(n)^3$ if f_{n_1} is known	$b_k(n)^3$ if f_{n_1} is unknown	f_{n_2}
II(b)	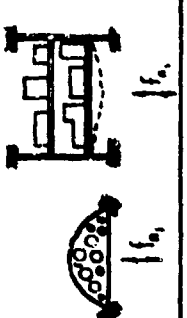	If 3 or more sides of the shelves are attached (other than at the corners) to the walls, bulkheads or outer structural surfaces (frames, stringers, etc.) use the criteria of 3.2.1. (Instr. panels only see II (b)	see I(b)		see Fig 519.2-10
III(a)			see I(a)		see Fig 519.2-10
III(b)	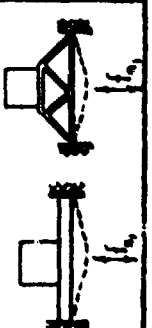		see I(b)		see Fig 519.2-10

TABLE 519.2-III Gunfire test tolerances

	Sine	Random
$W < 10$ lbs	A	A
$G_{r\ max} < .1\ g^2/Hz$	A	A
$W \geq 10$ lbs	A	A+C
$G_{r\ max} \geq .1\ g^2/Hz$	A	A+B
$G_{r\ max} \geq .1\ g^2/Hz$ and $W \geq 10$ lbs	A	A+B+C

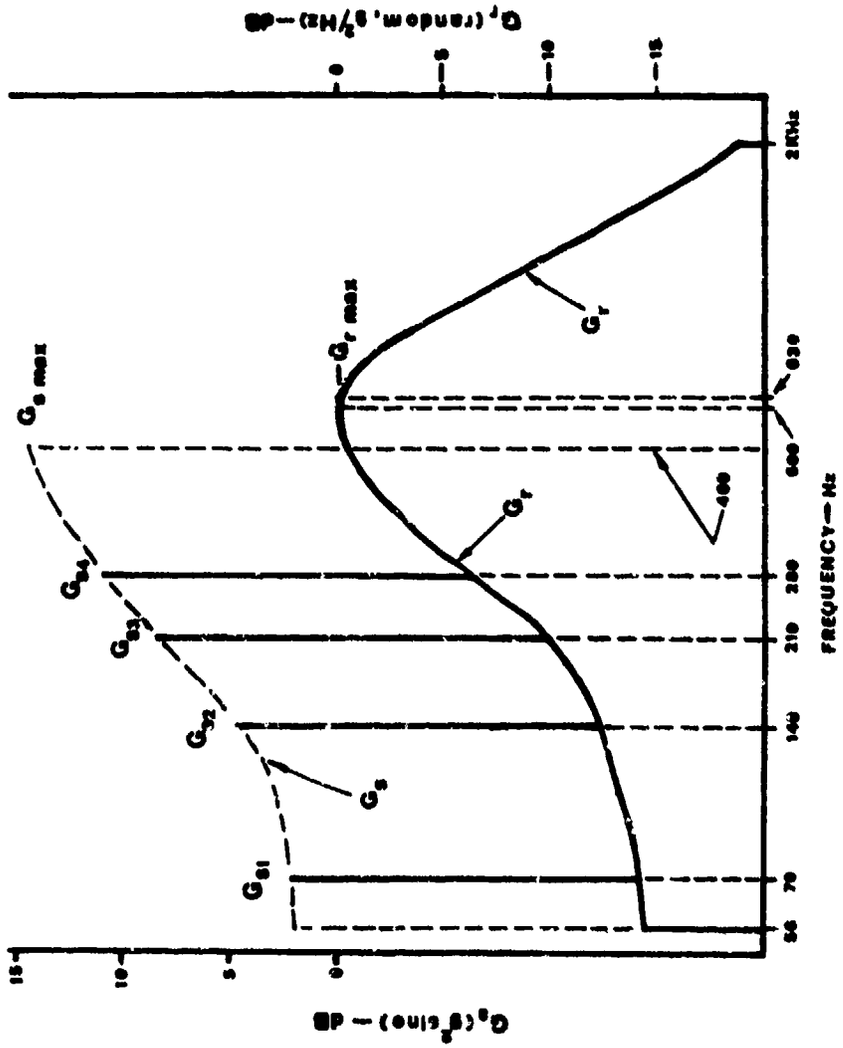

FIGURE 519.2-1. Low frequency sinusoidals superimposed on random vibration

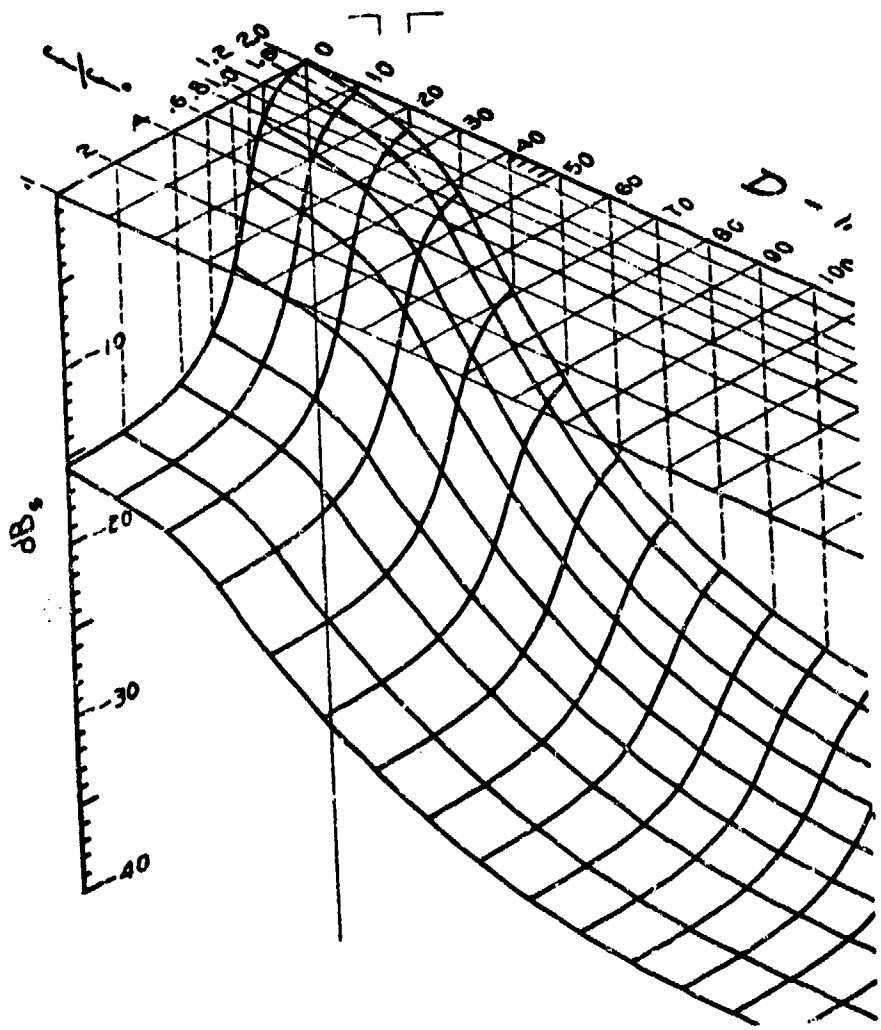

FIGURE 519.2-2. Sinusoidal vibration prediction surface

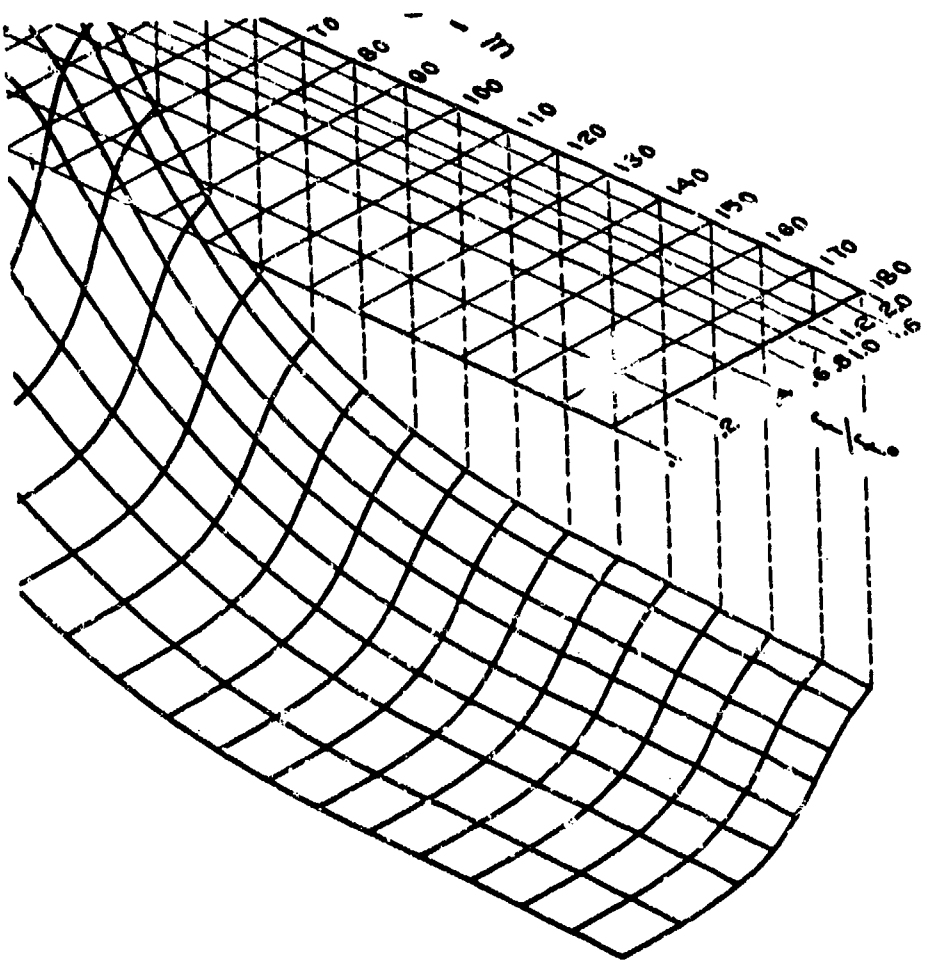

FIGURE 519.2-2. Sinusoidal vibration prediction surface (Cont'd)

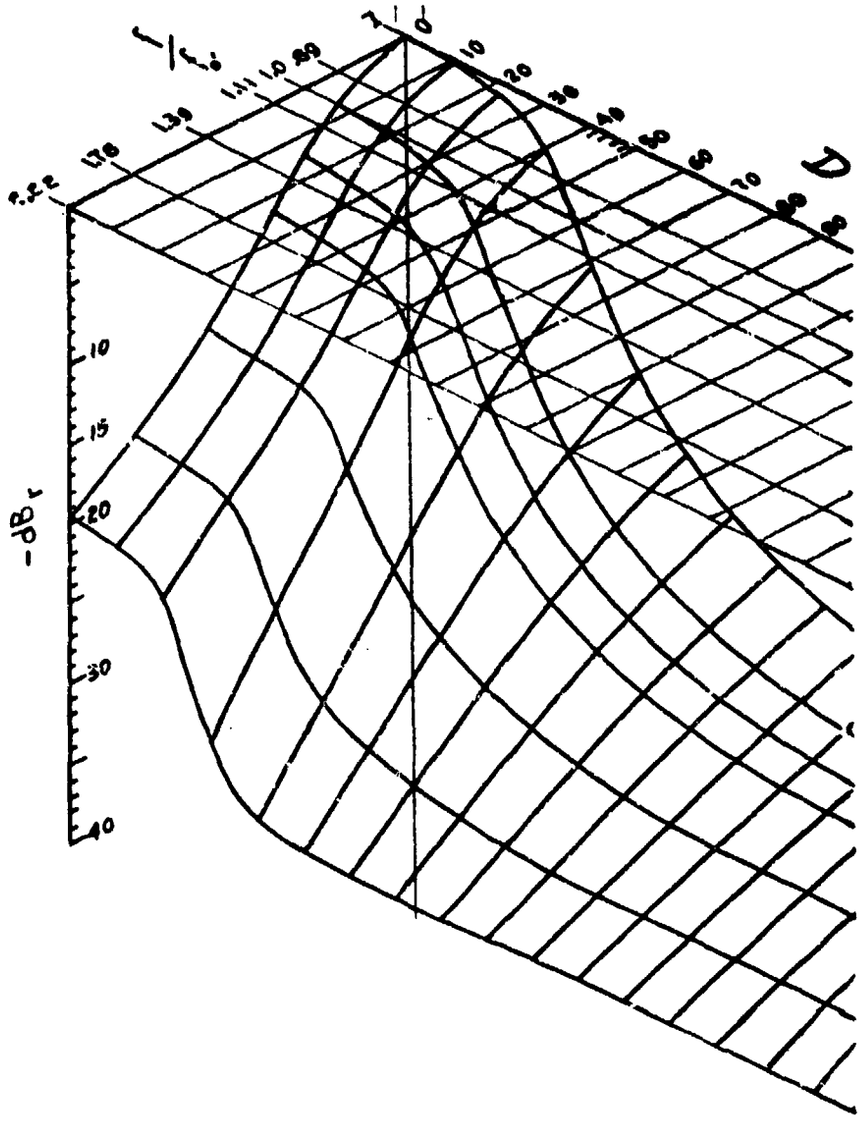

FIGURE 519.2-3. Random vibration prediction surface, high frequency

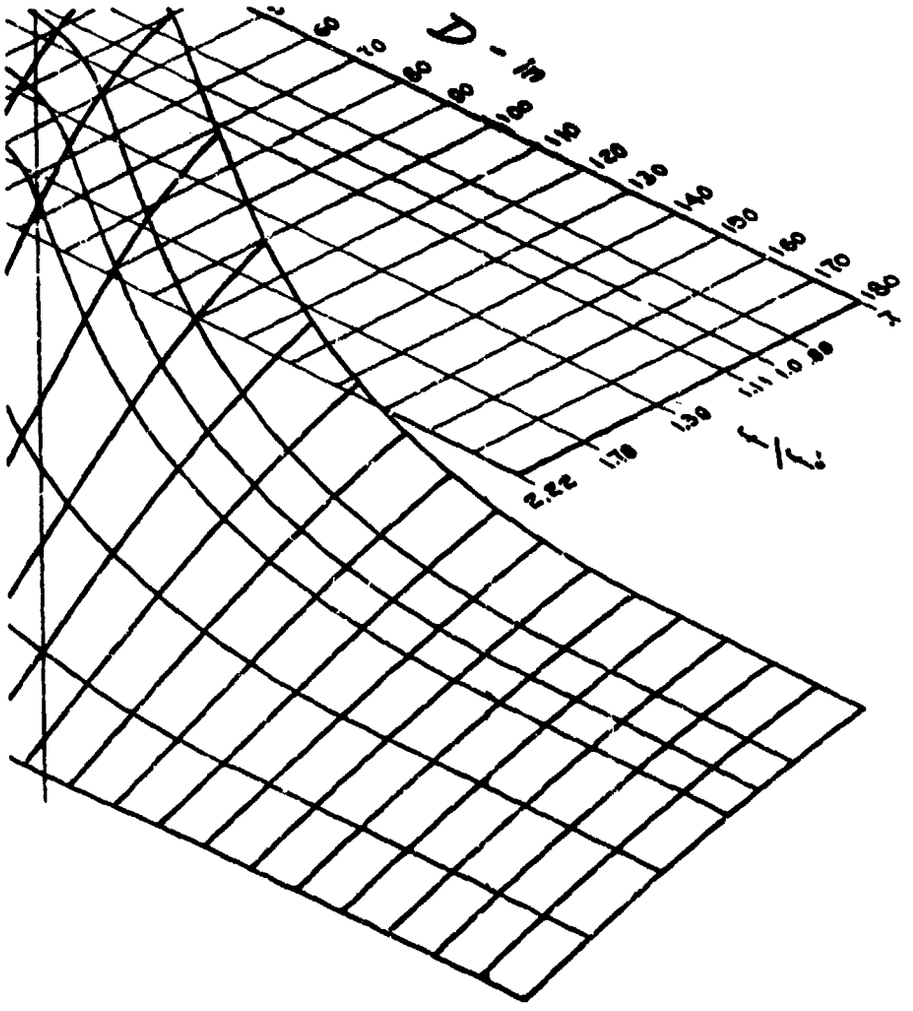

FIGURE 519.2-3. Random vibration prediction surface, high frequency (Cont'd)

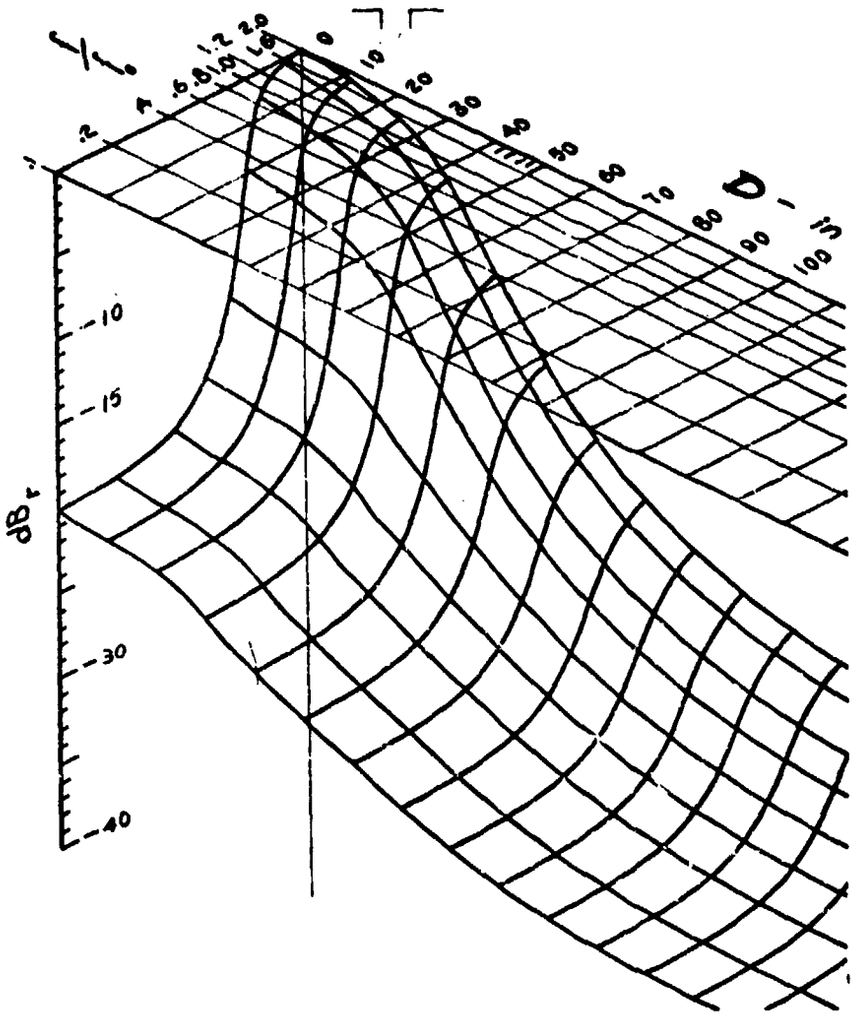

FIGURE 519.2-4. Random vibration prediction surface, low frequency

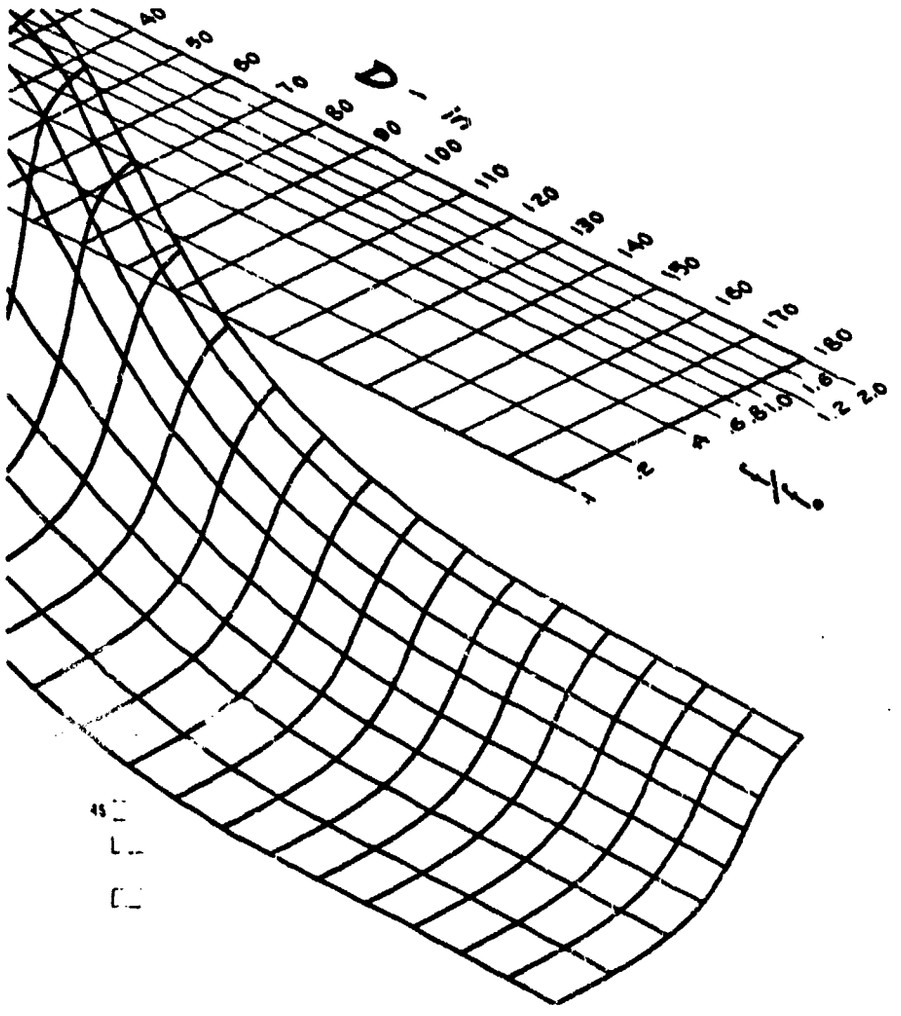

FIGURE 519.2-4. Random vibration prediction surface, low frequency (Cont'd)

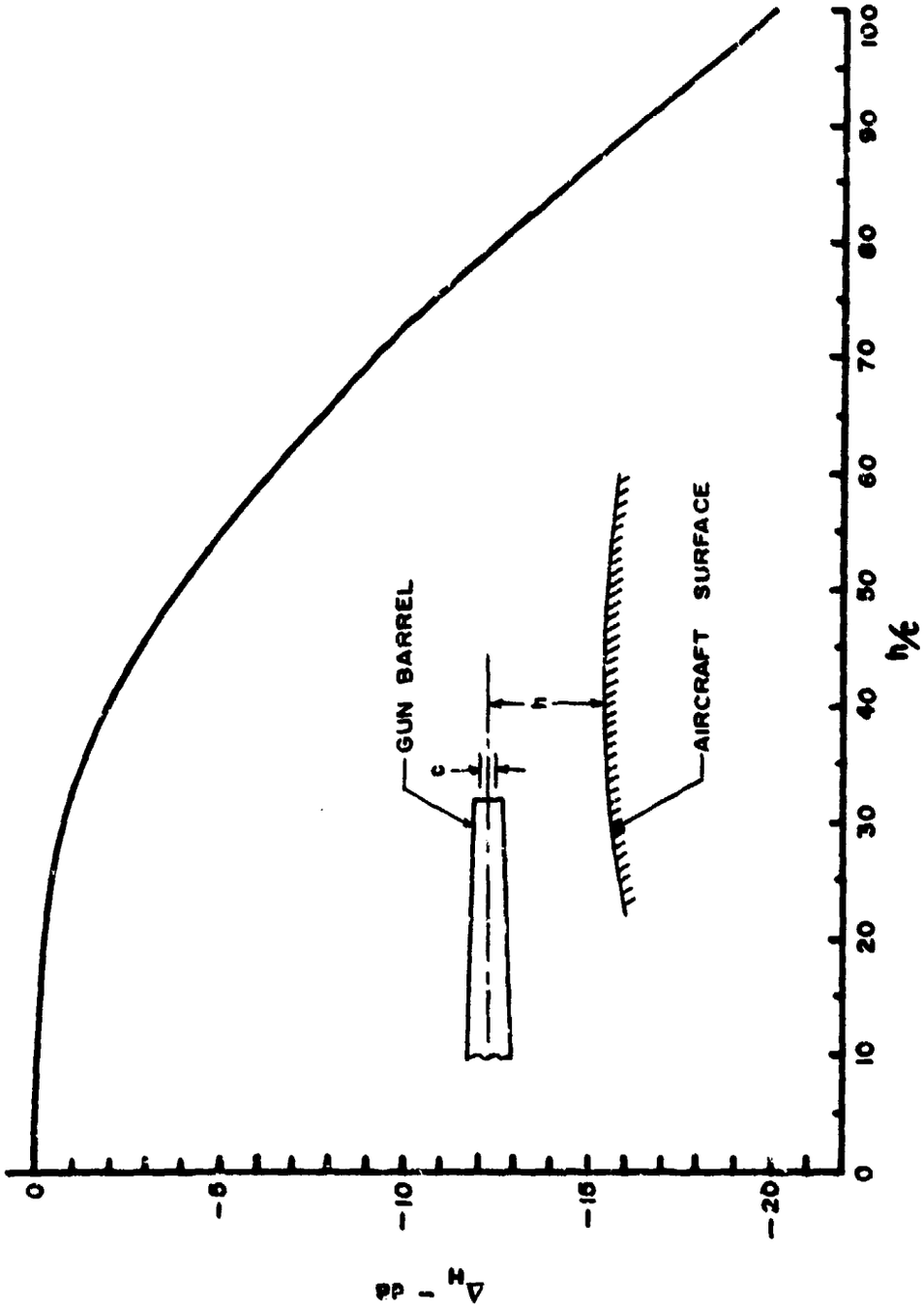

FIGURE 519.2-5. Test level reduction, A_H, due to gun standoff parameter, h/c

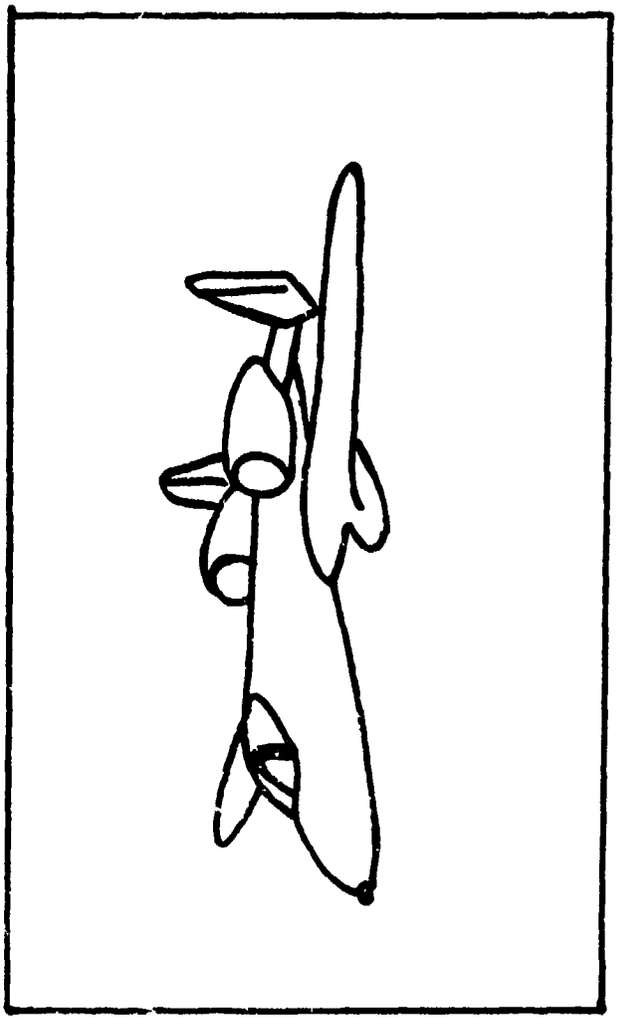

FIGURE 519.2-6. Example of gun configuration, free air

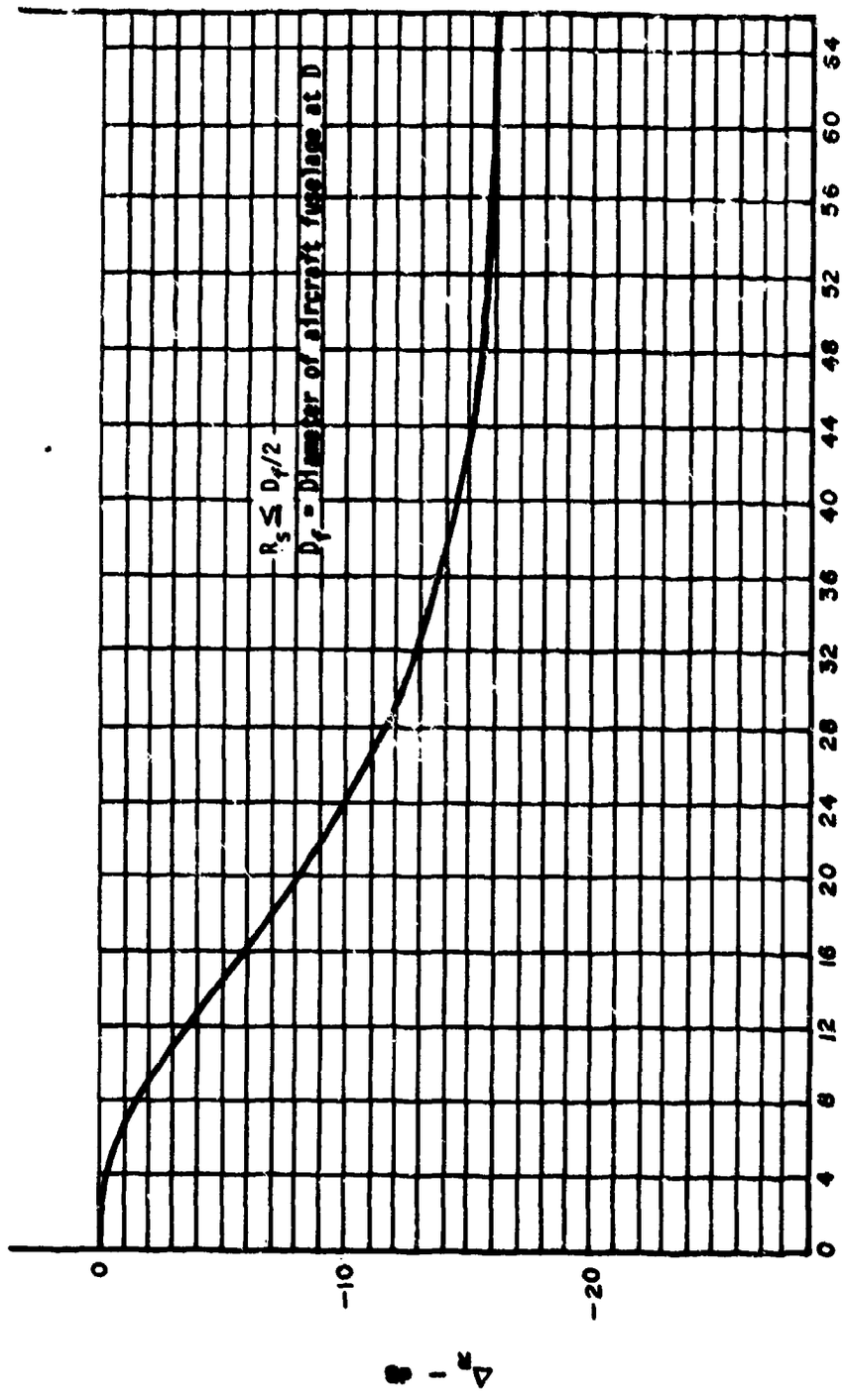

FIGURE 519.2-7. Test level reduction, Δ_R, due to depth parameter R_s.

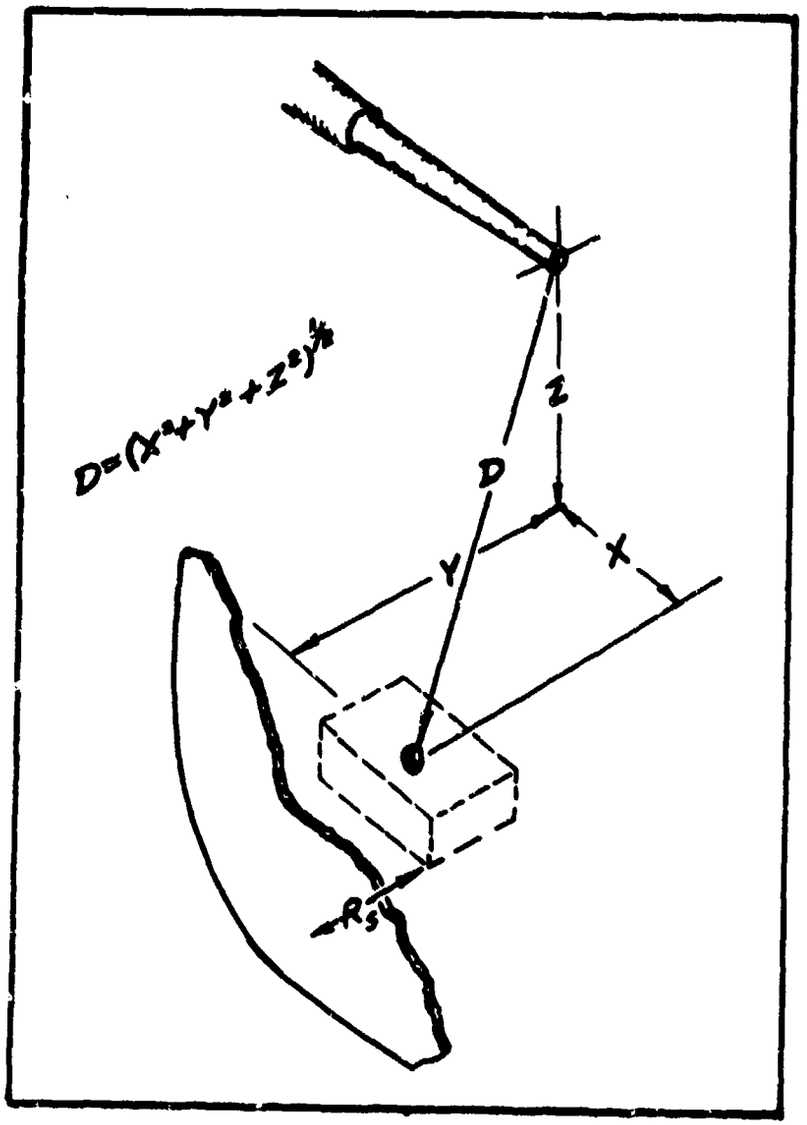

FIGURE 519.2-8. The distance parameter, D, and the depth parameter, R_s

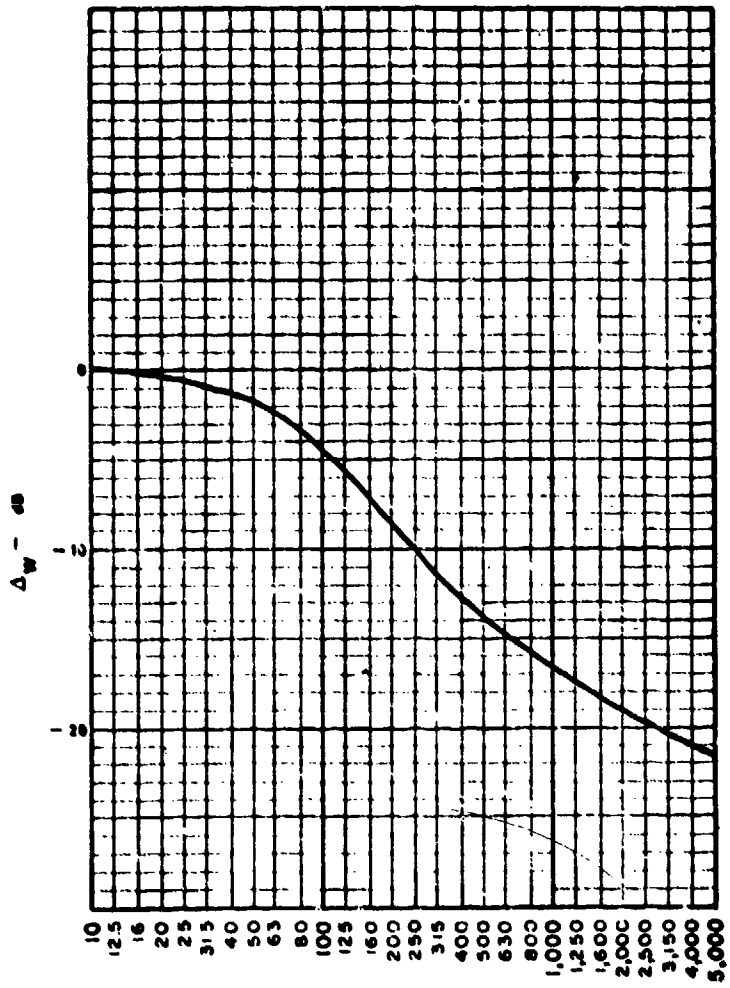

FIGURE 519.2-9. Test level reduction, Δ_W, due to equipment mass loading

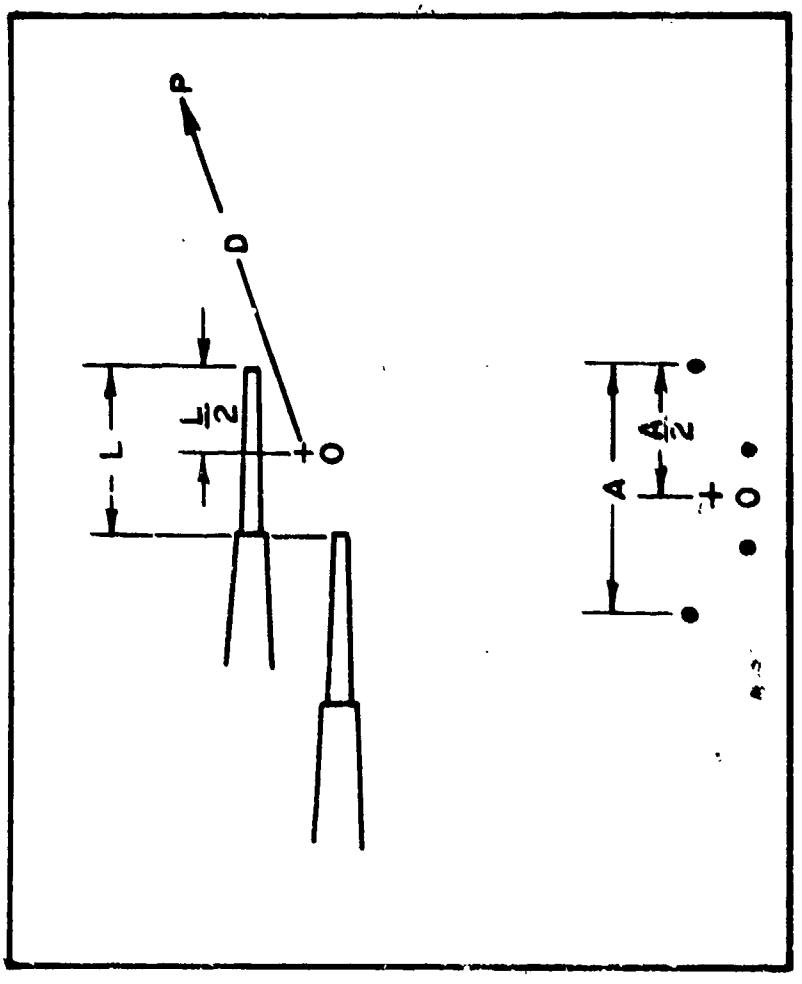

FIGURE 519.2-10. Multiple guns, closely grouped

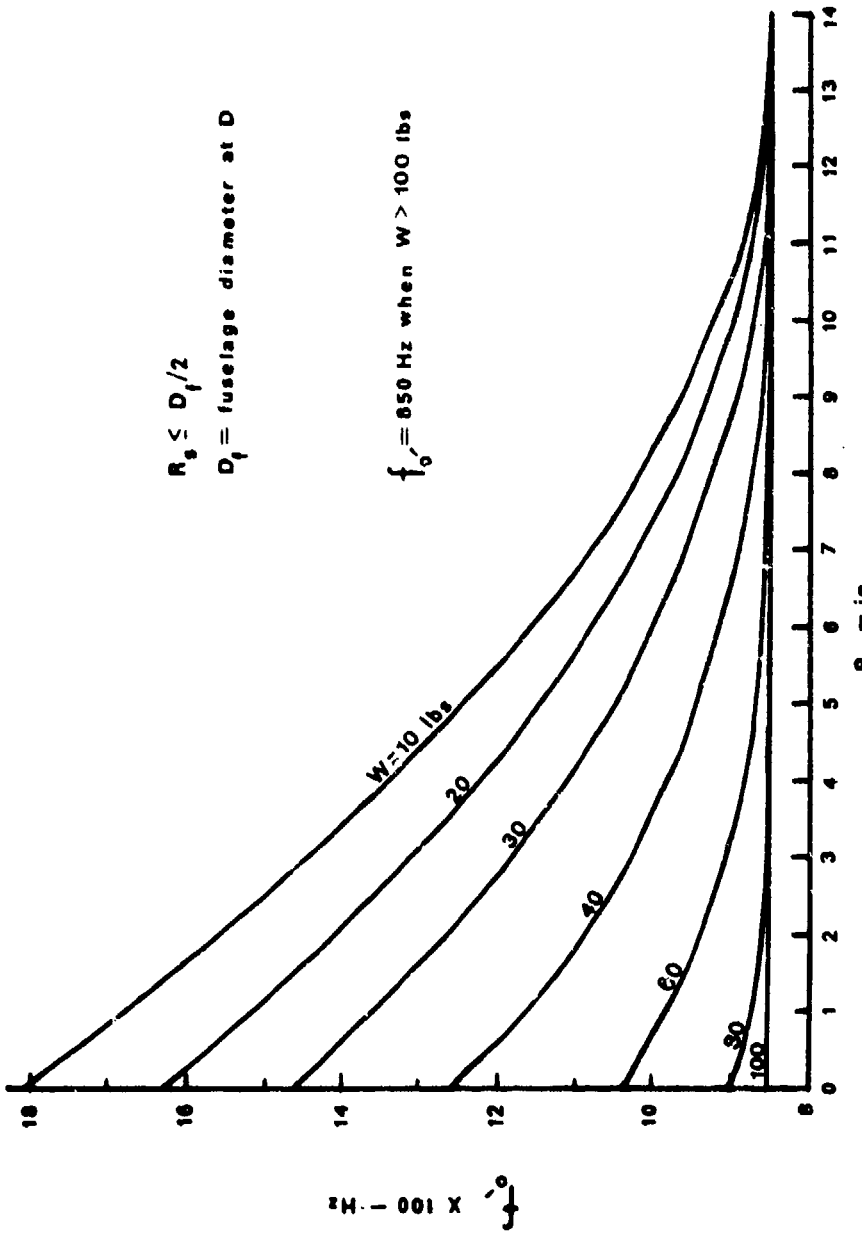

FIGURE 519.2-11. Locator frequency, f_o, for high frequency random prediction surface

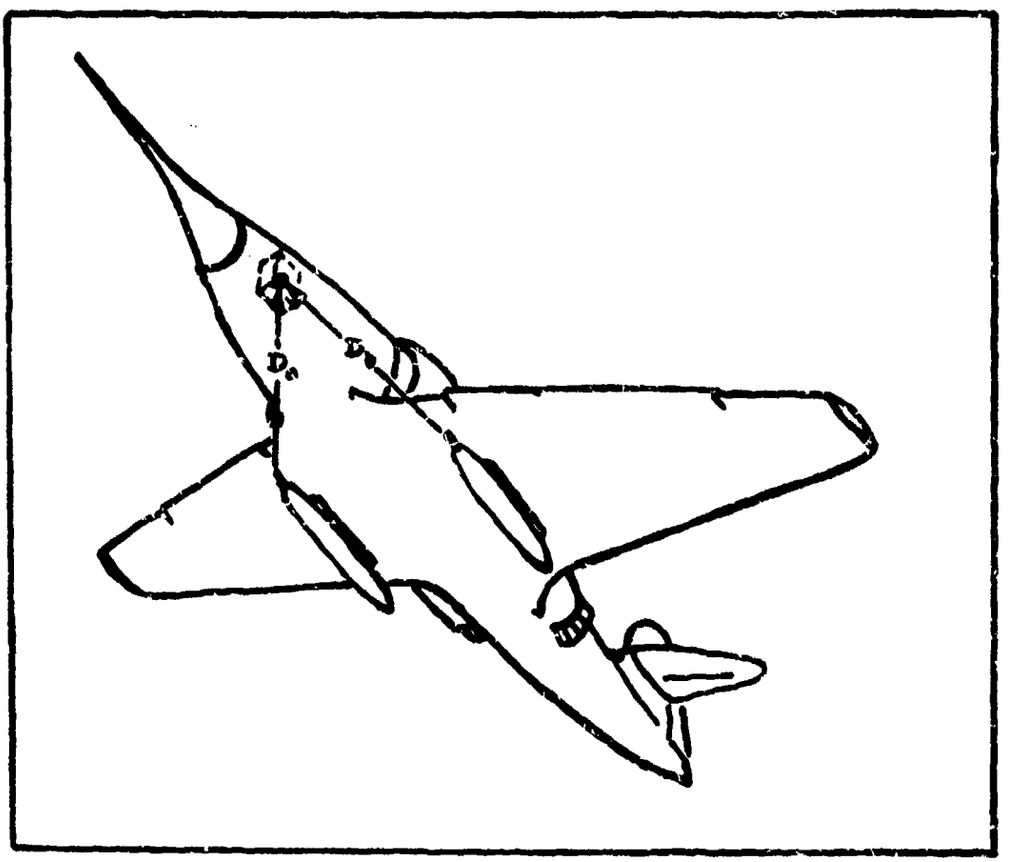

FIGURE 519.2-12. Multiple guns, dispersed

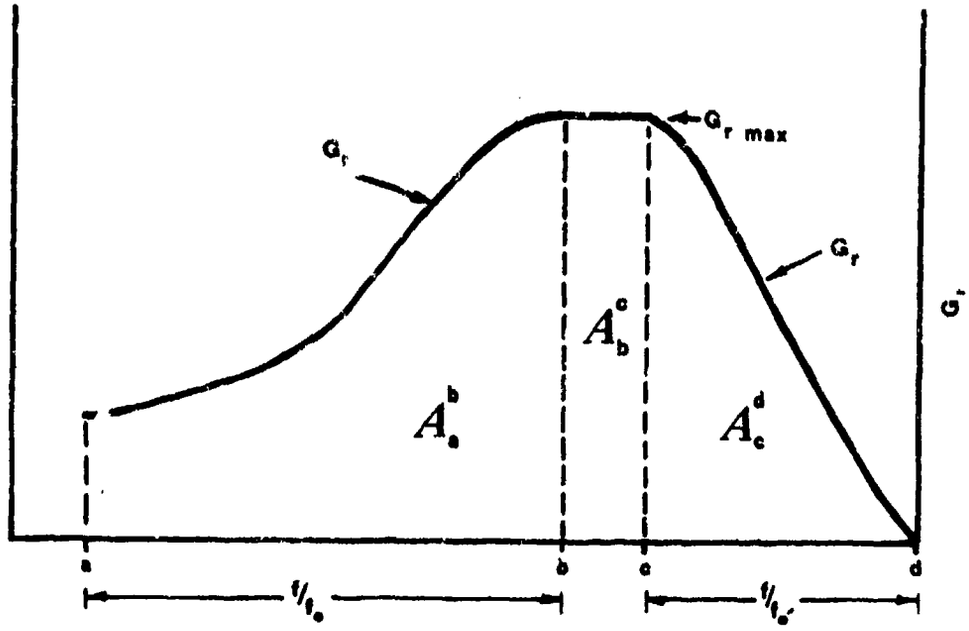

$A_a^b = G_{r\ max}\ f_o[I_b - I_a]$

$[I_b - I_a]$ = see Fig 519.2-14 and 3.3.7.1.1

where: f_o = 300 Hz

$a = 0.8\ f_1/f_o$

$b = f_b/f_o = 2.0$

$A_b^c = G_{r\ max}\ [f_c - f_b]$

where: f_o' = see Fig 519.2-11

$c = f_c/f_o' = 0.7$

$A_c^d = G_{r\ max}\ f_o'[I_d - I_c]$

$[I_d - I_c]$ = see Fig 519.2-15 and 3.3.7.1.1

where: $d = f_d/f_o'$

f_d = 2 KHz

FIGURE 519.2-13. Determining the OAMS from the random test curves

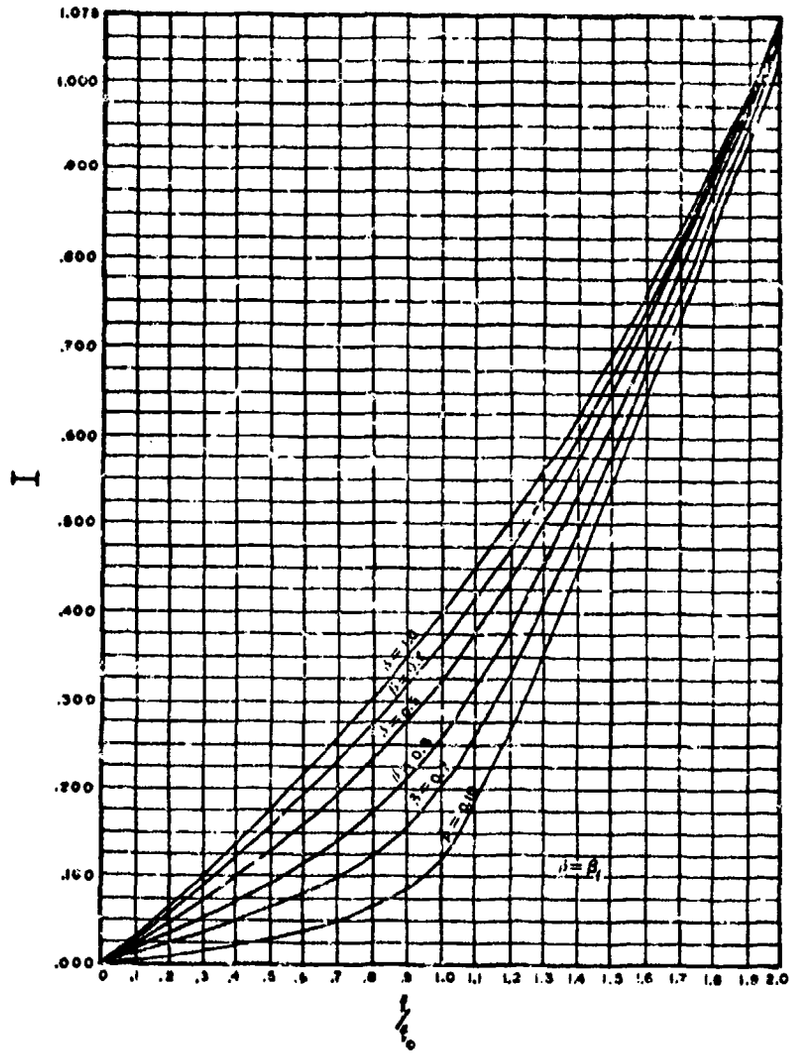

FIGURE 519.2-14. Normalized area under the low frequency random curve as a function of f/f_0 and β_f

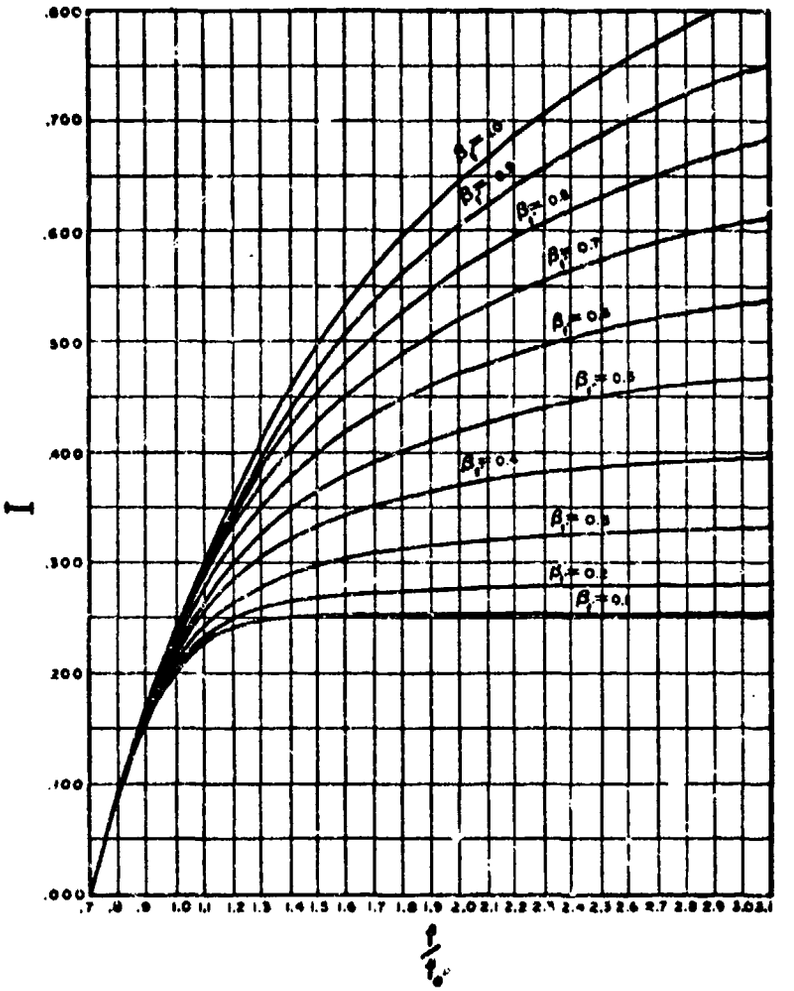

FIGURE 519.2-15. Normalized area under the high frequency random curve as a function of $f/f_{e'}$ and β_f.

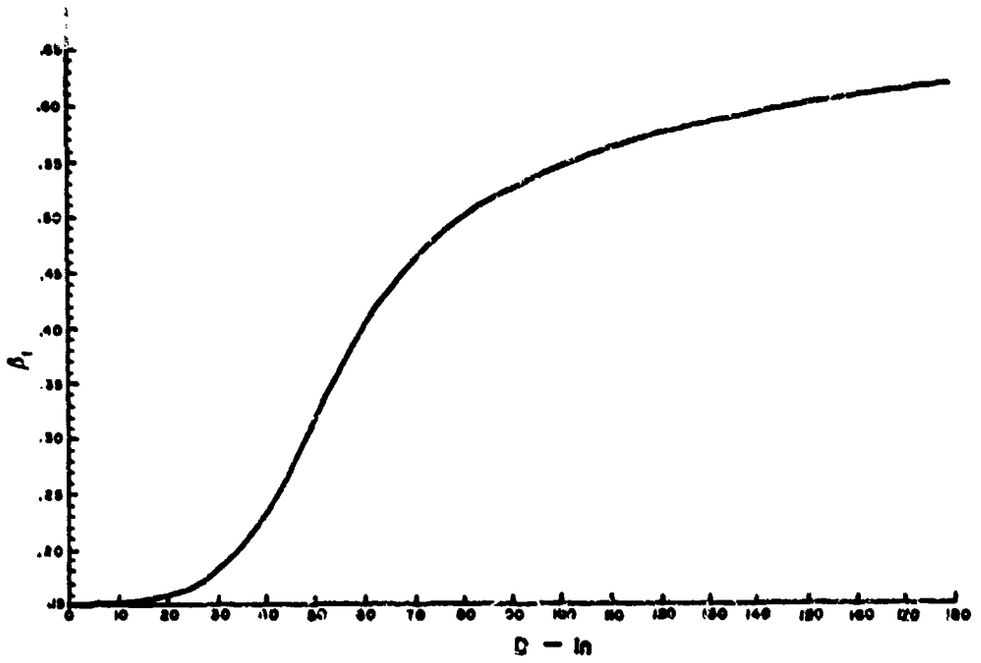

FIGURE 519.2-16. Slope factor, β_f, for the low frequency random surface

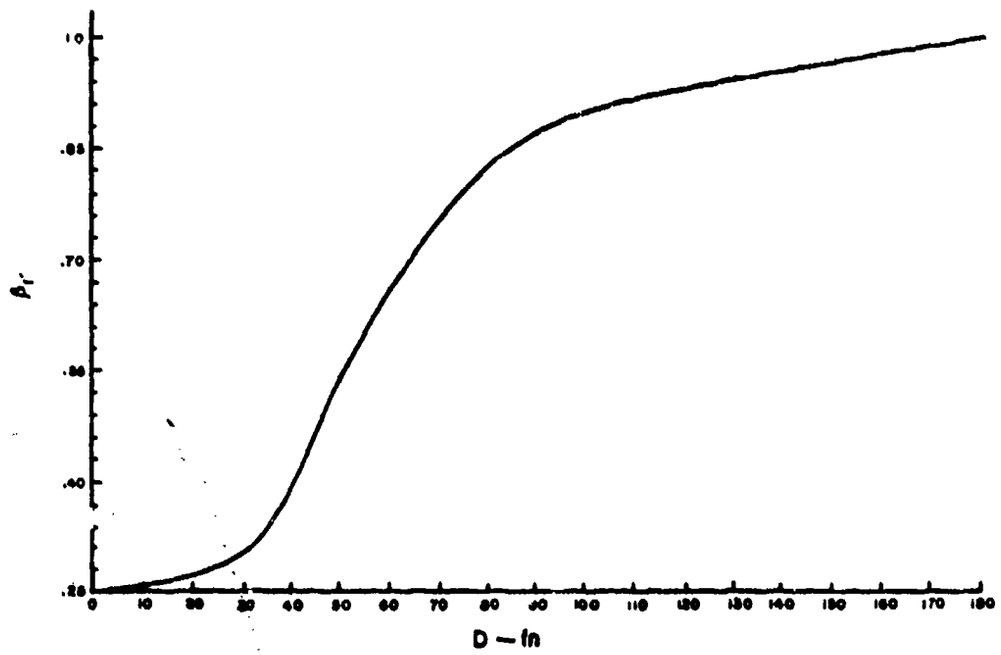

FIGURE 519.2-17. Slope factor, β_f, for the high frequency random surface

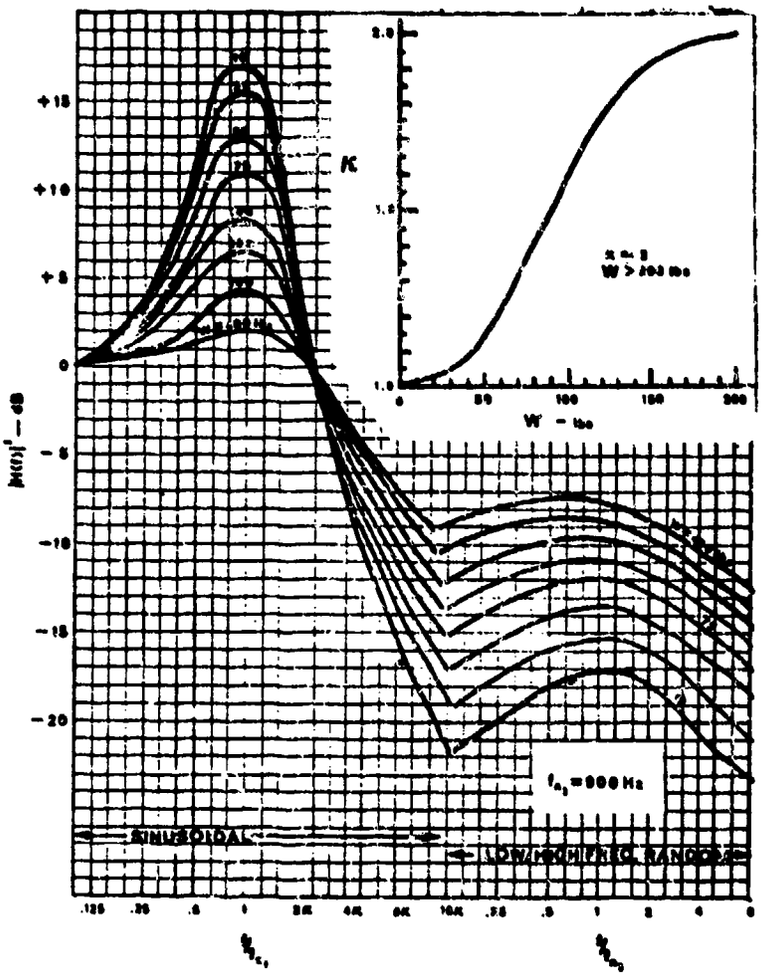

FIGURE 519.2-18 Transfer function for isolated equipments

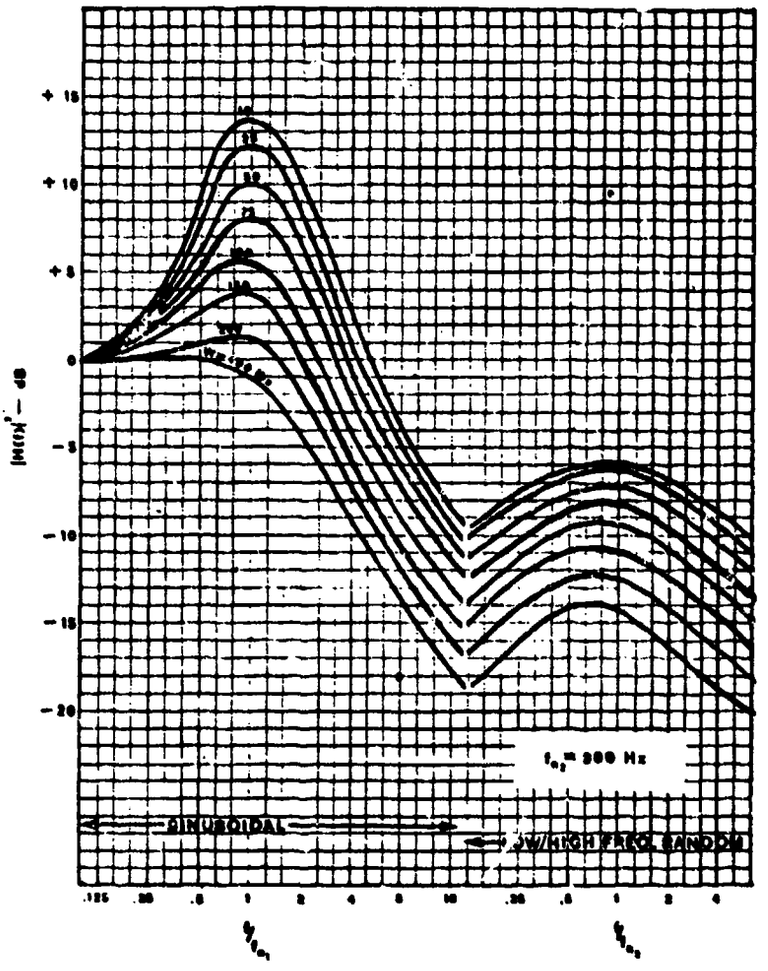

FIGURE 519.2-19 Transfer functions for non-isolated equipments

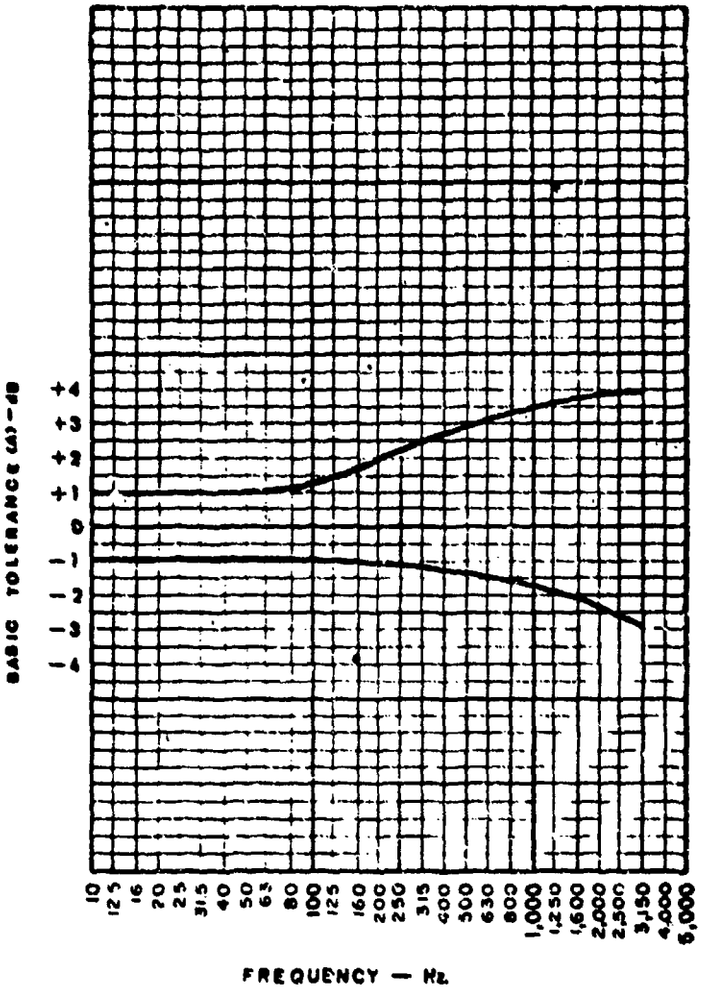

FIGURE 519.2-20 Basic test tolerance (A) for gunfire spectrum (W < 10 lbs.)

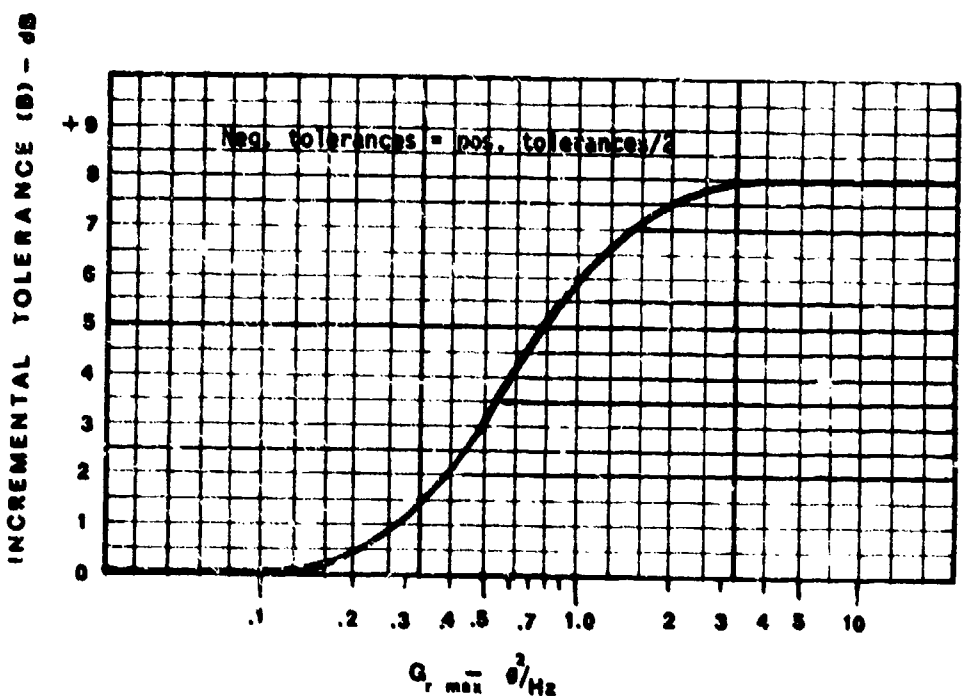

FIGURE 519.2-21 Gunfire test tolerance (B) for $G_{r\ max} \geq 0.1\ g^2/Hz$

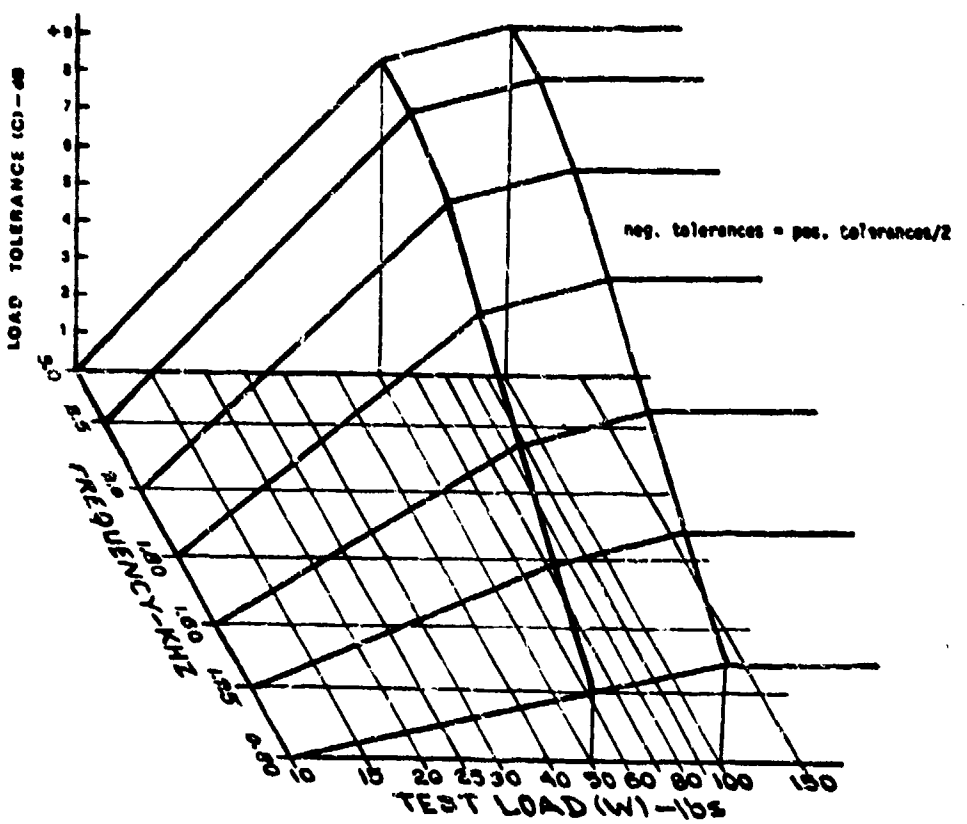

FIGURE 519.2-22 Gunfire test tolerance (C) for W ≥ 10 lbs

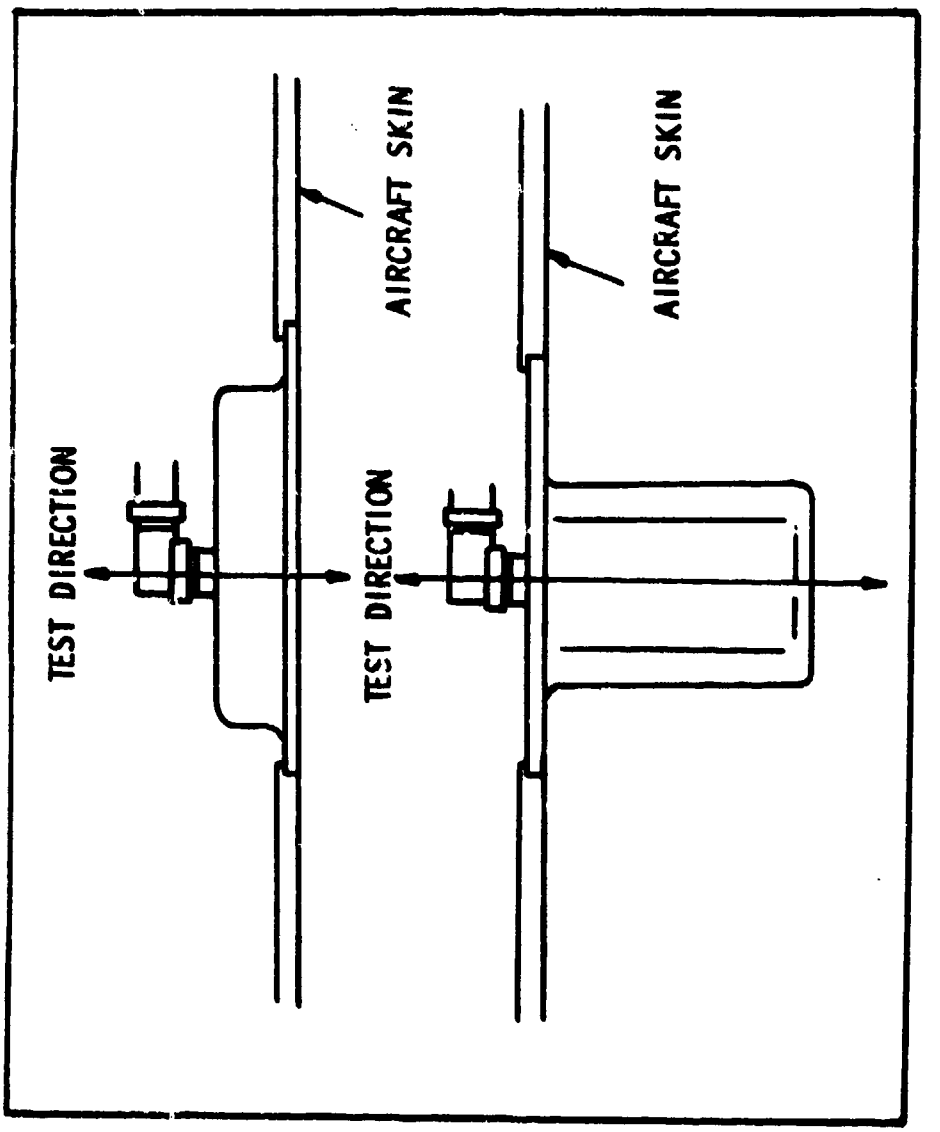

FIGURE 519.2-23 Single direction example

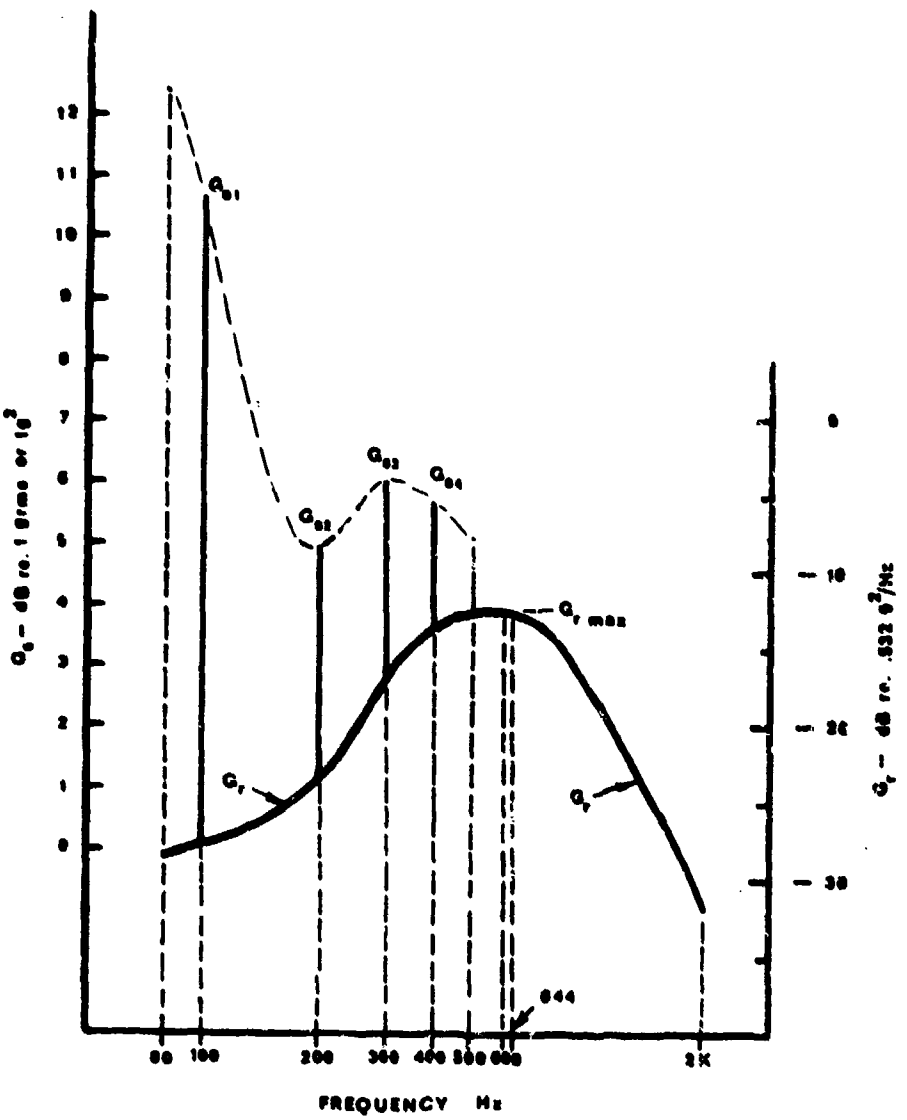

FIGURE 519.2-24 Example of test spectrum for secondary structure (instr. panel)

APPENDIX B

LOSS FACTOR VS FREQUENCY OF SUU-41 SKIN

1. INTRODUCTION

The objective of this laboratory study was to determine the Q vs frequency of the skin or surface of a structure that by its composition and form may be considered to be aircraft-like. A second objective was to supply a versatile function to provide a best fit for the data. The structure is an aircraft store (SUU-41) carried under the wing or fuselage of a variety of aircraft. The 0.063 inch aluminum housing envelopes 10 compartments; each one containing explosive cannisters of 35 pounds weight. During release the cannisters are ejected downward; propelled by explosive charges. Each cannister bottom is fitted with a flat metal rectangular shoe which, when the cannister is inserted into its compartment, provides a surface that is relatively flush with the underside of the store. The following sketch (Figure B-1) shows the side view of the SUU-41 with two cannisters outlined in their fore and aft compartments.

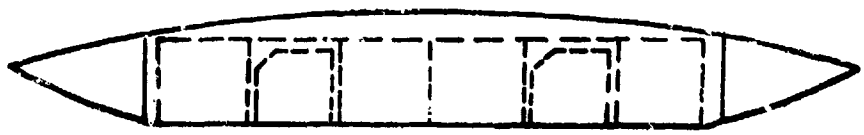

(a) Side

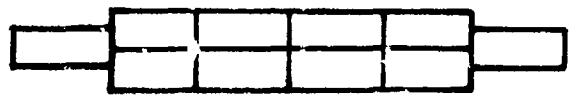

(b) Bottom

Figure B-1. SUU-41 Weapon Dispenser with Cannister Cavities

Looking from the bottom one can see the array of ten cannister compartments.

The skin was excited by a small shaker (MB-VA1500). Miniature accelerometers (Clevite E-1 and Endevco 2222) were distributed over the skin surface. No more than four accelerometers were used for recording and no more than one of these per panel was permitted in order to minimize mass loading. The shaker excitation point was changed from time to time and the shaker location was, for the most part, kept as far away from the response accelerometers as possible. In most cases the accelerometers were located on the store side opposite the shaker driving point. This precaution was observed in order to reduce the near field effects of the driver and to decouple damping contributions from the driving configuration. The accelerometers were periodically moved to new locations to obtain a good spatial average of the skin surface readings. A set of separate measurements were made on the store skin with: (1) all cannisters removed, (2) all cannisters in place. A constant 2 g peak sine sweep was used for the first case; 4 g's for the latter. The Q of the skin responses was determined by the 3dB down bandwidth method.

The following paragraphs describe in detail the laboratory setup and the data recording techniques employed.

2. LABORATORY SETUP

a. Test Item

Figure B-2 shows an early test setup which was later modified because it was feared that the straps around the fore and aft section of the SUU-41 might contribute undesirable damping of the skin. Apart from this departure the configuration as seen in Figure B-2 is, in essence, the same as the description which now follows.

The SUU-41 was suspended by bungee cords from an "A" Frame. Four bungee cords were used, two from each of the two hangar eyes on the SUU-41. The other end of the bungee cords was attached to each end of two channel irons bolted at right angles to the cross member of the "A" Frame. A third channel iron was placed across the top of these two

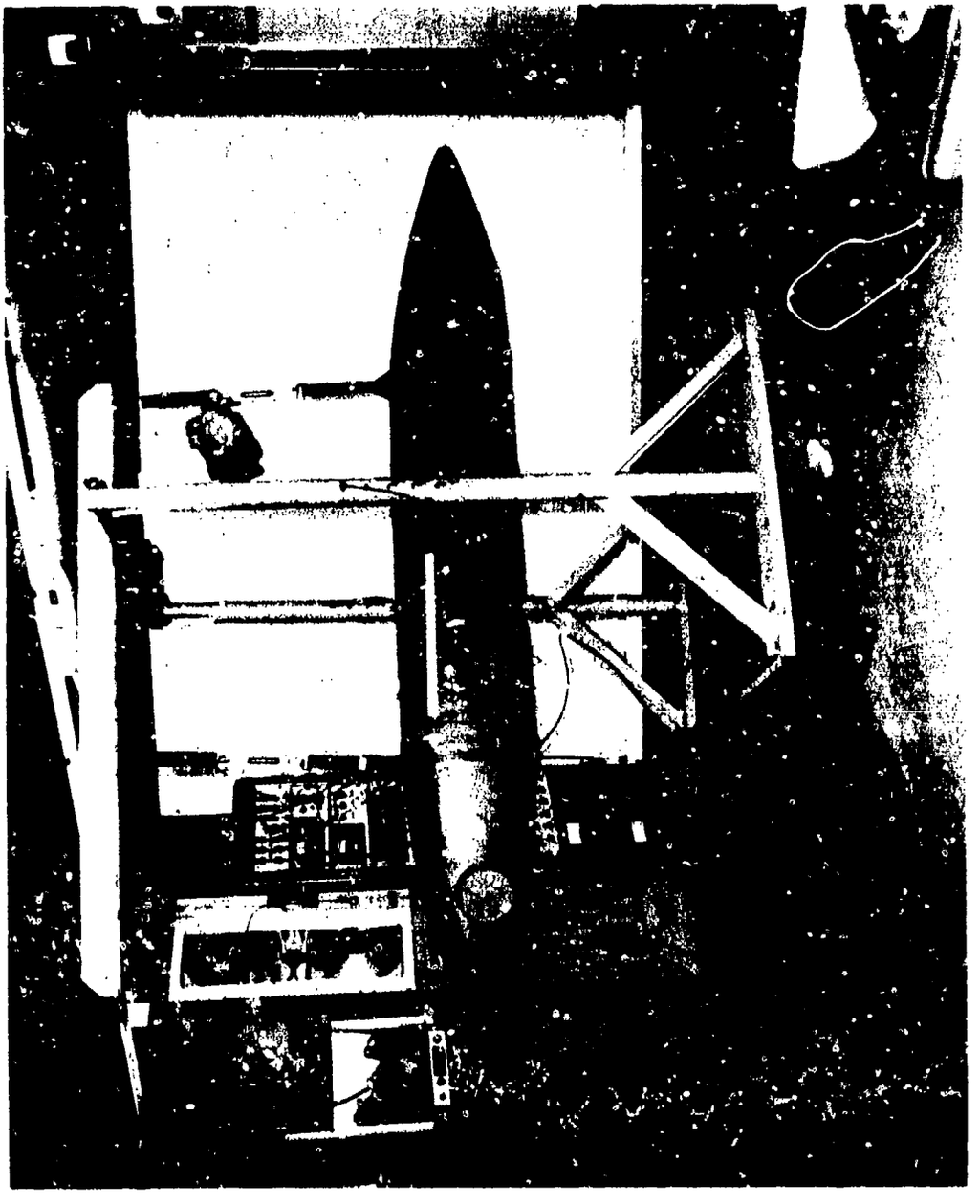

Figure B-2. Vibration Shaker Setup

channels in a direction parallel to the cross member of the "A" Frame. The third channel iron was used to support a 50 lb force permanent magnet shaker.

A trolley (using the third channel iron as the overhead rail) was implemented to permit translation of the shaker to any desired location along the longitudinal axis of the SUU-41.

The shaker was attached to the trolley via 1/8 inch steel cable and turnbuckles. A three point suspension was used at the shaker, two points at the front of the shaker and one point at the rear. This arrangement permitted ready adjustment of the turnbuckles to obtain vertical and perpendicular alignment of the shaker with respect to the driving point on the skin of the store.

Horizontal spacing of the shaker with respect to the driving point on the store was accomplished by sliding the third channel iron in or out on the two channel irons that were bolted to the cross member of the "A" Frame. After proper positioning, "C" Clamps were used to hold the channel iron in position. Horizontal positioning along the longitudinal axis of the store required merely moving the trolley along the rail until the proper location was reached; then locking the trolley in place.

b. Shaker to Store Attachment

Attachment of the shaker to the store was accomplished two different ways, depending whether the cannisters were in or out of their compartments. In either case an accelerometer at the driving point was required for servo control of the shaker.

In the case where the cannisters are removed from the store, attachment of the shaker and accelerometer is simplified. For this situation an adapter spacer was used (Figure B-3(a)). One end of the adapter spacer was made to attach to the shaker and the other end was drilled and tapped for the accelerometer mounting stud. The length of the spacer provided approximately 1 inch distance between the shaker and the store skin. A

clearance hole for the accelerometer mounting stud was drilled in the skin of the store at the driving point. After proper alignment of the shaker to the store the accelerometer was mounted on the inside surface of the skin with the mounting stud passing through the clearance hole at the driving point and entering the adapter spacer. Proper alignment was then checked by applying a low level vibration signal and observing the wave form on a oscilloscope. Final alignment was accomplished by adjusting the turnbuckles in the shaker suspension and by longitudinal adjustment on the trolley until a good sinusoidal waveform was displayed on the oscilloscope (See Figure B-2).

The second method of attaching the shaker to the store skin was used when the cannisters were installed in the cavity behind the driving point and the shaker was, from time to time, shifted from one excitation point to another. For this attachment, a drive linkage was fabricated to permit an accelerometer to be mounted close to the skin of the store but inside a cup on one end of the linkage (Figure B-3(b)). One side of the cup was slotted for the accelerometer lead exit.

c. Accelerometer Attachment

The accelerometer was attached to the SUU-41 skin with Eastman 910 cement. The cup of the driving linkage was attached to the skin area, about the accelerometer, by the rim surface of the cup with Eastmen 910 cement (Figure B-3(b)). This method turned out to be eminently suitable and permitted effective means by which the shaker could be cracked loose, moved, and recemented, without removing any of the cannisters.

d. Linkage Fastening

The shaker end of the linkage was aligned with the shaker mounting holes and secured with allen head cap screws. When proper alignment was achieved the two lock nuts on the drive linkage were secured.

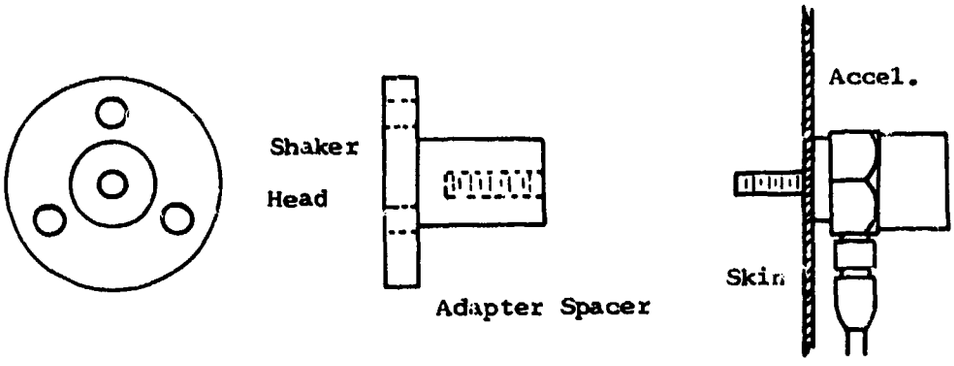

Figure B-3(a). Driver Attachment for Cases When Internal Space was Available

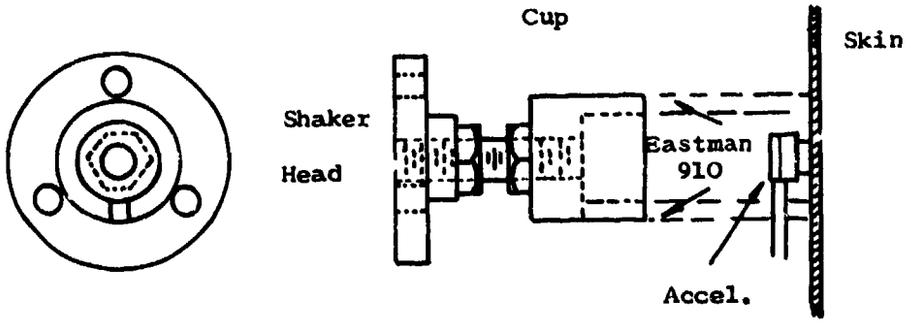

Figure B-3(b). Driver Attachment for Cases Where Internal Space was Limited by Cannister Occupancy

e. Accelerometer Calibration

All accelerometers were calibrated, together with their associated amplifiers, to a sensitivity of 100 mv/g. The output of the control accelerometer was attenuated to 10 mv/g for servo control input to the SD105.

The accelerometers were mounted at the specified location on the store and connected to their respective amplifiers.

f. Calibration of X-Y Recorders & Taping Calibration Signals

The instrumentation was interconnected as shown in Figure B-4. The X axes of the X-Y recorders were calibrated for a low limit of 50 Hz and a high limit of 3000 Hz. The Y axes were calibrated for 10 db/inch with 1 volt RMS as reference. After the recorders had been calibrated, the procedure was repeated, however this time the calibration signals were taped. The taped signals were for future use in calibrating the X and Y axes of the X-Y recorders prior to plotting from each channel of the tape recorder.

g. Data Recording and Plotting During Run

The equipment was interconnected as shown in Figure B-5. The SD104 was set to 200 Hz and the 2g level (or other as specified) set into the shaker and monitored from the control accelerometer. The SD105 was switched to Standby and the SD104 was reset to the low frequency limit. The SD105 was switched to Operate, the X-Y recorder pens were lowered, the tape deck record button was depressed and the vibration sweep was started. The sweep rate was changed for various frequency ranges as follows:

1.5	Decades/min	50-120 Hz
1.0	" "	120-300 Hz
0.75	" "	300-450 Hz
0.35	" "	450-900 Hz
0.2	"	900-3000 Hz

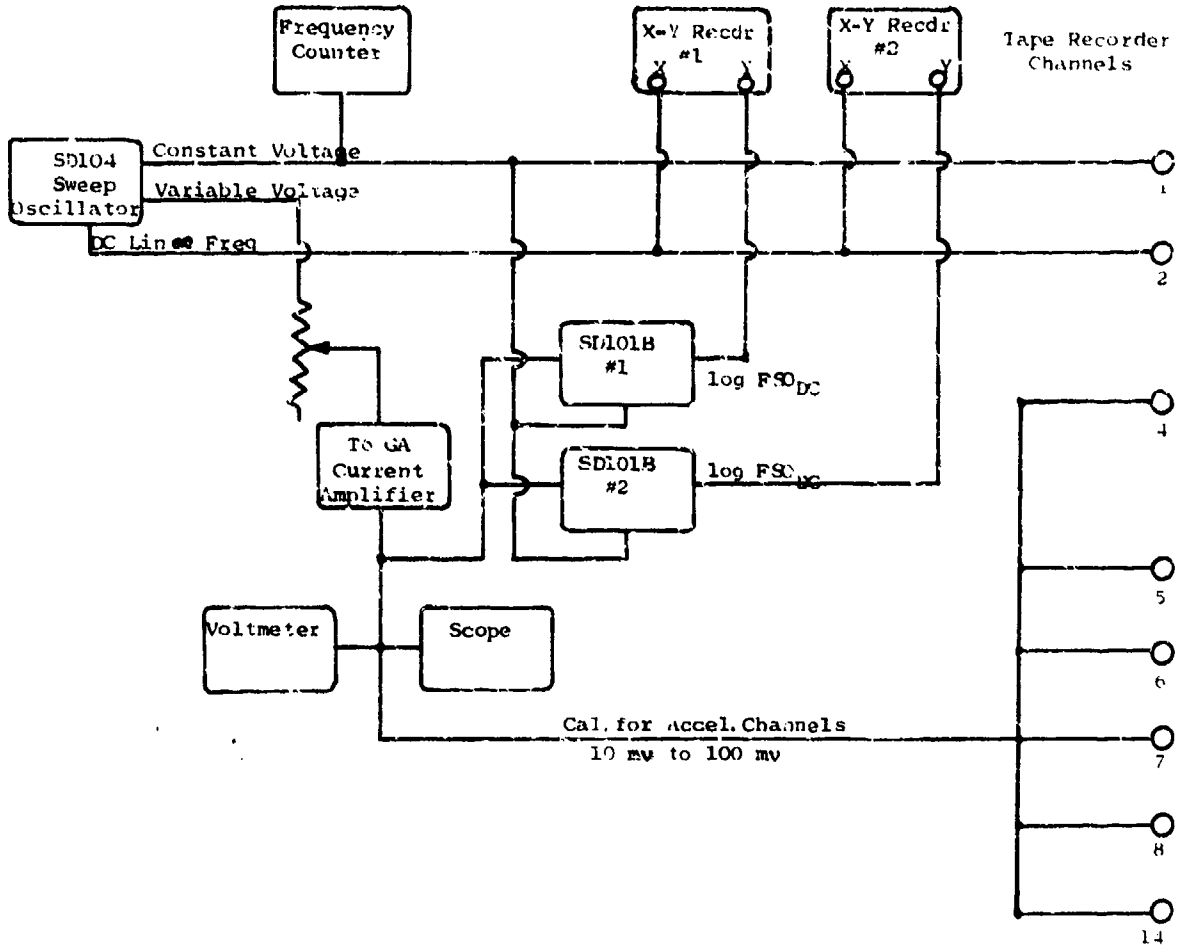

Figure B-4. Calibration Setup of Tape Recorder Signals and X-Y Recorders

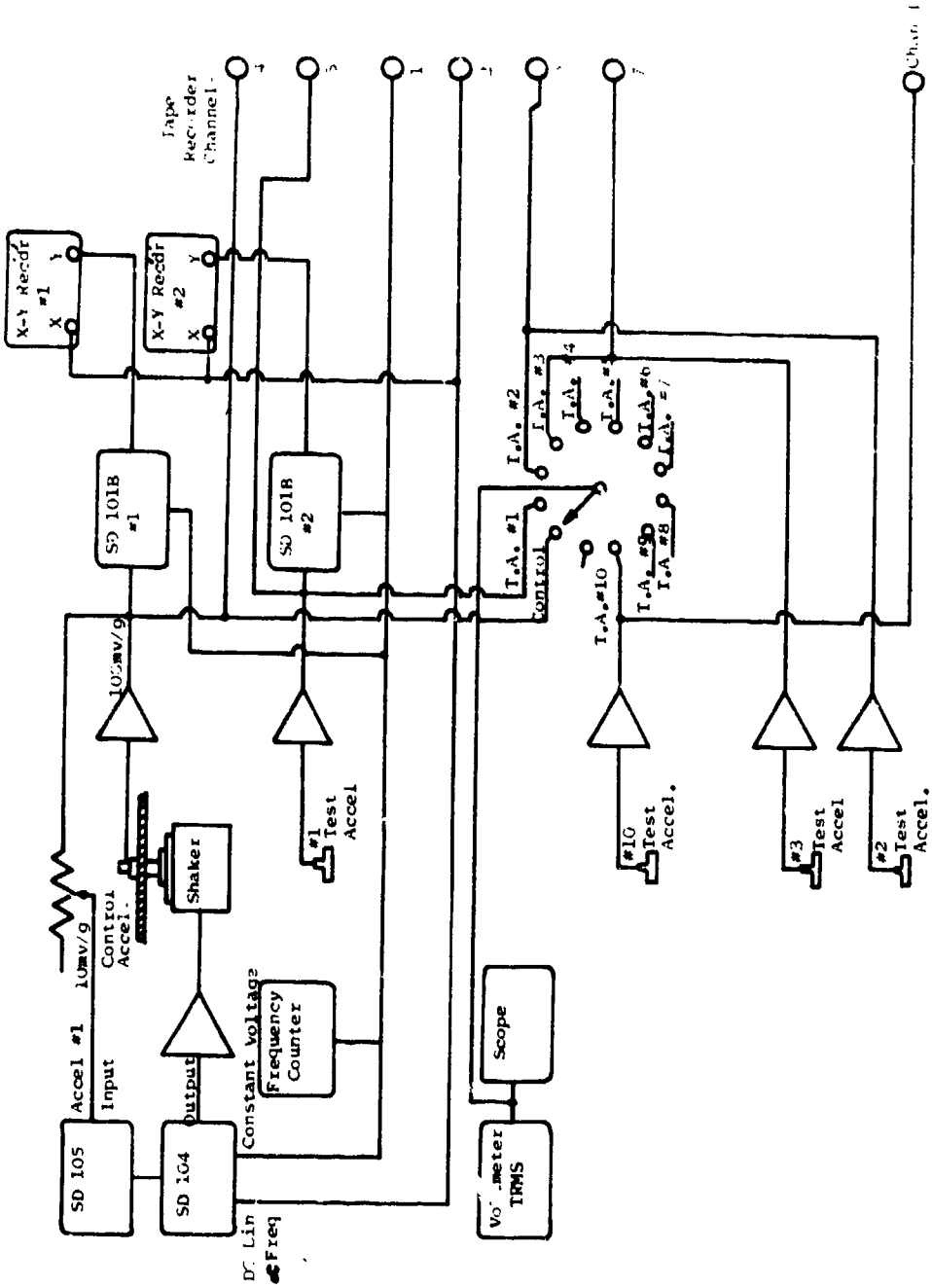

Figure B-5. Data Recording and Plotting Setup for Vibration Response Measurements

Sweep speeds were determined experimentally by sweeping through the sharpest resonances throughout the frequency range and slowing the rate for full response relative to steady state excitation. Note that both the control accelerometer and data accelerometer number 1 outputs were plotted during the vibration run.

h. Calibrate X and Y axes of X-Y Recorders from Tape and Plot Test Accelerometers number 2 and number 3 from Tape.

The equipment was interconnected as shown in Figure B-6. The tape was rewound to the calibration signals and the X and Y axes of the X-Y recorders were recalibrated as necessary. Note that the signals for driving the X axis of the X-Y recorder and for tuning the tracking filter are now coming from the tape playback. This procedure was repeated for all accelerometer channels that had been recorded on tape.

i. Expanded Frequency Scale Plots

The normal, coarse resolution frequency plots are not sufficient for performing high Q measurements, therefore it was deemed advisable to replot portions of the frequency range using an expanded scale for the X axis.

The General Radio Type 1142A Frequency Meter and Discriminator readily lends itself to such an application. Best results were obtained when an isolation amplifier was inserted between the 1142A and a low pass filter with the output from the filter supplying the DC proportional to frequency for the drive to the X axis of the recorder (Figure B-7). With this arrangement the frequency scale could be expanded to provide a 5 Hz/inch resolution; however, 20 Hz/inch provided sufficient resolution in most cases.

After determining the frequencies to be analyzed from the expanded scale plot the X axis of the X-Y recorder was calibrated to the desired frequency range (Figure B-8). Preparations were sufficient at this point to allow a plot of the data. Interconnections were made to the tape deck

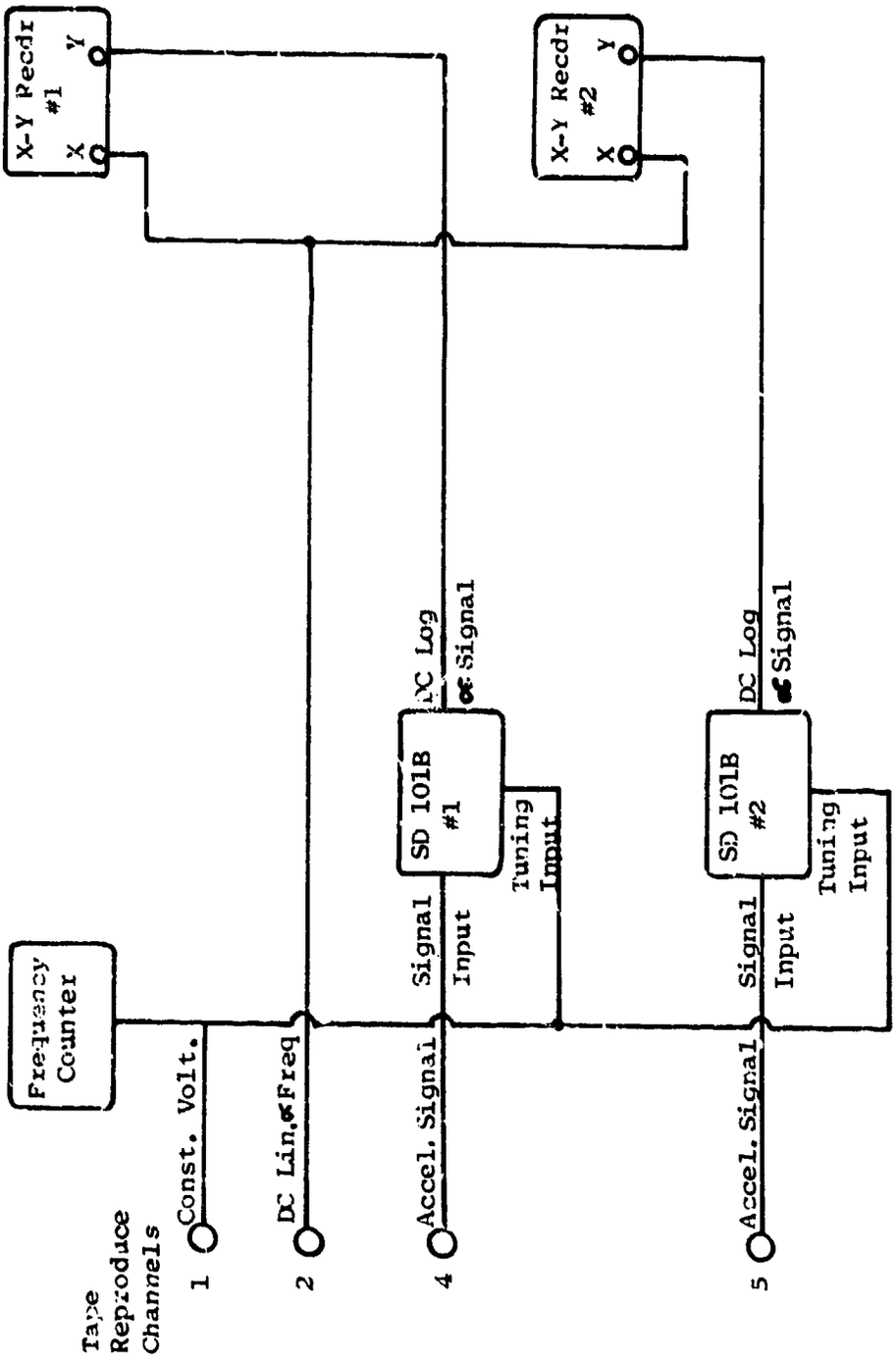

Figure B-6. Play back and Recording Setup of Acceleration Responses

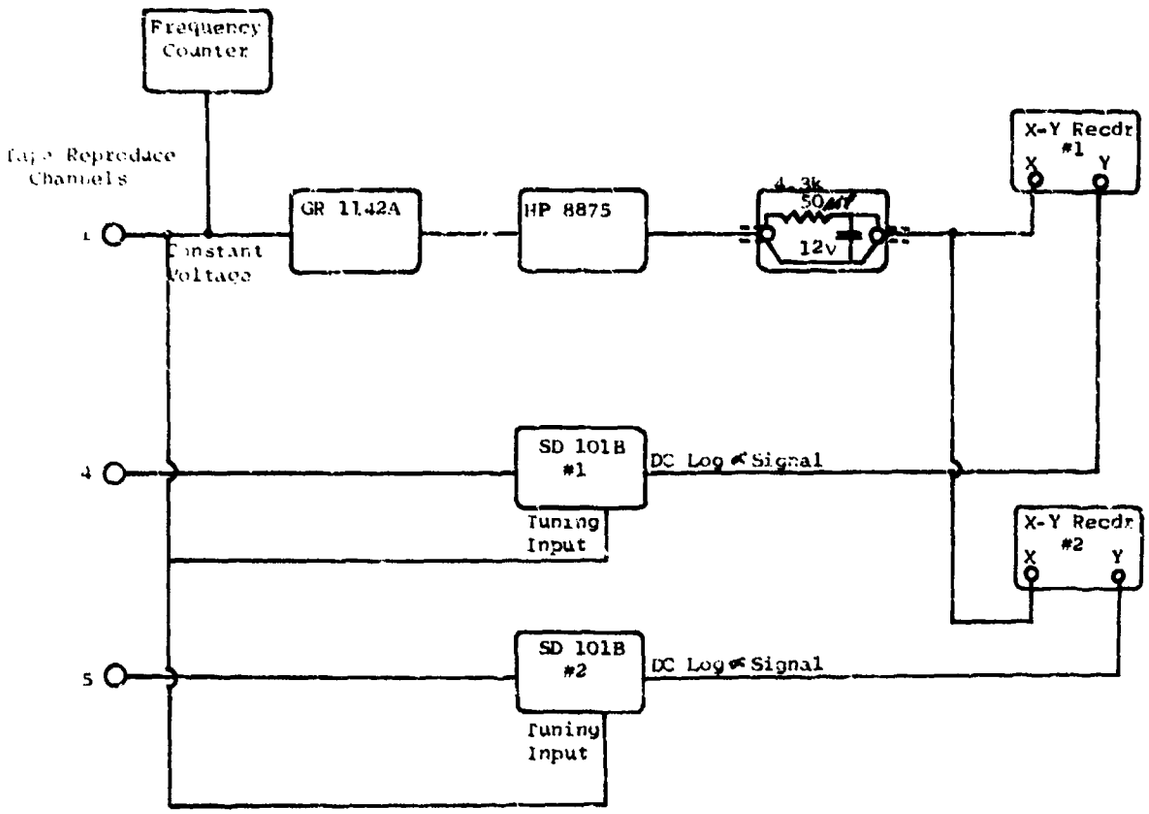

Figure B-7. Tape Play back Showing DC Proportional to Frequency Setup for X Axis of Recorders

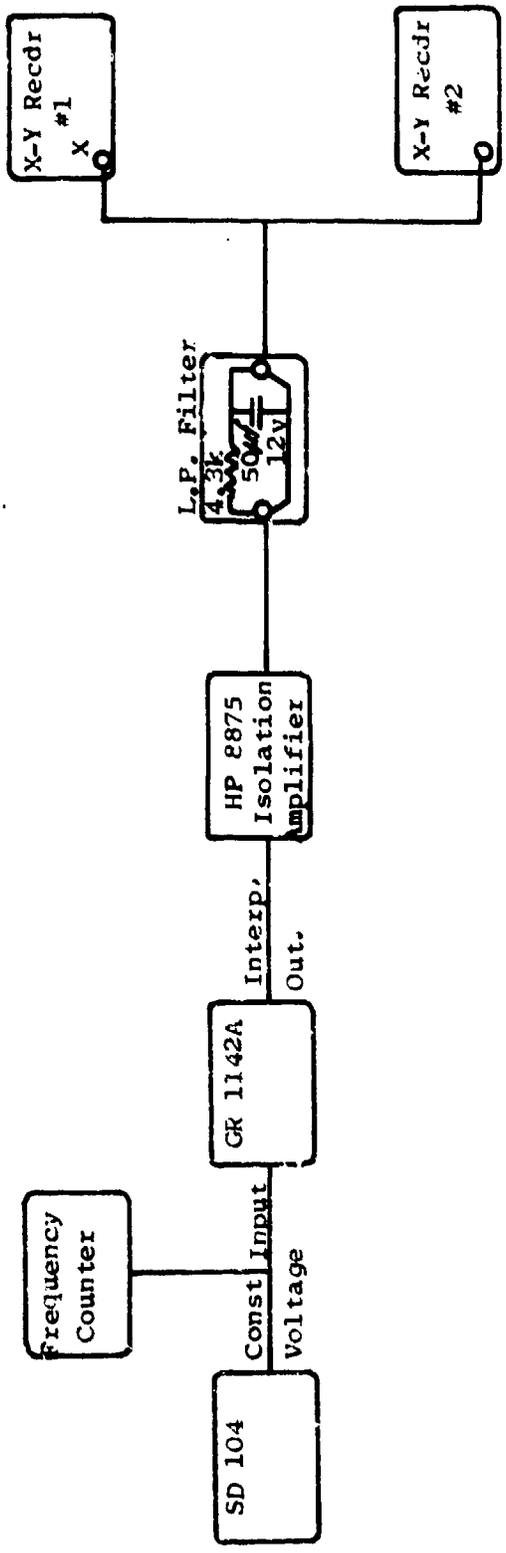

Figure B-8. Detailed View of Frequency Expansion Setup

per Figure B-7. The frequency counter was observed as the tape was played through the tape recorder. As the frequency counter approached the low frequency limit of the graph the X-Y recorder pen switch was thrown to the servo position, then, to the record position as the frequency counter and the pen reached the low frequency limit of the graph.

3. DATA REDUCTION

As noted earlier, a frequency resolution of 20 Hz/inch was found to be suitable for Q measurements using a filter bandwidth of 2.0 Hz. The X-Y recorder traces of the accelerometer response from the tape playback were recorded and assembled for each accelerometer location. The Q of each symmetrical response and its center frequency were noted and entered on computer cards for plotting purposes. A total of 74 data points were recorded for the store without cannisters (unloaded) and 101 data points were obtained for the store with cannisters in situ (loaded).

4. RESULTS

A plot of Q vs frequency for the SUU-41 skin (unloaded and loaded case) is shown in Figures B-9 and B-10. Their squared values vs frequency are shown in Figures B-11 and B-12.

A curve was chosen for a least squares fit. The function is of the form:

$$\theta = \tan^{-1} A$$

where: $$A = \frac{2\beta\, f/f_o}{1 - (f/f_o)^2}$$

β = a constant; to be determined

f_o = locator frequency; to be determined

Now, if we let $Q = k\theta$, where k is a proportionality constant

then, $Q = k\tan^{-1} A$

or , $$Q = k\tan^{-1} \frac{2\beta\, f/f_o}{1 - (f/f_o)^2}$$

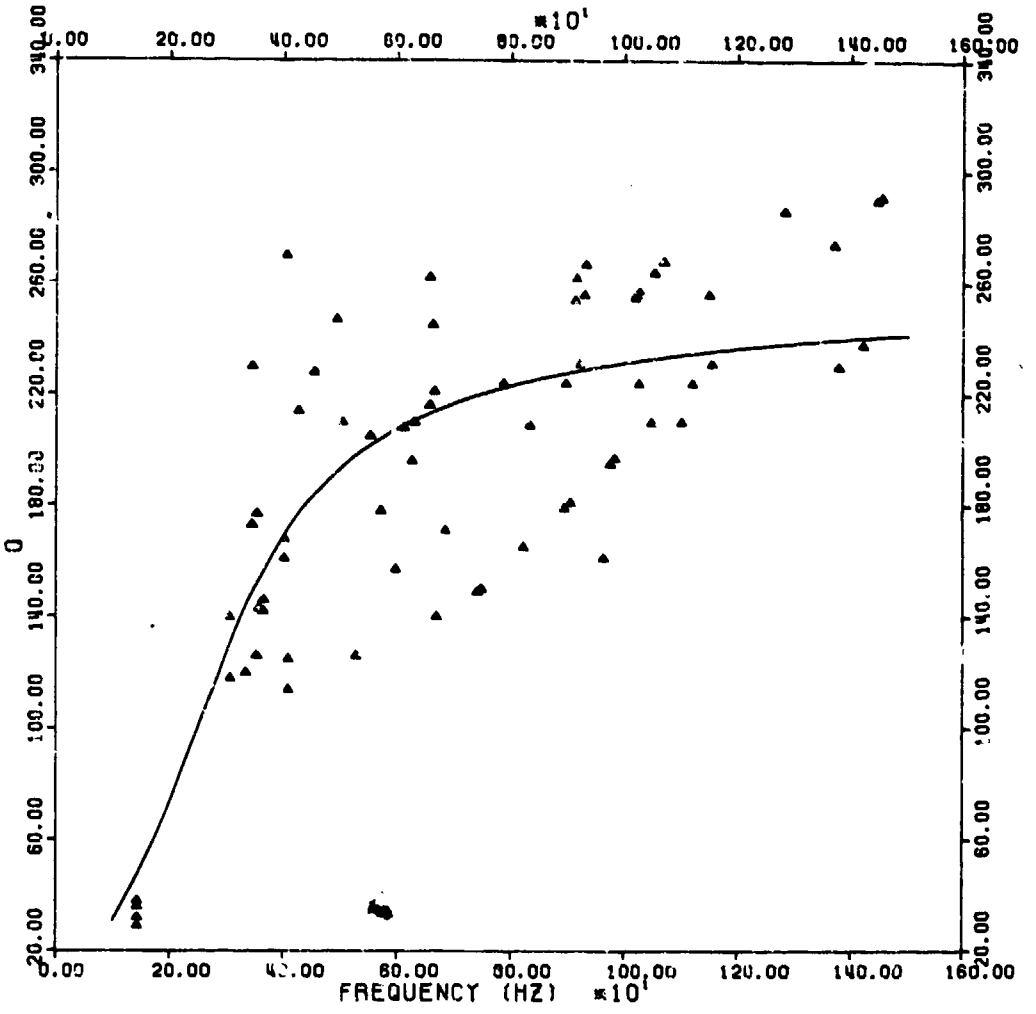

Figure B-9. Q vs Frequency Data Points for Unloaded Case

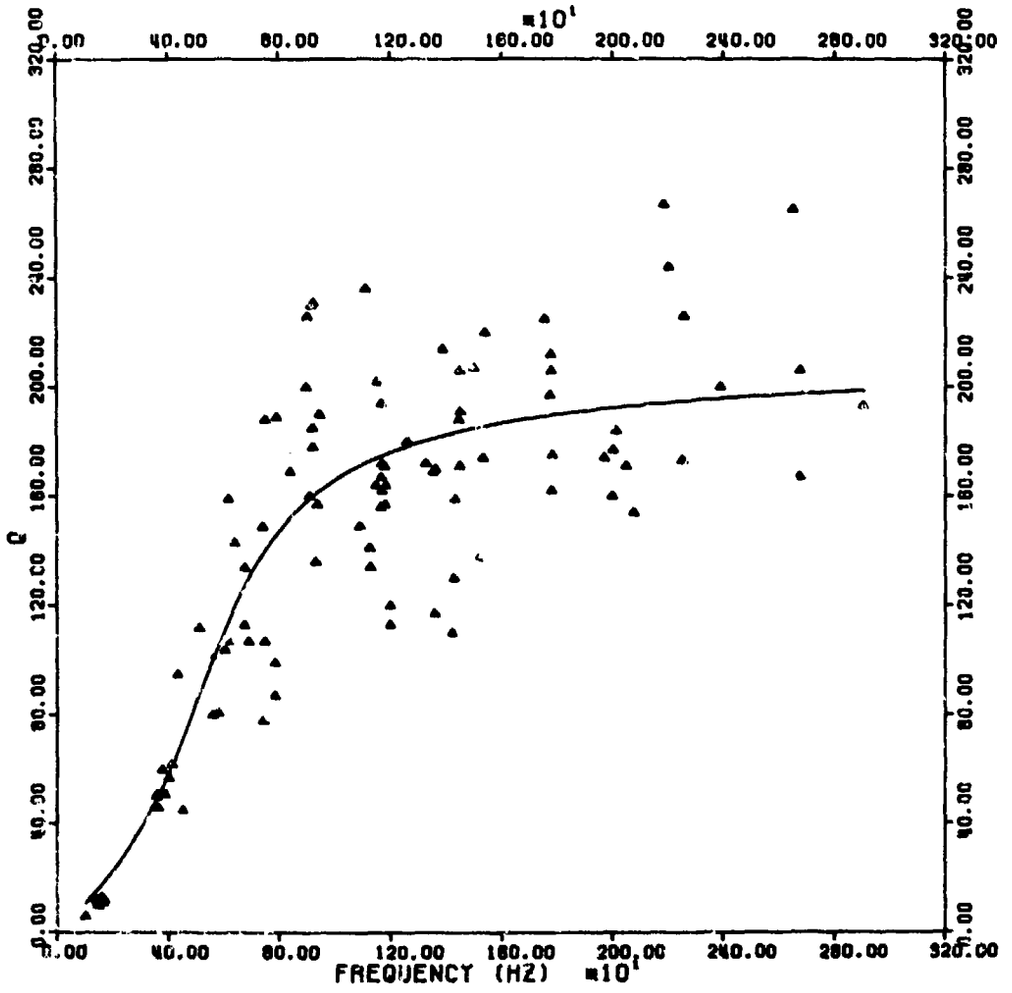

Figure B-10. Q vs Frequency Data Points for Loaded Case

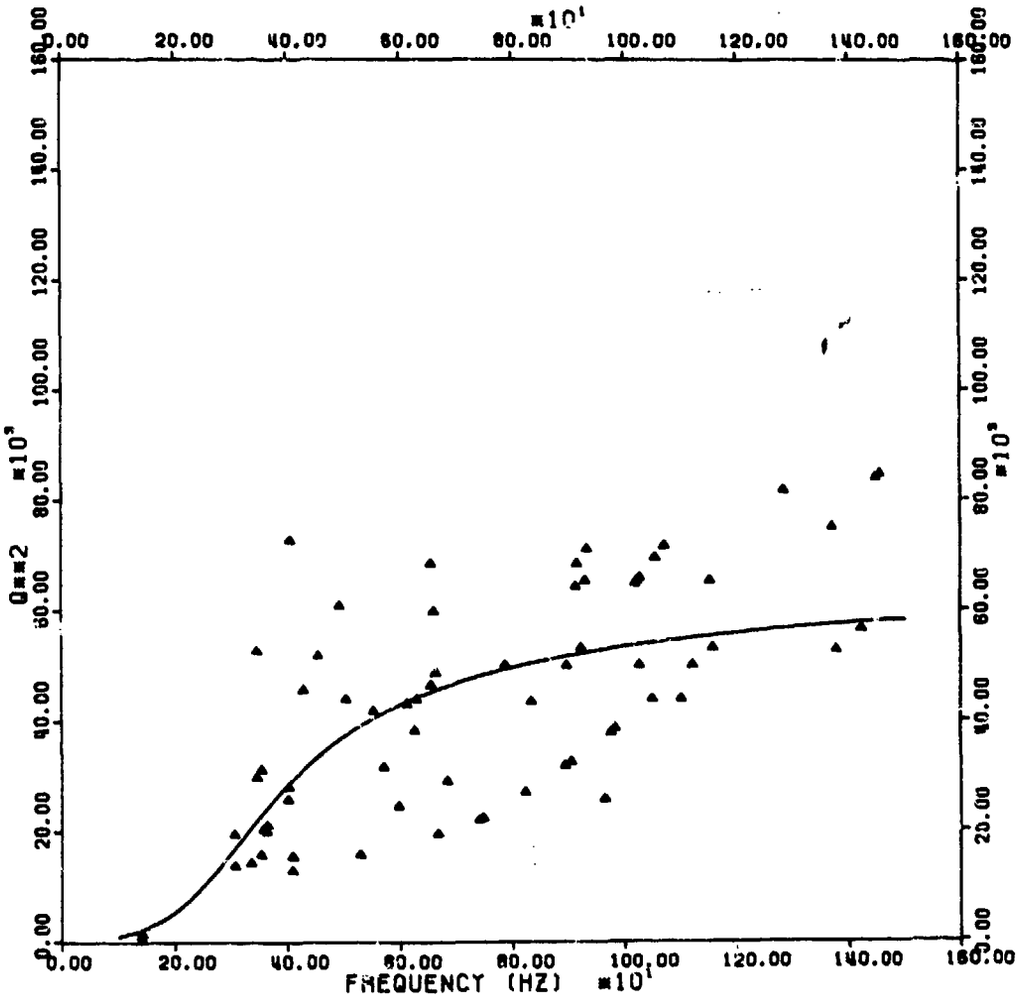

Figure B-11. Q^2 vs Frequency Data Points for Unloaded Case

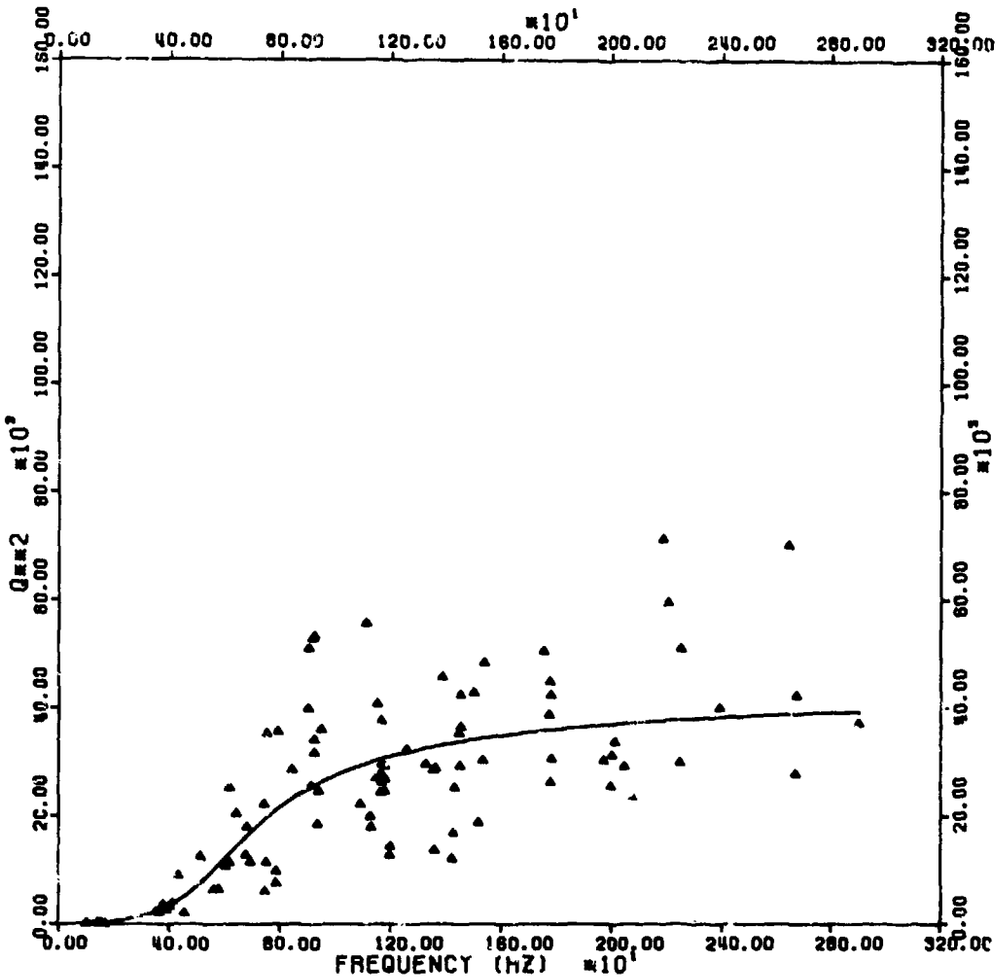

Figure B-12. Q^2 vs Frequency Data Points for Loaded Case

A computer regression program was introduced that utilizes step wise iteration for best fit. The program is initiated when first estimates of Q, f_o, and β are inserted into the program. The results are the curves shown together with the data plots of Figures B-9, B-10, B-11 and B-12. Table B-1 lists the best fit values of k, β, f_o, for the unloaded and the loaded case.

TABLE B-1

BEST FIT VALUES

f_o	β	k	
306	0.54	1.45	Unloaded
583	0.45	1.17	Loaded

It is more instructive to place the curves of Figures B-9 and B-10 together using the same scale (Figure B-13). Earlier, the fit for the unloaded case was restricted to 1600Hz. It was thought, at the time, that a better fit above that frequency could be had by introducing another curve that didn't asymptote as early as the arctan function. However, the strategem was not really worth all that and, in retrospect, the curve was extended as the original intended function out to 3 KHz in order to match the loaded curve. Anyway, as we shall soon see, the important curve is the regression curve for the loaded case because it is simply more representative of typical aircraft surface structure.

Note that the Q's have lowered when the cannisters were inserted. The cannister internal explosive was replaced with an equivalent weight of dry sand for this study, therefore the cannister load may be considered essentially resistive. It is interesting to note that structural response analyses based on energy concepts predict this type of behavior. The reduction in Q may be thought of as being the result of increased energy withdrawal from the skin due to an additional resistive load termination being introduced to the system when the cannisters are inserted. Put another way, the apparent loss factor of the skin has increased as a

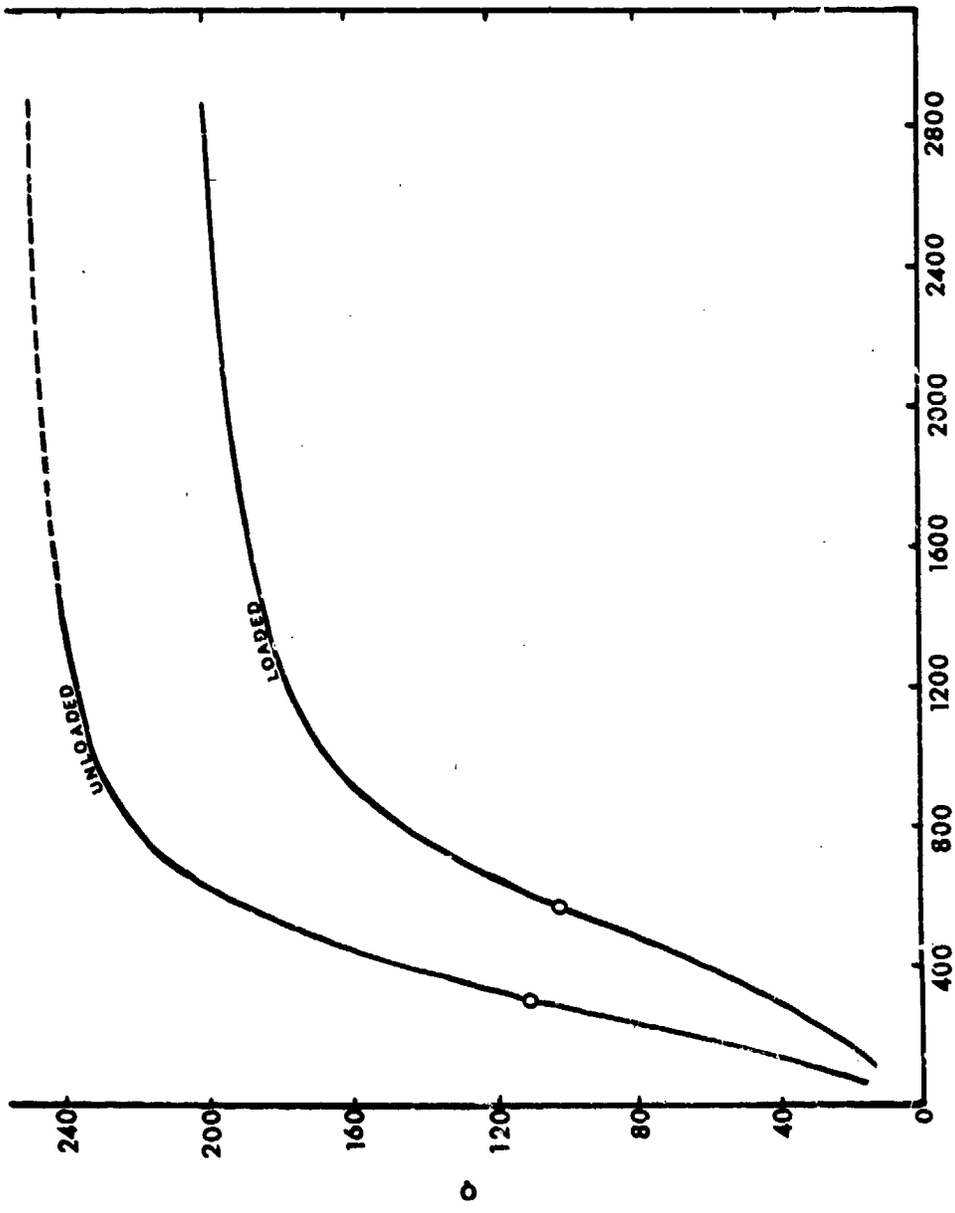

Figure B-13. Q vs Frequency Regression Curves for Unloaded and Loaded Conditions

result of the added internal load. This brings us to Figure B-14. Here, the apparent loss factor, η is set to the inverse of the Q and is plotted along with another interesting loss factor, that was determined by the decay method (Reference 4). This structure is an aircraft door taken from the nose section of the F-105.

On the whole, agreement is pretty good although the door appears to exhibit somewhat greater damping above 1 KHz. Perhaps this is not surprising since the door contains numerous reinforcing stringers and bulkheads, a multitude of rivets, spotwelds, inserts, and the door was painted on both sides. On the other hand, the SUU-41 skin is a relatively simple array of riveted panels, bulkheads, compartment dividers, and painted only on the exterior surface. Moreover, one can surmise that the coupling to the cannister loads is low since, mechanically, each unit is directly attached to the store structure by only two, small (1/8 inch dia.) vertical suspension rods that are ruptured during cannister release. Under the circumstances one should then expect a modest decrease in Q (increase in the loss factor) when the cannisters are introduced. This is the case since inspection of Figure B-13 shows the Q's down shifting about 3 dB or less.

Finally, the curve selected for the SUU-41 data seems to do a rather good fitting job. Note, too, that there is good agreement with the door loss factor in the low frequency region (below 1 KHz) and if we shift the arctan up a bit, we get a good fit for the data as a whole.

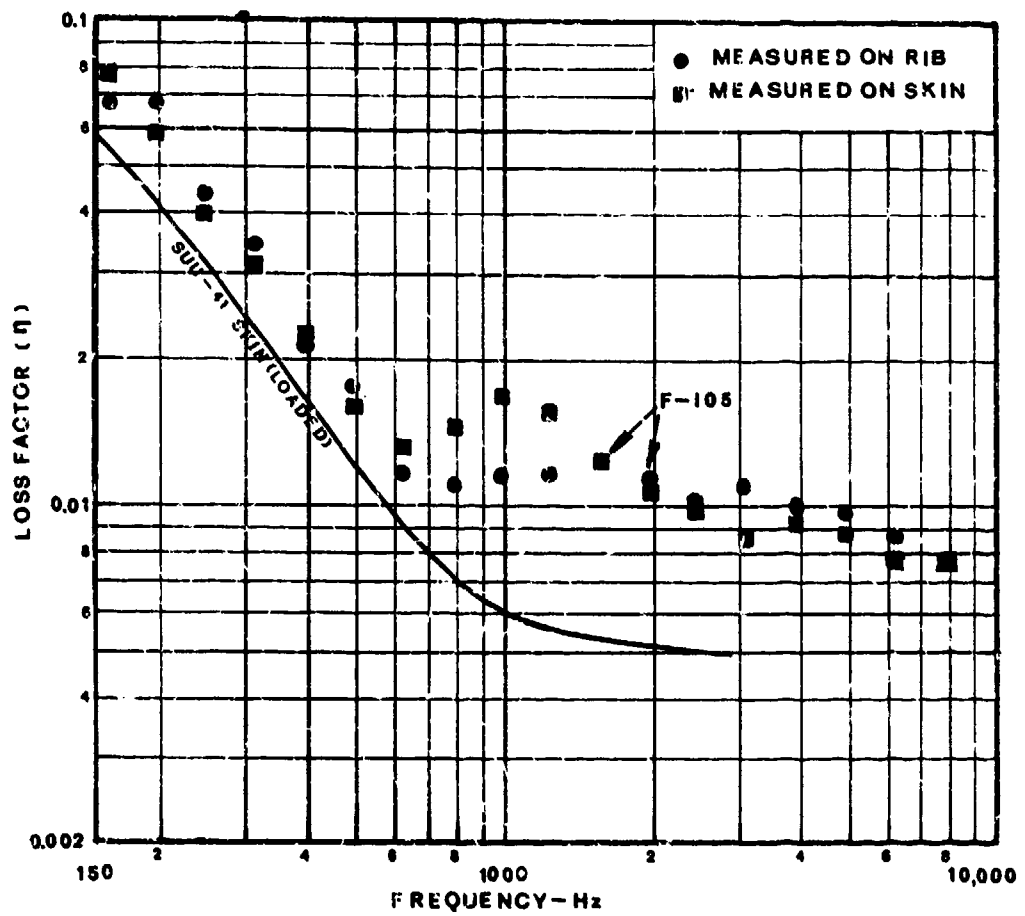

Figure B-14. Comparison Between Loss Factor of F105 Door and the Loss Factor for SUU-41 (Loaded)

APPENDIX C

SHAKER SYSTEM MODIFICATIONS

Circuit modifications were required for two equipment units of the MB T589 system. These equipments are designated MB models N-245 and N-275. They are discussed in this order.

1. N-245 SYSTEM MODIFICATIONS

a. Install two BNC connectors and two Pin Jack connectors to the front panel of the N-245 (Figure C-1). Electrically isolate each connector from panel.

b. MODIFICATION FOR EXTERNAL AMPLIFIER

(1). Disconnect lead from Terminal 4, Switch 1, Deck 2 (see Figure C-2) and connect this end of the lead to one BNC connector on the front panel. The high side of this connector is now tied directly to Terminal 1 on the Output Amplifier. Mark this connector "External Amplifier Input."

(2). Install a 50 uf 25v capacitor (C-25) between Terminal 4, Switch 1 (SW-1), Deck 2 and the second BNC connector on the front panel. Mark this connector "From External Amplifier Output."

(3). Connect a lead from the low side of both BNC connectors to one of the reference terminals on the Output Amplifier board.

> NOTE 1: For normal operation a jumper from one BNC connector to the other interconnects the circuit in the original configuration. For special application, insert a variable gain amplifier and/or filter between the two BNC connectors.

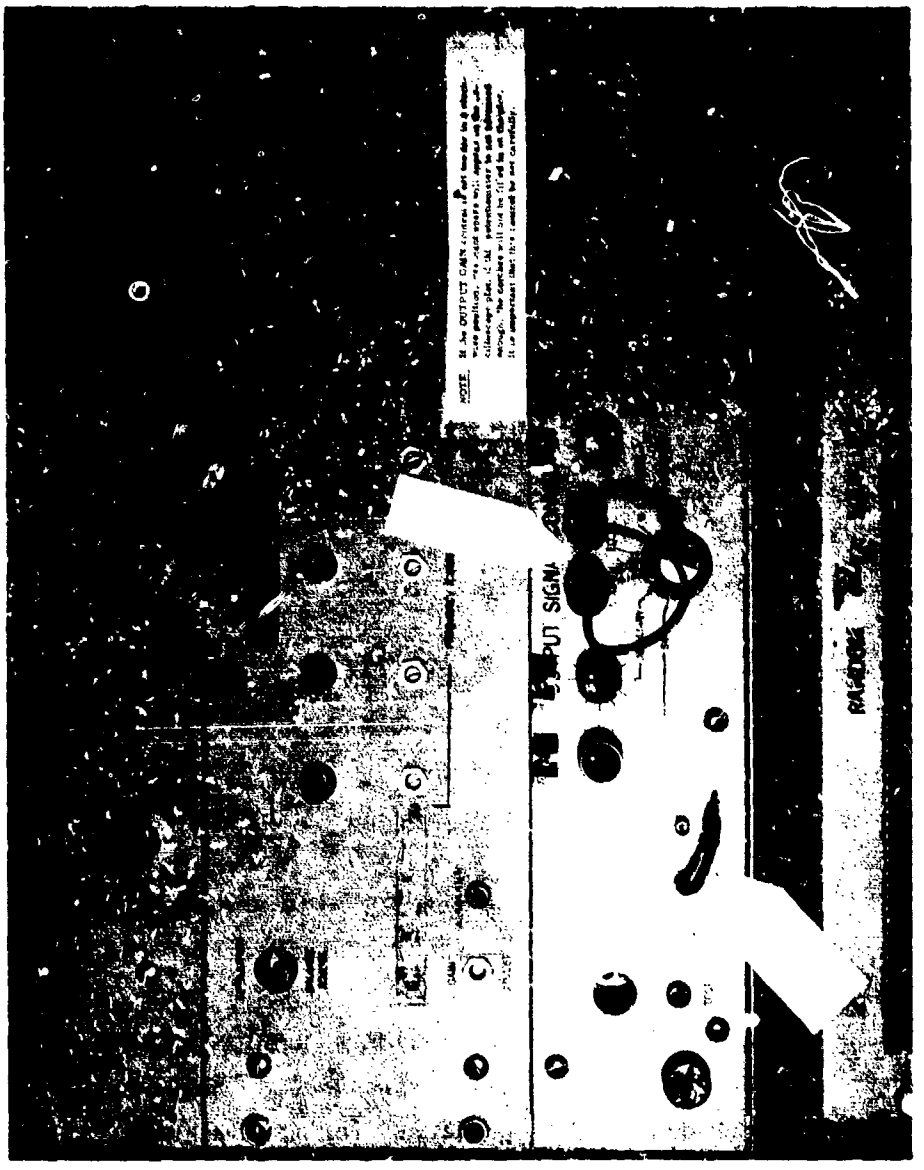

Figure C-1. Jumper Modifications of MB Model N-245

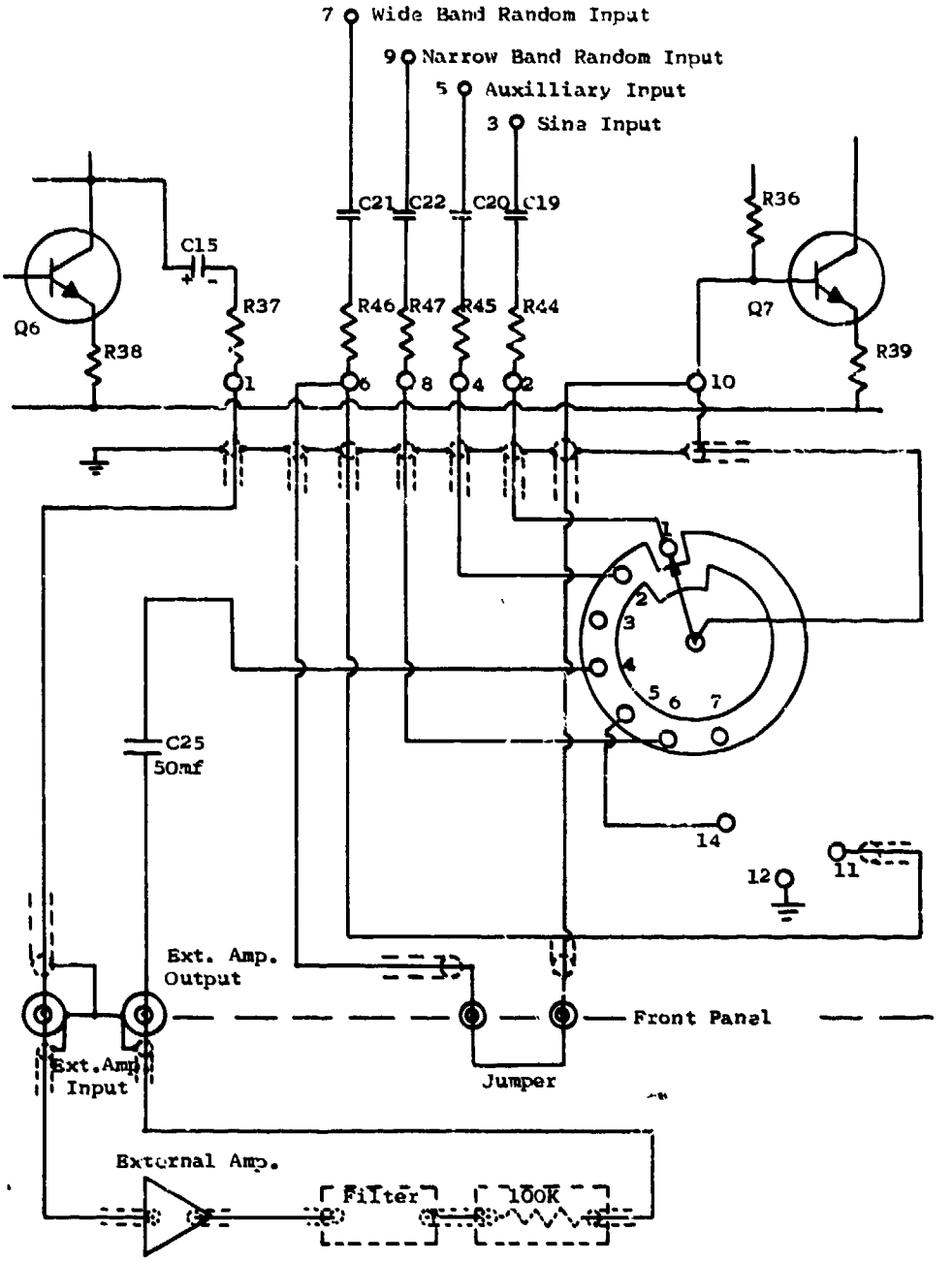

Figure C-2. Circuit Modifications of MB Model N-245

The amplifier used for this application should have a fairly high input impedance to prevent excess signal loss due to the voltage drop across R37 of the Output Amplifier. R37 may be paralleled with another resistor to somewhat compensate for an amplifier having a low impedance input. In any case, caution must be exercised to prevent overloading Q6.

Also, it may be necessary to insert a 100k resistor between the external amplifier output and the BNC connector marked "From External Amplifier Output" during "Mixed" operation. An isolation resistor is required if the output impedance of the external amplifier is sufficiently low to load the junction at summing resistors R44, 45, 46, and 47. This condition can be checked by applying a signal to the wide band random, narrow band random, auxiliary, and sine connectors and shorting the input to the external amplifier and observing the output drop of the N-245 when the external amplifier output is connected into the system.

c. Mod for Using Wide Band Random Input Connector for Mixing 4th Sine Signal

(1). Connect a shielded lead from terminal number 6 on the Output Amplifier board to one of the pin jacks on the front panel. Leave shield open at pin jack and connect other end of shield to a reference terminal on the Output Amplifier board.

(2). Connect a shielded lead from terminal number 10 on the Output Amplifier board to the other pin jack on the front panel. Leave shield open at pin jack and connect other end of shield to a reference terminal on the Output Amplifier board.

NOTE 2: Without the jumper between the two pin jacks the switch (SW-1) establishes the following circuit connections.

(a) SW-1 in "Sine" position: Sine input direct to Q-7; thence to the N-245 output. Wide band circuit is open. All other circuits are grounded thru summing resistors R45, R46, R47 and also thru R37 if BNC jumper is inserted.

(b) SW-1 in "Auxiliary" position. Same as par (a) except substitute Auxiliary in place of Sine and R44 in place of R45.

(c) SW-1 in "Mixed" position. Sine, Auxiliary Narrow Band Random are common thru summers R44, R45, and R46. This signal is also common with the output of Q6, which is the actual shaped spectrum. From here all signals input to Q7 thence to the N-245 output circuitry.

(d) SW-1 in "Equalized" position: From the Q6 output (shaped spectrum) to Q7, thence to the N-245 output. All other inputs, except wide band, grounded as in (a) and (b). Wide band is open.

(e) SW-1 in "Wide Band Random" position: Wide band random input to Q7, thence to N-245 output. All other inputs grounded as in (a) and (b).

(f) Switch in "Narrow Band Random" position. Same as (a) except substitute Narrow Band Random for Sine.

NOTE 3: With the pin jack jumpered: The same circuitry obtains as in Note 2 except for the following additions: Any signal on the Wide Band Random input connector (Wide Band pot turned up) will be mixed with a signal from: (1) Sine input when switch is in Sine position (2) Auxiliary input when switch is in Auxiliary position (3) Sine input,

Auxiliary input, shaped random signal, and the signal from the NB Random connector when SW-1 is in Equalized position; and (5) Signal at NB Random connector when in the NB random position. For the gunfire configuration SW-1 is in the "Mixed" position. In effect, the jumper provides an extra channel (wide band random) to sum with the other three inputs (Sine, Auxiliary, Narrow Band) thus providing the four required inputs for the gunfire sinusoids at f_1, f_2, f_3, and f_4. The original BNC input cable (the wide band input) is disconnected -- one of the sinusoids is substituted in its place. The other three sinusoids are connected to the Sine, the Auxiliary, and the Narrow Band input.

NOTE 4: When using the external amplifier and/or bypass filter, care should be exercised to see that Q7 is not over driven. An oscilloscope check across R39 will readily determine if overload occurs.

NOTE 5: For a complete layout of the N-245 Output Signal Converter see MB schematic diagram 9387361.

d. For our configuration, which utilized an external amplifier and filter (Note 4), the rolloff frequencies (1-3 dB down points) of the filter were set at 260 and 1200 Hz, the rolloff was approximately -18 dB/octave. An SKL Model 302 was used. It should be added that the filter settings, indeed the very use of the filter, depends upon the individual equalization problems of each test setup. For many test setups the filter is probably unnecessary.

2. N-275 MODIFICATIONS

a. Install a pair of banana jacks and a BNC connector on the front panel of the N-275 (Figure C-3). Install a gear and potentiometer assembly and a trimpot in the top section of the N-275 (Figure C-4). Install an operational amplifier and a solid state regulated power supply in the bottom section of the N-275 (Figure C-5).

b. Modification for driving the X axis of the X-Y recorder with the Channel Selector Switch.

(1). Obtain a gear that will mesh with the gear directly behind the front panel on the channel selector switch shaft. Using this gear and a 100K potentiometer, make up a gear and potentiometer assembly per Figure C-4. Install the gear and potentiometer assembly to the back side of the front panel, carefully spacing the assembly, so that the two gears mesh properly. Set the channel selector switch to Channel 1 and adjust the potentiometer so the X-Y recorder indicates Channel 1 on the graph paper.

(2). Install a pair of bannana jacks slightly to the left of "X" monitor jacks on the front panel of the N-275 (Figure C-3). Mark these jacks "Selector Switch X Axis."

(3). Install a trimpot (20K to 100K) in proximity to the gear and potentiometer assembly.

(4). Make electrical connections as shown in Figure C-4.

c. Modification for Narrow Band High Frequency Output.

(1). Install a ±15 power supply (Zeltex Model ZM1550 or other) and an operational amplifier (Fairchild ADO 60 or other) in the bottom section of the N-275 (Figure C-5).

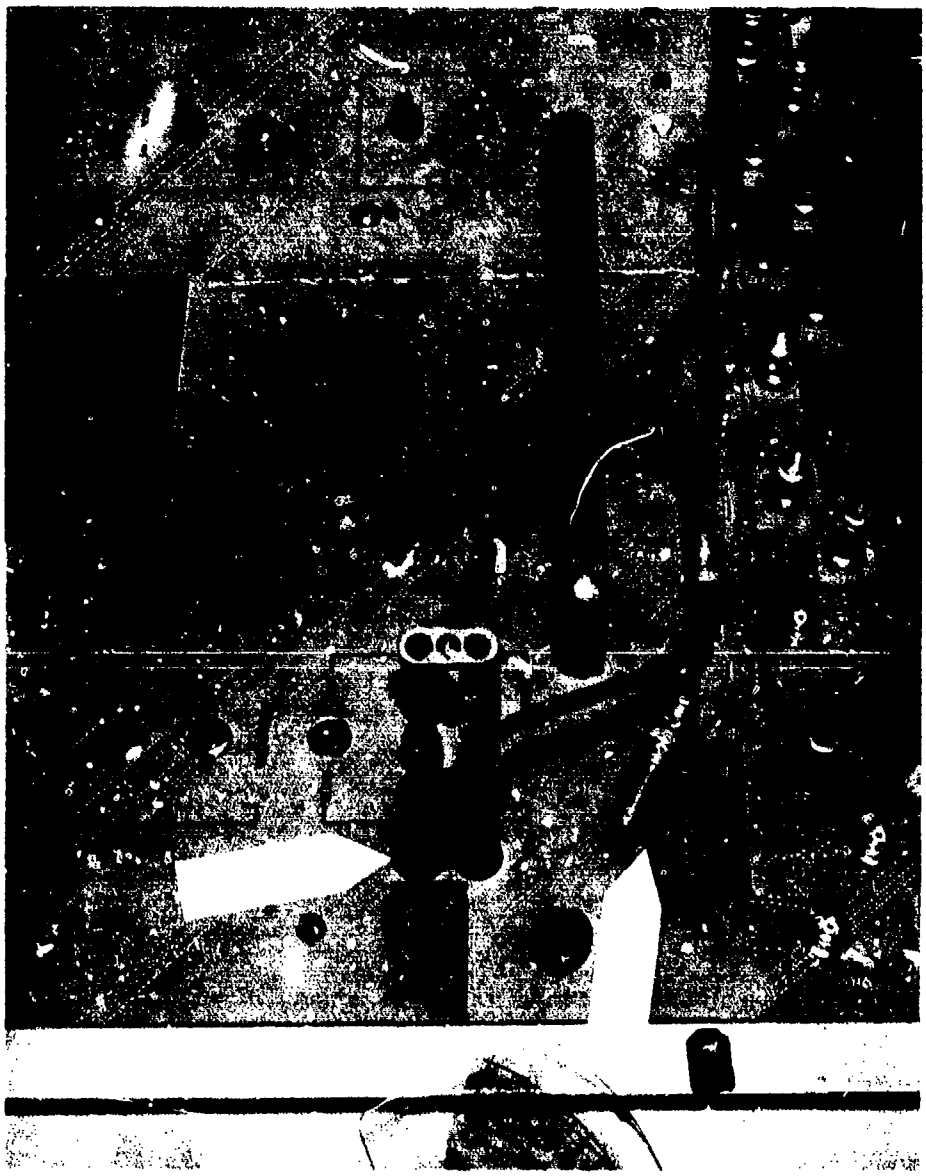

Figure C-3. Outlet Jacks Installed on Front Panel of N-275

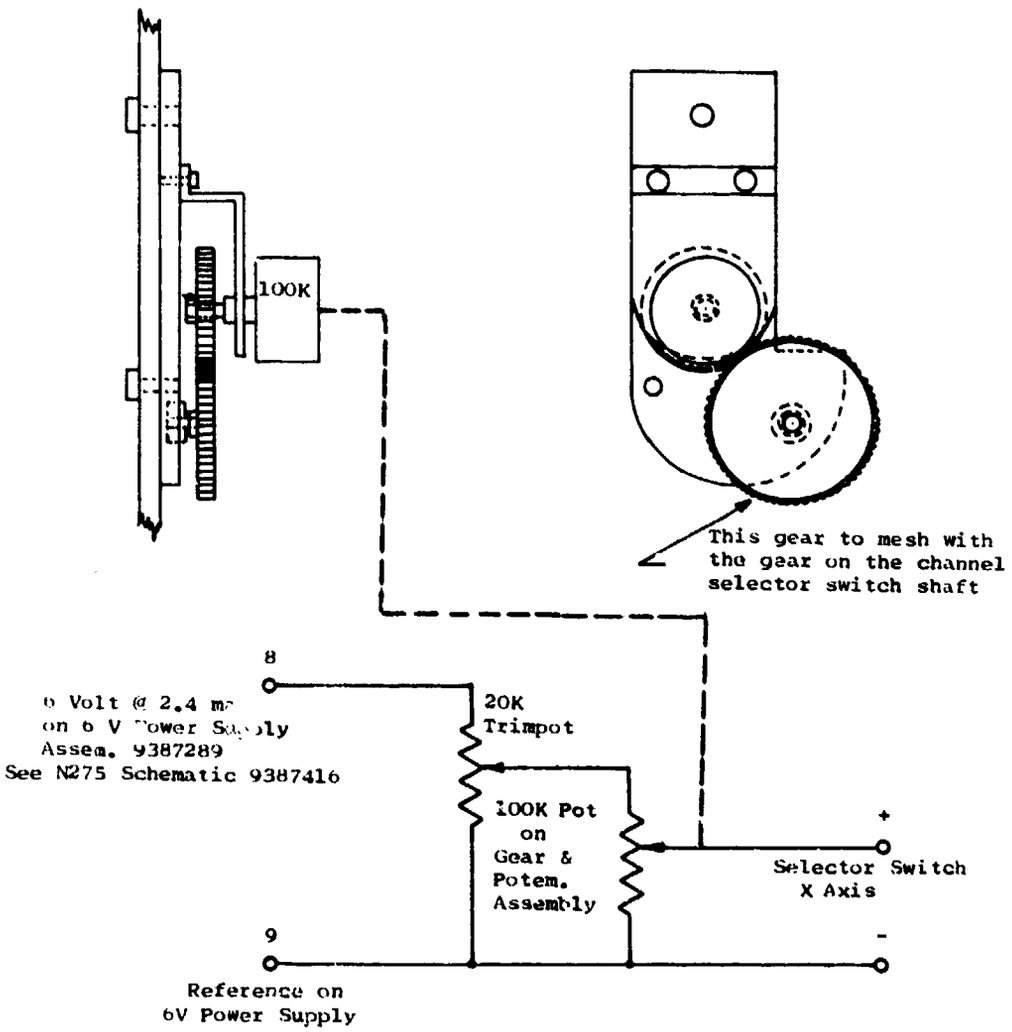

Figure C-4. Electromechanical Modification of MB N-275

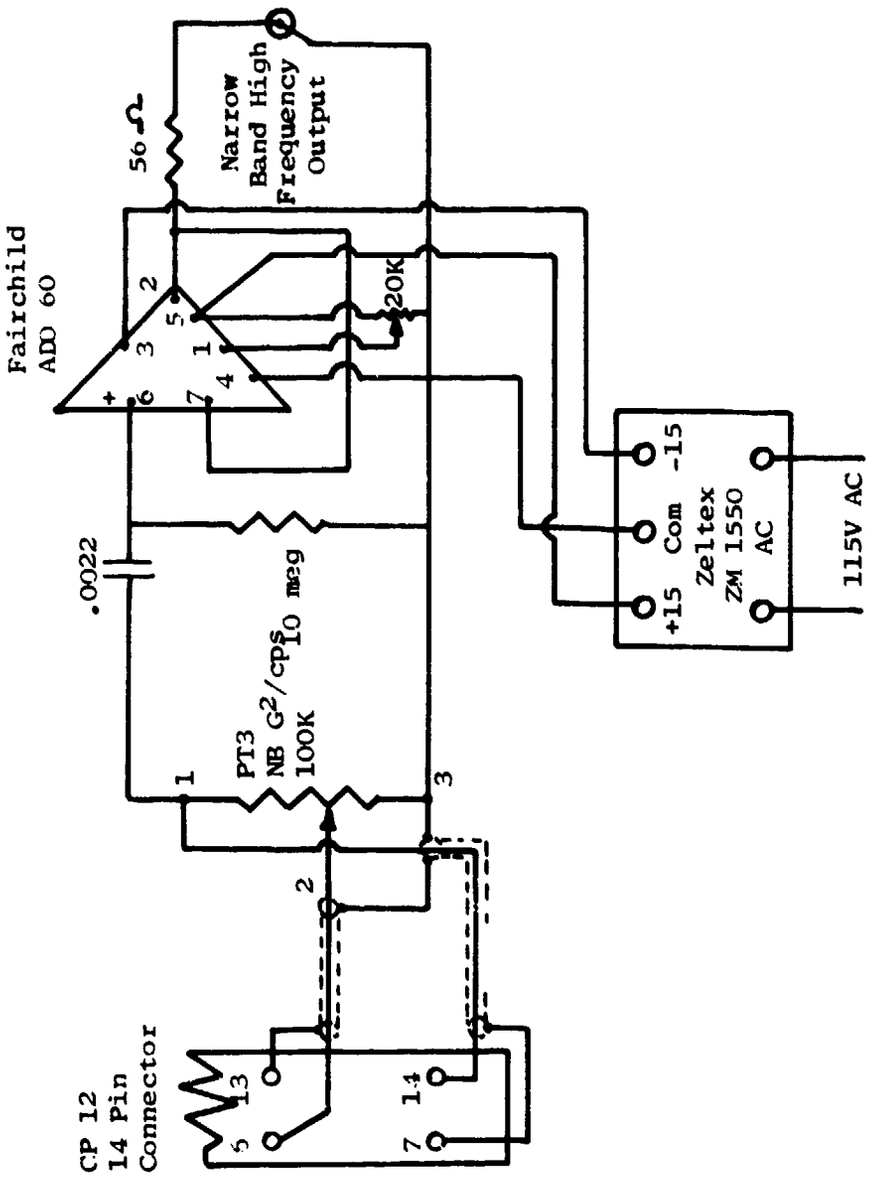

Figure C-5. Installation of High Frequency Amplifier Module of MB, N-275

(2). Connect the operational amplifier for unity gain. Connect the input of the op-amp to the "NB G^2/H_2 Pot" (PT3). Connect the output of the op-amp to the BNC connector installed on the front panel of the N-275. See Figure C-3.

3. CALIBRATION AND ADJUSTMENTS

a. We begin by normalizing the Channel Selector Switch X Axis Output so that the recorder X axis indicates the same relative position per channel whether driven by the External Monitor signal or by the Channel Selector Switch X Axis Signal.

(1). First, calibrate the X axis of the recorder using the External Monitor signal. Use the left writing pen (Y^2) as reference. This pen will be used for the Y External Monitor signal which is the normal plotter output.

(2). Next, connect the recorder X axis input to the Channel Selector Switch X Axis signal. Do not change the zero nor the X axis gain of the recorder.

(3). Select Channel 80 on the Channel Selector Switch. Adjust the Channel Selector Switch X Axis output signal, using the trimpot, so that the right pen (Y^1) is aligned with the Channel 80 position on the graph paper.

(4). Select Channel 1 on the Channel Selector Switch and observe whether the right pen (Y^1) is aligned with the Channel 1 position on the graph paper.

(5). During the initial calibration using the Channel Selector Switch X Axis output it will be necessary to change the potentiometer wiper position with respect to the gear on the channel selector switch shaft to obtain the proper position for Channel 1 and to adjust the trimpot to obtain the position for Channel 80. The potentiometer wiper

position with respect to the gear can be changed either by meshing different teeth of the gear on the channel selector shaft with the gear on the gear potentiometer assembly or by leaving the gears meshed and changing the potentiometer shaft position relative to the gear of the gear-potentiometer assembly.

(6). After normalization of Channels 1 and 80 for both inputs check all channels in between for channel correspondence of both pens.

a. This can best be accomplished by setting the odd channel sliders at +10db and the even channels at -10db then making a plot in closed loop operation from the monitor jacks. Change the recorder X axis input over to the Channel Selector X Axis connector and rotate the selector switch through the 80 channels and point plot each channel. The high frequency NB output is connected through a log converter to the recorder Y^2 input.

4. SUMMARY OF N-275 MODIFICATIONS

a. The modifications as detailed in this Appendix provide two main advantages. First, a spectral readout is made available that is independent of the present auto step scanning system. One can quickly switch to a desired channel (using the selector switch) without having to scan through the full 80 channels. In contrast, the modification permits each (or any) channel to be quickly monitored and this allows a spectrum to be checked and adjusted much more swiftly than was formerly possible. The second advantage has to do with increased accuracy. The log DC, as it normally comes from the N-275, contains nonlinear errors which though small at the center of the equalizer range show up noticeably at the lower positions of the equalizer slide wires. Figure C-6 shows a plot of a shaped spectrum of the N-275 Log DC output plotted together with the spectral output of the modification (Hi. Freq. output) and includes a spectral plot of an accelerometer input to the N-275 as seen from the log output of a SD 101B using a 10 Hz analyzer bandwidth. The high frequency output passes into a Pacific Measurements Model 1020 log converter, thence to the second channel of a two axis recorder. This versatile converter is accurate to within 0.1 dB -- the SD101B within a quarter of a dB. Note that at the chart lower extremities the N-274 plot is low by about 1 1/2 dB.

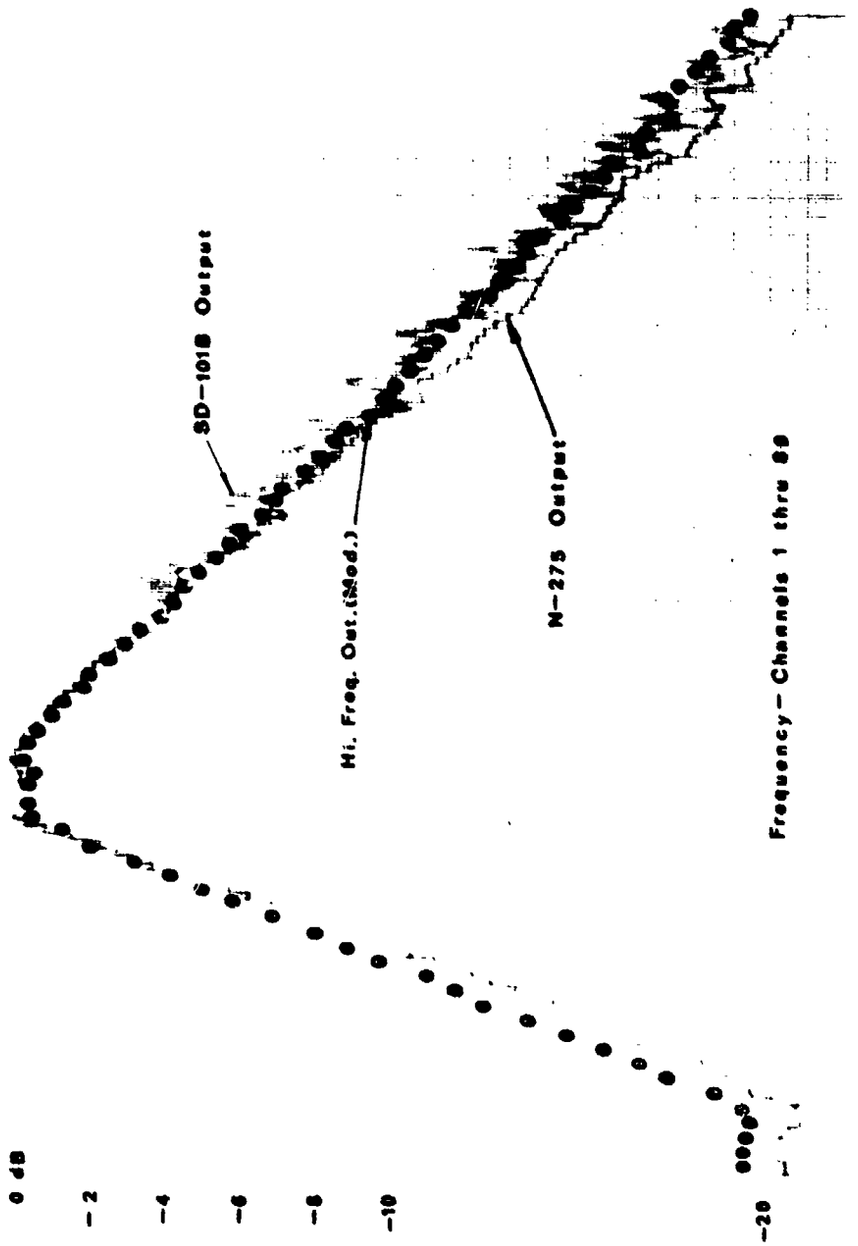

Figure C-6. Nonlinear Error of M8, Model N-275 DC Output

APPENDIX D

TEST PROCEDURE

1. PRELIMINARY PROCEDURE

A. EQUALIZER SYSTEM

(1). Debug the equalizer

(a). Adjust system for maximum performance with emphasis on achieving maximum servo control of the channels in the upper frequency range (1 KHz and above). This step is especially important for vibration levels run at 0.5 g^2/Hz and above and for test loads of 25 pounds or more. In general, the higher the levels and the larger the load the greater the demand on the dynamic range of the servo channels. In the high frequency range inadequate compression produces notching problems and this difficulty is often exacerbated by high Q resonances of the test assembly. Moreover, the difficulty is further accentuated by the asymmetric dynamic range of the equalizer channels resulting from adjacent skirt contributions that add in the plus (peak) direction and, also, in the negative (notch) direction. The latter effect is to subtract from the notching, or, compression capability.

(b). Having tweaked up to best equalizer performance additional compression range can be acheived by shifting the equalizer zero level up to, say, +10 dB. This subterfuge yields additional negative dynamic swing (compression or notching) at the expense of the peaking capability; an exchange that usually turns out to be profitable.

(c). For the larger test loads, approximately 50 pounds or larger, the low frequency part of the spectrum may require supplementary boost to assist the equalizer in the positive direction especially since, in this test configuration, the lower channels 1 to 19 (25 to 500 Hz) are switched to the manual position; thereby disabling their servo feedback loops. For the T589 system a single modification of the N-275 chassis provides convenient means by which a variable gain amplifier and

band pass filter may be inserted into the servo loop to provide adequate low frequency boost and, for that matter, to provide additional high frequency rolloff. See Appendix D for details.

B. PEAK - NOTCH FILTERS

(1). In all probability several peak notch filters (P-N) will be used, mostly in the notch mode, and usually located in the high frequency region. A major drawback to P-N's are the electrical loops that they tend to introduce into the system at 60, 120, 180 Hz. These are frequencies that are very close to, or are within, the cycling bandpass of the four sinusoids. It is important therefore to debug the P-N's for minimum noise contribution. If the P-N's are "tube" types check to see if there is D.C. on the filaments, if not, then convert. If 120 Hz is still present check the D.C. supply. Remember, that many of the preliminary adjustments in this procedure are conducted at -20 to -30 dB (re. the actual test level) and that it is therefore important to insure good signal-to-noise ratio in the low frequency part of the spectrum in order that the sinusoids remain easily identified as to magnitude and frequency.

(2). Finally, take care to observe "Frumps Fourth Law of P-N's" which asserts: "If fewer P-N's can be used -- then use them."

C. GROUND LOOPS - AC POWER

(1). For the same reasons cited in paragraph B the shaker system and associated equipment should feature a good common ground interconnect for the AC power which should, preferably, terminate at the incoming ground of the building power transformer. This termination should involve the shortest possible distance (Figure D-1).

D. GRAPHIC DISPLAY INNOVATIONS

(1). Sine Pre-Graphing

Amplitude vs frequency curves are entered on the two console X-Y recorders in order to describe the cycling and control profile for the four sinusoids. Each of the two recorders (one for

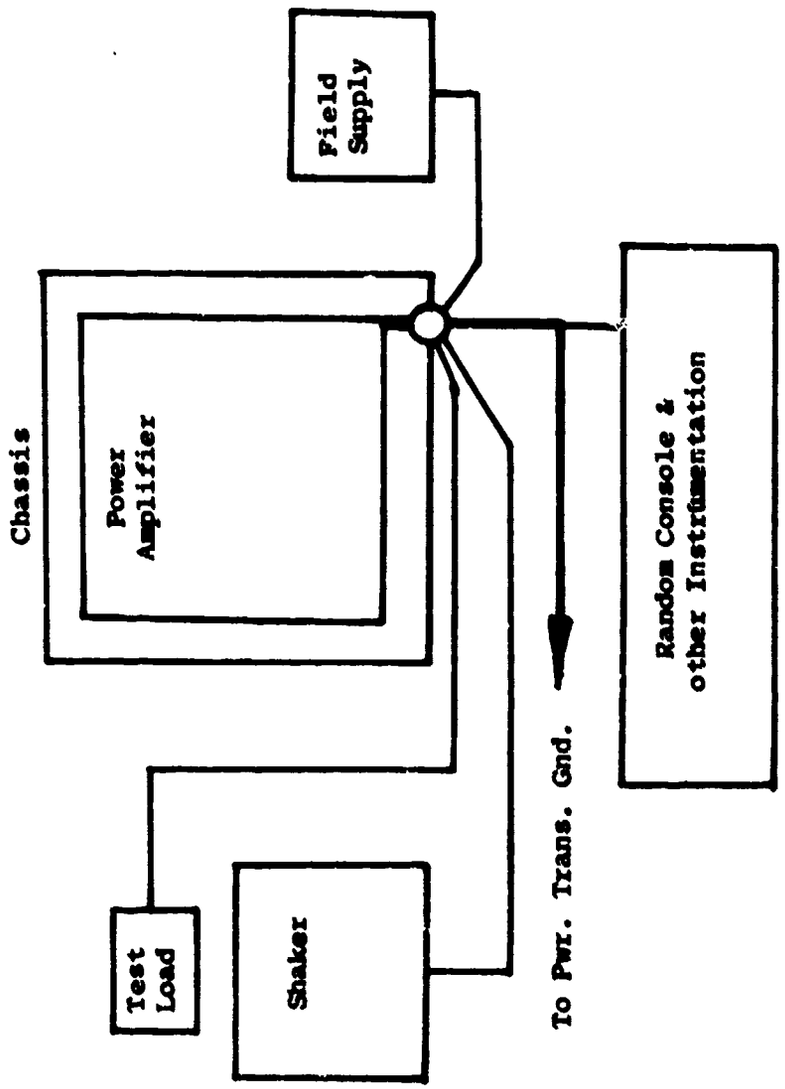

Figure D-1. Basic Grounding of Shaker System

console number 1 and one for console number 2) accommodates a pair of sinusoids as shown in Figure D-2. In practice, upper and lower boundary lines, indicating the amplitude tolerance limits, should also be entered on each curve. For details concerning the setup procedure see Paragraph E.

(2). Oscilloscope Spectral Display

A large screen scope provides an effective spectral display. Spectral information is further enhanced when the random and sine spectra together with their tolerance boundary lines are drawn on the face of the scope. Colored grease pencils were found to be effective means for delineating amplitudes and tolerance limits. Figure D-3 illustrates the display arrangement. Also, the scope display provides a quick means by which ground loop presence can be detected at 60, 120, 180, 240 and 300 Hz.

E. SETUP FOR SINE SUPERIMPOSED ON RANDOM

(1). Obtaining Swept Sines from Four Wavetek Model 144 Generators (VCG).

(a). Determine the main dial settings and the external VCG input control signal required to obtain the center frequency (CF) and the $\pm$20% CF for each generator using the VCG voltage-to-frequency nomograph.

(b). Note from the nomograph that if the main dial of each generator is set to the center frequency that the voltage required at the VCG input to obtain CF is zero, and, that the output frequency for each generator is proportional to the plus and minus voltages applied to the VCG input.

Example: Suppose the desired center frequencies are 100, 200, 300, and 400 Hz. Center frequencies minus 20% are then 80, 160, 240 and 320 Hz, while center frequencies plus 20% are 120, 240, 360 and 480 Hz. With the main dials set at 100, 200, 300, and 400 Hz,

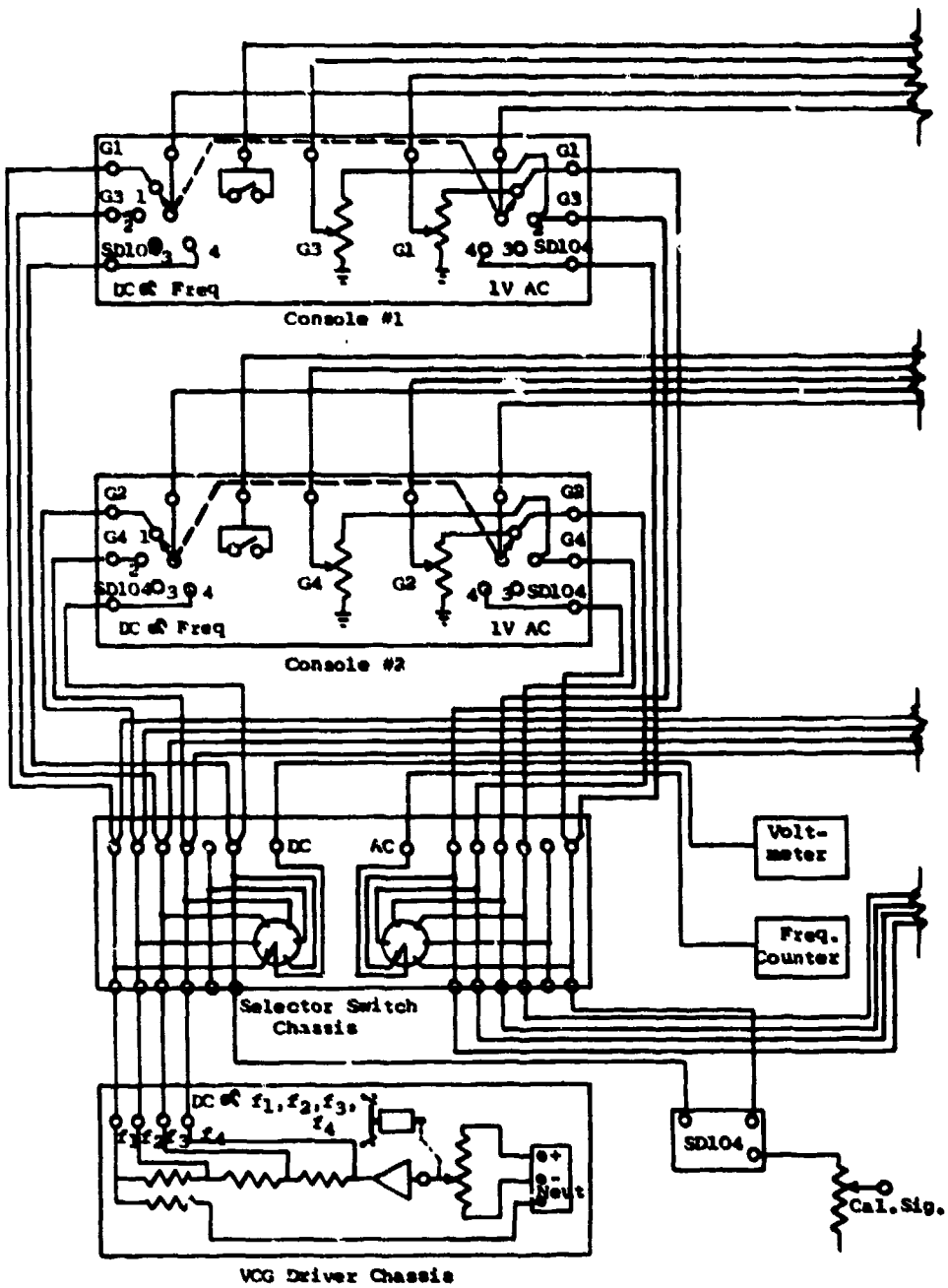

Figure D-2(a). Schematic for Control Console

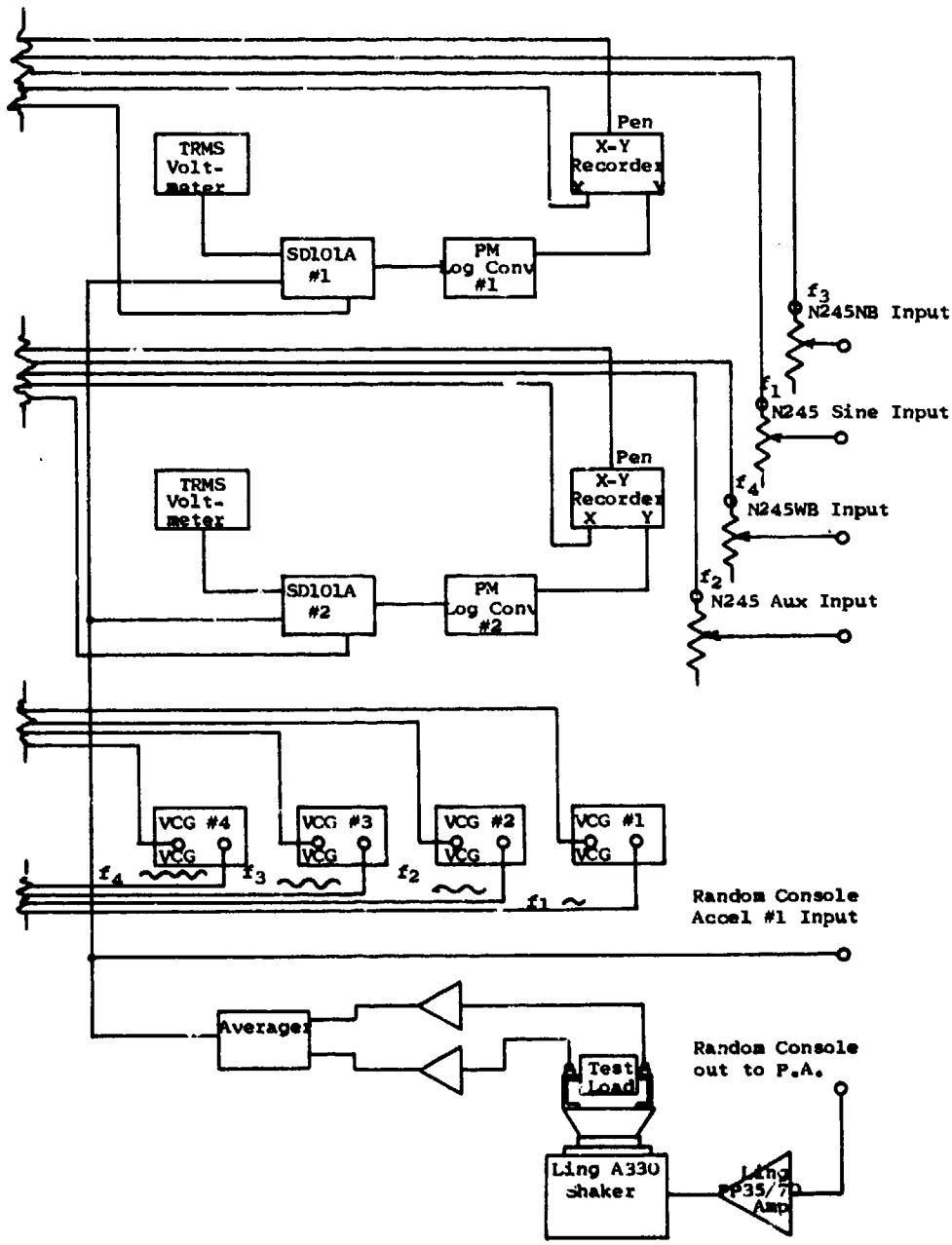

Figure D-2(b). Schematic for Control Console

Figure D-3. Tolerance Limits Marked on Oscilloscopes

the negative voltages at the VCG inputs required are 100 mv, 200 mv, 300 mv, and 400 mv for 80, 160, 240, and 320 Hz, respectively. Also, the positive voltages required at the VCG inputs are 100 mv, 200 mv, 300 mv, and 400 mv for 120, 240, 360, and 480 Hz, respectively. This permits the use of a simple dividing voltage network supplied by a single plus and minus supply to obtain the desired frequencies from each of the four generators. See Figure D-4.

If the $\pm$ regulated voltage into the potentiometer is less than the minimum VCG required for VCG number 4, the variable gain amplifier can be used to adjust the VCG's for the desired frequencies. Turn the $\pm$ potentiometer to full positive or full negative position, then adjust the amplifier to obtain f_4 + 20% f_4 or f_4 - 20% f_4, respectively. Check frequencies of all generators. Slight trimming of R_1, R_2, or R_3 may be necessary to obtain the required frequencies.

A reversible motor connected to the shaft of the $\pm$ potentiometer will provide automatic sweep. Sweep rate is determined by motor speed.

To prevent override of the $\pm$ potentiometer stops, the reversing switches should be actuated a few degrees before the limits are reached. The reversing switches determine the full positive or negative voltage when adjusting the amplifier for the required VCG input voltage to obtain the desired VCG number 4 output frequency.

(2). Connecting Sine Inputs to Random Console

The sine inputs are mixed with the shaped random spectrum before the master gain in order that master gain has full control. The random spectrum and the sine inputs can be mixed using an external summing network, or when using the MB T-589 Random Console the random spectrum and up to four sine signals can be mixed in the N245 Output Signal Converter.

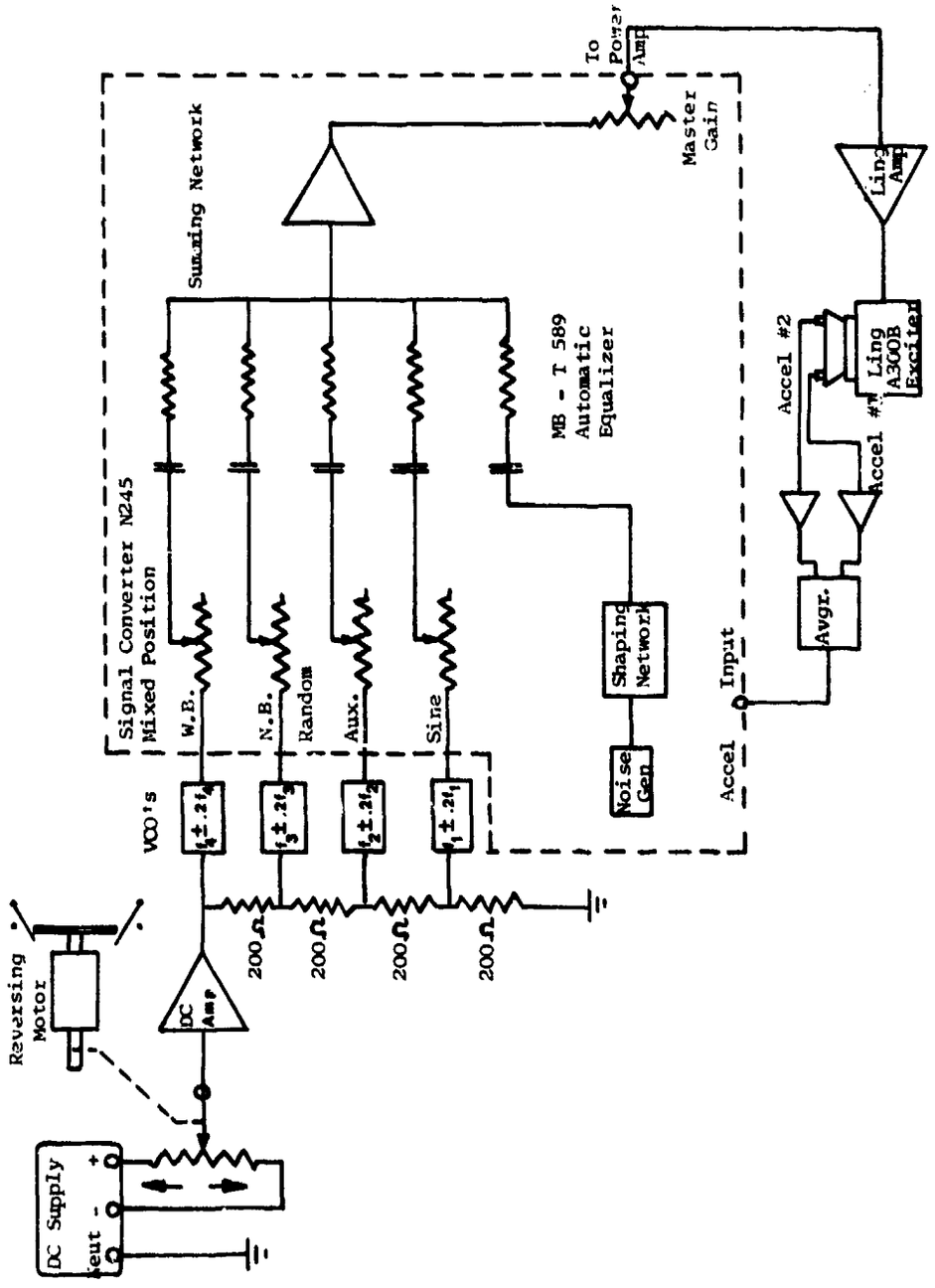

Figure D-4. Sinusoidal Generation and Sweep System

When using the MB T-589 and mixing the signals in the N245, the output signal converter selector switch is set to the "Mixed" position, and the sine inputs are connected to the sine, auxillary, wide band random, and narrow band random inputs. (NOTE: Since the wide band random input is not connected to the N245 Output Amplifier when in the mixed mode, it is necessary to jumper the signal around the switch. This is accomplished by a jumper between terminals 6 and 10 or the N245.) For further details see Appendix C.

(3). Equalizer Automatic-Manual Switch Positions

Determine the portion of the random spectrum over which the sine signals are to be swept and set these switches in the manual mode. Set the remaining switches in the automatic position. For the T589 system this amounts to setting channels 1 thru 19 to manual and channels 20 thru 80 to automatic.

(4). External Instrumentation (Figure D-2)

Two tracking filters with 5 Hz BW filters and two X-Y recorders should be used for monitoring the sine input levels. If the tracking filters do not provide a DC Log output proportional to signal, external log converters should be inserted between the tracking filter outputs and the X-Y recorders.

Switched outputs from VCG's 1 and 3 are connected to the tuning input of one tracking filter while the switched outputs from VCG's 2 and 4 are connected to the tuning input of the other tracking filter.

By using the DC VCG input signals in conjunction with the switched outputs of the VCG's, the X axis of the X-Y recorders can be calibrated to correspond to the frequencies of the VCG's.

A true RMS voltmeter connected to the filtered signal of the tracking filters is beneficial for monitoring the sine levels during initial setup. However, the required time constant of the meter is too long for practical application during rapid amplitude changes.

A sweep oscillator with a constant amplitude for tuning a tracking filter and with a DC proportional to frequency for driving the X axis of the X-Y recorder can assist greatly in determining ground loops and other extraneous signals.

A frequency counter is required for setting in the sine frequencies, locating notch frequencies, and determining extraneous signal frequencies.

(5) Calibration and use of Tracking Filters

The following paragraphs include some useful details concerning recorder calibrations and narrow band filter uses; both done in conjunction with some special switching capabilities of the control console.

Two cycle by 150 division graph paper was determined to be appropriate for adjusting and plotting the swept sine levels. This scale permits sufficient spacing between the sets of curves such that overlapping will not occur and the curves will still be spaced sufficiently close such that the 1 secord time constant for the 5 Hz filter does not constitute a delay problem during rapid switching from one sinusoid to the other. Good resolution for frequency is obtained if the X or horizontal axis is calibrated to 20 Hz/inch.

To pregraph the sine test curves, the curves were first plotted on 2x3 cycle graph paper where the amplitude vs frequency profile plot has, for this study, been simplified to a straight line. The voltage vs frequency points were then transferred to the semi-logarithmic paper.

With the above preliminaries out of the way, calibration can be started (See Figure D-2).

(a). Select Range and Multipier switch positions that will accept full test level operations without overloading the tracking filter.

(b). Disconnect the averager output lead from the tracking filter inputs and connect the calibration signal lead from the sine oscillator to the tracking filter inputs. Connect a voltmeter in parallel with the tracking filter inputs.

NOTE: In our case, the SD104 was used for preliminary narrow band checks and therefore was readily accessible for calibration. However, if an oscillator was not used as the SD104 is shown in the circuit diagram, one of the VCG's can be used for calibration.

(c). Tune the tracking filters with the same oscillator or VCG that is used to supply the calibration voltage using the switches on consoles 1 and 2.

(d). Disconnect the leads from the X axis of the X-Y recorders and adjust the X zero for an abscissa value equal to the center frequencies of f_1, f_2, f_3, and f_4.

(e). Adjust the calibration signal for 100 mv, 200 Hz.

(f). Turn the X-Y Recorder Servo on and proceed to calibrate over a 20 db range (10-100 mv) so the ordinate position agrees with values on the graph paper.

(g). Position the cycler to the low end of the sweep range.

(h). Switch the AC channel of the selector switch chassis to G4 and observe the frequency counter. The frequency of G4 should be 320 Hz (f_4 - 20%). If not, adjust the VCG driver variable gain amplifier to obtain 320 Hz. With G4 now adjusted for 320 Hz, the frequencies of G1, G2, and G3 will be 80, 160, and 240 Hz, respectively if the procedure of paragraph E.(1).(b) has been accomplished. These frequencies can be checked on the frequency counter by switching the AC channel of the selector switch chassis to G1, G2, and G3.

(i). Reconnect the console DC proportional-to-frequency leads to the X axis of each recorder. Switch consoles 1 and 2 to G3 and G4, respectively. Adjust the X axis gain of each recorder to drive the X or horizontal axis with abscissa values equal to G3 and G4 frequencies.

(6). Narrow Band Analysis During Preliminary Setup

During the preliminary setup stage, a narrow band analysis of the spectrum can be very beneficial in determining ground loops, oscillation, etc., and also in setting in the peak-notch filters.

The outputs of the Spectral Dynamics SD104 was incorporated into the Control Monitors for this purpose as well as for a calibration signal (see Figure D-2 and D-5).

With console 1 and 2 switches in position SD104, the tuning frequency to the tracking filters is supplied by the SD104, and the X axis of each X-Y recorder is fed from the Log DC proportional to frequency output from the SD104. Thus, by switching to position SD104 on console 1 or 2 a narrow band plot of the accelerometer is readily available. The frequency of the oscillator is displayed on the frequency counter when the AC switch on the Selector Switch Panel is in position SD104.

(a). Shaping Spectrum and Adjusting Sine Levels (Bare Table)

That portion of the spectrum not containing sine can be set in on closed loop operation when using an automatic system. Adjust spectrum for 20 db below final level.

For that portion of the spectrum which is on manual control (or for manual control systems) manually adjust for the desired spectrum level before applying the sine signals.

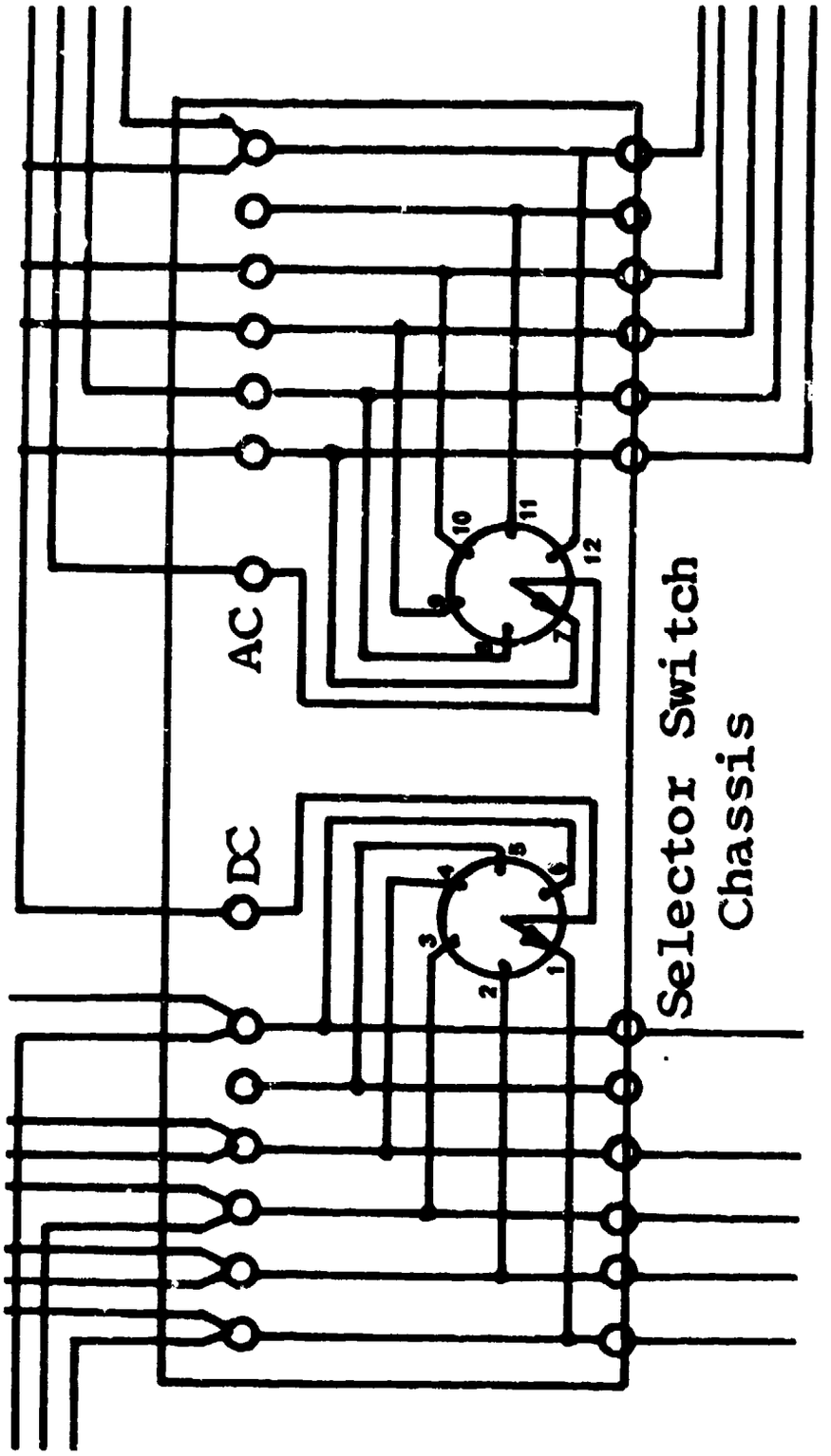

Figure D-5. Detail View of Console Selector Switch System

Switch from closed loop operation to shaker operation and check instrumentation readout for ground loop content. If excessive -- troubleshoot (see Paragraphs B and C).

Energize shaker and adjust the attenuators to set the entire random spectrum preferably at a level 30 db below final level or in any case, at least 20 db down.

Adjust the VCG's to the center frequencies by disconnecting the VCG inputs (DC tracking voltage).

Switch the tracking filter to the desired f_1.

Observe the filtered signal accelerometer output on the voltmeter and X-Y recorder and adjust the sine generator f_1 output in conjunction with the appropriate summing input potentiometer for a g value at f_1 that is at least 20 db below the final test level.

Switch the tracking filter to f_2, f_3 and f_4 in turn and adjust for g values 20 db below final values.

Increase the shaker amplitude by 10 db (switch the N263 Input Attenuator when using the MB T-589 system), observe the random spectrum and the sine levels and make any necessary adjustments.

Increase the shaker amplitude to the final level and again make any necessary adjustments in the levels.

Decrease the shaker amplitude 10 or 20 db, reconnect the VCG inputs to the VCO's and start the sine sweep. Observe the sweep rate and upper and lower frequency limits and make any necessary final adjustments.

Cut down shaker operation and mount specimen on shaker.

2. TEST PROCEDURE

A. At - 30 dB (PE FINAL TEST LEVEL)

(1). Sine pots down, P-N's in bypass. Set servo operating level. Monitor (via scope) the servo output (MB N245) for proper operation.

(2). Shape random spectrum to the curve drawn on the N275 recorder and make visual check with curve drawn on large screen oscilloscope (see Figure D-3).

B. At - 20 dB

(1). Check servo output of N245.

(2). If required, bring up low frequency boost amplifier and adjust associated bandpass filter. Do this in conjunction with equalizer pots for optimum spectral shaping. NOTE: During this operation monitor the N245. Overloading is indicated by clipping and, as characteristic of the T589 system, a marked increase in the high frequency content. If overload appears, back off the gain of the variable gain amplifier, readjust bandpass filter, reset equalizer pots, and, if necessary, touch in servo operating point (N245 output when using the T589).

(3). Switch in P-N's at required spectral locations. A tracking filter and counter may be used to pinpoint the desired notching frequencies whereupon the shaker can be shut down to reduce the vibration time exposure to which equipments are necessarily exposed during such preparatory steps. Alternatively, one can tape the spectrum at this point, shut down the shaker, and use the oscillator and tracking filter to set the frequencies of the P-N's; it being understood that subsequent touch-in adjustments of the P-N's are sometimes required as the vibration levels are changed.

(4). Check the low frequency end for excessive noise contributions from the P-N's. If excessive, troubleshoot (see paragraph B).

(5). Touch-in random spectrum as necessary.

(6). Switch down to -30 dB.

C. At -30 dB

(1). Set in the four sines at their approximate g levels (review paragraph E. (5).

(2). Check the N245 (servo output).

(3). Switch to -20 dB.

D. At -20 dB

(1). Set cycler to low frequency end of sine sweep. Sweep through the full cycling range controlling the four sinusoids as described in Section IV and para. E. (5). The object of this sweep is to adjust the levels of the console control pots in conjunction with the four mixer pots (Figures D-2 and D-4). This is done in order to obtain adequate sine levels and sensitivity to accommodate the shaker driving needs thus ensuring full control over the dynamic range of the test level response. With this done, return the cycler to center frequency conditions (f_1 = 100 Hz, f_2 = 200 Hz, f_3 = 300 Hz and f_4 = 400 Hz) and set the four control pots to obtain the proper acceleration levels for the four sinusoids. Leave the four pots at this setting, quick cycle down to the low frequency end and then slow cycle up and return. Do not adjust the four control pots. Record the frequency response of two sinusoids during the up cycle; switching to the other two sinusoids during the down cycle. NOTE: This last step does two things. First, the graphical display of the recording indicates which of the four sinusoids exhibit the greatest dynamic (peak-notch) range; therefore require the greatest control. The appropriate sine channels may then be reapportioned between the two operators in order to balance up the monitoring load, as described in Section IV. Second, since the plots are left on the X-Y recorder platens and new, pregraphed sheets are placed

over these the console operators now have visible background curves to use as anticipatory indicators that prepare the operators for sudden changes in pot control when major peak notch areas are encountered during the cycling period. This measure eases operator fatigue and facilitates amplitude control.

(2). Switch down to -30 dB.

E. At -30 dB

Check and set all monitor and recording systems for go.

F. Switch Sequentially up to 0 dB

(1). Immediately check the N245 output; if OK, proceed at this level.

(2). Touch-in the four sines to their proper levels.

(3). Touch-in random spectrum.

(4). Check the N245.

G. Start cycler and begin controlled sweep of sinusoids. NOTE: During this phase it is advantageous to have a third operator available to touch-in the random spectrum, monitor the servo output, check the spectra levels, and so on.

REFERENCES

1. R. W. Sevy, J. Clark, Aircraft Gunfire Vibration; The Development of Prediction Methods and the Synthesis of Equipment Vibration Techniques, AFFDL-TR-70-131, November 1970.

2. Peter S. Westine, Structural Responses of Helicopters to Muzzle and Breech Blast, (Vol. I of Final Technical Report, Blast Field about Weapons), Southwest Research Institute Technical Report 02-2029, November 1968.

3. V. C. McIntosh, P. G. Bolds, Vibration and Acoustic Environment of UH-1C Helicopter Configured with and Using M-5 and XM-21 Armament, AFFDL-TR-73-160, February 1974.

4. Manfred A. Heckl, Richard H. Lyon, Gideon Maidanik and Eric E. Ungar, New Approaches to Flight Vehicle Structural Vibration Analysis and Control, ASD TDR-62-237, October 1962.

BIBLIOGRAPHY

Crandall. "Random Vibration," Vol. I, MIT Press.

The Chemical Rubber Co., "Handbook of Mathematical Tables", 2nd Edition, 1964.

Harris and Crede. "Shock and Vibration Handbook", Vol. I, McGraw-Hill, 1961.

☆ U. S. GOVERNMENT PRINTING OFFICE: 1976 — 657-650/565